Host Inflammatory Responses to Adenovirus Respiratory Infection

by

Mary Katherine McCarthy

A dissertation submitted in partial fulfillment
of the requirements for the degree of
Doctor of Philosophy
(Microbiology and Immunology)
in The University of Michigan
2014

Doctoral Committee:

Associate Professor Jason B. Weinberg, Chair
Associate Professor David M. Aronoff, Vanderbilt University
Professor Nicholas W. Lukacs
Professor Bethany B. Moore
Professor Katherine R. Spindler

DEDICATION

To my family and friends

ACKNOWLEDGMENTS

First and foremost, I would like to thank my mentor, Dr. Jason Weinberg for welcoming me into his lab when I first came to the University of Michigan. Jason is unequivocally the most supportive and enthusiastic mentor and friend that a graduate student could ever hope to have. I would like to thank him for encouraging all of my pursuits, both inside and outside of science. Jason and I have tolerated (and at times, incited) each other's crazy ideas for experiments over the years, and he continually urged me to think critically about my work. Jason's humor and lightheartedness made the lab a fantastic place to work these past four years. Jason allowed me a great deal of autonomy over my projects, especially in the early stages of the myocarditis work, which gave me confidence that I could develop into a capable, independent researcher. Jason has always made time for each of his lab members while juggling the immense responsibilities of a clinician scientist, and his patience with and dedication to those who work with him is something that I will strive to emulate going forward.

Members of my thesis committee (a.k.a. "The Dream Team") have been instrumental to my success in graduate school. I would like to thank my committee members for encouraging me in my graduate school projects, being very positive when I introduced new things (like the myocarditis work), providing thoughtful questions and comments, and advising me in my career. I thank Kathy Spindler, for great discussions during joint lab meetings, for being willing to read

my grant proposals and manuscripts, and for all of her assistance and advice for my career. I thank Beth Moore for all of her assistance and helpful conversations on the bone marrow transplant project in particular and for making my GSI experience during the undergraduate virology course a very positive one. Dave Aronoff provided excellent advice, asked perceptive questions, and showed all-around enthusiasm for my projects. Nick Lukacs continually gave important input, provided critical reagents (namely, the IFN-γ neutralizing antibody), and encouraged me to become somewhat of a T cell immunologist. I also thank Mike Imperiale, my “honorary thesis committee member,” for providing feedback on my manuscripts, asking insightful questions during joint virology lab meetings, having a sense of humor, and providing a quiet lab environment conducive to writing. Suzy Dawid has also been an important source of graduate school and career advice.

I would also like to thank my labmates, especially Megan Procario and Rachael Levine, for making the Weinberg Virology Lab a positively wonderful place. Lab would undoubtedly not be the same without you. I would like to thank members of the Dawid lab, especially Natalie Maricic, for all of the good times. Megan, Rachael, and Natalie have been fantastic friends through the ups and downs of graduate school and I am thankful to have spent the past few years with them.

I am thankful to those who have provided critical feedback on manuscripts (Mike Imperiale, Kathy Spindler, Beth Moore, and Mike Watson). Carol Wilke was a crucial resource for our bone marrow transplant experiments. I also thank Joel

Whitfield from the Cancer Center Immunology Core for performing cytokine and chemokine ELISA measurements, Paula Arrowsmith from the ULAM Pathology Cores for Animal Research for providing histology, and Kimber Converso-Baran from the Physiology Phenotyping Core for performing echocardiography. Dan Michele, Sharlene Day, and Saul Powell provided important feedback, suggestions, and resources for the myocarditis project. Many others in the Department of Microbiology & Immunology have provided reagents or instruction in the past few years. I would also like to thank members of the administrative staff in the Department of Pediatrics & Communicable Diseases, in particular Judith Green, Laura Bismack, and Sandy Klaus. Staff members in the Microbiology & Immunology departmental office, particularly Heidi Thompson, have been very helpful as well. I also thank the following funding sources: R01 AI083334, R21 AI103452, the Molecular Mechanisms of Microbial Pathogenesis Training Program (T32), American Society for Virology Student Travel Awards, the University of Michigan Endowment for the Development of Graduate Education (EDGE) Award, Rackham Graduate Student Research Grants, and a Rackham Conference Travel Award.

Last, but certainly not least, I would like to thank my friends and family. I have been blessed with the most incredible friends that I could ever ask for. It would require hundreds of pages to adequately express my gratitude for their support, their encouragement, and the fun that I had with them these past four years. I am similarly grateful for my family, especially my parents, without whose love and support this would not have been possible.

TABLE OF CONTENTS

LIST OF TABLES

LIST OF FIGURES

LIST OF ACRONYMS AND ABBREVIATIONS

5-LO	5-lipoxygenase
AA	arachidonic acid
AdV	adenovirus
AHR	airway hyperreactivity
AM	alveolar macrophage
AMP	antimicrobial peptide
APC	antigen presenting cell
BAL	bronchoalveolar lavage
BLT	B leukotriene receptor
BMT	bone marrow transplant
Btk	Bruton's tyrosine kinase
cAMP	cyclic adenosine monophosphate
CCL5	chemokine (CC motif) ligand 5
COPD	chronic obstructive pulmonary disease
COX	cyclooxygenase
cPGES	cytosolic prostaglandin E2 synthase
cTEC	cortical thymic epithelial cell
CVB3	coxsackievirus B3
cysLT	cysteinyl leukotriene
DC	dendritic cell
DC	dendritic cell
DCM	dilated cardiomyopathy
dpi	days post infection
DRiP	defective ribosomal product
E1A	early region 1 A
EKC	epidemic keratoconjunctivitis
EP	E prostanoid
ER	endoplasmic reticulum
FLAP	5-LO-activating protein
G-CSF	granulocyte colony stimulating factor
GM-CSF	granulocyte macrophage colony-stimulating factor
HAdV	human adenovirus
HBV	hepatitis B virus
HCMV	human cytomegalovirus
hMPV	human metapneumovirus
HSCT	hematopoietic stem cell transplant
i.p.	intraperitoneal
i.v.	intravenous
IFN	interferon

IGF-1	insulin-like growth factor-1
IL	interleukin
IRF	interferon regulatory factor
Kb	kilobase
LAP	leucine aminopeptidase
LCMV	lymphocytic choriomeningitis virus
LMP	low molecular weight protein
LT	leukotriene
LV	left ventricle
MAV-1	mouse adenovirus type 1
MCMV	mouse cytomegalovirus
MECL-1	multicatalytic endopeptidase complex-like 1
MHC	major histocompatibility complex
MLN	mediastinal lymph node
mPGES	microsomal prostaglandin E_2 synthase
MPO	myeloperoxidase
MRP	multidrug resistance protein
NF-κB	nuclear factor-kappa B
ng	nanogram
NK	natural killer
NO	nitric oxide
NOD	nonobese diabetic
OVA	ovalbumin
PBS	phosphate buffered saline
PCR	polymerase chain reaction
pfu	plaque forming units
PG	prostaglandin
PIV	parainfluenza virus
PLA_2	phospholipase A_2
PMA	phorbol-12-myristate-13-acetate
PVM	pneumonia virus of mice
RORgt	RAR-related orphan receptor gamma t
ROS	reactive oxygen species
RSV	respiratory syncytial virus
RT-qPCR	reverse transcriptase quantitative real-time PCR
RV	rhinovirus
SV40	simian virus 40
TAP	transporter for antigen processing
TLR	toll-like receptor
TNF-α	tumor necrosis factor alpha
TXA_2	thromboxane A_2

ABSTRACT

Adenoviruses are common causes of acute respiratory infection and myocarditis, but limited therapies exist. It is unclear if the clinical manifestations of adenovirus disease are mediated by virus-induced tissue damage or the host immune response to the virus. The main focus of this dissertation was to identify host factors that regulate inflammatory responses and contribute to pathogenesis of acute adenovirus respiratory infection. Due to the species-specificity of adenoviruses, which precludes animal studies with a human adenovirus, I used mouse adenovirus type 1 (MAV-1) to study the pathogenesis of an adenovirus in its natural host.

PGE_2 is a lipid mediator that can promote proinflammatory cytokine production and pulmonary inflammation. Exaggerated PGE_2 production in the setting of hematopoietic stem cell transplantation has been linked to increased susceptibility to microbial infections. Using pharmacologic inhibitors and mice deficient in PGE_2, I determined that while PGE_2 promotes the expression of a variety of cytokines in response to acute MAV-1 infection, PGE_2 synthesis is not essential for generating pulmonary immunity to MAV-1 in immunocompetent mice. IL-17, a cytokine that is highly induced during MAV-1 infection and can be upregulated by PGE_2, is likewise not essential for control of virus infection or for virus-induced pulmonary inflammation. Adenovirus infections are an important

complication in immunocompromised individuals, such as transplant patients. I demonstrated that bone marrow transplant (BMT) mice display exaggerated PGE_2 production and significantly delayed clearance of virus from the lungs. BMT-induced T cell dysfunction likely contributes to impaired virus clearance. However, T cell dysfunction is independent of excess PGE_2 production.

In addition to causing respiratory disease, adenoviruses are important causes of myocarditis. I used MAV-1 to establish a mouse model of adenovirus myocarditis in neonatal mice. I demonstrated that IFN-γ is a proinflammatory mediator during MAV-1 myocarditis, and persistent MAV-1 infection may contribute to ongoing cardiac dysfunction. The immunoproteasome, a specialized type of proteasome that can be induced by IFN-γ and regulate inflammatory responses, is robustly induced during MAV-1 myocarditis. IFN-γ is important for induction of the immunoproteasome following MAV-1 infection, and the immunoproteasome likely has organ-specific effects. Inhibition of the constitutive proteasome or the immunoproteasome impairs induction of some proinflammatory cytokines during MAV-1 myocarditis.

By determining contributions of various host factors to MAV-1 pathogenesis and viral clearance, we have gained insight into mechanisms of acute disease and persistence. My work suggests that minimizing some host immune responses during acute infection of immunocompetent hosts may be a useful strategy to prevent excess inflammation without impacting antiviral immunity. In immunocompromised hosts, in which viral clearance is impaired, interventions to restore anti-adenoviral immunity could prevent prolonged

disease associated with excess viral replication. Finally, approaches to clear persistent adenovirus may lessen the impact of chronic disease in the lungs or heart. Understanding the role that host factors play during adenovirus pathogenesis is an essential step in determining whether modulation of adenovirus-induced inflammation could provide an alternative to antiviral drugs to treat patients with adenovirus infection.

Chapter 1:
Adenoviruses

Adenovirus Biology

Adenoviruses (AdVs) are non-enveloped icosahedral viruses with a double-stranded DNA genome of 26-45 Kb (1). They were first identified in 1953 during attempts to establish cell culture lines from surgically removed tonsils and adenoid tissue (2). Multiple serotypes of AdV were identified soon after and a nomenclature was adopted before being reclassified in 1999 (3). Phylogenetic analyses have grouped the family *Adenoviridae* into four genera: *Mastadenovirus*, originating from mammals and containing all human AdV (HAdV); *Aviadenovirus*, from birds; and *Atadenovirus* and *Siadenovirus*, isolated from a wide range of hosts including reptiles, birds, and mammals. A fifth genus contains the only fish adenovirus isolated to date (4). Human adenoviruses (HAdVs) are grouped into seven species (A, B, C, D, E, F, and G) based on their ability to agglutinate red blood cells and based on sequence. Species B AdV are further divided into species B1 and B2. HAdVs are named based on the format "type HAdV-C5," where the letter "C" indicates the species and each type has a unique number (5). There are currently 58 known human types, which are increasingly defined based on DNA sequence and bioinformatics rather than serology.

Adenovirus Infections in Humans

AdV have been associated with a number of clinical conditions in humans, including acute respiratory disease, conjunctivitis (including epidemic keratoconjunctivitis, EKC), acute hemorrhagic cystitis, hepatitis, gastroenteritis, and myocarditis (6). Some generalizations can be made regarding the relationship between the serotype and disease. Species C and some B1 serotypes (Ad3 and Ad7) are common in infants and younger children, while species E AdV (Ad4 and Ad7) cause acute respiratory distress (ARD) in military recruits. Species B2 affects the kidney and urinary tract. Adenoviruses in species F (Ad40 and Ad41) are common causes of gastroenteritis. Species D (especially Ad8, Ad19, and Ad37) cause EKC.

Much of the information regarding adenovirus epidemiology in civilian populations was learned from two virus watch studies that were undertaken in New York and Seattle (7, 8). While initial spread of HAdV can occur by the respiratory route, fecal-oral transmission accounts for most infections, especially in young children. A large number of HAdV infections are asymptomatic or subclinical, but there is a high incidence of recurrent shedding in fecal samples. Live virus can be isolated and grown from the gastrointestinal tract many months after the initial infection and immune response.

HAdV are responsible for approximately 5-10% of upper respiratory infections in early childhood (7, 9). Adenoviruses can also cause lower respiratory tract infections in children, and a few epidemics have resulted in substantial mortality (10-12). Neonates, in particular, are at increased risk for

morbidity and mortality due to HAdV infection, especially when infection is disseminated and involves the respiratory tract (13). Fatal HAdV respiratory infections in military recruits and children with severe HAdV disease are characterized by necrotizing bronchitis, bronchiolitis, and interstitial pneumonia (14). Persistent HAdV infections in the respiratory tract have been implicated in the development and pathogenesis of asthma and chronic obstructive pulmonary disease (COPD) (15, 16).

Immunocompromised populations are at particular risk for severe HAdV disease. Human adenoviruses cause considerable morbidity and mortality in hematopoietic stem cell transplant (HSCT) patients (17, 18) and solid organ transplant patients (19). Depending on the assay used and clinical sample analyzed, adenovirus infection rates in HSCT patients vary from 5% to 47% ((20, 21) and reviewed in (22)). Disease rates as high as 6.5% have been reported, with >50% mortality rates in some studies of HSCT patients with HAdV disease (21, 23). Pediatric patients are at a higher risk for HAdV disease (24, 25), likely due to higher infection rates of lower serotypes of species C HAdV in this population, and a relative lack of species cross-reactive T and B cell responses compared to adults where some adenovirus-specific immunity has been established (26). Severe graft versus host disease (27), T-cell-depleted grafts, and leukopenia (28) are additional risk factors for adenovirus infection following transplant. Depending on the patient age, HAdV serotype and affected organ, clinical manifestations of HAdV infections in immunocompromised patients include pneumonia, hepatitis, hemorrhagic cystitis, pancreatitis,

meningoencephalitis, and disseminated disease (reviewed in (22)). Immune recovery appears to play a significant role in HAdV infection post-HSCT. A number of studies have documented a strong association between lymphocyte count (both absolute lymphocyte count and CD4 count) and clearance of HAdV and survival (28-30). Clearance of HAdV is also associated with an increase in titers of serotype-specific antibodies (29), indicating that both B and T cell function may be important for control HAdV post-HSCT.

It is unknown whether HAdV infections post-transplant occur as a result of endogenous reactivation of persistent virus or primary infection, although evidence suggests that both routes could contribute. In a subset of liver transplant recipients who developed HAdV hepatitis, concomitant HAdV infection with the same serotype was demonstrated in a close relative, suggesting that infection occurred as a result of spread rather than virus reactivation (31). Persistence of HAdV DNA has been documented in T lymphocytes of tonsil and adenoid tissue (32, 33), supporting the possibility that persistently infected lymphocytes within the transplant may be the source of infection in transplant patients. However, a previous study demonstrated absence or low (<2%) frequency of HAdV DNA in peripheral blood of healthy volunteers, suggesting that there is very little HAdV found in circulation (34). Whether HAdV DNA can be found in cells within the bone marrow or in bone marrow progenitors elicited into the bloodstream by GM-CSF (a common source of stem cells for HSCT) is unknown. Still, endogenous reactivation from T cells could be a significant source

of infection in solid organ transplant recipients, where there are likely to be numerous persistently infected lymphocytes within the transplanted organ.

Adenoviruses are also common causes of myocarditis. HAdV genome was detected in 38% of pediatric (<18 years old) patients with clinical and histologic diagnosis of myocarditis (35). In a study of over 600 patients with clinically diagnosed myocarditis, HAdV genome was detected by PCR in endomyocardial biopsy samples in 23% of patients (n = 142) (36). Approximately 80% of these patients were positive for Ad2 and the rest were positive for Ad5, except for one patient who was positive for Ad6. HAdV was the most common virus detected regardless of age group. Interestingly, only 40% of HAdV -positive patients had acute myocarditis by histology, in contrast to the majority of enterovirus-positive patients. This suggests that HAdV myocarditis is associated with less inflammation than enterovirus myocarditis. The presence of HAdV genome in endomyocardial biopsies of pediatric heart transplant recipients is associated with coronary vasculopathy and graft loss (37).

Dilated cardiomyopathy (DCM) is a long-term sequella of acute myocarditis. HAdV was detected by PCR in endomyocardial biopsy samples of 18 of 149 (12%) of patients with DCM (36). In another study, HAdV DNA was detected in 8% of DCM patients (38). Left ventricular (LV) ejection fraction significantly improved in patients where viral genomes were cleared, while persistence of viral genome was associated with decreased LV function. Another study from the same group documented AdV DNA in only 1.6% of patients with DCM (39). The reason for the relatively low rate of AdV detection in this study

compared to previous studies is unknown. HAdV DNA was detected in 12 of 94 adult patients with idiopathic LV dysfunction, which is also called idiopathic DCM (40). In a follow-up phase II clinical study of patients with persistent LV dysfunction who tested positive for enterovirus or HAdV genomes, IFN-β treatment led to clearance of virus that was accompanied by improved LV function (41).

HAdV clearly cause a wide variety of diseases in humans, with many involving the respiratory tract or the heart. The manifestations and outcome of disease vary widely and depend on the HAdV serotype involved, the affected organ(s), and the immune status of the host. Persistent HAdV infections are implicated as causes or major contributors to the development of a number of diseases, including COPD, asthma, and DCM.

Immune Responses to Adenoviruses

Studies on the pathogenesis of adenovirus infection have been limited by the strict species-specificity of adenoviruses. Although HAdV can infect cells of most mammals, they do not replicate well even in simian species. Early proteins (which are expressed prior to the onset of DNA replication) are highly expressed in nonhuman mammals, but adenovirus DNA does not replicate and therefore late genes are expressed at very low levels or not expressed at all. HAdV replication can be achieved in monkey cells, although this requires either coinfection with simian virus 40 (SV40) or infection with an adenovirus host range mutant (Ad5hr404), which contains a point mutation in the DNA-binding protein

(42). Inoculation of mice with HAdV does not result in a fully permissive infection, as the virus does not replicate in mouse tissue (43). Pneumonia can be induced in mice following intranasal inoculation with Ad5, but this requires an infectious dose $>10^{10}$ plaque-forming units (pfu) (43). Although cotton rats have been used in some HAdV models and are permissive for HAdV replication, a high virus inoculum is required to cause respiratory disease (43, 44). Syrian hamsters are permissive for HAdV replication in the lung (45), but this model is not well characterized.

Most information regarding the immune response to adenoviruses has been gleaned from *in vitro* studies or from exposure of mice to high doses of non-replicating HAdV vectors. *In vitro* studies do not provide an adequate way to comprehensively study interactions between a virus and host inflammatory responses. While *in vivo* studies using non-replicating AdV provide a means to study immune responses to some AdV early proteins and capsid proteins, this does not fully recapitulate steps that occur during a natural infection, in which the immune system would encounter an actively replicating virus. Nevertheless, much has been learned about early AdV-host interactions through nonpermissive infection studies.

In mouse pneumonia models following nonpermissive infection with species C HAdV, the inflammatory response is characterized by early infiltration of lymphocytes, monocytes, and macrophages (43, 46). Early viral gene expression is detected in bronchiolar epithelial cells and bronchioles of the lung and nasal mucosa, with some damage occurring in these cells. The late phase of

cellular infiltration is thought to consist almost entirely of virus-specific lymphocytes, because this response does not occur in athymic nude mice. Inflammation in HAdV -exposed lungs is accompanied by induction of IL-1β, IL-6, IFN-γ, IL-12 and TNF-α. Each of these cytokines may be playing major roles during AdV infection. Signaling of TNF-α through two of its receptors, p55 and p75, plays an important role in determining the scale of humoral immune responses to HAdV. Mice deficient in TNF-α or the p55 TNF receptor show significantly reduced humoral responses compared to wild-type mice following intratracheal instillation with HAdV vector (47). Although IL-12 is induced in many animal models of HAdV infection, the generation of Th1-responses and humoral responses is not reduced in IL-12-deficient mice exposed intranasally to high doses of human AdV (48). IL-18, a cytokine that can compensate for IL-12 in some settings, is required for induction of IFN-γ after HAdV infection, but does not affect Th1 responses (48).

Alveolar macrophages provide a first line of defense in the respiratory tract through immune surveillance and the initiation and regulation of inflammation. Upon intratracheal administration of HAdV vectors to the mouse lung, alveolar macrophages recovered within the first 30 min contain large amounts of vector genome (49). In another study, HAdV labeled with a fluorescent dye was localized in alveolar macrophages within 1 min of administration (50). Because they are among the first cells to encounter AdV in the lung, alveolar macrophages are an important source of initial cytokine signaling during AdV infection. Alveolar macrophages isolated 30 min after infection, but not airway

epithelial or vascular endothelial cells, express TNF-α and IL-6 mRNA (50). Activation of alveolar macrophages by HAdV can be caused by detection of HAdV capsid proteins or by detection of HAdV and vector DNA via Toll-like receptors (TLRs) (51).

Human macrophages produce IL-1α and IL-1β after exposure to HAdV. Induction of IL-1β in bone marrow-derived macrophages requires HAdV endosomal membrane penetration and TLR9 sensing of HAdV DNA in order to activate the NLRP3 inflammasome (52). IL-1α induction occurs independently of TLR9 and NLRP3, and instead requires interactions between RGD motifs on virus capsid proteins and β3 integrins on the surface of macrophages (53). Interference with the IL-1 signaling pathway through genetic deletion of IL-1R1 results in significantly reduced inflammatory responses to intravenously administered HAdV vectors in mice (54). Intranasal administration of replication-deficient HAdV vectors to mice results in signs of acute respiratory distress and high mortality (55). However, mice deficient in caspase-1 or $P2X_7R$ (an extracellular ATP receptor that activates the inflammasome) have increased survival compared to control mice that correlates with reduced IL-1β, IL-6, and neutrophil recruitment early during infection. These results indicate that activation of the inflammasome pathway through diverse mechanisms plays an important role in the regulation of inflammatory responses to HAdV.

Dendritic cells (DCs) also play important roles in immune responses in the lung through efficient antigen presentation and initiation of the adaptive immune response. HAdV can trigger DC activation through viral capsid proteins (56-58),

and viral gene expression is not required for DC activation (59, 60). Although DCs can be activated through TLRs during HAdV infection (51), accumulating evidence suggests that TLR-independent pathways may be important for DC activation in response to HAdV as well (61, 62). Elimination of tissue macrophages and splenic DCs *in vivo* in mice results in significantly reduced IL-6, IL-12, and TNF-α release and an impaired HAdV -specific CD8 T cell response (63). Interestingly, HAdV infection of lung-resident murine DCs suppresses DC-induced T cell proliferation by making T cells nonresponsive to IL-2 (64). Suppression is not due to factors secreted by DCs or downregulation of MHC or costimulatory molecules, but it does require viral protein synthesis and DC-T cell contact. These effects are not observed in mouse bone marrow- or monocyte-derived DCs, suggesting that HAdV may have different effects in DCs depending on their source and activation/maturation state. It also suggests that results obtained from DC-depleted or DC-deficient mice systemically exposed to HAdV vectors may not fully reflect the role that lung-resident DCs play during natural AdV respiratory infections.

Type I IFN-deficient mice exhibit a similar phenotype to that of DC-depleted mice, with less IL-6, IL-12, and T cell activation compared to wild-type mice following exposure to HAdV (65). DCs and macrophages appear to be important producers of type I IFNs in response to HAdV (61, 62, 66). A specialized type of DC, the plasmacytoid DC (pDC), produces large amounts of type I IFNs when stimulated and is known as a professional IFN-producing cell (67, 68). pDCs express only the endosomal nucleic acid sensors TLR7 and TLR9

(69). When exposed to HAdV vectors, TLR9-deficient mice secrete significantly less IL-6 and IL-12 than wild-type mice (70). This suggests a role for TLR9 sensing of AdV DNA in the induction of proinflammatory cytokines, possibly through the induction of type I IFNs in pDCs. However, a later study suggested that type I IFN induction in response to HAdV does not occur through TLR9 at all. In mice administered high doses of HAdV intraperitoneally (i.p.), myeloid DCs (mDCs) rather than pDCs are the primary producers of type I IFN (62). Production of type I IFN in this model occurs independently of TLR signaling. Furthermore, distinct pathways mediate initial IL-6 and type I IFN production, although type I IFNs positively regulate the IL-6 response. The induction of type I IFN and proinflammatory cytokines clearly involves a complicated interplay between multiple cell types, mechanisms of AdV sensing, and feedback loops. Many redundant pathways are likely involved in this process and more studies are required to assess the contribution of these pathways to inflammatory responses during a natural AdV infection.

Neutrophil recruitment to the lung following exposure to HAdV is a common finding in a number of animal models (44, 71-73). HAdV induces robust production of the chemokine IL-8 in human airway epithelial cells (74-76). Increased levels of the neutrophil chemokines CXCL1 and CXCL2 (mouse IL-8 homologs, also known as KC and MIP-2, respectively) have been observed in lungs of mice exposed to HAdV (46). Neutrophils are the main cell type recovered by bronchoalveolar lavage in mice at early times following intratracheal administration of HAdV-B3 or HAdV-B7 (46). Neutrophils can

internalize HAdV in the presence of complement or IgG (77) and may be a prominent source of proinflammatory cytokines during AdV infection.

Many of the observed proinflammatory cytokine responses to HAdV vectors in nonpermissive models have also been observed in HAdV infections in humans. Increased concentrations of circulating IL-6, IL-8, and TNF-α are significantly associated with severity of HAdV infection in children (78). IL-6, in particular, was detected in children with severe and fatal HAdV infection, but not in children with HAdV infections classified as moderate in severity. Serum IL-8 levels also correlated with clinical outcome in children with HAdV pneumonia. In another study, high IL-6 serum levels correlated with serum concentrations of C-reactive protein and also associated with severity of HAdV infection (79).

While there are indications that some of the cytokines induced during severe HAdV infections and studies with animal models are similar, it is difficult to use nonpermissive animal models to assess the role of these cytokines or other factors at different stages during an infection. The distribution of virus, as well as the kinetics and magnitude of inflammatory responses are likely to be quite different in natural human infections, when the immune system is faced with an AdV that is actively spreading and evading these responses, compared to animal infections by non-replicating HAdV vectors. A permissive animal model is particularly important for the study of persistent AdV infections, which may play important roles in a number of patient populations and disease states, including BMT, asthma, COPD, and DCM.

MAV-1 as a Model for Adenovirus Pathogenesis

Mouse adenovirus type 1 (MAV-1, also known as MAdV-1) was first identified in 1960 and designated Ad-FL (80). MAV-1 causes disseminated infections and replicates to high titers in multiple organs of susceptible mouse strains (81-84). Shortly after identification of MAV-1, a second mouse adenovirus (K87) was identified and later designated MAV-2 (85). MAV-2 replicates in the intestinal tract of neonatal and adult mice without causing overt signs of disease, and it is shed in the feces for a long period of time (86). Recently, another mouse adenovirus was isolated from tissue culture and designated MAV-3, as it is genetically and serologically distinct from MAV-1 and MAV-2 (87). Following intravenous (i.v.) inoculation, MAV-3 DNA was detected at high levels in heart tissue and, unlike MAV-1, was undetectable in the brain. Detailed studies of pathogenesis have yet to be carried out using MAV-2 or MAV-3, and MAV-1 is the best characterized of the mouse adenoviruses to date. MAV-1 provides a useful model system to study adenovirus pathogenesis. The virion morphology and genomic organization of MAV-1 are similar to that of HAdV (88, 89). However, there are some notable differences in one early region 1A (E1A) protein, the early region 3 (E3) proteins, and some early region 4 (E4) open reading frames (90-96). MAV-1 also lacks virus-associated RNAs (VA-RNAs) that are found in all HAdV (89).

MAV-1 causes both acute and persistent infections in mice, just as human AdV cause acute and persistent infections in human hosts. Susceptibility to and the outcome of MAV-1 infection depend on the dose of virus and the inoculation

route, as well as the strain and age of mice infected (81, 84, 97, 98). Although mice of all ages are susceptible to MAV-1 infection, morbidity and mortality are generally observed in mice infected as neonates [at least in outbred NMRI mice (Swiss type strain) and the unknown mouse strain used in Hartley & Rowe, 1960], but not in newly weaned or adult mice (2, 99). In the original 1960 paper detailing the identification of MAV-1, it was noted that i.p., intracerebral, or intranasal (i.n.) inoculation of neonatal mice resulted in disseminated pathological changes in the adrenal gland, myocardium, salivary glands, and kidney (80). In these studies, no transplacental transmission of virus was observed between an infected mother and pups, and mice born of previously infected mothers were not susceptible to MAV-1 infection, presumably due to protection by maternal antibodies. Infection of neonatal outbred Swiss Webster mice resulted in viral replication in the heart, as well as lesions of necrosis and inflammatory cells in the myocardium, endocardium, and heart valves (100). Another study observed necrosis in the kidney, heart, spleen and brain in neonatal (9 day old) mice infected with a high dose of MAV-1, with the most severe necrosis and highest concentration of viable virus present in heart tissue, although the mouse strain used in this study was not specified (101).

MAV-1 disease outcome also depends on the strain of mice infected, as some strains of adult mice develop signs of overt disease after MAV-1 infection (81, 83, 97, 102). BALB/c mice are generally resistant to MAV-1-induced disease, while i.p. inoculation of C57BL/6 mice results in a dose-dependent encephalomyelitis (81). Susceptibility to MAV-1-induced encephalomyelitis is

associated with a major quantitative trait locus *Msq1* that maps to a 0.75 megabase region of mouse Chromosome 15 and contains genes of the *Ly6* family (102-104). Following i.p. inoculation, virus can be found in cells of the monocyte/macrophage linage and in vascular endothelial cells (81-83). Infection of outbred NIH Swiss Webster mice results in a persistent infection, with viral DNA detected in kidneys, brain, spleen, and lymph nodes up to 55 weeks post infection (105). Another study detected MAV-1 shed in the urine of outbred Swiss mice for 2 years after either i.p. or i.n. inoculation (106).

Immune Response to MAV-1 Infection

The immune response to MAV-1 is multifaceted. MAV-1 is relatively resistant to the inhibitory effects of type I and II IFN in vitro (107), but there are few published studies documenting MAV-1 pathogenesis in type I or II IFN-deficient mice. Little is known about the contribution of other cytokines and chemokines to MAV-1 pathogenesis. As previously mentioned, i.p. infection of C57BL/6 mice results in acute encephalomyelitis. The inflammatory response in the brain is characterized by recruitment of macrophages, T cells, B cells, and neutrophils (108).

Depletion of macrophages by administration of clodronate-loaded liposomes results in increased viral loads in the spleens of BALB/cJ mice (109), a strain that is largely resistant to MAV-1-induced encephalitis. However, spleen viral loads do not differ in wild-type or mice deficient in CCR2, a chemokine receptor that is important for macrophage recruitment in many models. Viral

loads in the brain are unaffected by macrophage depletion or CCR2 deficiency. This suggests that resident splenic or peritoneal macrophages are important for protection from MAV-1 infection in the spleen. However, viral dissemination to other organs such as the brain may occur by independent or redundant mechanisms. The role of resident macrophages in other organs during MAV-1 pathogenesis, such as Kupffer cells in the liver or alveolar macrophages in the lung, has not been investigated.

Mice deficient in α/β T cells, MHC class I, or the cytolytic granule perforin do not show signs of acute MAV-1 encephalomyelitis following i.p. inoculation (110). MHC class II-deficient mice display no difference in the development MAV-1-induced encephalomyelitis compared to wild-type mice. This suggests a critical role for T cells, and CD8 T cells in particular, in the development of immunopathology during MAV-1 encephalomyelitis. Clearance of MAV-1 from the spleen and brain following i.p. infection occurs in mice deficient in perforin, MHC class I or II, CD4 T cells, or CD8 T cells. However, mice deficient in α/β T cells fail to control MAV-1 replication and succumb between 9 and 16 weeks post infection, indicating that either CD4 or CD8 T cells are required for long-term host survival of MAV-1 i.p. infection. In contrast to T cells, natural killer (NK) cells are not required for control of viral replication or survival following i.p. MAV-1 inoculation (111). The role of various T cell subsets during MAV-1-induced disease in other organs, such as the lung or heart, and through other inoculation routes is largely undefined.

Mice infected either i.p. or i.n. develop MAV-1-specific neutralizing antibodies in the first 2-3 weeks post infection (106). Mice lacking B cells or Bruton's tyrosine kinase (Btk) show increased susceptibility to MAV-1, and antiserum from immune wild-type mice protects $Btk^{-/-}$ mice (112), suggesting that B cells play an important role in control of MAV-1 replication.

Recent studies have provided insight into the immune response to MAV-1 during respiratory infection. Following i.n. inoculation of adult mice, MAV-1 gene expression and infectious virus is present in lung tissue (113). MAV-1 E3 protein can be detected in respiratory epithelial cells by immunohistochemistry. Pulmonary inflammation during MAV-1 respiratory infection is characterized by the accumulation of mononuclear cell infiltrates around medium and large airways, along with interstitial pneumonitis and thickened alveolar walls. The percentage of neutrophils is significantly increased in bronchoalveolar lavage fluid of infected mice. Cellular inflammatory responses peak between 7 and 14 dpi, and largely resolve by 21 dpi. Intranasal inoculation of MAV-1 does not increase overall mucus production in the lung (109). Mice deficient in Muc1, a mucin that is a major constituent of mucus barriers in the lung, have marginally higher viral loads at early times post infection, indicating that Muc1 may contribute to a protective physical barrier against MAV-1 respiratory infection.

Several chemokines are upregulated in the lungs of mice after infection, notably CXCL1 and CCL5 (113, 114). Macrophage inflammatory proteins (MIP)-1α and MIP-1β (now called CCL3 and CCL4, respectively) are significantly upregulated in lungs of infected mice. These cytokines are important in

recruitment of immune cells to sites of infection and induction of proinflammatory cytokines in other models of inflammation (115).

A Th1 cytokine response is observed in the lungs of MAV-1-infected mice, with upregulation of IFN-γ, but not the Th2 cytokines IL-4 or IL-13. Lung viral loads are slightly higher at both 7 and 14 dpi in adult IFN-$\gamma^{-/-}$ mice (on a BALB/cJ background) than wild-type mice, suggesting that IFN-γ may make a small contribution to control of MAV-1 replication in the lung. Following infection, there is an increase in the overall percentage of $CD8^+$ T cells in the lungs. Effector memory CD4 and CD8 T cells ($CD62L^{low}CD4^+$ and $CD62L^{low}CD8^+$) begin to appear in lungs as early as 7 dpi. BALB/cJ mice infected as neonates (7 days of age) have significantly higher lung viral loads during the acute phase of infection that correlate with blunted pulmonary inflammation and cytokine responses compared to adults. Although lung IFN-γ responses are substantially lower in neonates than in adults, administration of exogenous IFN-γ to neonates does not affect viral loads, suggesting that the blunted IFN-γ responses in neonate lungs do not explain increased susceptibility to infection. Neonates exhibit similar kinetics and magnitude of T cell responses in the lung compared to adults, and they are able to develop protective immunity to virus rechallenge. Therefore, although neonates are more susceptible to acute MAV-1 respiratory infection than adults, the development of protective immunity to MAV-1 is intact (114).

Chapter Outlines

In Chapter II, *Eicosanoids and Respiratory Viral Infection*, I discuss eicosanoid synthesis and functions, and their role during respiratory viral infection. In Chapter III, *Immunoproteasome*, I provide an overview of the MHC class I antigen processing pathway and the role of the immunoproteasome in CD8 T cell responses and other aspects of inflammation relevant to viral infection.

In Chapter IV, PGE_2-deficient mice were infected with MAV-1 to assess the role of PGE_2 during MAV-1 respiratory infection. While PGE_2 promotes the expression of a variety of cytokines in response to acute MAV-1 infection, PGE_2 synthesis does not appear to be essential for generating pulmonary immunity in immunocompetent mice.

In Chapter V, I used a mouse model of bone marrow transplant (BMT) to determine the susceptibility of BMT mice to MAV-1 respiratory infection. BMT increases susceptibility to MAV-1 infection, but this is not due to exaggerated PGE_2 overproduction following infection. Instead, BMT-induced T cell dysfunction likely contributes to impaired virus clearance.

Due to substantial evidence that PGE_2 promotes IL-17 responses during inflammation, I studied the role of IL-17 during MAV-1 infection. In Chapter VI, I characterized T cell polarization and IL-17 responses to MAV-1 in wild-type mice. Although MAV-1 induces robust Th17 responses during MAV-1 respiratory infection, these responses are not essential for control of virus infection or for virus-induced pulmonary inflammation.

Adenoviruses are important causes of myocarditis. In Chapter VII, I established a model of MAV-1-induced myocarditis in neonatal mice. I demonstrate that IFN-γ is a proinflammatory mediator during MAV-1 myocarditis, and persistent MAV-1 infection may contribute to ongoing cardiac dysfunction.

In Chapter VIII, I show that the immunoproteasome is significantly induced during MAV-1 myocarditis. IFN-γ is important for induction of the immunoproteasome following MAV-1 infection. While treatment of mice with a nonspecific proteasome inhibitor leads to decreased proinflammatory cytokine induction after MAV-1 infection, an immunoproteasome-specific inhibitor does not have seem to have a similar effect.

Finally, in Chapter VIV, I summarize findings of the dissertation, discuss implications of this work, and propose directions for future research.

References

1. **Knipe D, Howley P, Griffin D, Lamb R, Martin M, Roizman B, Straus S.** 2007. Fields Virology, 5th ed. Lippincott Williams & Wilkins, Philadelphia, PA.
2. **Rowe W, Huebner R, Gilmore L, Parrott R, Ward T.** 1953. Isolation of a cytopathogenic agent from human adenoids undergoing spontaneous degeneration in tissue culture. Proc Soc Exp Biol Med **84:**570-573.
3. **van Regenmortel MH, M FC, HL BD.** 2000. Virus taxonomy: classification and nomenclature of viruses. Academic Press, San Diego, CA.
4. **Davison AJ, Benko M, Harrach B.** 2003. Genetic content and evolution of adenoviruses. J Gen Virol **84:**2895-2908.
5. **Seto D, Chodosh J, Brister JR, Jones MS, Community motAR.** 2011. Using the whole genome sequence to characterize and name human adenoviruses. J Virol.
6. **Knipe D, Howley P, Griffin D, Lamb R, Martin M, Roizman B, Straus S.** 2007. Adenoviridae: The Viruses and Their Replication, p. 2355-2436, Fields Virology, vol. 1.
7. **Fox JP, Brandt CD, Wassermann FE, Hall CE, Spigland I, Kogon A, Elveback LR.** 1969. The virus watch program: a continuing surveillance of viral infections in metropolitan New York families. VI. Observations of adenovirus infections: virus excretion patterns, antibody response, efficiency of surveillance, patterns of infections, and relation to illness. Am J Epidemiol **89:**25-50.
8. **Fox JP, Hall CE, Cooney MK.** 1977. The Seattle Virus Watch. VII. Observations of adenovirus infections. Am J Epidemiol **105:**362-386.
9. **Brandt CD, Kim HW, Vargosko AJ, Jeffries BC, Arrobio JO, Rindge B, Parrott RH, Chanock RM.** 1969. Infections in 18,000 infants and children in a controlled study of respiratory tract disease. I. Adenovirus pathogenicity in relation to serologic type and illness syndrome. Am J Epidemiol **90:**484-500.
10. **Carballal G, Videla C, Misirlian A, Requeijo PV, Aguilar MdC.** 2002. Adenovirus type 7 associated with severe and fatal acute lower respiratory infections in Argentine children. BMC pediatrics **2:**6.
11. **Murtagh P, Cerqueiro C, Halac A, Avila M, Kajon A.** 1993. Adenovirus type 7h respiratory infections: a report of 29 cases of acute lower respiratory disease. Acta Paediatrica **82:**557-561.
12. **Faden H, Wynn RJ, Campagna L, Ryan RM.** 2005. Outbreak of adenovirus type 30 in a neonatal intensive care unit. J Pediatr **146:**523-527.
13. **Ronchi A, Doern C, Brock E, Pugni L, Sánchez PJ.** 2014. Neonatal adenoviral infection: a seventeen year experience and review of the literature. J Pediatr **164:**529-535.e521-524.

14. **Dudding BA, Wagner SC, Zeller JA, Gmelich JT, French GR, Top FH.** 1972. Fatal pneumonia associated with adenovirus type 7 in three military trainees. NEJM **286:**1289-1292.
15. **Hayashi S, Hogg JC.** 2007. Adenovirus infections and lung disease. Curr Opin Pharmacol **7:**237-243.
16. **Hogg JC.** 2001. Role of latent viral infections in chronic obstructive pulmonary disease and asthma. Am J Respir Crit Care Med **164:**S71-75.
17. **Walls T, Shankar AG, Shingadia D.** 2003. Adenovirus: an increasingly important pathogen in paediatric bone marrow transplant patients. Lancet Infect Dis **3:**79-86.
18. **Kojaoghlanian T, Flomenberg P, Horwitz MS.** 2003. The impact of adenovirus infection on the immunocompromised host. Rev Med Virol **13:**155-171.
19. **Ison MG, Green M, Practice AIDCo.** 2009. Adenovirus in solid organ transplant recipients. Am J Transplant **9 Suppl 4:**S161-165.
20. **Runde V, Ross S, Trenschel R, Lagemann E, Basu O, Renzing-Köhler K, Schaefer UW, Roggendorf M, Holler E.** 2001. Adenoviral infection after allogeneic stem cell transplantation (SCT): report on 130 patients from a single SCT unit involved in a prospective multi center surveillance study. Bone Marrow Transplantation **28:**51-57.
21. **Flomenberg P, Babbitt J, Drobyski WR, Ash RC, Carrigan DR, Sedmak GV, McAuliffe T, Camitta B, Horowitz MM, Bunin N.** 1994. Increasing incidence of adenovirus disease in bone marrow transplant recipients. J Infect Dis **169:**775-781.
22. **Echavarría M.** 2008. Adenoviruses in immunocompromised hosts. Clin Microbiol Rev **21:**704-715.
23. **Hierholzer JC.** 1992. Adenoviruses in the immunocompromised host. Clin Microbiol Rev **5:**262-274.
24. **Howard DS, Phillips II GL, Reece DE, Munn RK, Henslee-Downey J, Pittard M, Barker M, Pomeroy C.** 1999. Adenovirus infections in hematopoietic stem cell transplant recipients. Clin Infect Dis **29:**1494-1501.
25. **Baldwin A, Kingman H, Darville M, Foot AB, Grier D, Cornish JM, Goulden N, Oakhill A, Pamphilon DH, Steward CG, Marks DI.** 2000. Outcome and clinical course of 100 patients with adenovirus infection following bone marrow transplantation. Bone Marrow Transplantation **26:**1333-1338.
26. **Leen AM, Bollard CM, Myers GD, Rooney CM.** 2006. Adenoviral infections in hematopoietic stem cell transplantation. Biol Blood Marrow Transplant **12:**243-251.
27. **Shields AF, Hackman RC, Fife KH, Corey L, Meyers JD.** 1985. Adenovirus infections in patients undergoing bone-marrow transplantation. N Engl J Med **312:**529-533.
28. **Chakrabarti S, Mautner V, Osman H, Collingham KE, Fegan CD, Klapper PE, Moss PAH, Milligan DW.** 2002. Adenovirus infections following allogeneic stem cell transplantation: incidence and outcome in

relation to graft manipulation, immunosuppression, and immune recovery. Blood **100:**1619-1627.

29. **Heemskerk B, Lankester AC, van Vreeswijk T, Beersma MFC, Claas ECJ, Veltrop-Duits LA, Kroes ACM, Vossen JMJJ, Schilham MW, van Tol MJD.** 2005. Immune reconstitution and clearance of human adenovirus viremia in pediatric stem-cell recipients. J Infect Dis **191:**520-530.
30. **Van Tol MJD, Claas ECJ, Heemskerk B, Veltrop-Duits LA, De Brouwer CS, Van Vreeswijk T, Sombroek CC, Kroes ACM, Beersma MFC, De Klerk EPA, Egeler RM, Lankester AC, Schilham MW.** 2005. Adenovirus infection in children after allogeneic stem cell transplantation: diagnosis, treatment and immunity. Bone Marrow Transplantation **35 Suppl 1:**S73-76.
31. **Cames B, Rahier J, Burtomboy G, de Ville de Goyet J, Reding R, Lamy M, Otte JB, Sokal EM.** 1992. Acute adenovirus hepatitis in liver transplant recipients. J Pediatr **120:**33-37.
32. **Garnett CT, Erdman D, Xu W, Gooding LR.** 2002. Prevalence and quantitation of species C adenovirus DNA in human mucosal lymphocytes. J Virol **76:**10608-10616.
33. **Garnett CT, Talekar G, Mahr JA, Huang W, Zhang Y, Ornelles DA, Gooding LR.** 2009. Latent Species C Adenoviruses in Human Tonsil Tissues. J Virol **83:**2417-2428.
34. **Flomenberg P, Gutierrez E, Piaskowski V, Casper JT.** 1997. Detection of adenovirus DNA in peripheral blood mononuclear cells by polymerase chain reaction assay. J Med Virol **51:**182-188.
35. **Calabrese F, Rigo E, Milanesi O, Boffa GM, Angelini A, Valente M, Thiene G.** 2002. Molecular diagnosis of myocarditis and dilated cardiomyopathy in children: clinicopathologic features and prognostic implications. Diagn Mol Pathol **11:**212-221.
36. **Bowles NE, Ni J, Kearney DL, Pauschinger M, Schultheiss H-P, McCarthy R, Hare J, Bricker JT, Bowles KR, Towbin JA.** 2003. Detection of viruses in myocardial tissues by polymerase chain reaction. evidence of adenovirus as a common cause of myocarditis in children and adults. J Am Coll Cardiol **42:**466-472.
37. **Moulik M, Breinholt JP, Dreyer WJ, Kearney DL, Price JF, Clunie SK, Moffett BS, Kim JJ, Rossano JW, Jefferies JL, Bowles KR, O'Brian Smith E, Bowles NE, Denfield SW, Towbin JA.** 2010. Viral endomyocardial infection is an independent predictor and potentially treatable risk factor for graft loss and coronary vasculopathy in pediatric cardiac transplant recipients. J Am Coll Cardiol **56:**582-592.
38. **Kühl U, Pauschinger M, Seeberg B, Lassner D, Noutsias M, Poller W, Schultheiss H-P.** 2005. Viral persistence in the myocardium is associated with progressive cardiac dysfunction. Circulation **112:**1965-1970.
39. **Kühl U, Pauschinger M, Noutsias M, Seeberg B, Bock T, Lassner D, Poller W, Kandolf R, Schultheiss H-P.** 2005. High prevalence of viral

genomes and multiple viral infections in the myocardium of adults with "idiopathic" left ventricular dysfunction. Circulation **111:**887-893.

40. **Pauschinger M, Bowles NE, Fuentes-Garcia FJ, Pham V, Kühl U, Schwimmbeck PL, Schultheiss HP, Towbin JA.** 1999. Detection of adenoviral genome in the myocardium of adult patients with idiopathic left ventricular dysfunction. Circulation **99:**1348-1354.
41. **Kühl U, Pauschinger M, Schwimmbeck PL, Seeberg B, Lober C, Noutsias M, Poller W, Schultheiss H-P.** 2003. Interferon-beta treatment eliminates cardiotropic viruses and improves left ventricular function in patients with myocardial persistence of viral genomes and left ventricular dysfunction. Circulation **107:**2793-2798.
42. **Klessig DF, Grodzicker T.** 1979. Mutations that allow human Ad2 and Ad5 to express late genes in monkey cells map in the viral gene encoding the 72K DNA binding protein. Cell **17:**957-966.
43. **Ginsberg HS, Moldawer LL, Sehgal PB, Redington M, Kilian PL, Chanock RM, Prince GA.** 1991. A mouse model for investigating the molecular pathogenesis of adenovirus pneumonia. Proc Natl Acad Sci USA **88:**1651-1655.
44. **Prince GA, Porter DD, Jenson AB, Horswood RL, Chanock RM, Ginsberg HS.** 1993. Pathogenesis of adenovirus type 5 pneumonia in cotton rats (Sigmodon hispidus). J Virol **67:**101-111.
45. **Thomas MA, Spencer JF, La Regina MC, Dhar D, Tollefson AE, Toth K, Wold WSM.** 2006. Syrian hamster as a permissive immunocompetent animal model for the study of oncolytic adenovirus vectors. Cancer Res **66:**1270-1276.
46. **Kajon AE, Gigliotti AP, Harrod KS.** 2003. Acute inflammatory response and remodeling of airway epithelium after subspecies B1 human adenovirus infection of the mouse lower respiratory tract. J Med Virol **71:**233-244.
47. **Minter RM, Rectenwald JE, Fukuzuka K, Tannahill CL, La Face D, Tsai V, Ahmed I, Hutchins E, Moyer R, Copeland EM, Moldawer LL.** 2000. TNF-alpha receptor signaling and IL-10 gene therapy regulate the innate and humoral immune responses to recombinant adenovirus in the lung. J Immunol **164:**443-451.
48. **Xing Z, Zganiacz A, Wang J, Divangahi M, Nawaz F.** 2000. IL-12-independent Th1-type immune responses to respiratory viral infection: requirement of IL-18 for IFN-gamma release in the lung but not for the differentiation of viral-reactive Th1-type lymphocytes. J Immunol **164:**2575-2584.
49. **Worgall S, Leopold PL, Wolff G, Ferris B, Van Roijen N, Crystal RG.** 1997. Role of alveolar macrophages in rapid elimination of adenovirus vectors administered to the epithelial surface of the respiratory tract. Hum Gene Ther **8:**1675-1684.
50. **Zsengellér Z, Otake K, Hossain SA, Berclaz PY, Trapnell BC.** 2000. Internalization of adenovirus by alveolar macrophages initiates early

proinflammatory signaling during acute respiratory tract infection. J Virol **74:**9655-9667.
51. **Hensley SE, Amalfitano A.** 2007. Toll-like receptors impact on safety and efficacy of gene transfer vectors. Molecular Therapy **15:**1417-1422.
52. **Barlan AU, Griffin TM, Mcguire KA, Wiethoff CM.** 2011. Adenovirus Membrane Penetration Activates the NLRP3 Inflammasome. J Virol **85:**146-155.
53. **Di Paolo NC, Miao EA, Iwakura Y, Murali-Krishna K, Aderem A, Flavell RA, Papayannopoulou T, Shayakhmetov DM.** 2009. Virus binding to a plasma membrane receptor triggers interleukin-1 alpha-mediated proinflammatory macrophage response in vivo. Immunity **31:**110-121.
54. **Shayakhmetov DM, Li Z-Y, Ni S, Lieber A.** 2005. Interference with the IL-1-signaling pathway improves the toxicity profile of systemically applied adenovirus vectors. J Immunol **174:**7310-7319.
55. **Lee BH, Hwang DM, Palaniyar N, Grinstein S, Philpott DJ, Hu J.** 2012. Activation of P2X(7) receptor by ATP plays an important role in regulating inflammatory responses during acute viral infection. PloS one **7:**e35812.
56. **Philpott NJ, Nociari M, Elkon KB, Falck-Pedersen E.** 2004. Adenovirus-induced maturation of dendritic cells through a PI3 kinase-mediated TNF-alpha induction pathway. Proc Natl Acad Sci USA **101:**6200-6205.
57. **Molinier-Frenkel V, Prévost-Blondel A, Hong S-S, Lengagne R, Boudaly S, Magnusson MK, Boulanger P, Guillet J-G.** 2003. The maturation of murine dendritic cells induced by human adenovirus is mediated by the fiber knob domain. J Biol Chem **278:**37175-37182.
58. **Molinier-Frenkel V, Lengagne R, Gaden F, Hong S-S, Choppin J, Gahery-Ségard H, Boulanger P, Guillet J-G.** 2002. Adenovirus hexon protein is a potent adjuvant for activation of a cellular immune response. J Virol **76:**127-135.
59. **Morelli AE, Larregina AT, Ganster RW, Zahorchak AF, Plowey JM, Takayama T, Logar AJ, Robbins PD, Falo LD, Thomson AW.** 2000. Recombinant adenovirus induces maturation of dendritic cells via an NF-kappaB-dependent pathway. J Virol **74:**9617-9628.
60. **Hirschowitz EA, Weaver JD, Hidalgo GE, Doherty DE.** 2000. Murine dendritic cells infected with adenovirus vectors show signs of activation. Gene therapy **7:**1112-1120.
61. **Nociari M, Ocheretina O, Schoggins JW, Falck-Pedersen E.** 2007. Sensing infection by adenovirus: Toll-like receptor-independent viral DNA recognition signals activation of the interferon regulatory factor 3 master regulator. J Virol **81:**4145-4157.
62. **Fejer G, Drechsel L, Liese J, Schleicher U, Ruzsics Z, Imelli N, Greber UF, Keck S, Hildenbrand B, Krug A, Bogdan C, Freudenberg MA.** 2008. Key role of splenic myeloid DCs in the IFN-alphabeta response to adenoviruses in vivo. PLoS Pathog **4:**e1000208.
63. **Zhang Y, Chirmule N, Gao GP, Qian R, Croyle M, Joshi B, Tazelaar J, Wilson JM.** 2001. Acute cytokine response to systemic adenoviral vectors

in mice is mediated by dendritic cells and macrophages. Molecular Therapy **3:**697-707.

64. **Thiele AT, Sumpter TL, Walker JA, Xu Q, Chang C-H, Bacallao RL, Kher R, Wilkes DS.** 2006. Pulmonary immunity to viral infection: adenovirus infection of lung dendritic cells renders T cells nonresponsive to interleukin-2. J Virol **80:**1826-1836.
65. **Zhu J, Huang X, Yang Y.** 2007. Innate immune response to adenoviral vectors is mediated by both Toll-like receptor-dependent and -independent pathways. J Virol **81:**3170-3180.
66. **Iacobelli-Martinez M, Nemerow GR.** 2007. Preferential Activation of Toll-Like Receptor Nine by CD46-Utilizing Adenoviruses. J Virol **81:**1305-1312.
67. **Liu Y-J.** 2005. IPC: professional type 1 interferon-producing cells and plasmacytoid dendritic cell precursors. Annu Rev Immunol **23:**275-306.
68. **Zhang Z, Wang FS.** 2005. Plasmacytoid dendritic cells act as the most competent cell type in linking antiviral innate and adaptive immune responses. Cell Mol Immunol **2:**411-417.
69. **Kawai T, Akira S.** 2011. Toll-like receptors and their crosstalk with other innate receptors in infection and immunity. Immunity **34:**637-650.
70. **Cerullo V, Seiler MP, Mane V, Brunetti-Pierri N, Clarke C, Bertin TK, Rodgers JR, Lee B.** 2007. Toll-like receptor 9 triggers an innate immune response to helper-dependent adenoviral vectors. Molecular Therapy **15:**378-385.
71. **Boyce JT, Giddens WE, Valerio M.** 1978. Simian adenoviral pneumonia. Am J Pathol **91:**259-276.
72. **Ginsberg HS, Lundholm-Beauchamp U, Horswood RL, Pernis B, Wold WS, Chanock RM, Prince GA.** 1989. Role of early region 3 (E3) in pathogenesis of adenovirus disease. Proc Natl Acad Sci USA **86:**3823-3827.
73. **Pacini DL, Dubovi EJ, Clyde WA.** 1984. A new animal model for human respiratory tract disease due to adenovirus. J Infect Dis **150:**92-97.
74. **Booth JL, Metcalf JP.** 1999. Type-specific induction of interleukin-8 by adenovirus. Am J Respir Cell Mol Biol **21:**521-527.
75. **Booth JL, Coggeshall KM, Gordon BE, Metcalf JP.** 2004. Adenovirus type 7 induces interleukin-8 in a lung slice model and requires activation of Erk. J Virol **78:**4156-4164.
76. **Alcorn MJ, Booth JL, Coggeshall KM, Metcalf JP.** 2001. Adenovirus type 7 induces interleukin-8 production via activation of extracellular regulated kinase 1/2. J Virol **75:**6450-6459.
77. **Cotter MJ, Zaiss AK, Muruve DA.** 2005. Neutrophils Interact with Adenovirus Vectors via Fc Receptors and Complement Receptor 1. J Virol **79:**14622-14631.
78. **Mistchenko AS, Diez RA, Mariani AL, Robaldo J, Maffey AF, Bayley-Bustamante G, Grinstein S.** 1994. Cytokines in adenoviral disease in children: association of interleukin-6, interleukin-8, and tumor necrosis factor alpha levels with clinical outcome. J Pediatr **124:**714-720.

79. **Kawasaki Y, Hosoya M, Katayose M, Suzuki H.** 2002. Correlation between serum interleukin 6 and C-reactive protein concentrations in patients with adenoviral respiratory infection. Pediatr Infect Dis J **21:**370-374.
80. **Hartley J, Rowe W.** 1960. A new mouse virus apparently related to the adenovirus group. Virology **11:**645-647.
81. **Guida JD, Fejer G, Pirofski LA, Brosnan CF, Horwitz MS.** 1995. Mouse adenovirus type 1 causes a fatal hemorrhagic encephalomyelitis in adult C57BL/6 but not BALB/c mice. J Virol **69:**7674-7681.
82. **Kajon AE, Brown CC, Spindler KR.** 1998. Distribution of mouse adenovirus type 1 in intraperitoneally and intranasally infected adult outbred mice. J Virol **72:**1219-1223.
83. **Charles PC, Guida JD, Brosnan CF, Horwitz MS.** 1998. Mouse adenovirus type-1 replication is restricted to vascular endothelium in the CNS of susceptible strains of mice. Virology **245:**216-228.
84. **Kring SC, King CS, Spindler KR.** 1995. Susceptibility and signs associated with mouse adenovirus type 1 infection of adult outbred Swiss mice. J Virol **69:**8084-8088.
85. **Hashimoto K, Sugiyama T, Sasaki S.** 1966. An adenovirus isolated from the feces of mice I. Isolation and identification. Jpn J Microbiol **10:**115-125.
86. **Sugiyama T, Hashimoto K, Sasaki S.** 1967. An adenovirus isolated from the feces of mice. II. Experimental infection. Jpn J Microbiol **11:**33-42.
87. **Klempa B, Krüger DH, Auste B, Stanko M, Krawczyk A, Nickel KF, Uberla K, Stang A.** 2009. A novel cardiotropic murine adenovirus representing a distinct species of mastadenoviruses. J Virol **83:**5749-5759.
88. **Wigand R, Gelderblom H, Ozel M.** 1977. Biological and biophysical characteristics of mouse adenovirus, strain FL. Arch Virol **54:**131-142.
89. **Meissner JD, Hirsch GN, LaRue EA, Fulcher RA, Spindler KR.** 1997. Completion of the DNA sequence of mouse adenovirus type 1: sequence of E2B, L1, and L2 (18-51 map units). Virus Res **51:**53-64.
90. **Ball AO, Beard CW, Redick SD, Spindler KR.** 1989. Genome organization of mouse adenovirus type 1 early region 1: a novel transcription map. Virology **170:**523-536.
91. **Ball AO, Beard CW, Villegas P, Spindler KR.** 1991. Early region 4 sequence and biological comparison of two isolates of mouse adenovirus type 1. Virology **180:**257-265.
92. **Ball AO, Williams ME, Spindler KR.** 1988. Identification of mouse adenovirus type 1 early region 1: DNA sequence and a conserved transactivating function. J Virol **62:**3947-3957.
93. **Beard CW, Ball AO, Wooley EH, Spindler KR.** 1990. Transcription mapping of mouse adenovirus type 1 early region 3. Virology **175:**81-90.
94. **Cauthen AN, Spindler KR.** 1996. Sequence of the mouse adenovirus type-1 DNA encoding the 100-kDa, 33-kDa and DNA-binding proteins. Gene **168:**183-187.

95. **Kring SC, Ball AO, Spindler KR.** 1992. Transcription mapping of mouse adenovirus type 1 early region 4. Virology **190:**248-255.
96. **Kring SC, Spindler KR.** 1990. Sequence of mouse adenovirus type 1 DNA encoding the amino terminus of protein IVa2. Nucleic Acids Res **18:**4003.
97. **Spindler KR, Fang L, Moore ML, Hirsch GN, Brown CC, Kajon A.** 2001. SJL/J mice are highly susceptible to infection by mouse adenovirus type 1. J Virol **75:**12039-12046.
98. **Pirofski L, Horwitz MS, Scharff MD, Factor SM.** 1991. Murine adenovirus infection of SCID mice induces hepatic lesions that resemble human Reye syndrome. Proc Natl Acad Sci USA **88:**4358-4362.
99. **Wigand R.** 1980. Age and susceptibility of Swiss mice for mouse adenovirus, strain FL. Arch Virol **64:**349-357.
100. **Blailock ZR, Rabin ER, Melnick JL.** 1968. Adenovirus myocarditis in mice. An electron microscopic study. Exp Mol Pathol **9:**84-96.
101. **Heck FC, Sheldon WG, Gleiser CA.** 1972. Pathogenesis of experimentally produced mouse adenovirus infection in mice. Am J Vet Res **33:**841-846.
102. **Welton AR, Chesler EJ, Sturkie C, Jackson AU, Hirsch GN, Spindler KR.** 2005. Identification of quantitative trait loci for susceptibility to mouse adenovirus type 1. J Virol **79:**11517-11522.
103. **Hsu T-H, Althaus IW, Foreman O, Spindler KR.** 2012. Contribution of a single host genetic locus to mouse adenovirus type 1 infection and encephalitis. mBio **3**.
104. **Spindler KR, Welton AR, Lim ES, Duvvuru S, Althaus IW, Imperiale JE, Daoud AI, Chesler EJ.** 2010. The major locus for mouse adenovirus susceptibility maps to genes of the hematopoietic cell surface-expressed LY6 family. J Immunol **184:**3055-3062.
105. **Smith K, Brown CC, Spindler KR.** 1998. The role of mouse adenovirus type 1 early region 1A in acute and persistent infections in mice. J Virol **72:**5699-5706.
106. **van der Veen J, Mes A.** 1973. Experimental infection with mouse adenovirus in adult mice. Arch Gesamte Virusforsche **42:**235-241.
107. **Kajon AE, Spindler KR.** 2000. Mouse adenovirus type 1 replication in vitro is resistant to interferon. Virology **274:**213-219.
108. **Gralinski LE, Ashley SL, Dixon SD, Spindler KR.** 2009. Mouse adenovirus type 1-induced breakdown of the blood-brain barrier. J Virol **83:**9398-9410.
109. **Ashley SL, Welton AR, Harwood KM, Rooijen NV, Spindler KR.** 2009. Mouse adenovirus type 1 infection of macrophages. Virology **390:**307-314.
110. **Moore ML, Brown CC, Spindler KR.** 2003. T cells cause acute immunopathology and are required for long-term survival in mouse adenovirus type 1-induced encephalomyelitis. J Virol **77:**10060-10070.
111. **Welton AR, Gralinski LE, Spindler KR.** 2008. Mouse adenovirus type 1 infection of natural killer cell-deficient mice. Virology **373:**163-170.

112. **Moore ML, McKissic EL, Brown CC, Wilkinson JE, Spindler KR.** 2004. Fatal disseminated mouse adenovirus type 1 infection in mice lacking B cells or Bruton's tyrosine kinase. J Virol **78:**5584-5590.
113. **Weinberg JB, Stempfle GS, Wilkinson JE, Younger JG, Spindler KR.** 2005. Acute respiratory infection with mouse adenovirus type 1. Virology **340:**245-254.
114. **Procario MC, Levine RE, McCarthy MK, Kim E, Zhu L, Chang C-H, Hershenson MB, Weinberg JB.** 2012. Susceptibility to acute mouse adenovirus type 1 respiratory infection and establishment of protective immunity in neonatal mice. J Virol **86:**4194-4203.
115. **Maurer M, von Stebut E.** 2004. Macrophage inflammatory protein-1. Int J Biochem Cell Biol **36:**1882-1886.

Chapter 2:
Eicosanoids and Respiratory Viral Infection: Coordinators of Inflammation and Potential Therapeutic Targets

Abstract

Viruses are frequent causes of respiratory infection, and viral respiratory infections are significant causes of hospitalization, morbidity, and sometimes mortality in a variety of patient populations. Lung inflammation induced by infection with common respiratory pathogens such as influenza and respiratory syncytial virus is accompanied by increased lung production of prostaglandins and leukotrienes, lipid mediators with a wide range of effects on host immune function. Deficiency or pharmacologic inhibition of prostaglandin and leukotriene production often results in a dampened inflammatory response to acute infection with a respiratory virus. These mediators may therefore serve as appealing therapeutic targets for disease caused by respiratory viral infection.

Respiratory Viruses

Viruses are the most frequent cause of respiratory infection in humans. It has been estimated that viruses cause up to 90% of lower respiratory infection (LRI) hospitalizations in children less than 5 years of age and up to 40% of hospitalizations in children age 5-18 years (1). Among the most common causes of viral respiratory infection in children and adults are respiratory syncytial virus (RSV), influenza, rhinovirus (RV), adenovirus, parainfluenza virus (PIV), and

human metapneumovirus (hMPV) (2). Viral respiratory infection also causes substantial disease burden in the elderly and immunocompromised populations (3, 4).

The host immune system faces the task of effectively clearing a virus while limiting local tissue damage and inflammation. The immune response to viruses can be protective, aiding with clearance of virus from the lungs and resolution of disease caused by viral replication. Disease associated with respiratory viruses can also be caused by immune-mediated pathology. Virus-induced inflammation can be detrimental to the host, causing symptoms during acute infection and leading to damage that contributes to long-term residual lung disease. Eicosanoids are potent lipid mediators that play a role in many biological processes, including inflammation and immune function. Two classes of eicosanoids, the prostaglandins (PG) and leukotrienes (LT), have been increasingly studied in the context of respiratory viral infection. Because of these effects, eicosanoids are likely to make significant contributions to the pathogenesis of respiratory virus infection.

Eicosanoid Synthesis

Eicosanoids are generated from arachidonic acid and other related polyunsaturated fatty acids derived from phospholipid membranes. There are three major metabolic pathways for eicosanoid biosynthesis: the cyclooxygenase pathway (COX-1 and COX-2), the lipoxygenase pathway (5-LOX, 12-LOX, and 15-LOX), and the cytochrome P450 pathway. For the purposes of this review, the

discussion is limited to the role of PGE_2, the major product of the COX-1 and COX-2 pathway, and the leukotrienes, the major products of the 5-LOX pathway, during respiratory viral infection.

Prostaglandins

PGs are generated when phospholipase A_2 (PLA_2) releases arachidonic acid (AA) from membrane glycerophospholipids (Figure 2-1). Released AA is oxidized to the intermediate prostaglandin H_2 (PGH_2) by cyclooxygenase (COX). COX exists in three isoforms. COX-1 is generally constitutively expressed, while COX-2 expression is rapidly induced by growth factors and cytokines (5). COX-3 is a recently discovered isoform whose biological role, if any, remains poorly understood (6, 7). Once formed, PGH_2 can be converted by specific synthases to thromboxane A_2 (TXA_2), PGD_2, PGE_2, PGF_2, and PGI_2. As described below, PGE_2 has multiple effects on host immune function. PGE_2 is transported from the cell by multidrug resistance protein (MRP) 4 and possibly by other unknown transporters (8). The effects of PGE_2 are mediated by its signaling through four distinct G protein-coupled E prostanoid (EP) receptors, EP1-4. The EP1 receptor is coupled to an unidentified G protein and mediates PGE_2-induced increases in intracellular Ca^{2+} (9). The EP2 and EP4 receptors mediate increases in cyclic AMP (cAMP) concentration by coupling to $G\alpha_s$. Four isoforms of the EP3 receptor are coupled to different G proteins, although the major EP3 receptor signaling pathway involves adenylate cyclase inhibition via $G\alpha_i$ coupling with subsequent decreases in intracellular cAMP (10). The EP2 and EP4 receptors

are expressed in almost all mouse tissues, while expression of EP1 is restricted to several organs, including the lung. EP2 expression is the least abundant of the EP receptors, however several stimuli induce expression of EP2 (10).

Leukotrienes

LTs are also generated by liberation of AA from cell membranes (Figure 2-1). This is modified by a series of enzymes beginning with 5-lipoxygenase (5-LOX), which acts in concert with 5-LOX-activating protein (FLAP) to form leukotriene A_4 (LTA_4) (11). LTA_4 can then be metabolized by LTA_4 hydrolase to form leukotriene B_4 (LTB_4). Alternatively, LTA_4 can be conjugated to reduced glutathione by leukotriene C_4 (LTC_4) synthase to form LTC_4. LTC_4 is exported from the cell by specific transporters (12) and can be acted on by extracellular peptidases to form LTD_4 or LTE_4. Leukotrienes C_4, D_4, or E_4 are collectively known as the cysteinyl leukotrienes (cysLTs).

Expression of 5-LOX is tightly regulated and is primarily restricted to cells of the myeloid lineage, such as monocytes/macrophages, mast cells, eosinophils, and neutrophils. Although LT synthesis was once thought to be restricted to leukocytes, it has subsequently been shown that human bronchial epithelial cells and fibroblasts are capable of producing both cysLTs and LTB_4 (13, 14). In addition, the intermediate LTA_4 can be transferred from an activated donor cell to a recipient cell. LTA_4 can then be metabolized to either LTB_4 or LTC_4 by LTA_4 hydrolase or LTC_4 synthase, respectively, in a process termed

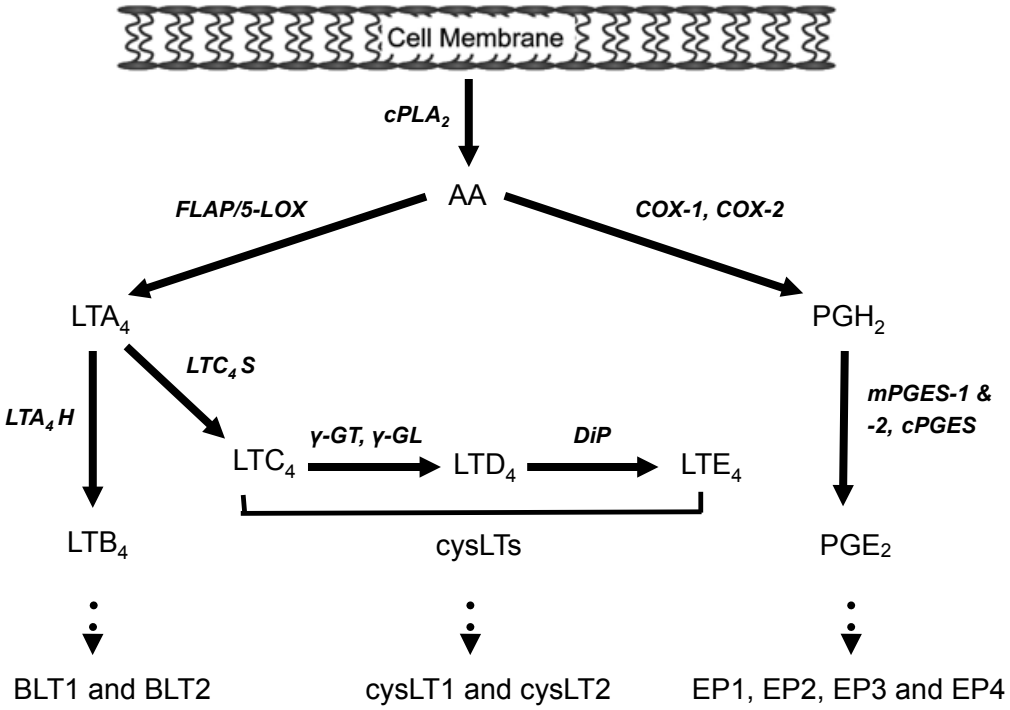

Figure 2-1. Synthesis of PGE_2 and the leukotrienes.

$cPLA_2$ – cytosolic phospholipase A_2, AA – arachidonic acid, FLAP – 5-lipoxygenase activating protein, 5-LOX – 5-lipoxygenase, LTA_4 – leukotriene A_4, LTA_4H – leukotriene A_4 hydrolase, LTB_4- leukotriene B_4, BLT1 & BLT2 – B leukotriene receptor 1 and 2, LTC_4S – leukotriene C_4 synthase, LTC_4 – leukotriene C_4, γ-GT - γ-glutamyl transpeptidase, γ-GL - γ-glutamyl leukotrienease, LTD_4 – leukotriene D_4, DiP – dipeptidase, LTE_4 – leukotriene E_4, cysLTs – cysteinyl leukotrienes, cysLT1 & cysLT2 – cysteinyl leukotriene receptor 1 and 2, COX-1 & COX-2 – cyclooxygenase 1 & 2, PGH_2 – prostaglandin H_2, mPGES-1 & -2 – microsomal prostaglandin E synthase-1 and -2, PGE_2 – prostaglandin E_2, EP1-4 – E prostanoid receptors 1-4

"transcellular biosynthesis" (15). These enzymes are expressed in most tissues. In this way, other cell types, such as epithelial cells, can become an important source of LTs during an inflammatory response.

Like PGE_2, the effects of LTs are mediated by signaling through G protein-coupled receptors. Among the receptors for cysLTs, two have been thoroughly characterized. The cysLT1 receptor binds LTD_4 with high affinity and binds LTC_4 and LTE_4 with lower affinities (16). The cysLT2 receptor binds LTC_4 and LTD_4 with equal affinity. A number of studies have alluded to the existence of additional cysLTR subtypes, although these have yet to be characterized (17). The chemoattractant and proinflammatory effects of LTB_4 are mediated by the high affinity B leukotriene receptor 1 (BLT1). A second receptor, B leukotriene receptor 2 (BLT2), binds LTB_4 with lower affinity, but its biological function remains poorly understood (18). Studies in transfected cell lines have shown that the four LT receptors can couple to both $G\alpha_i$ and $G\alpha_q$ proteins to decrease cAMP and increase intracellular Ca^{2+}, respectively (19-23). Studies in primary cells have yielded differing results and the specific signaling programs initiated by GPCRs remain to be dissected (24). Within the human lung, cysLT1 mRNA is expressed in epithelial cells, bronchial smooth muscle cells, interstitial macrophages, and the nasal mucosa. CysLT2 is expressed by bronchial smooth muscle cells, interstitial macrophages, and nasal mucosa (17). Human BLT1 is expressed primarily in leukocytes and its expression can be altered in response to various inflammatory stimuli (18, 25). BLT2 is expressed more ubiquitously,

with high mRNA expression detected in the spleen and low levels in most human tissues, including the lung (26).

Eicosanoids and Immune Function

Prostaglandin E_2

PGE_2 regulates immune function in a myriad of ways that are likely to affect viral pathogenesis (Table 2-1). Widespread expression of COX-2 has been demonstrated in airway epithelial and resident inflammatory cells in the absence of overt inflammation, suggesting a role for COX-2 in regulation of human airway homeostasis (27). High concentrations of COX products are present in the epithelial lining fluid of human airways, potentially playing a role in inhibiting lymphocyte activity and fibroblast proliferation in the absence of inflammation (28). Additionally, constitutive secretion of PGE_2 by airway epithelial cells contributes to modulation of DCs under homeostatic conditions (29). PGE_2 can promote inflammation through vasodilatory mechanisms, yielding edema, warmth, erythema, and passive leukocyte recruitment. However, PGE_2 is also capable of inhibiting neutrophil chemotaxis, phagocytosis, and bacterial killing (30, 31). PGE_2 suppresses phagocytosis by non-alveolar monocytes/macrophages (32-35), and PGE_2 inhibits alveolar macrophage (AM) phagocytosis via a mechanism that involves EP2 activation and increases in cAMP (36). Bacterial killing and reactive oxygen intermediate generation by AMs is also inhibited by PGE_2 in an EP2/EP4- and cAMP-dependent manner (37).

The production of various pro-inflammatory cytokines and chemokines is inhibited in the presence of PGE_2 (38, 39), while production of the anti-inflammatory cytokine interleukin (IL)-10 is enhanced (40). PGE_2 suppresses production of the Th1 cytokines interferon (IFN)-γ and IL-12, leading to a Th2-polarized environment (41, 42). However, a number of studies have also reported PGE_2-mediated enhancement of Th1 cytokine secretion and differentiation *in vivo* (43, 44). The role of PGE_2 is not strictly suppressive, as it has been shown to promote certain pathways in immune differentiation. For example, PGE_2 can act on uncommitted B lymphocytes to promote isotype switching to IgE or IgG1 (45-47). COX inhibitors inhibit antibody production in activated human B lymphocytes (48, 49). PGE_2 augments IL-17 production and Th17 differentiation by increasing IL-23 production in T cells and dendritic cells (44, 50-53), an activity that likely occurs via EP2- and EP4-mediated increases in cAMP (54, 55). Additionally, PGE_2 enhances the production of the proinflammatory cytokine IL-6 by leukocytes (56) and airway epithelial cells (57). PGE_2 potently inhibits the production of a number of antimicrobial peptides (AMPs) such as human β-defensin by epithelial cells (58). This effect of PGE_2 is likely to be relevant for viral pathogenesis, because AMPs can inhibit the replication of viruses (59, 60).

Leukotrienes

The diverse effects of LTs on innate immunity have been reviewed elsewhere (61) and are briefly summarized in Table 2-1. LTB_4 promotes neutrophil migration and survival (62, 63) and enhances neutrophil granule

enzyme secretion (64) and superoxide anion generation (65, 66). T lymphocyte recruitment to sites of inflammation can be induced by LTB_4 (67-70). In addition to neutrophil and T cell trafficking, LTB_4 can promote the migration of dendritic cells (DCs) *in vitro* (71) and to draining lymph nodes as mice deficient in BLT1/2 show reduced DC migration (72). Both cysLTs and LTB_4 can enhance Fcγ receptor-mediated phagocytosis by AMs, though by different mechanisms (24, 73, 74). LTB_4 induces antimicrobial peptide release from neutrophils *in vivo,* in some cases inhibiting viral replication (75-77). Lung generation of the proinflammatory cytokine TNF-α is enhanced by LTB_4 (78). A number of studies have reported that LTB_4 acts synergistically with IL-4 to induce activation, proliferation, and differentiation of human B lymphocytes (79-81), although a separate study reported that 5-LOX inhibitors actually enhanced B lymphocyte proliferation (82).

CysLTs can promote microvascular leak (11), enhance leukocyte survival (83, 84), and induce nitric oxide (NO) generation in neutrophils (85, 86). CysLTs induce DC chemotaxis to CCL19 and DC trafficking to lymph nodes is impaired in LTC_4 transporter-deficient mice (87). In addition, cysLTs have been suggested to play a role in allergen-induced DC migration from blood (88). Addition of LTD_4 to activated B lymphocytes leads to a modest upregulation of IgE and IgG production (89). CysLTs also play a role in regulation of a pulmonary Th2 response as mice deficient in LTC_4 synthase showed reduced Th2 cytokine mRNA expression and Ag-specific IgE and IgG1 in the lung (90). CysLTs are recognized as important mediators in the pathogenesis of asthma by their ability

Table 2-1. Effects of PGE_2 and Leukotrienes on Immune Function

	PGE_2	***LTB_4***	***cysLTs***
Neutrophils	• Inhibits neutrophil chemotaxis, phagocytosis, and bacterial killing	• Promotes neutrophil chemotaxis, ROS generation, and survival	• Induces NO generation in neutrophils
Macrophages	• Inhibits AM phagocytosis, ROS generation, and bacterial killing	• Enhances AM phagocytosis	• Enhance AM phagocytosis
T cells	• Promotes Th17 differentiation	• Induces T cell recruitment	• Enhances Th2 response
B cells/Antibody Production	• Promotes isotype switching to IgE and IgG1	• Induces activation, differentiation, and proliferation of B cells	• Upregulate IgE and IgG1 production by B cells
Dendritic Cells	• Varies	• Promotes DC migration	• Promotes DC migration
Cytokines	• Suppresses IFN-γ and IL-12 production • Enhances IL-10 and IL-6 production	• Enhances TNF-α production	• Enhances IL-5, IL-13, and eotaxin expression
Antimicrobial Peptides	• Inhibits AMP production by epithelial cells	• Induces AMP production by neutrophils	• Unknown

to promote airway microvascular permeability, mucus secretion and smooth muscle contraction (91-95). The prostaglandins and leukotrienes modulate many host immune responses that are important contributors to viral pathogenesis, such as cytokine signaling, neutrophil and macrophage phagocytosis, trafficking and activation of DCs and T cells, and antibody production by B cells.

Eicosanoids and Respiratory Viruses

Influenza

Influenza infections account for over 200,000 hospitalizations annually in the US (96). In addition to hospitalizations, influenza is also associated with a substantial number of outpatient visits each year, causing considerable healthcare burden and economic costs. Influenza upregulates COX-2 expression both *in vitro* and *in vivo,* and it has been suggested that COX hyperinduction contributes to the exaggerated cytokine response observed in severe human H5N1 infections (97-99). Alteration of the COX pathway has contrasting effects on inflammatory responses to influenza virus depending on the model of pharmacologic inhibition (COX-1- or COX-2-specific or dual inhibition) or of genetic deficiency. Treatment of influenza-infected mice with celecoxib, a selective COX-2 inhibitor, did not significantly affect viral titers or disease severity, although treatment did suppress production in the lung of the proinflammatory cytokines tumor necrosis factor (TNF)-α, IL-6 and granulocyte-colony stimulating factor (G-CSF) (100). In contrast, influenza infection of mice

genetically deficient in COX-2 resulted in reduced mortality, inflammation and cytokine responses compared to infection of wild-type control (101). Peak lung viral titers were significantly elevated in COX-$2^{-/-}$ mice but returned to levels seen in wild-type mice by day 6, suggesting a role for COX-2 in controlling early viral replication but not in virus clearance. Interestingly, levels of PGE_2 in influenza-infected COX-$2^{-/-}$ mice were equivalent to levels measured in infected wild-type mice. The lack of PGE_2 deficiency in COX-$2^{-/-}$ mice could be due to compensatory upregulation of COX-1 activity, as has been described before (102).

Mice infected with highly virulent H5N1 and treated with a combination of celecoxib, the neuraminidase inhibitor zanamivir, and mesalazine (an aminosalicylate drug that exhibits weak 5-LOX and COX inhibition (103)) showed significantly improved survival even when treatment was delayed 48 hours (104). The beneficial effect of celecoxib and mesalazine likely stemmed from their effects on immunopathology, as mice treated with triple therapy had similar viral loads as those treated with zanamivir alone. Triple therapy significantly reduced levels of the proinflammatory cytokines IL-6, TNF-α and IFN-γ.

Another group treated influenza-infected mice with paracetamol (acetominophen), a selective inhibitor of COX-2 (105, 106), although it does exhibit some inhibitory activity toward heme oxidases, such as myeloperoxidase (107). Paracetamol-treated mice had improved lung function and reduced immunopathology compared to control mice. A separate group of mice treated with celecoxib also showed improvements in cellular infiltrates, lung function and

pathology. However, the degree of improvement was generally less than that seen in paracetamol-treated mice. In contrast to mice genetically deficient in COX-2 (101), paracetamol- and celecoxib-treated mice had viral loads equivalent to those in untreated control mice. Virus-specific $CD4^+$ and $CD8^+$ T cell numbers were not altered in treated mice, and treatment with paracetamol or celecoxib did not interfere with the establishment of protective immunity to a second infection with a different influenza subtype.

The significantly increased viral titers seen in COX-$2^{-/-}$ mice but not observed in mice treated with COX-2 inhibitors could be due to a functional defect in innate immunity, as COX products are known to be involved in modulating the innate immune response (108). In addition, COX-$2^{-/-}$ mice have a complete loss of COX-2 activity, whereas mice treated with inhibitors still retain some COX-2 activity due to insufficient inhibition by the drug. COX-$2^{-/-}$ mice had levels of PGE_2 in bronchoalveolar lavage (BAL) fluid similar to wild-type mice, suggesting that the effects of COX-2 deficiency in this model may not be due to lack of PGE_2. As COX-$2^{-/-}$ deficiency is likely to affect the production of other prostaglandins (such as TXA_2, PGD_2, PGF_2, and PGI_2), it is possible that decreased levels of one of the other COX products are responsible for increased survival.

Influenza infection upregulates 5-LOX expression and/or levels of LTs in cell lines as well as in lungs of infected mice and humans (109-111). However, few studies have examined influenza infection in the context of altered 5-LOX production (either due to genetic deficiency or pharmacologic inhibition). One

study has reported a beneficial effect of exogenous LTB_4 administration during influenza infection of mice (75). Mice treated daily with LTB_4 had significantly reduced lung viral loads. The lungs of LTB_4-treated mice showed increased levels of multiple antimicrobial peptides, decreased inflammatory cell infiltration, and partially restored lung architecture. The antiviral effect of LTB_4 was mediated by neutrophils and the high affinity BLT1 receptor, as viral loads were unaffected in neutrophil-depleted or BLT1-deficient mice. LTB_4 treatment of primary human neutrophils in this study induced antimicrobial peptide release and decreased influenza titers, demonstrating that the effects of LTB_4 on neutrophils are similar in both mice and humans. This is in agreement with another study, in which human neutrophils treated with LTB_4 showed significantly more myeloperoxidase (MPO) activity and α-defensin production than untreated cells, and LTB_4-treated neutrophils had enhanced virucidal activity against influenza virus, human coronavirus, and RSV (112). The role of cysLTs during influenza infection has yet to be defined in detail. Enhanced levels of cysLTs seen in COX-$2^{-/-}$ mice infected with influenza are associated with increased survival (101), but whether the decreased mortality in COX-2 deficient mice is directly due to cysLTs in this model is unknown. High levels of proinflammatory 5-LOX mediators, particularly the cysLT LTE_4, are tightly correlated with the highly pathogenic phase of sublethal influenza infection in mice (113). Similarly, in nasopharyngeal lavage fluid collected from patients during the 2009-2011 influenza seasons, increasing levels of 5-LOX-derived mediators (LTB_4 and the cysLT LTE_4) and decreasing

levels of 12-LOX-derived mediators correlated with increasing clinical symptoms and immune response (113).

The beneficial effects of COX-2 deficiency may also be due to shunting of released AA to the 5-LOX pathway. A number of reports suggest that COX inhibitors enhance production of LTs (114, 115). Indeed, COX-$2^{-/-}$ mice showed higher BAL fluid levels of cysLTs than wild-type mice following infection with influenza. However, in mice treated with a combination of zanamivir, celecoxib, and mesalazine, increased survival was associated with lower LT levels and higher PGE_2 levels in the treated mice compared to wild-type. The discrepancies in COX and 5-LOX products in these models may reflect the different pathophysiology of the influenza strains used. Perhaps increased LT production during severe H5N1 infection promotes inflammation and local tissue damage, while PGE_2 provides a balancing protective influence. In contrast, during infection with the less virulent H3N2 virus, enhanced LT production may contribute to virus clearance without a detrimental effect on host inflammation. However, in the case of either virus lower levels of the proinflammatory cytokines IL-6, TNF-α and IFN-γ were correlated with decreased morbidity and increased survival. Other differences in the studies could be accounted for by differences in virus subtype, virus inoculum, mouse strain, or drug dose and delivery method. However, partial COX inhibition by pharmacologic intervention appears to be beneficial in reducing immunopathology while still controlling viral replication during influenza infection in mice.

Respiratory Syncytial Virus

Respiratory syncytial virus (RSV) is the leading cause of bronchiolitis and pneumonia in infants (116, 117). RSV is also a significant pathogen in the elderly population, particularly those living in long-term care facilities or with underlying cardiopulmonary disease (118). The immunocompromised are at risk for severe RSV infection, with mortality rates of up to 80% reported for RSV pneumonia (119). RSV induces PGE_2 release *in vitro,* in animal models, and in lungs of infants with RSV bronchiolitis (120-123). Treatment with COX inhibitors reduces RSV replication *in vitro* and diminishes immunopathology *in vivo.* Blocking PG production with NS-398, celecoxib, or the $cPLA_2$ inhibitor pyrrophenone reduced virus particle production in the A549 airway epithelial cell line (120). COX inhibition also reduced transcription and production of the proinflammatory cytokines IL-8 and RANTES (CCL5). RSV-induced activation of interferon regulatory factor (IRF) and NF-κB activation was suppressed by a high concentration of celecoxib. Another study demonstrated that the nonselective COX inhibitor indomethacin decreased lung histopathology in RSV-infected cotton rats, but COX inhibition did not significantly affect viral replication (121).

RSV also induces production of LTB_4 and cysLTs in both animal models and infants afflicted with RSV bronchiolitis (123-129). LT concentrations during RSV infection have been correlated with development of symptoms and in some reports are associated with disease severity (110, 126, 130, 131). Treatment of RSV-infected mice with the 5-LOX inhibitor zileuton reduced inflammatory cell numbers in the lung, prevented RSV-induced weight loss, and decreased RSV-

induced airway constriction (126). Viral titers were somewhat lower in the lungs of zileuton-treated mice, although the difference was not statistically significant. Even when administered after the emergence of respiratory symptoms, zileuton reduced airway resistance and weight loss compared to untreated mice. Treatment with the cysLTR1 antagonist MK-571 decreased RSV-induced airway hyperreactivity (AHR) (125). In contrast to treatment with zileuton, MK-571 did not affect inflammatory cell recruitment or production of IL-4 and IFN-γ in RSV-infected mice. A possible effect of MK-571 on viral titers was not examined in this study.

Similar to highly virulent influenza H5N1, successful treatment of RSV infection may require the use of an antiviral agent in combination with an anti-inflammatory agent that limits immunopathology. In support of this, treatment of RSV-infected cotton rats with the RSV-specific humanized monoclonal antibody palivizumab and a glucocorticoid resulted in enhanced clearance of RSV and limited lung histopathology compared to controls (132). Further support comes from a model of pneumonia virus of mice (PVM), a paramyxovirus that is a close phylogenetic relative of RSV. PVM infection increased levels of cysLTs in the lung (133). In this model, administration of either the cysLT1 antagonist montelukast or the nucleoside analog ribavirin did not affect disease severity. However, combined therapy of montelukast with ribavirin substantially decreased morbidity and mortality of PVM-infected mice.

Administration of montelukast during primary RSV infection prevented enhanced AHR, airway eosinophil recruitment, and mucus overproduction upon

reinfection (124). Montelukast administered only during secondary infection did not affect this enhanced response. Previous studies have shown that LTs are only transiently elevated during the acute phase of infection and that levels drop to baseline shortly after (134). This suggests that LT inhibitors may have a beneficial effect during the early phase of infection but may no longer be useful as treatment for the long-term airway dysfunction observed post-RSV infection when LT levels are no longer elevated.

The above reports demonstrate a beneficial effect of 5-LOX product inhibitors or cysLT1 receptor antagonists during primary infection with RSV. However, the studies in animal models used pharmacologic agents given to mice starting on the day before infection, whereas treatment in humans is typically initiated later during the course of infection after the emergence of symptoms. Delaying zileuton treatment until 3 days post infection, after respiratory symptoms emerged, still reduced clinical signs during primary RSV infection in mice. However, there have been conflicting results when 5-LOX inhibitors and cysLT antagonists were used as treatment in children with RSV bronchiolitis. One study suggested a beneficial effect of the cysLTR1 antagonist montelukast on lung symptoms post-RSV bronchiolitis (135), but further studies have failed to corroborate these findings (136-138). To our knowledge, there are no human studies that examine prophylactic administration of 5-LOX pathway inhibitors or receptor antagonists to high-risk children. Further studies are needed to define the role of LT inhibitors in patients with primary RSV infection and in those experiencing persistent airway dysfunction post-RSV.

While many viruses are capable of causing respiratory infections, relatively little is known about the contributions made by eicosanoids to the pathogenesis of respiratory viruses other than influenza and RSV. Rhinovirus (RV) infection increases expression of 5-LOX, FLAP, and COX-2 in human bronchial cells (139). In addition, cysLT levels in BAL fluid are increased upon rhinovirus infection in humans and correlate with emergence of upper respiratory symptoms (110, 139). Adenovirus induces COX-2 expression and PGE_2 release in murine fibroblasts (140) and in human primary synovial fibroblasts (141). Additional studies are necessary to examine adenovirus-induced PG production in lung-relevant cell types, but in vivo studies of human adenovirus pathogenesis are limited by the strict species specificity of adenoviruses. Using mouse adenovirus type 1 to study the pathogenesis of adenovirus respiratory infection (142) will provide a useful tool to define the roles of eicosanoids to adenovirus respiratory infection.

Human cytomegalovirus (HCMV) can also cause respiratory infections, although symptomatic disease is uncommon in immunocompetent individuals (143). HCMV induces 5-LOX expression and LTB_4 production (144) in vascular smooth muscle cells as well as COX-2 expression and PGE_2 production in fibroblasts (145). COX-2 inhibition reduces levels of the immediate-early 2 mRNA and protein in addition to viral DNA replication and transcription of some early and late mRNAs. Treatment of HCMV-infected fibroblasts with COX inhibitors inhibits cell-to-cell spread of virus (146). Of note, while many reports with other viruses have shown inhibition of viral replication or gene transcription by COX

inhibitors at non-physiologic concentrations, these results with HCMV were obtained with concentrations of COX inhibitors that are achievable in human plasma. Although few studies have examined the effect of 5-LOX products on HCMV pathogenesis, one study reported that exogenous LTB_4 inhibited reactivation of CMV following allogeneic bone marrow transplantation (BMT) in mice, demonstrating a beneficial effect for this LT (147).

Common Themes

From the data summarized above, it is clear that the effect of COX or 5-LOX inhibition or antagonism of cysLT receptors on host responses to respiratory viral infection is variable and in some cases may be pathogen- and/or model-specific (Table 2-2). In general, COX inhibition or deficiency is associated with less exuberant inflammation and in some cases improved survival. COX products may play a role in controlling early viral replication, although this possible role is only evident for influenza infection in mice completely lacking COX-2 activity and not in mice treated with a COX-2 inhibitor. These data are consistent with the role of PGE_2 as an immunomodulatory mediator, balancing pro-inflammatory actions with suppressive effects on innate and adaptive immune function. Inhibition of LT production or signaling during respiratory viral infection is associated with less inflammation accompanied by variable (but generally beneficial) effects on lung physiology. However, administration of exogenous LTB_4 also blunted inflammatory responses to influenza virus in one

Table 2-2. Effects of PGE_2 and Leukotrienes on Respiratory Syncytial Virus and Influenza Infection

	PGE_2		*Leukotrienes*
	COX Inhibition	**COX-2 Deficiency**	
RSV	• Reduction in viral replication *in vitro* • Suppression of virus-induced cytokine production *in vitro* • No effect on viral replication in the lungs *in vivo* • Decreased lung pathology *in vivo*		• Reduction in pulmonary inflammatory, weight loss, and RSV-induced airway constriction in mice treated with 5-LO inhibitor • CysLTR1 antagonism during primary infection prevents enhanced AHR upon reinfection • Decreased RSV-induced AHR but no effect on cytokine production in mice treated with cysLTR1 antagonist
Influenza	• No effect on viral replication or disease severity in mice treated with celecoxib • Suppression of virus-induced cytokine production in mice treated with celecoxib • Improved survival and reduced proinflammatory cytokine levels in mice treated with zanamivir, celecoxib, and mesalazine • Improved lung function and reduced immunopathology in mice treated with paracetamol	• Decreased mortality, pulmonary inflammation and cytokine responses in COX-$2^{-/-}$ mice • Increased viral titers in lungs of COX-$2^{-/-}$ mice compared to controls	• Reduced lung viral loads and decreased pulmonary inflammatory in mice treated with exogenous LTB_4

study (75), suggesting that various 5-LOX products may be differentially involved in promoting inflammation and affecting host immune responses to viral infection.

Therapeutic Implications

Respiratory viral infections cause substantial disease and are associated with significant morbidity, mortality, and healthcare utilization. Many antiviral drugs are available to treat infection with human immunodeficiency virus, and a smaller number of drugs such as acyclovir and ganciclovir are available to treat infections with herpesviruses such as herpes simplex virus, varicella zoster virus, and HCMV. In contrast, far fewer drugs are available to treat viruses that most frequently cause respiratory infections. Neuraminidase inhibitors such as oseltamivir and zanamavir can be used as prophylaxis to prevent infection by influenza virus or used to treat infection. Older drugs such as amantadine and rimantadine can also be used to prevent or treat influenza. However, the emergence of drug-resistant influenza strains has the potential to increasingly limit the utility of these drugs. The nucleoside analog cidofovir has been used to treat adenovirus infections, although it has substantial toxicities and no randomized clinical trials have been performed to show clinical benefit. Currently, there are no drugs that have consistently been shown to be safe and effective for the treatment of disease caused by infection with RSV, rhinovirus, human metapneumovirus, or other viruses that commonly cause respiratory infections.

Preventing virus-induced inflammation may serve as an important adjunct to any antiviral therapy. When antiviral drugs are not available, modulation of

virus-induced inflammation by itself may serve as an effective strategy to treat disease caused by viruses. Drugs with the ability to modulate eicosanoid production, such as ibuprofen and acetaminophen, are already frequently used in patients with respiratory infections to alleviate fevers, myalgias, and nonspecific symptoms. Studies described above that show decreased virus-induced inflammation and increased survival in animals treated with an inhibitor of PG or LT synthesis or in PG- or LT-deficient animals support the potential benefit of this approach. Drugs that modulate eicosanoid production may be particularly useful to prevent or treat infections in patients with exaggerated eicosanoid production at baseline. For instance, exaggerated PGE_2 production in the setting of bone marrow transplantation has been associated with increased susceptibility to bacterial infection that is linked to impaired neutrophil and macrophage phagocytosis and killing (148, 149). Increased PGE_2 production has been reported in humans with a variety of disease states including cancer (150), aging (151), HIV infection (152), malnutrition (153, 154), and stem cell and solid organ transplant recipients (155, 156), making the potential benefits of this approach more widespread.

Any therapy that involves modulation of eicosanoid production must consider the potential for deleterious effects on the development of adaptive immunity and subsequent protection from secondary infection. PGE_2 plays an important role in optimal antibody synthesis, as COX inhibitors reduce antibody production in activated human B lymphocytes (48, 49). In addition, mice genetically deficient in COX-2 produce significantly less IgM and IgG than wild-

type mice (48). There is evidence that COX-2 plays a role in potentiating antibody production in humans as well. Human volunteers challenged with RV showed increased nasal symptoms and a suppressed serum neutralizing antibody response when treated with aspirin or acetaminophen, suggesting a protective role for COX products in reducing symptoms and promoting an antibody response (157). One large-scale study has been performed in which children were administered prophylactic paracetamol when receiving routine childhood vaccinations (158). Antibody responses to several of the vaccine antigens were less robust in patients receiving prophylactic paracetamol. Evidence also exists that LTs, like PGE_2, promote appropriate antibody responses (79-81, 89), but the effect of 5-LOX inhibitors and receptor antagonists on antibody production has not yet been described.

Conclusions

Eicosanoids modulate many host immune responses that are important contributors to viral pathogenesis. It will be essential to better define mechanisms underlying the effects of eicosanoids on both innate and adaptive immune responses to respiratory viral infection in order to develop therapies with maximal anti-inflammatory benefit and minimal impact on protective immune responses. For instance, the use of specific receptor agonists or antagonists may eventually provide a better-tailored approach than inhibitors of PG or LT synthesis to treat patients with respiratory viral infections. In general terms, however, alteration of

eicosanoid production or antagonism of eicosanoid receptors has the potential to serve as a useful treatment strategy for respiratory viral infections.

References

1. **Henrickson KJ, Hoover S, Kehl KS, Hua W.** 2004. National disease burden of respiratory viruses detected in children by polymerase chain reaction. Pediatr Infect Dis J **23:**S11-18.
2. **Pavia AT.** 2011. Viral infections of the lower respiratory tract: old viruses, new viruses, and the role of diagnosis. Clin Infect Dis **52 Suppl 4:**S284-289.
3. **Greenberg SB.** 2002. Viral respiratory infections in elderly patients and patients with chronic obstructive pulmonary disease. Am J Med **112 Suppl 6A:**28S-32S.
4. **Nichols WG, Peck Campbell AJ, Boeckh M.** 2008. Respiratory viruses other than influenza virus: impact and therapeutic advances. Clin Microbiol Rev **21:**274-290, table of contents.
5. **Funk CD.** 2001. Prostaglandins and leukotrienes: advances in eicosanoid biology. Science **294:**1871-1875.
6. **Chandrasekharan NV, Dai H, Roos KLT, Evanson NK, Tomsik J, Elton TS, Simmons DL.** 2002. COX-3, a cyclooxygenase-1 variant inhibited by acetaminophen and other analgesic/antipyretic drugs: cloning, structure, and expression. Proc Natl Acad Sci USA **99:**13926-13931.
7. **Kis B, Snipes JA, Busija DW.** 2005. Acetaminophen and the cyclooxygenase-3 puzzle: sorting out facts, fictions, and uncertainties. J Pharmacol Exp Ther **315:**1-7.
8. **Reid G, Wielinga P, Zelcer N, van der Heijden I, Kuil A, de Haas M, Wijnholds J, Borst P.** 2003. The human multidrug resistance protein MRP4 functions as a prostaglandin efflux transporter and is inhibited by nonsteroidal antiinflammatory drugs. Proc Natl Acad Sci USA **100:**9244-9249.
9. **Watabe A, Sugimoto Y, Honda A, Irie A, Namba T, Negishi M, Ito S, Narumiya S, Ichikawa A.** 1993. Cloning and expression of cDNA for a mouse EP1 subtype of prostaglandin E receptor. J Biol Chem **268:**20175-20178.
10. **Narumiya S, Sugimoto Y, Ushikubi F.** 1999. Prostanoid receptors: structures, properties, and functions. Physiol Rev **79:**1193-1226.
11. **Okunishi K, Peters-Golden M.** 2011. Leukotrienes and airway inflammation. Biochimica et biophysica acta.
12. **Robbiani DF, Finch RA, Jäger D, Muller WA, Sartorelli AC, Randolph GJ.** 2000. The leukotriene C(4) transporter MRP1 regulates CCL19 (MIP-3beta, ELC)-dependent mobilization of dendritic cells to lymph nodes. Cell **103:**757-768.
13. **Jame AJ, Lackie PM, Cazaly AM, Sayers I, Penrose JF, Holgate ST, Sampson AP.** 2007. Human bronchial epithelial cells express an active and inducible biosynthetic pathway for leukotrienes B4 and C4. Clin Exp Allergy **37:**880-892.

14. **James AJ, Penrose JF, Cazaly AM, Holgate ST, Sampson AP.** 2006. Human bronchial fibroblasts express the 5-lipoxygenase pathway. Respir Res **7:**102.
15. **Sala A, Folco G, Murphy RC.** 2010. Transcellular biosynthesis of eicosanoids. Pharmacol Rep **62:**503-510.
16. **Kanaoka Y, Boyce JA.** 2004. Cysteinyl leukotrienes and their receptors: cellular distribution and function in immune and inflammatory responses. J Immunol **173:**1503-1510.
17. **Capra V, Thompson MD, Sala A, Cole DE, Folco G, Rovati GE.** 2007. Cysteinyl-leukotrienes and their receptors in asthma and other inflammatory diseases: critical update and emerging trends. Med Res Rev **27:**469-527.
18. **Tager AM, Luster AD.** 2003. BLT1 and BLT2: the leukotriene B(4) receptors. Prostaglandins Leukot Essent Fatty Acids **69:**123-134.
19. **Lynch KR, O'Neill GP, Liu Q, Im DS, Sawyer N, Metters KM, Coulombe N, Abramovitz M, Figueroa DJ, Zeng Z, Connolly BM, Bai C, Austin CP, Chateauneuf A, Stocco R, Greig GM, Kargman S, Hooks SB, Hosfield E, Williams DL, Ford-Hutchinson AW, Caskey CT, Evans JF.** 1999. Characterization of the human cysteinyl leukotriene CysLT1 receptor. Nature **399:**789-793.
20. **Yokomizo T, Izumi T, Chang K, Takuwa Y, Shimizu T.** 1997. A G-protein-coupled receptor for leukotriene B4 that mediates chemotaxis. Nature **387:**620-624.
21. **Sarau HM, Ames RS, Chambers J, Ellis C, Elshourbagy N, Foley JJ, Schmidt DB, Muccitelli RM, Jenkins O, Murdock PR, Herrity NC, Halsey W, Sathe G, Muir AI, Nuthulaganti P, Dytko GM, Buckley PT, Wilson S, Bergsma DJ, Hay DW.** 1999. Identification, molecular cloning, expression, and characterization of a cysteinyl leukotriene receptor. Mol Pharmacol **56:**657-663.
22. **Pollock K, Creba J.** 1990. Leukotriene D4 induced calcium changes in U937 cells may utilize mechanisms additional to inositol phosphate production that are pertussis toxin insensitive but are blocked by phorbol myristate acetate. Cell Signal **2:**563-568.
23. **Crooke ST, Mattern M, Sarau HM, Winkler JD, Balcarek J, Wong A, Bennett CF.** 1989. The signal transduction system of the leukotriene D4 receptor. Trends Pharmacol Sci **10:**103-107.
24. **Peres CM, Aronoff DM, Serezani CH, Flamand N, Faccioli LH, Peters-Golden M.** 2007. Specific leukotriene receptors couple to distinct G proteins to effect stimulation of alveolar macrophage host defense functions. J Immunol **179:**5454-5461.
25. **Pettersson A, Sabirsh A, Bristulf J, Kidd-Ljunggren K, Ljungberg B, Owman C, Karlsson U.** 2005. Pro- and anti-inflammatory substances modulate expression of the leukotriene B4 receptor, BLT1, in human monocytes. J Leukoc Biol **77:**1018-1025.

26. **Yokomizo T, Kato K, Terawaki K, Izumi T, Shimizu T.** 2000. A second leukotriene B(4) receptor, BLT2. A new therapeutic target in inflammation and immunological disorders. J Exp Med **192:**421-432.
27. **Watkins DN, Peroni DJ, Lenzo JC, Knight DA, Garlepp MJ, Thompson PJ.** 1999. Expression and localization of COX-2 in human airways and cultured airway epithelial cells. Eur Respir J **13:**999-1007.
28. **Ozaki T, Rennard SI, Crystal RG.** 1987. Cyclooxygenase metabolites are compartmentalized in the human lower respiratory tract. J Appl Physiol **62:**219-222.
29. **Schmidt LM, Belvisi MG, Bode KA, Bauer J, Schmidt C, Suchy M-T, Tsikas D, Scheuerer J, Lasitschka F, Gröne H-J, Dalpke AH.** 2011. Bronchial epithelial cell-derived prostaglandin E2 dampens the reactivity of dendritic cells. J Immunol **186:**2095-2105.
30. **Aronoff DM, Canetti C, Serezani CH, Luo M, Peters-Golden M.** 2005. Cutting edge: macrophage inhibition by cyclic AMP (cAMP): differential roles of protein kinase A and exchange protein directly activated by cAMP-1. J Immunol **174:**595-599.
31. **Armstrong RA.** 1995. Investigation of the inhibitory effects of PGE2 and selective EP agonists on chemotaxis of human neutrophils. British Journal of Pharmacology **116:**2903-2908.
32. **Oropeza-Rendon RL, Speth V, Hiller G, Weber K, Fischer H.** 1979. Prostaglandin E1 reversibly induces morphological changes in macrophages and inhibits phagocytosis. Exp Cell Res **119:**365-371.
33. **Fernández-Repollet E, Mittler RS, Tiffany S, Schwartz A.** 1982. In vivo effects of prostaglandin E2 and arachidonic acid on phagocytosis of fluorescent methacrylate microbeads by rat peritoneal macrophages. J Histochem Cytochem **30:**466-470.
34. **Davidson J, Kerr A, Guy K, Rotondo D.** 1998. Prostaglandin and fatty acid modulation of Escherichia coli O157 phagocytosis by human monocytic cells. Immunology **94:**228-234.
35. **Canning BJ, Hmieleski RR, Spannhake EW, Jakab GJ.** 1991. Ozone reduces murine alveolar and peritoneal macrophage phagocytosis: the role of prostanoids. Am J Physiol **261:**L277-282.
36. **Aronoff DM, Canetti C, Peters-Golden M.** 2004. Prostaglandin E2 inhibits alveolar macrophage phagocytosis through an E-prostanoid 2 receptor-mediated increase in intracellular cyclic AMP. J Immunol **173:**559-565.
37. **Serezani CH, Chung J, Ballinger MN, Moore BB, Aronoff DM, Peters-Golden M.** 2007. Prostaglandin E2 suppresses bacterial killing in alveolar macrophages by inhibiting NADPH oxidase, p. 562-570, Am J Respir Cell Mol Biol, vol. 37.
38. **Aronoff DM, Carstens JK, Chen G-H, Toews GB, Peters-Golden M.** 2006. Short communication: differences between macrophages and dendritic cells in the cyclic AMP-dependent regulation of lipopolysaccharide-induced cytokine and chemokine synthesis. J Interferon Cytokine Res **26:**827-833.

39. **Kunkel SL, Spengler M, May MA, Spengler R, Larrick J, Remick D.** 1988. Prostaglandin E2 regulates macrophage-derived tumor necrosis factor gene expression. J Biol Chem **263:**5380-5384.
40. **Harizi H, Juzan M, Pitard V, Moreau J-F, Gualde N.** 2002. Cyclooxygenase-2-issued prostaglandin e(2) enhances the production of endogenous IL-10, which down-regulates dendritic cell functions. J Immunol **168:**2255-2263.
41. **Betz M, Fox BS.** 1991. Prostaglandin E2 inhibits production of Th1 lymphokines but not of Th2 lymphokines. J Immunol **146:**108-113.
42. **Snijdewint FG, Kaliński P, Wierenga EA, Bos JD, Kapsenberg ML.** 1993. Prostaglandin E2 differentially modulates cytokine secretion profiles of human T helper lymphocytes. J Immunol **150:**5321-5329.
43. **Bloom D, Jabrane-Ferrat N, Zeng L, Wu A, Li L, Lo D, Turck CW, An S, Goetzl EJ.** 1999. Prostaglandin E2 enhancement of interferon-gamma production by antigen-stimulated type 1 helper T cells. Cell Immunol **194:**21-27.
44. **Yao C, Sakata D, Esaki Y, Li Y, Matsuoka T, Kuroiwa K, Sugimoto Y, Narumiya S.** 2009. Prostaglandin E2-EP4 signaling promotes immune inflammation through Th1 cell differentiation and Th17 cell expansion. Nat Med **15:**633-640.
45. **Roper RL, Brown DM, Phipps RP.** 1995. Prostaglandin E2 promotes B lymphocyte Ig isotype switching to IgE. J Immunol **154:**162-170.
46. **Fedyk ER, Phipps RP.** 1996. Prostaglandin E2 receptors of the EP2 and EP4 subtypes regulate activation and differentiation of mouse B lymphocytes to IgE-secreting cells. Proc Natl Acad Sci USA **93:**10978-10983.
47. **Roper RL, Graf B, Phipps RP.** 2002. Prostaglandin E2 and cAMP promote B lymphocyte class switching to IgG1. Immunol Lett **84:**191-198.
48. **Ryan EP, Pollock SJ, Pollack SJ, Murant TI, Bernstein SH, Felgar RE, Phipps RP.** 2005. Activated human B lymphocytes express cyclooxygenase-2 and cyclooxygenase inhibitors attenuate antibody production. J Immunol **174:**2619-2626.
49. **Bancos S, Bernard MP, Topham DJ, Phipps RP.** 2009. Ibuprofen and other widely used non-steroidal anti-inflammatory drugs inhibit antibody production in human cells. Cell Immunol **258:**18-28.
50. **Khayrullina T, Yen J-H, Jing H, Ganea D.** 2008. In vitro differentiation of dendritic cells in the presence of prostaglandin E2 alters the IL-12/IL-23 balance and promotes differentiation of Th17 cells. J Immunol **181:**721-735.
51. **Napolitani G, Acosta-Rodriguez EV, Lanzavecchia A, Sallusto F.** 2009. Prostaglandin E2 enhances Th17 responses via modulation of IL-17 and IFN-gamma production by memory CD4+ T cells. Eur J Immunol **39:**1301-1312.
52. **Sheibanie AF, Tadmori I, Jing H, Vassiliou E, Ganea D.** 2004. Prostaglandin E2 induces IL-23 production in bone marrow-derived dendritic cells. FASEB J **18:**1318-1320.

53. **Chizzolini C, Chicheportiche R, Alvarez M, de Rham C, Roux-Lombard P, Ferrari-Lacraz S, Dayer J-M.** 2008. Prostaglandin E2 synergistically with interleukin-23 favors human Th17 expansion. Blood **112:**3696-3703.
54. **Schnurr M, Toy T, Shin A, Wagner M, Cebon J, Maraskovsky E.** 2005. Extracellular nucleotide signaling by P2 receptors inhibits IL-12 and enhances IL-23 expression in human dendritic cells: a novel role for the cAMP pathway. Blood **105:**1582-1589.
55. **Boniface K, Bak-Jensen KS, Li Y, Blumenschein WM, McGeachy MJ, McClanahan TK, McKenzie BS, Kastelein RA, Cua DJ, de Waal Malefyt R.** 2009. Prostaglandin E2 regulates Th17 cell differentiation and function through cyclic AMP and EP2/EP4 receptor signaling. J Exp Med **206:**535-548.
56. **McCoy JM, Wicks JR, Audoly LP.** 2002. The role of prostaglandin E2 receptors in the pathogenesis of rheumatoid arthritis. J Clin Invest **110:**651-658.
57. **Tavakoli S, Cowan MJ, Benfield T, Logun C, Shelhamer JH.** 2001. Prostaglandin E(2)-induced interleukin-6 release by a human airway epithelial cell line. Am J Physiol Lung Cell Mol Physiol **280:**L127-133.
58. **Aronoff DM, Hao Y, Chung J, Coleman N, Lewis C, Peres CM, Serezani CH, Chen G-H, Flamand N, Brock TG, Peters-Golden M.** 2008. Misoprostol impairs female reproductive tract innate immunity against Clostridium sordellii. J Immunol **180:**8222-8230.
59. **Carriel-Gomes MC, Kratz JM, Barracco MA, Bachére E, Barardi CRM, Simões CMO.** 2007. In vitro antiviral activity of antimicrobial peptides against herpes simplex virus 1, adenovirus, and rotavirus. Mem Inst Oswaldo Cruz **102:**469-472.
60. **Nguyen EK, Nemerow GR, Smith JG.** 2010. Direct Evidence from Single-Cell Analysis that Human -Defensins Block Adenovirus Uncoating To Neutralize Infection. J Virol **84:**4041-4049.
61. **Peters-Golden M, Canetti C, Mancuso P, Coffey MJ.** 2005. Leukotrienes: underappreciated mediators of innate immune responses. J Immunol **174:**589-594.
62. **Lee E, Lindo T, Jackson N, Meng-Choong L, Reynolds P, Hill A, Haswell M, Jackson S, Kilfeather S.** 1999. Reversal of human neutrophil survival by leukotriene B(4) receptor blockade and 5-lipoxygenase and 5-lipoxygenase activating protein inhibitors. Am J Respir Crit Care Med **160:**2079-2085.
63. **Ford-Hutchinson A, Bray M, Doig M.** 1980. Leukotriene B4, a potent chemokinetic and aggregating substance released from polymorphonuclear leukocytes. Nature **286:**264.
64. **Hafstrom I, Palmblad J, Malmsten CL, Rådmark O, Samuelsson B.** 1981. Leukotriene B4--a stereospecific stimulator for release of lysosomal enzymes from neutrophils. FEBS Lett **130:**146-148.
65. **Serhan CN, Radin A, Smolen JE, Korchak H, Samuelsson B, Weissmann G.** 1982. Leukotriene B4 is a complete secretagogue in

human neutrophils: a kinetic analysis. Biochem Biophys Res Commun **107:**1006-1012.

66. **Lärfars G, Lantoine F, Devynck MA, Palmblad J, Gyllenhammar H.** 1999. Activation of nitric oxide release and oxidative metabolism by leukotrienes B4, C4, and D4 in human polymorphonuclear leukocytes. Blood **93:**1399-1405.
67. **Tager AM, Bromley SK, Medoff BD, Islam SA, Bercury SD, Friedrich EB, Carafone AD, Gerszten RE, Luster AD.** 2003. Leukotriene B4 receptor BLT1 mediates early effector T cell recruitment. Nat Immunol **4:**982-990.
68. **Ott VL, Cambier JC, Kappler J, Marrack P, Swanson BJ.** 2003. Mast cell-dependent migration of effector CD8+ T cells through production of leukotriene B4. Nat Immunol **4:**974-981.
69. **Costa MFdS, de Souza-Martins R, de Souza MC, Benjamim CF, Piva B, Diaz BL, Peters-Golden M, Henriques MdG, Canetti C, Penido C.** 2010. Leukotriene B4 mediates gammadelta T lymphocyte migration in response to diverse stimuli. J Leukoc Biol **87:**323-332.
70. **Goodarzi K, Goodarzi M, Tager AM, Luster AD, Von Andrian UH.** 2003. Leukotriene B4 and BLT1 control cytotoxic effector T cell recruitment to inflamed tissues. Nat Immunol **4:**965-973.
71. **Shin EH, Lee HY, Bae Y-S.** 2006. Leukotriene B4 stimulates human monocyte-derived dendritic cell chemotaxis. Biochem Biophys Res Commun **348:**606-611.
72. **Del Prete A, Shao W-H, Mitola S, Santoro G, Sozzani S, Haribabu B.** 2007. Regulation of dendritic cell migration and adaptive immune response by leukotriene B4 receptors: a role for LTB4 in up-regulation of CCR7 expression and function. Blood **109:**626-631.
73. **Mancuso P, Peters-Golden M.** 2000. Modulation of alveolar macrophage phagocytosis by leukotrienes is Fc receptor-mediated and protein kinase C-dependent. Am J Respir Cell Mol Biol **23:**727-733.
74. **Canetti C, Hu B, Curtis JL, Peters-Golden M.** 2003. Syk activation is a leukotriene B4-regulated event involved in macrophage phagocytosis of IgG-coated targets but not apoptotic cells. Blood **102:**1877-1883.
75. **Gaudreault E, Gosselin J.** 2008. Leukotriene B4 induces release of antimicrobial peptides in lungs of virally infected mice. J Immunol **180:**6211-6221.
76. **Gaudreault E, Gosselin J.** 2007. Leukotriene B4-mediated release of antimicrobial peptides against cytomegalovirus is BLT1 dependent. Viral Immunol **20:**407-420.
77. **Flamand L, Borgeat P, Lalonde R, Gosselin J.** 2004. Release of anti-HIV mediators after administration of leukotriene B4 to humans. J Infect Dis **189:**2001-2009.
78. **Goldman G, Welbourn R, Kobzik L, Valeri C, Shepro D, Hechtman H.** 1993. Lavage with leukotriene B4 induces lung generation of tumor necrosis factor-α that in turn mediates neutrophil diapedesis. Surgery **113:**297.

79. **Yamaoka KA, Dugas B, Paul-Eugene N, Mencia-Huerta JM, Braquet P, Kolb JP.** 1994. Leukotriene B4 enhances IL-4-induced IgE production from normal human lymphocytes. Cell Immunol **156:**124-134.
80. **Yamaoka KA, Claésson HE, Rosén A.** 1989. Leukotriene B4 enhances activation, proliferation, and differentiation of human B lymphocytes. J Immunol **143:**1996-2000.
81. **Dugas B, Paul-Eugene N, Cairns J, Gordon J, Calenda A, Mencia-Huerta JM, Braquet P.** 1990. Leukotriene B4 potentiates the expression and release of Fc epsilon RII/CD23, and proliferation and differentiation of human B lymphocytes induced by IL-4. J Immunol **145:**3406-3411.
82. **Behrens TW, Lum LG, Lianos EA, Goodwin JS.** 1989. Lipoxygenase inhibitors enhance the proliferation of human B cells. J Immunol **143:**2285-2294.
83. **Herbert M, Takano T, Holthofer H, Brady H.** 1996. Sequential morphologic events during apoptosis of human neutrophils: modulation by lipoxygenase derived eicosanoids. J Immunol **157:**3105.
84. **Lee E, Robertson T, Smith J, Kilfeather S.** 2000. Leukotriene receptor antagonists and synthesis inhibitors reverse survival in eosinophils of asthmatic individuals. Am J Respir Crit Care Med **161:**1881-1886.
85. **Schmidt H, Seifert R, Bohme E.** 1989. Formation and release of nitric oxide from human neutrophils and HL-60 cells induced by a chemotactic peptide, platelet activating factor and leukotriene B4. FEBS Lett **244:**357.
86. **Larfars G, Lantoine F, Deynck M, Palmblad J, Gyllenhammar H.** 1999. Activation of nitric oxide release and oxidative metabolism by leukotrienes B4, C4, and D4 in human polymorphonuclear leukocytes. Blood **93:**1399.
87. **Robbiani D, Finch R, Jager D, Muller W, Sartorelli A, Randolph G.** 2000. The leukotriene C4 transporter MRP1 regulates CCL19 (MIP-3b, ELC)-dependent mobilization of dendritic cells to lymph nodes. Cell **103:**757.
88. **Parameswaran K, Liang H, Fanat A, Watson R, Snider DP, O'Byrne PM.** 2004. Role for cysteinyl leukotrienes in allergen-induced change in circulating dendritic cell number in asthma. J Allergy Clin Immunol **114:**73-79.
89. **Lamoureux J, Stankova J, Rola-Pleszczynski M.** 2006. Leukotriene D4 enhances immunoglobulin production in CD40-activated human B lymphocytes. J Allergy Clin Immunol **117:**924-930.
90. **Kim DC, Hsu FI, Barrett NA, Friend DS, Grenningloh R, Ho I-C, Al-Garawi A, Lora JM, Lam BK, Austen KF, Kanaoka Y.** 2006. Cysteinyl leukotrienes regulate Th2 cell-dependent pulmonary inflammation. J Immunol **176:**4440-4448.
91. **Holgate ST, Peters-Golden M, Panettieri RA, Henderson WR.** 2003. Roles of cysteinyl leukotrienes in airway inflammation, smooth muscle function, and remodeling. J Allergy Clin Immunol **111:**S18-34; discussion S34-16.

92. **Dahlén SE, Hedqvist P, Hammarström S, Samuelsson B.** 1980. Leukotrienes are potent constrictors of human bronchi. Nature **288:**484-486.
93. **Montuschi P, Peters-Golden ML.** 2010. Leukotriene modifiers for asthma treatment. Clin Exp Allergy **40:**1732-1741.
94. **Dahlén S-E.** 2006. Treatment of asthma with antileukotrienes: first line or last resort therapy? Eur J Pharmacol **533:**40-56.
95. **Ogawa Y, Calhoun WJ.** 2006. The role of leukotrienes in airway inflammation. J Allergy Clin Immunol **118:**789-798; quiz 799-800.
96. **Thompson WW, Shay DK, Weintraub E, Brammer L, Bridges CB, Cox NJ, Fukuda K.** 2004. Influenza-associated hospitalizations in the United States. JAMA **292:**1333-1340.
97. **Lee Suki MY, Cheung CY, Nicholls John M, Hui Kenrie PY, Leung Connie YH, Uiprasertkul M, Tipoe George L, Lau YL, Poon Leo LM, Ip Nancy Y, Guan Y, Peiris JSM.** 2008. Hyperinduction of Cyclooxygenase‐2‐Mediated Proinflammatory Cascade: A Mechanism for the Pathogenesis of Avian Influenza H5N1 Infection. J Infect Dis **198:**525-535.
98. **Woo PCY, Tung ETK, Chan K-H, Lau CCY, Lau SKP, Yuen K-Y.** 2010. Cytokine profiles induced by the novel swine-origin influenza A/H1N1 virus: implications for treatment strategies. J Infect Dis **201:**346-353.
99. **Darwish I, Mubareka S, Liles WC.** 2011. Immunomodulatory therapy for severe influenza. Expert Rev Anti Infect Ther **9:**807-822.
100. **Carey MA, Bradbury JA, Rebolloso YD, Graves JP, Zeldin DC, Germolec DR.** 2010. Pharmacologic inhibition of COX-1 and COX-2 in influenza A viral infection in mice. PLoS ONE **5:**e11610.
101. **Carey MA, Bradbury JA, Seubert JM, Langenbach R, Zeldin DC, Germolec DR.** 2005. Contrasting effects of cyclooxygenase-1 (COX-1) and COX-2 deficiency on the host response to influenza A viral infection. J Immunol **175:**6878-6884.
102. **Hodges RJ, Jenkins RG, Wheeler-Jones CPD, Copeman DM, Bottoms SE, Bellingan GJ, Nanthakumar CB, Laurent GJ, Hart SL, Foster ML, Mcanulty RJ.** 2004. Severity of lung injury in cyclooxygenase-2-deficient mice is dependent on reduced prostaglandin E(2) production. Am J Pathol **165:**1663-1676.
103. **Allgayer H.** 2003. Review article: mechanisms of action of mesalazine in preventing colorectal carcinoma in inflammatory bowel disease. Aliment Pharmacol Ther **18 Suppl 2:**10-14.
104. **Zheng B-J, Chan K-W, Lin Y-P, Zhao G-Y, Chan C, Zhang H-J, Chen H-L, Wong SSY, Lau SKP, Woo PCY, Chan K-H, Jin D-Y, Yuen K-Y.** 2008. Delayed antiviral plus immunomodulator treatment still reduces mortality in mice infected by high inoculum of influenza A/H5N1 virus. Proc Natl Acad Sci USA **105:**8091-8096.
105. **Lauder SN, Taylor PR, Clark SR, Evans RL, Hindley JP, Smart K, Leach H, Kidd EJ, Broadley KJ, Jones SA, Wise MP, Godkin AJ, O'Donnell V, Gallimore AM.** 2011. Paracetamol reduces influenza-

induced immunopathology in a mouse model of infection without compromising virus clearance or the generation of protective immunity. Thorax **66:**368-374.
106. **Hinz B, Cheremina O, Brune K.** 2008. Acetaminophen (paracetamol) is a selective cyclooxygenase-2 inhibitor in man. FASEB J **22:**383-390.
107. **Graham GG, Davies MJ, Day RO, Mohamudally A, Scott KF.** 2013. The modern pharmacology of paracetamol: therapeutic actions, mechanism of action, metabolism, toxicity and recent pharmacological findings. Inflammopharmacology **21:**201-232.
108. **Rocca B, FitzGerald GA.** 2002. Cyclooxygenases and prostaglandins: shaping up the immune response. Int Immunopharmacol **2:**603-630.
109. **Li C, Bankhead A, Eisfeld AJ, Hatta Y, Jeng S, Chang JH, Aicher LD, Proll S, Ellis AL, Law GL, Waters K, Neumann G, Katze MG, McWeeney S, Kawaoka Y.** 2011. Host Regulatory Network Response to Infection with Highly Pathogenic H5N1 Avian Influenza Virus. J Virol.
110. **Gentile DA, Fireman P, Skoner DP.** 2003. Elevations of local leukotriene C4 levels during viral upper respiratory tract infections. Annals of Allergy, Asthma and Immunology **91:**270-274.
111. **Hennet T, Ziltener HJ, Frei K, Peterhans E.** 1992. A kinetic study of immune mediators in the lungs of mice infected with influenza A virus. J Immunol **149:**932-939.
112. **Widegren H, Andersson M, Borgeat P, Flamand L, Johnston S, Greiff L.** 2011. LTB4 increases nasal neutrophil activity and conditions neutrophils to exert antiviral effects. Respir Med.
113. **Tam VC, Quehenberger O, Oshansky CM, Suen R, Armando AM, Treuting PM, Thomas PG, Dennis Ea, Aderem A.** 2013. Lipidomic profiling of influenza infection identifies mediators that induce and resolve inflammation. Cell **154:**213-227.
114. **Duffield-Lillico AJ, Boyle JO, Zhou XK, Ghosh A, Butala GS, Subbaramaiah K, Newman RA, Morrow JD, Milne GL, Dannenberg AJ.** 2009. Levels of prostaglandin E metabolite and leukotriene E(4) are increased in the urine of smokers: evidence that celecoxib shunts arachidonic acid into the 5-lipoxygenase pathway. Cancer Prev Res **2:**322-329.
115. **Schenkelaars EJ, Bonta IL.** 1986. Cyclooxygenase inhibitors promote the leukotriene C4 induced release of beta-glucuronidase from rat peritoneal macrophages: prostaglandin E2 suppresses. Int J Immunopharmacol **8:**305-311.
116. **Lee M-S, Walker RE, Mendelman PM.** 2005. Medical burden of respiratory syncytial virus and parainfluenza virus type 3 infection among US children. Implications for design of vaccine trials. Hum Vaccin **1:**6-11.
117. **Collins CL, Pollard AJ.** 2002. Respiratory syncytial virus infections in children and adults. J Infect **45:**10-17.
118. **Falsey AR, Hennessey PA, Formica MA, Cox C, Walsh EE.** 2005. Respiratory syncytial virus infection in elderly and high-risk adults. N Engl J Med **352:**1749-1759.

119. **Falsey AR, Walsh EE.** 2000. Respiratory syncytial virus infection in adults. Clin Microbiol Rev **13:**371-384.
120. **Liu T, Zaman W, Kaphalia BS, Ansari GAS, Garofalo RP, Casola A.** 2005. RSV-induced prostaglandin E2 production occurs via cPLA2 activation: role in viral replication. Virology **343:**12-24.
121. **Richardson JY, Ottolini MG, Pletneva L, Boukhvalova M, Zhang S, Vogel SN, Prince GA, Blanco JCG.** 2005. Respiratory syncytial virus (RSV) infection induces cyclooxygenase 2: a potential target for RSV therapy. J Immunol **174:**4356-4364.
122. **Radi ZA, Meyerholz DK, Ackermann MR.** 2010. Pulmonary cyclooxygenase-1 (COX-1) and COX-2 cellular expression and distribution after respiratory syncytial virus and parainfluenza virus infection. Viral Immunol **23:**43-48.
123. **Sznajer Y, Westcott JY, Wenzel SE, Mazer B, Tucci M, Toledano BJ.** 2004. Airway eicosanoids in acute severe respiratory syncytial virus bronchiolitis. J Pediatr **145:**115-118.
124. **Han J, Jia Y, Takeda K, Shiraishi Y, Okamoto M, Dakhama A, Gelfand EW.** 2010. Montelukast during primary infection prevents airway hyperresponsiveness and inflammation after reinfection with respiratory syncytial virus. Am J Respir Crit Care Med **182:**455-463.
125. **Fullmer JJ, Khan AM, Elidemir O, Chiappetta C, Stark JM, Colasurdo GN.** 2005. Role of cysteinyl leukotrienes in airway inflammation and responsiveness following RSV infection in BALB/c mice. Pediatr Allergy Immunol **16:**593-601.
126. **Welliver RC, Hintz KH, Glori M, Welliver RC.** 2003. Zileuton reduces respiratory illness and lung inflammation, during respiratory syncytial virus infection, in mice. J Infect Dis **187:**1773-1779.
127. **Keun Kim C, Yeon Koh J, Hee Han T, Kyun Kim D, Il Kim B, Yull Koh Y.** 2006. Increased levels of BAL cysteinyl leukotrienes in acute RSV bronchiolitis. Acta Paediatrica **95:**479-485.
128. **Piedimonte G, Renzetti G, Auais A, Di Marco A, Tripodi S, Colistro F, Villani A, Di Ciommo V, Cutrera R.** 2005. Leukotriene synthesis during respiratory syncytial virus bronchiolitis: influence of age and atopy. Pediatr Pulmonol **40:**285-291.
129. **Da Dalt L, Callegaro S, Carraro S, Andreola B, Corradi M, Baraldi E.** 2007. Nasal lavage leukotrienes in infants with RSV bronchiolitis. Pediatr Allergy Immunol **18:**100-104.
130. **Volovitz B, Welliver RC, De Castro G, Krystofik DA, Ogra PL.** 1988. The release of leukotrienes in the respiratory tract during infection with respiratory syncytial virus: role in obstructive airway disease. Pediatr Res **24:**504-507.
131. **van Schaik SM, Tristram DA, Nagpal IS, Hintz KM, Welliver RC, Welliver RC.** 1999. Increased production of IFN-gamma and cysteinyl leukotrienes in virus-induced wheezing. J Allergy Clin Immunol **103:**630-636.

132. **Prince G, Mathews A, Curtis S, Porter D.** 2000. Treatment of Respiratory Syncytial Virus Bronchiolitis and Pneumonia in a Cotton Rat Model with Systemically Administered Monoclonal Antibody (Palivizumab) and Glucocorticosteroid. J Infect Dis **182:**1326-1330.
133. **Bonville CA, Rosenberg HF, Domachowske JB.** 2006. Ribavirin and cysteinyl leukotriene-1 receptor blockade as treatment for severe bronchiolitis. Antiviral Res **69:**53-59.
134. **Wedde-Beer K, Hu C, Rodriguez MM, Piedimonte G.** 2002. Leukotrienes mediate neurogenic inflammation in lungs of young rats infected with respiratory syncytial virus. Am J Physiol Lung Cell Mol Physiol **282:**L1143-1150.
135. **Bisgaard H, Virus SGoMaRS.** 2003. A randomized trial of montelukast in respiratory syncytial virus postbronchiolitis. Am J Respir Crit Care Med **167:**379-383.
136. **Bisgaard H, Flores-Nunez A, Goh A, Azimi P, Halkas A, Malice M-P, Marchal J-L, Dass SB, Reiss TF, Knorr BA.** 2008. Study of Montelukast for the Treatment of Respiratory Symptoms of Post-Respiratory Syncytial Virus Bronchiolitis in Children. Am J Respir Crit Care Med **178:**854-860.
137. **Proesmans M, Sauer K, Govaere E, Raes M, De Bilderling G, De Boeck K.** 2009. Montelukast does not prevent reactive airway disease in young children hospitalized for RSV bronchiolitis. Acta Paediatrica **98:**1830-1834.
138. **Wright M, Piedimonte G.** 2011. Respiratory syncytial virus prevention and therapy: past, present, and future. Pediatr Pulmonol **46:**324-347.
139. **Seymour ML, Gilby N, Bardin PG, Fraenkel DJ, Sanderson G, Penrose JF, Holgate ST, Johnston SL, Sampson AP.** 2002. Rhinovirus infection increases 5-lipoxygenase and cyclooxygenase-2 in bronchial biopsy specimens from nonatopic subjects. J Infect Dis **185:**540-544.
140. **Culver CA, Laster SM.** 2007. Adenovirus type 5 exerts multiple effects on the expression and activity of cytosolic phospholipase A2, cyclooxygenase-2, and prostaglandin synthesis. J Immunol **179:**4170-4179.
141. **Crofford LJ, McDonagh KT, Guo S, Mehta H, Bian H, Petruzelli LM, Roessler BJ.** 2005. Adenovirus binding to cultured synoviocytes triggers signaling through MAPK pathways and induces expression of cyclooxygenase-2. J Gene Med **7:**288-296.
142. **Weinberg JB, Stempfle GS, Wilkinson JE, Younger JG, Spindler KR.** 2005. Acute respiratory infection with mouse adenovirus type 1, p. 245-254, Virology, vol. 340.
143. **Knipe D, Howley P, Griffin D, Lamb R, Martin M, Roizman B, Straus S.** 2007. Fields Virology, 5th ed. Lippincott Williams & Wilkins, Philadelphia, PA.
144. **Qiu H, Stråat K, Rahbar A, Wan M, Söderberg-Nauclér C, Haeggström JZ.** 2008. Human CMV infection induces 5-lipoxygenase expression and leukotriene B4 production in vascular smooth muscle cells. J Exp Med **205:**19-24.

145. **Zhu H, Cong J-P, Yu D, Bresnahan WA, Shenk TE.** 2002. Inhibition of cyclooxygenase 2 blocks human cytomegalovirus replication. Proc Natl Acad Sci USA **99:**3932-3937.
146. **Schröer J, Shenk T.** 2008. Inhibition of cyclooxygenase activity blocks cell-to-cell spread of human cytomegalovirus. Proc Natl Acad Sci USA **105:**19468-19473.
147. **Gosselin J, Borgeat P, Flamand L.** 2005. Leukotriene B4 protects latently infected mice against murine cytomegalovirus reactivation following allogeneic transplantation. J Immunol **174:**1587-1593.
148. **Ballinger MN, Aronoff DM, McMillan TR, Cooke KR, Olkiewicz K, Toews GB, Peters-Golden M, Moore BB.** 2006. Critical role of prostaglandin E2 overproduction in impaired pulmonary host response following bone marrow transplantation. J Immunol **177:**5499-5508.
149. **Ojielo CI, Cooke K, Mancuso P, Standiford TJ, Olkiewicz KM, Clouthier S, Corrion L, Ballinger MN, Toews GB, Paine R, 3rd, Moore BB.** 2003. Defective phagocytosis and clearance of *Pseudomonas aeruginosa* in the lung following bone marrow transplantation. J. Immunol. **171:**4416-4424.
150. **Chaimoff C, Malachi T, Halbrecht I.** 1985. Prostaglandin E2 and cyclic nucleotides in plasma and urine of colonic cancer patients. J Cancer Res Clin Oncol **110:**153-156.
151. **Fraifeld V, Kaplanski J, Kukulansky T, Globerson A.** 1995. Increased prostaglandin E2 production by concanavalin A-stimulated splenocytes of old mice. Gerontology **41:**129-133.
152. **Ramis I, Rosello-Catafau J, Gomez G, Zabay JM, Fernandez Cruz E, Gelpi E.** 1991. Cyclooxygenase and lipoxygenase arachidonic acid metabolism by monocytes from human immune deficiency virus-infected drug users. J Chromatogr **557:**507-513.
153. **Anstead GM, Zhang Q, Melby PC.** 2009. Malnutrition promotes prostaglandin over leukotriene production and dysregulates eicosanoid-cytokine crosstalk in activated resident macrophages. Prostaglandins Leukotrienes Essent Fatty Acids **in press**.
154. **Redmond HP, Shou J, Kelly CJ, Schreiber S, Miller E, Leon P, Daly JM.** 1991. Immunosuppressive mechanisms in protein-calorie malnutrition. Surgery **110:**311-317.
155. **Cayeux SJ, Beverley PC, Schulz R, Dorken B.** 1993. Elevated plasma prostaglandin E2 levels found in 14 patients undergoing autologous bone marrow or stem cell transplantation. Bone Marrow Transplant **12:**603-608.
156. **el-Sharabasy MM, el-Naggar MM.** 1992. Prostaglandin E2 in renal transplant recipients. Int Urol Nephrol **24:**447-451.
157. **Graham NM, Burrell CJ, Douglas RM, Debelle P, Davies L.** 1990. Adverse effects of aspirin, acetaminophen, and ibuprofen on immune function, viral shedding, and clinical status in rhinovirus-infected volunteers. J Infect Dis **162:**1277-1282.
158. **Prymula R, Siegrist C-A, Chlibek R, Zemlickova H, Vackova M, Smetana J, Lommel P, Kaliskova E, Borys D, Schuerman L.** 2009.

Effect of prophylactic paracetamol administration at time of vaccination on febrile reactions and antibody responses in children: two open-label, randomised controlled trials. Lancet **374:**1339-1350.

Notes

This chapter was reprinted and modified from McCarthy, MK and Weinberg, JB. 2012. Eicosanoids and respiratory viral infection: coordinators of inflammation and potential therapeutic targets. *Mediators of Inflammation*. Vol 2012. DOI: 10.1155/2012/236345

Chapter 3:
Immunoproteasome

MHC Class I Antigen Presentation Pathway

CD8 T cells recognize peptides bound to MHC class I molecules. The generation of peptide-MHC class I complexes involves many steps (Figure 3-1). Peptides that bind tightly to MHC class I are 8-11 amino acids in length and have anchor residues, which are generally in the C-terminus, but can be present elsewhere in the peptide sequence (1). In humans, C-terminal anchor residues can be either basic or hydrophobic, whereas MHC class I molecules from mice only accept peptides that contain hydrophobic C-terminal anchor residues. The vast majority of these peptides are generated by proteasomes (2), although extended versions can be trimmed by aminopeptidases in the cytosol (3) or endoplasmic reticulum (ER) (4, 5). Peptides are transported from the cytoplasm to the ER by an ER-resident heterodimeric protein called TAP (transporter for antigen processing) (6). TAP is a subunit of the MHC class-I-loading complex, a ~1 MDa complex within the ER, that clusters the molecules involved in MHC class I loading in order to increase efficiency of the process. Within the complex, TAP interacts with 3-4 copies of tapasin, a molecular chaperone that binds empty MHC class I molecules and is required for loading of peptides (7, 8). Tapasin interacts with ERp57, which in turn interacts with the molecular chaperone

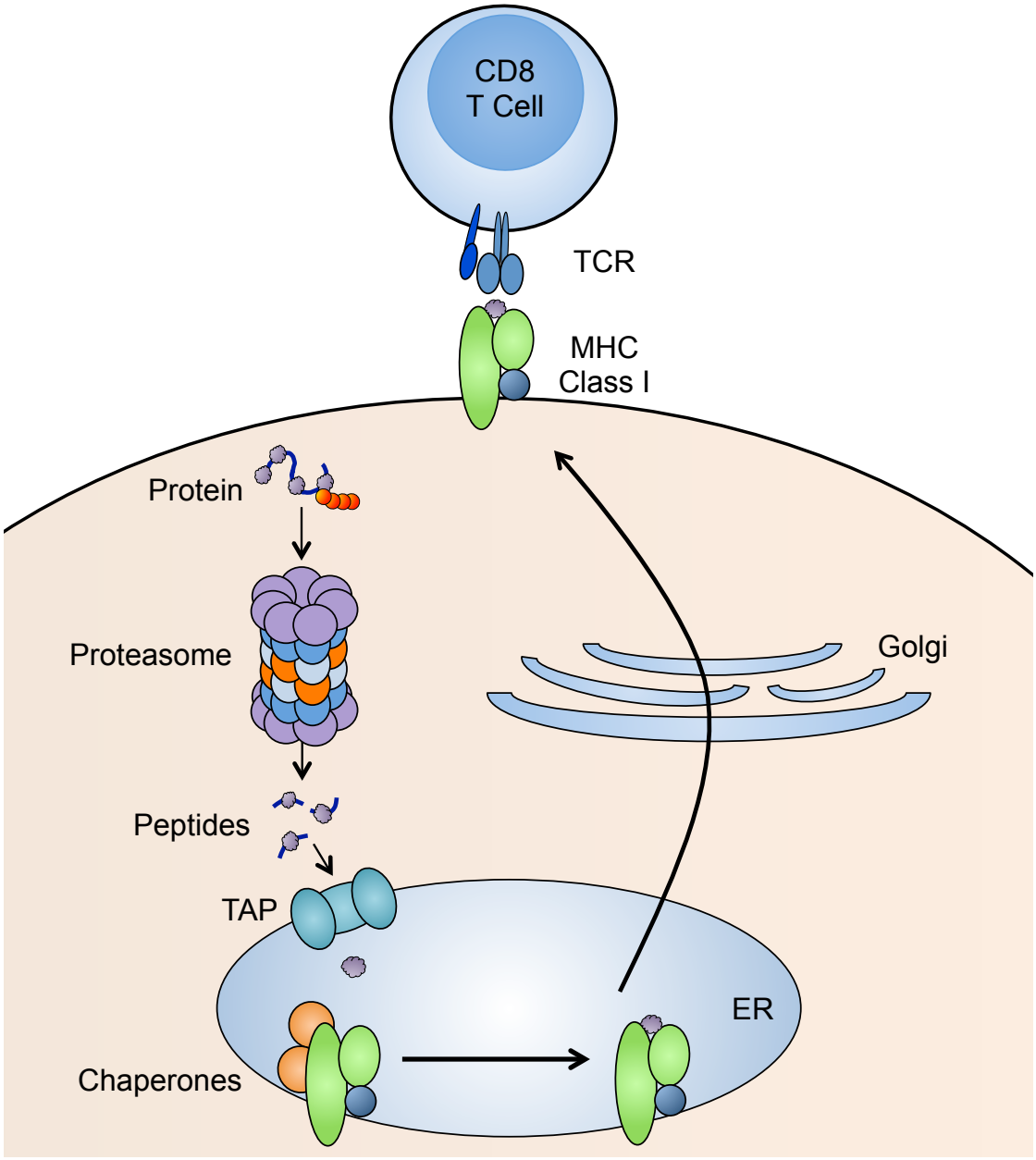

Figure 3-1. MHC Class I Antigen Presentation Pathway.

Proteins with ubiquitin tags (red spheres) are degraded by proteasomes and the resulting peptides are transported into the ER by TAP. In the ER, the peptide is loaded onto MHC class I molecules by many molecular chaperones. The peptide-MHC class I complex is then transported to the cell surface for presentation to CD8 T cells.

calreticulin and is required for peptide loading (8, 9). Once a peptide is successfully bound, the MHC class I molecule is released from the MHC class-I-loading complex and delivered to the cell surface for presentation to CD8 T cells.

Standard Proteasomes and Immunoproteasomes

Proteasomes are large complexes responsible for the regulated degradation of almost all cellular proteins, and as such proteasome activity is required for cell viability (2, 10). Proteasomes also play a primary role in generation of antigenic peptides for presentation on MHC class I molecules, but not on MHC class II (2, 11, 12). The 20S proteasome core is a barrel-shaped complex that is composed of four stacked heptameric rings: two outer alpha rings (dark blue) and two inner beta rings (light blue and orange) (Figure 3-1) (13, 14). The proteasome may be associated with activator caps (lavender), discussed below. The catalytic activity is restricted to three of the beta subunits, β1 (also called Y in vertebrates), β2 (Z) and β5 (X), that account for the caspase-like, trypsin-like, and chymotrypsin-like activities of the proteasome, respectively (15). The active sites of each of these proteins face toward the lumen of the proteasome cylinder, preventing unrestricted exposure of cytosolic proteins to proteolysis.

Almost 25 years ago, two more β-type proteasome subunits that are homologous to β1 and β5 were identified: proteasome subunit β1i (also known as PSMB9 and LMP2, low molecular weight protein 2) and proteasome subunit β5i (also known as PSMB8 and LMP7) (16-18). These subunits are encoded by

genes in the MHC class II region and are induced by IFN-γ and TNF-α (19), leading to the designation of these subunits as “immunosubunits” and the complex they form as the “immunoproteasome” (20) (Figure 3-2). A third IFN-γ-inducible proteasome subunit, this one outside of the MHC region, was subsequently identified: proteasome subunit β2i (also known as PSMB10, LMP10, and MECL-1, multicatalytic endopeptidase complex-like 1), which is homologous to β2 (21-23). Expression of the three immunosubunits following IFN-γ stimulation is mediated by interferon regulatory factor-1 (IRF-1) (24-27). Type I IFNs can also upregulate the immunoproteasome, although higher concentrations are needed to achieve the same upregulation induced by IFN-γ (28-30).

An additional type of specialized proteasome, termed the thymoproteasome, was identified in cortical thymic epithelial cells (cTECs). This proteasome contains the immunosubunits β1i and β2i as well as a cTEC-specific proteasome subunit β5t (also known as PSMB11). Expression of β5t is essential for positive selection of T cells, and expression of the homologous subunits β5 or β5i cannot compensate for deficiency in this specialized subunit (31-33).

Immunoproteasome Formation and Tissue Expression

Immunoproteasome assembly occurs in a cooperative manner whereby the immunosubunits interact with one another to favor the assembly of homogenous immunoproteasomes containing all three immunosubunits.

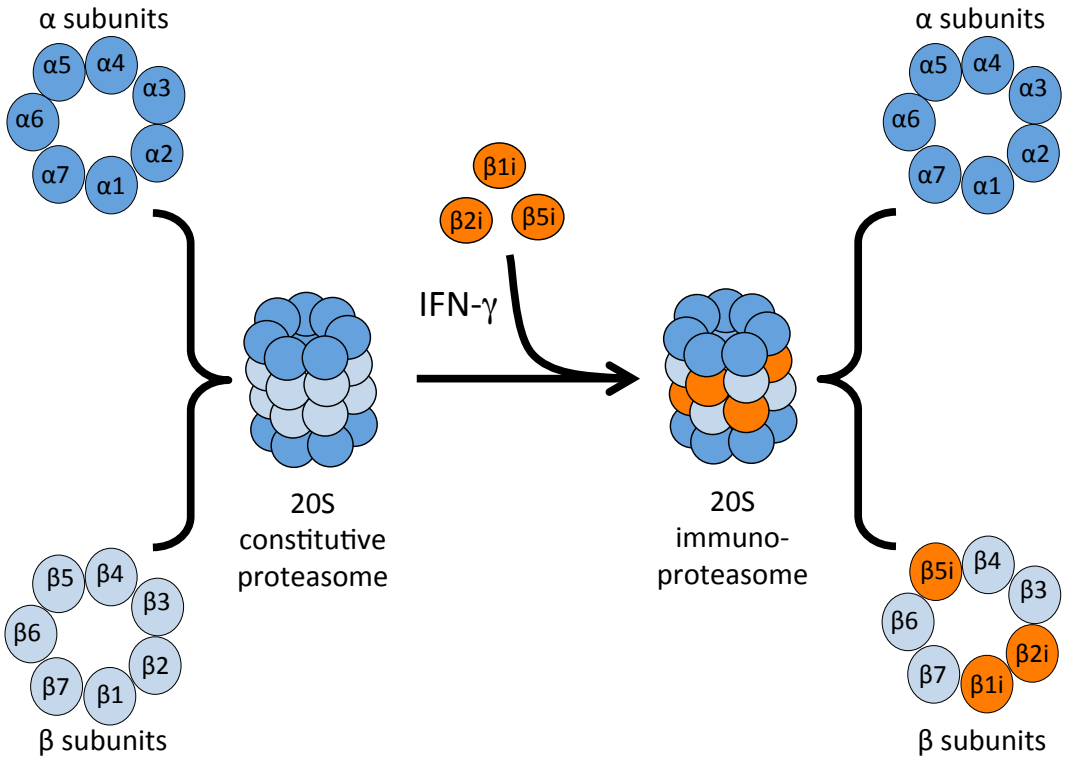

Figure 3-2. Immunoproteasome Formation.

The catalytic core of the 20S proteasome is comprised of two outer α rings and two inner β rings. IFN-γ exposure induces the synthesis of three β "immunosubunits," which are incorporated into newly formed proteasomes in place of their constitutive counterparts to form the 20S immunoproteasome.

This occurs even in cells that coexpress both standard and immunosubunits (34). The immunosubunit β1i is incorporated more quickly than β1, and incorporation of β2i depends on that of β1i (35, 36). Incorporation of β5i is required for the maturation (removal of the propeptides) of β1i and β2i, which would otherwise prevent their catalytic activity (34, 35). β5i is the only subunit that can be incorporated into immunoproteasomes independently of the other subunits, allowing for the existence of “mixed” or intermediate proteasomes that contain both β1i-β5i or β5i without other immunosubunits (34, 37). Mixed proteasomes are present in some human tissue types in the absence of stimulation or inflammation, especially the liver and colon, but not the heart. They are particularly abundant (50% or greater of the proteasomes in cell lysates) in antigen presenting cells (APCs), such as monocytes and both immature and mature DCs (38).

The spleen has the highest level of immunoproteasome expression and activity compared to other organs (39, 40). This makes sense given that the immunoproteasome is abundantly expressed in cells of hematopoietic origin, including professional APCs such as macrophages and B cells, found in the spleen (41, 42). Malignant cell lines derived from B cells or multiple myeloma express high levels of immunoproteasome subunits (43, 44). There has been some disagreement regarding the regulation of immunoproteasome expression in DCs. Initial reports suggested that immature DCs constitutively express immunoproteasomes at equal levels to that of the standard proteasome. Upon maturation, immunosubunit expression is dramatically upregulated and synthesis

of new proteasomes switches exclusively to immunoproteasomes (45). Later reports showed that immunoproteasome content is unchanged or even decreased in DCs following maturation (46-48). The disagreements regarding immunoproteasome expression in DCs may have been due to lack of immunosubunit-specific antibodies at the time of those studies. A more recent study demonstrated the presence of mostly immunoproteasomes and mixed proteasomes (β1-β2-β5i and β1i-β2-β5i) in immature DCs that does not change after maturation (38). In response to TLR stimulation, the immunosubunits are only upregulated transcriptionally in maturing DCs, and this upregulation is not followed by an increase at the protein level (49).

The constitutive expression of immunoproteasome subunits by immune cells appears to be independent of external signaling requirements, such as persistent stimulation by cytokines *in vivo*, because immune cells maintain their immunoproteasome expression *in vitro* in the absence of cytokines or other external stimuli. Rather, the high basal levels of immunoproteasome expression in immune cells are likely due to permanent activation of intracellular signaling pathways. One report demonstrated minor reductions in β1i and β5i mRNA in thymus and spleen tissue of mice lacking either type I or type II IFN receptors (50), but a second study demonstrated that the spleens of IFN-γ-deficient mice have levels of immunoproteasome protein expression similar to that of wild-type mice (51). In STAT1$^{-/-}$ mice, however, mRNA and protein expression of immunoproteasome subunits is markedly reduced (50, 51), suggesting that basal immunoproteasome expression does not require IFN-γ signaling (and therefore

phosphorylated STAT1), but is at least partially dependent on nonphosphorylated STAT1. This is supported by evidence that nonphosphorylated STAT1 and IRF1 form a complex that occupies the IFN-γ-activated sequence (GAS) elements of the β1i promoter to support its constitutive expression (52). There is still some basal immunoproteasome expression in spleens and thymus of STAT1$^{-/-}$ mice. This may reflect equal reduction of immunoproteasome subunits in all immune cell types present in these tissues (i.e., STAT1 greatly enhances basal expression), or could be due to complete absence of immunoproteasome expression in some cell types and not others (i.e., a cell-type-specific dependence on STAT1 for basal expression).

While nonimmune cells express standard proteasomes almost exclusively, immunoproteasome expression can be induced in such cells following exposure to IFN-γ. As mentioned above, type I IFNs can also upregulate the immunoproteasome, although less efficiently than IFN-γ (28-30). An initial report suggested that TNF-α could act synergistically with IFN-γ to upregulate β5i expression (53), implying that other proinflammatory cytokines may be capable of regulating immunoproteasome expression. However, in three murine cell lines of non-hematopoietic origin, only IFN-γ was capable of upregulating immunoproteasome subunits, and there was no effect of IL-1, IL-4, IL-6, TNF-α, TGF-β, IL-3, or GM-CSF treatment on immunoproteasome subunit protein levels (51). Therefore, it seems that other proinflammatory cytokines cannot regulate immunoproteasome expression and that IFN signaling is required for immunoproteasome induction in non-hematopoietic cells. There are some

exceptions to reports that nonimmune cells express exclusively standard proteasomes. Constitutive immunoproteasome expression has been reported in immune-privileged sites that are highly unlikely to receive persistent cytokine stimulation, such as the eye and brain (54-56), suggesting a role for immunoproteasomes in non-immune processes.

26S and 20S Proteasomes

Proteasomes exist in many forms in cells, with different regulatory or activator cap complexes that associate with the 20S core to control access to the proteolytic inner chamber (57). The α rings serve as scaffolds for the β subunits during proteasome assembly, but also as binding sites for regulatory and activator complexes. The 26S proteasome, which is composed of a 20S core particle and one or two 19S (also known as PA700) regulatory caps, degrades proteins in an ATP- and largely polyubiquitin-dependent manner. The 19S regulator complex recognizes and binds polyubiquitin moieties, then unfolds and feeds substrate proteins into the 20S core for degradation (58). Although 26S proteasomes preferentially degrade ubiquitinated proteins, degradation can occur without ubiquitination if the protein is first denatured (59). The 26S proteasome is responsible for the majority of normal protein turnover within cells. Because the α subunits are unchanged between different types of proteasomes, the 19S regulator complex can associate with 20S cores containing either standard or immunosubunits. This makes possible a number of different proteasome and immunoproteasome combinations: 20S alone, asymmetric 26S proteasomes

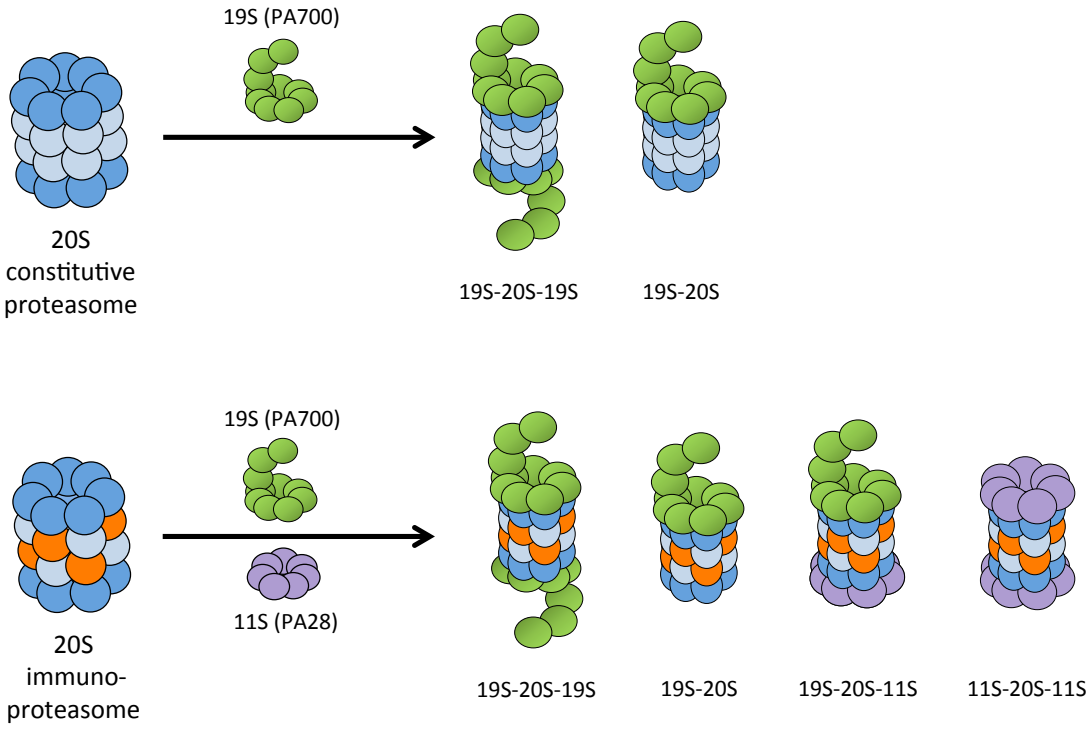

Figure 3-3. Possible combinations of 20S proteasome core with proteasome activator complexes.

The 19S (PA700) regulatory cap can associate at one or both ends of the 20S proteasome core to form an asymmetric 26S proteasome or a 26S proteasome, respectively. The IFN-γ-induced 11S (PA28) regulatory complex can bind at the free end of a 19S-20S complex to form a hybrid proteasome, or it can associate with both ends of the 20S immunoproteasome core.

(19S-20S), or 26S (19S-20S-19S), with each capable of having either the standard or immunosubunits in the 20S core (Figure 3-3).

It was originally thought that cells have little to no free 20S proteasome, and that the 20S complex is incapable of acting independently of its regulators or activators (60). Without the 19S regulatory cap, the 20S proteasome does not have the ability to recognize and unfold polyubiquitinated proteins. The 20S core seems to exist in an autoinhibited state, where the N-terminal tails of the α subunits at the openings on either end of the complex prevent substrate access to the internal proteolytic chamber (61). Binding of activator or regulatory complexes to the 20S core displaces the N-terminal tails, opening a channel into the lumen of the proteasome (62, 63). However, even in the absence of activating agents (such as heating or low detergent concentrations (64)), the 20S core is capable of degrading proteins at low, albeit detectable and reproducible, rates. Degradation of proteins by the 20S core probably involves partial or transient opening of the inner channel and is not an active process (62, 65-67). Indeed, the 26S proteasome and immunoproteasome hydrolyze unstructured polypeptides at rates nearly 10-fold higher compared to 20S proteasomes and immunoproteasomes (59, 68, 69). However, the free 20S core is capable of binding to and degrading proteins in a process that is both ATP- and ubiquitin-independent (64, 70). Rather than recognizing ubiquitin moieties, the 20S proteasome has a selective preference for degradation of damaged or oxidized proteins, while the 26S proteasome does not (71-73). Thus, it appears that the majority of normal protein turnover occurs through the 26S proteasome, while the

20S proteasome plays a specialized role in degradation of damaged or oxidized proteins. It has been suggested that oxidation may act as a marker for targeting proteins to the MHC class I pathway (74). This notion, termed the PrOxI (protein oxidation and immunoproteasome) hypothesis, would represent a new mechanism of substrate generation by the proteasome and may act in concert with other pathways (such as the DRiPs pathway discussed below) to efficiently generate peptides for MHC class I presentation.

Proteasome Processing of Peptides for MHC Class I

Depending on the cell type, up to 30% or more of translation products are defective, found as incorrect (mistranslated or prematurely stopped), misfolded, or misassembled proteins. This group of proteins is known as defective ribosomal products, or DRiPs. Because peptides generated for MHC class I molecules are generated by proteasomes, they are derived either from DRiPs or from proteins undergoing normal turnover (proteins termed by Yewdell as ‘retirees’ (75)), a process that occurs stochastically (76, 77) or due to age-associated damage and folding (78). Yewdell was the first to suggest that DRiPs are a major source of peptides for MHC class I molecules (79). Multiple lines of evidence have supported this notion (80, 81). The majority of peptides bound to TAP originate from newly synthesized proteins, and turnover from ‘retirees’ appears to be a relatively insignificant source of peptide for MHC class I molecules (82). DRiPs likely play a crucial role during viral infection, as the majority of abundant viral proteins are stable and long-lived. Rather than wait

hours or days for a stable viral protein to be degraded, DRiPs allow for the generation of suitable MHC class-I-binding peptides almost immediately after these proteins are synthesized. In this way, CD8 T cells can respond immediately to a viral infection and begin to eradicate a virus before it spreads (83).

The efficiency of proteasomes in generating antigenic peptides is quite low. Based on *in vitro* observations of rates of various steps in MHC class I antigen presentation (84, 85), Yewdell has estimated this efficiency to be on the order of 1 per 10,000. This means that only one MHC class-I-binding peptide is produced for every 10,000 proteins degraded. Thus, out of the estimated 2 million peptides generated in a cell per second, only 150 MHC class I molecules are loaded with peptides (75, 86). While these values are based on estimates obtained from a single cell line and may vary widely depending on different cell types or activation states, other studies have confirmed the low generation of MHC class I peptides by proteasomes. When ovalbumin (OVA) is used as a proteasome substrate, purified proteasomes produce SIINFEKL, a well-studied OVA-derived MHC class I peptide, or N-extended versions (that could be trimmed to the correct length by cytosolic or ER peptidases) only ~5% of the time (69, 87). It is likely that much of the SIINFEKL peptide is lost after generation due to peptidase activities in the cytosol. In fluorescence loss in photobleaching (FLIP) experiments, less than 2% of microinjected peptides enter the ER (84). Less than 1% of cytosolic peptides are recruited for MHC class I presentation, and this efficiency is at least 2 log units lower for peptides with low affinity for TAP (88). When vaccinia virus is used to encode various forms of SIINFEKL

peptide, only ~2% of proteasome-generated SIINFEKL is successfully loaded on H-2K^b molecules (85). Given that proteasomes produce SIINFEKL only 5% of the time, this would predict an efficiency of SIINFEKL-MHC class I complex generation of 5% x 2%, or 0.1%. Pamer and Cresswell estimated that from every 100 molecules of *Listeria* proteins degraded *in vivo,* between 3 and 30 MHC class I peptides were generated, depending on the epitope (89). Others have estimated the efficiency to be closer to 1 MHC class I peptide for every 30 *Listeria* proteins degraded (90). This is a significantly higher efficiency than has been reported using different antigens in other systems, and it may relate to cross-presentation mechanisms in phagocytic cells such as DCs and macrophages. More studies are needed to determine efficiencies of MHC class I peptide generation using different antigens and cell types, and under varying conditions (including viral infections). The low efficiency of MHC class I epitope generation by proteasomes underscores that their main function is to degrade proteins to amino acids, and that the cleavages that yield MHC class I peptides are relatively rare occurrences.

The changes in proteasome subunit composition from standard to immunosubunits in response to IFN-γ stimulation alter the proteolytic activity of the complex. Purified 20S and 26S immunoproteasomes from IFN-γ-treated cells substantially increase the rate at which they cleave after hydrophobic and basic residues (19, 91, 92) and decrease the rate of cleavage after acidic residues (93). As the vast majority of peptides presented on MHC class I have hydrophobic or basic C-termini, the immunoproteasome is thought to generate

peptides better suited to binding to MHC class I molecules compared to the constitutive proteasome and thus be more efficient at eliciting immune responses (91, 94). Rates of OVA degradation by 26S proteasomes and immunoproteasomes, or 20S proteasomes and immunoproteasomes, are indistinguishable (69). All produce peptides of similar sizes ranging between 3 and 22 residues. 26S particles yield peptides with a mean size of 7-8 residues, while the mean size of products from 20S particles is slightly larger, at 8-9 residues (95). So the different β subunits do not affect rates of protein degradation or peptide size, but rather seem to affect the cleavage sites within a protein to generate peptides with more hydrophobic C-termini.

It was uncertain whether proteasomes cleave proteins to the exact length (8-10 residues) that would be directly loaded onto MHC class I molecules, or whether they produce larger precursors that are further cleaved by other peptidases. Some initial experiments indicated that isolated 20S proteasomes could cleave larger peptides to antigenic epitopes (96-98). However, these experiments used short (less than 50 amino acid) precursors that are likely very different from the ubiquitinated or damaged full-length protein substrates that the proteasome would encounter under normal conditions. 20S proteasomes also release a different spectrum of products than do 26S proteasomes (95, 99). A number of studies have indicated that proteasomes release N-extended versions of antigenic peptides, which are then trimmed by aminopeptidases in the cytosol (3) or ER (4, 5). Moreover, one of these aminopeptidases, leucine aminopeptidase (LAP), is induced by IFN-γ (100). Following IFN-γ treatment,

cytosolic LAP activity accounted for all trimming of an N-terminal extended version of the well-studied OVA-derived epitope SIINFEKL to the correct length.

Although immunoproteasomes degrade proteins at the same rate as standard proteasomes, immunoproteasomes generate more antigenic peptides than standard proteasomes (69). Degradation of OVA by standard 26S proteasomes isolated from muscle tissue produces SIINFEKL or an N-extended version only 6-8% of the time. When 26S immunoproteasomes from the spleen are used, the percentage of peptides containing SIINFEKL at the C-terminus increases to 11%. This is not due to an increase in the amount of final SIINFEKL peptide generated, as standard proteasomes and immunoproteasomes release the same amount of SIINFEKL. Instead, 20S or 26S immunoproteasomes generate 2-4 times the amount of N-extended versions of this peptide, which could be trimmed by the cytosolic enzyme LAP, compared to their standard proteasome counterparts. Therefore, it seems that the effect of IFN-γ on antigenic peptide generation within cells is at least three-fold: changes from standard to immunosubunits in the 20S proteasome core directly affect C-terminal processing and generate more N-extended versions of antigenic peptides, while induction of aminopeptidase activity in the cytosol alters N-terminal processing.

IFN-γ-induced Proteasome Regulator PA28

Another protein complex induced by IFN-γ is PA28 (also known as REG or 11S), a large regulatory complex that binds the ends of the 20S proteasome in

an ATP-independent manner (Figure 3-3). In mammals, PA28 is made of two homologous subunits, PA28α (REGα or PSME1) and PA28β (REGβ or PSME2) (101-107). It was originally predicted that PA28 either enhanced the rate of protein degradation by proteasomes or generated peptides better suited to binding to MHC class I. However, the biological functions of PA28 are still relatively unknown. PA28 does not enhance rates of protein degradation by either the standard proteasome or the immunoproteasome. In fact, PA28-20S particles degrade proteins at the same slow rate as 20S particles alone (68). PA28 appears to enhance the ability of the 20S proteasome to degrade short peptide substrates, but not proteins or polyubiquitinated proteins (108, 109). PA28 is also able to associate with asymmetric 26S proteasomes (20S proteasomes with only one 19S regulatory complex, usually denoted as 19S-20S) to form hybrid proteasomes (19S-20S-PA28) (Figure 3-3) (110-113). Hybrid proteasomes hydrolyze 3- and 4-residue peptides at faster rates than standard 26S particles.

An extensive study of the molecular mechanisms of PA28 was recently undertaken by Raule et al., who performed *in vitro* degradation of full-length proteins (insulin-like growth factor-1, or IGF-1, and casein) by 20S, 26S and PA28α/β-20S immunoproteasomes and analyzed the range of peptides released (68). Rather than increase the fraction of 8-10 residue peptides that is generated, association of PA28 with 20S immunoproteasomes reduces it from 10% to approximately 6% of the total, with the majority of peptides being <6 amino acids in length. This may occur through allosteric modification of proteasome active

sites by PA28α/β. Alternatively, PA28α/β may control the efflux of longer peptides out of the proteolytic chamber and contribute to their ongoing hydrolysis (68, 114).

Binding of PA28 to the 20S catalytic core also appears to favor the release of a specific subset of longer peptides with an acidic C terminus, several of which contain the correct C-terminal anchor residue required for binding to MHC class I (68). Several studies have demonstrated that PA28 expression enhances MHC class I presentation of certain antigens (115-118) but not others (119). It was proposed that this small fraction of peptides specifically generated by PA28-20S immunoproteasomes may be important in stimulating an effective CD8 T cell response under certain pathophysiological conditions in which a ubiquitin-independent proteolytic pathway is favored. However, since the vast majority of peptides released by PA28-20S immunoproteasomes are too short to serve as MHC class I antigens, an alternative possibility is that PA28 may play a regulatory role by preventing excessive cytotoxic response against self-antigens, and decrease the risk of autoimmune reactions. A recent study demonstrated that purified PA28α/β increases the capacity of both the constitutive 20S proteasome and the immunoproteasome to selectively degrade oxidized proteins in response to hydrogen peroxide-induced oxidative stress, supporting a role for PA28 that is independent of MHC class I antigen processing (120).

Although PA28 does not stimulate proteolytic degradation under normal conditions, PA28 does increase catalytic rates of the immunoproteasome under conditions of ATP depletion (29). The implications of PA28 regulation by cellular

ATP levels are unknown. Proinflammatory cytokines, such as IL-1 and IFNs, significantly decrease total cellular ATP levels (121, 122). It is possible that decreases in ATP levels that could occur during inflammatory conditions such as viral infection trigger increased association of PA28 with 20S immunoproteasomes and enhance rates of protein degradation. However, given that the majority of peptides degraded by PA28-20S proteasomes and immunoproteasomes are not suitable for binding to MHC class I, it seems unlikely that this added level of regulation is related to MHC class I antigen processing. It may instead be related to possible roles for PA28 in degradation of oxidized proteins or decreasing the potential for autoimmune reactions at sites of inflammation, as discussed above. If PA28 does dampen autoimmunity, then one would expect to see an increase in autoimmune responses in PA28-deficient mice after an inflammatory response. These are intriguing possibilities that bear further investigation.

Strategies to Study Immunoproteasome Function

Until recently, traditional gene deletion has been the main strategy employed to study immunoproteasome function. There are numerous drawbacks to this approach. Due to cooperative assembly of immunoproteasomes, deficiency in one subunit could affect the structure and assembly of the 20S core, as well as impair binding or activity of regulatory subunits. Mice deficient in one or more of the immunosubunits since birth could develop compensatory mechanisms of proteasome or immunoproteasome assembly, leading to

alteration in subunit composition that could detrimentally affect peptide processing. They also could also have defects in maturation of the immune system, since the thymoproteasome (composed of β1i, β2i and the cTEC-specific subunit β5t) is important for positive selection of T cells (31). Most studies of immunoproteasome function have been undertaken with mice in which only one or two immunosubunits are deleted, rather than all three. It is possible that a standard proteasome subunit is able to compensate when only one or two immunosubunits are missing, in which case a phenotype would not be observed unless the mice are lacking all immunoproteasome activity. Therefore, caution must be taken in drawing conclusions from studies using mice deficient in one or more immunosubunits.

Small molecule peptide screens have led to the identification of inhibitors specific to immunoproteasome activity. The use of small molecule inhibitors offers several advantages over traditional gene deletion approaches, the most obvious of which is their potential for use as therapeutics. Because small molecule inhibitors are unlikely to affect the assembly or structure of the immunoproteasome, they allow for the study of how the catalytic activity of a specific subunit affects immune responses. Furthermore, these inhibitors are unlikely to affect the positive selection of T cells in the thymus, since most studies are undertaken in adult mice after maturation of the immune system.

The first reported immunoproteasome-specific inhibitor, PR-957 (now known as ONX 0914), inhibits β5i with an IC_{50} value of approximately 10 nM (123). ONX 0914 is 20- to 40-fold more selective for β5i than for the next two

most sensitive subunits, β1i and β5. Another β5i-specific inhibitor, PR-924, targets β5i and has less specificity toward other subunits compared to ONX 0914 (124). UK-101 was the first identified compound to specifically inhibit β1i (125, 126), with two more (IPSI-001 and YU-102) identified shortly thereafter (127, 128). Leupeptin is a recently described inhibitor of the trypsin-like activity of the proteasome (β2 and β2i) that does not affect activity of other β subunits (129, 130). There are currently no available compounds that specifically inhibit the activity of β2i. A recent crystal structure of the murine constitutive proteasome and the immunoproteasome in complex with ONX 0914 revealed important structural differences in the binding pockets of the different subunits (131). While the crystal structures demonstrated that β1 and β5 have distinct substrate binding pockets from their immunosubunit counterparts, the substrate binding pockets of β2 and β2i are essentially identical. Therefore, it will be difficult to develop β2i inhibitors that do not also target its constitutive counterpart. Several other proteasome- and immunoproteasome- specific inhibitors are in development and are of significant interest as potential therapeutic agents (127).

Immunoproteasome and Activation of the NF-κB Pathway

The nuclear factor-κB (NF-κB/Rel) family of transcription factors plays a central role in regulation of immunity and inflammation. NF-κB transcription factors interact as homodimers or heterodimers with other NF-κB family members, including p65 (RelA), RelB, c-Rel, p50 (NF-κB1), and p52 (NF-κB2).

Under normal conditions, these factors exist in the cytoplasm in an inactive state because of interaction with inhibitory IκB proteins (IκBα, IκBβ, IκBε) or the unprocessed forms of NF-κB1 and NF-κB2 (p105 and p100, respectively). The NF-κB pathway is activated in response to many different stimuli, including exposure to inflammatory cytokines such as TNF-α or IL-1 family members (132). In the canonical or classical pathway of NF-κB activation, the proteasome degrades IκBα, releasing the active NF-κB dimer (usually p65/p50) and allowing translocation to the nucleus. In the noncanonical or alternative pathway of NF-κB activation, the proteasome degrades the inhibitory portion of p105 or p100 to generate the active transcription factors p50 or p52. These transcription factors can then associate with p65, RelB, or each other to form homodimers and heterodimers. The classical and alternative NF-κB pathways regulate distinct sets of target genes, in part because different populations of NF-κB dimers are regulated by either IκBα degradation or p100 processing (133).

It is widely accepted that the standard proteasome plays a crucial role in the processing of the p105 precursor of the p50 subunit and in the degradation of IκBα (134, 135). However, a role for the immunoproteasome in NF-κB pathway activation is controversial. Nonobese diabetic (NOD) mice were reported to have a specific defect in β1i production that resulted in defective activation of NF-κB (136). This finding has been debated, but contradictory results were likely due to different cell populations and the phenotype (non-diseased versus diseased) of NOD mice analyzed (136-138). Nevertheless, Hayashi et al. did directly demonstrate impaired NF-κB activation in lymphocytes from $\beta 1i^{-/-}$ mice (136).

The human lymphocyte cell line T2, which lacks both β1i and β5i, has substantial defects in NF-κB activation compared to the parental T1 cell line and is sensitive to TNF-α-induced apoptosis (139).

In support of a role for the immunoproteasome in NF-κB activation, another study reported delayed termination of the classical NF-κB activation pathway and reduced activation of transcription factors associated with the alternative NF-κB pathway in β1i$^{-/-}$ mice, but not β1i/β5i double knockout mice (140). B cells isolated from β1i$^{-/-}$ mice exhibit slightly delayed NF-κB signaling, although the authors posited that defects in these mice were likely due to the presence of mixed proteasomes containing β1, β2i and β5i because a B cell phenotype was not observed in mice lacking both β1i and β2i (141). It is important to note that the mixed proteasomes may have abnormal function that is directly responsible for observed defects in NF-κB activation in β1i$^{-/-}$ mice (discussed in more detail below). If that is the case, then the deficiencies in these cell types in β1i$^{-/-}$ mice are not a true reflection of immunoproteasome function.

In support of this possibility, another study used two small molecule inhibitors of the immunoproteasome, UK-101 and LKS01, which target β1i and β5i, respectively, to study the role of the immunoproteasome in NF-κB activation in lung and pancreatic adenocarcinoma cells (142). Their results suggest that the catalytic activity of β1i and β5i is not required for canonical NF-κB activation, and they support the notion that deficiencies in NF-κB activation in β1i$^{-/-}$ mice may instead be an artifact of mixed proteasomes. One study demonstrated reduced

NF-κB activation in cardiomyocytes and B-cell-depleted splenocytes in β5i$^{-/-}$ mice following exposure to IFN-γ (143). However, because NF-κB activation in this study was measured by assessing p50 levels in whole cell homogenates, it is unknown whether the reduced levels in β5i$^{-/-}$ mice were due to impaired activation of the classical or alternative NF-κB pathway.

Since some studies have reported impaired activation of the alternative NF-κB pathway in β1i$^{-/-}$ mice, it will be important to repeat the UK-101 and LKS01 inhibitor studies to determine whether the catalytic activity of β1i or β5i is important in the alternative pathway of NF-κB activation. Additionally, it remains to be determined whether other cell types, such as those of the immune system that express the immunoproteasome constitutively, use immunoproteasome activity in the either the classical or alternative pathway of NF-κB activation.

Immunoproteasome Functions in Antigen Processing and Viral Infection

Because β1i and β5i are encoded on the MHC locus, it was originally thought that the major function of the immunoproteasome is to regulate the immune response via optimization of MHC class I peptide processing. Although proteasome activity in general is required for MHC class I antigen presentation, the immunoproteasome does not appear to be essential for that function. In fact, some epitopes are processed more efficiently by the 20S proteasome than the immunoproteasome (144, 145). However, the immunoproteasome is certainly more effective than the standard proteasome at producing many MHC class I epitopes, particularly when it comes to immunodominant epitopes derived from

infectious organisms. Many of the epitopes processed inefficiently by the immunoproteasome are derived from self proteins (145). While these epitopes may be important for generating an immune response to tumor antigens and could have implications for design of cancer vaccines, it is unlikely that they play a role in the immune response to an infectious organism.

The immunoproteasome appears to play important roles in T cell responses that are independent of MHC class I antigen presentation. A common phenotype of immunoproteasome-deficient mice is reduced number of CD8+ T cells in the spleen, supporting a role for the immunoproteasome in T cell development or maturation (141, 146, 147). A number of studies have reported increased CD4/CD8 T cell ratios $\beta 2i^{-/-}$ mice (148-150), and this has recently been ascribed to a T-cell-intrinsic process that occurs independently of both thymic selection and antigen processing (151). T cells from $\beta 1i^{-/-}$, $\beta 2i^{-/-}$, or $\beta 5i^{-/-}$ mice are impaired in proliferation and survival when transferred into virus-infected wild-type mice, suggesting a role for the immunoproteasome in the expansion and maintenance of T cell populations during an immune response (149, 152, 153).

The immunoproteasome may also play a critical role in B cell development, as mice deficient in $\beta 1i$, but not $\beta 1i/\beta 2i$ or $\beta 5i/\beta 2i$, have reduced numbers of mature B cells in the spleen (141). These authors reported reduced survival and impaired immunoglobulin (Ig) isotype switching in B cells from $\beta 1i^{-/-}$ mice compared to wild-type B cells. However, the observed defects have been attributed to the presence of mixed proteasomes containing $\beta 2i$ and $\beta 5i$ in these mice, and may not be a true reflection of immunoproteasome function. A

separate report was unable to recapitulate the finding of reduced B cells in $\beta1i^{-/-}$ mice, and it demonstrated equivalent numbers of $CD19^{+}$ B cells in the spleens of mice deficient in β1i, β2i, or both β1i/β2i (146). B cell responses were not examined in detail in that study. Therefore, the role of the immunoproteasome in B cell development or induction of a humoral response following a viral infection is still largely undefined.

The immunoproteasome, or at least the β5i subunit, plays a critical role in generating nearly all mouse cytomegalovirus (MCMV)-derived epitopes (154). Interestingly, memory "inflating" epitopes, or epitopes for which the pool of specific CD8 T cells is sustained or even increased over time, show a reduced dependence on the immunoproteasome compared to non-inflating epitopes. This suggests that immunoproteasomes play a role in stimulating immune responses during acute infection, but not during chronic MCMV infection. Although this study did not monitor the effect of β5i deficiency on MCMV viral loads over time, it was suggested that β5i deficiency likely would not have an impact on MCMV replication because neither CD8 nor MHC class I deficiency have an impact on viral loads in this model.

The immunoproteasome (subunits β1i and β5i) moderately influences the magnitude and specificity of CD8 T cell responses to hepatitis B virus (HBV) polymerase and envelope proteins (155). Although type I IFNs and IFN-γ inhibit HBV replication, the antiviral effect of IFNs occurs independently of their induction of β1i and β5i.

The majority of studies examining the effect of immunoproteasome deficiency on the generation of antigenic epitopes during viral infection have been performed with influenza virus or lymphocytic choriomeningitis virus (LCMV), two well-studied viruses for which the immunodominant CD8 T cell epitopes are known. APCs from $\beta1i^{-/-}$ mice show a reduced capacity to generate an influenza virus nucleoprotein-specific epitope, while presentation of OVA-derived antigens was unaffected (147). Two later studies using seven defined peptides from influenza virus showed that $\beta1i$ (and to a lesser extent the other immunoproteasome subunits) plays a major role in establishing the immunodominance hierarchy of responding CD8 T cells (149, 156). Responses to the two most immunodominant epitopes significantly decreased in $\beta1i^{-/-}$ mice. One of these was due to decreased generation of the epitope by APCs, while the other was due to reduced frequency of epitope-specific T cells in the CD8 T cell repertoire. The overall number of influenza virus-specific CD8 T cells was decreased in $\beta1i^{-/-}$ mice, even when $\beta1i^{-/-}$ CD8 T cells were restimulated with influenza virus-infected splenocytes from wild-type mice as APCs. Because this defect was observed for epitopes produced equally by standard proteasomes and immunoproteasomes, it was suggested that immunoproteasomes might play a role in T cell activation and proliferation.

Interestingly, influenza virus titers are reduced approximately 50% in sera of $\beta1i^{-/-}$ mice. While B cells from influenza virus-infected $\beta1i^{-/-}$ mice proliferate as well as those from wild-type mice, they display a survival defect and impaired Ig isotype switching. DCs from the same mice show reduced innate cytokine

production in response to influenza virus infection (141). The altered response of many cell types in β1i$^{-/-}$ mice to influenza virus is likely due to the presence of mixed proteasomes containing β2i and β5i.

Care must be taken in the interpretation of results obtained using β1i$^{-/-}$ mice, since results cannot be attributed solely to absence of β1i catalytic activity, but may rather be due to dysregulated proteasome assembly and function. While mixed proteasomes containing both standard and immunosubunits have recently been isolated, these mixed proteasomes contain either β1i-β5i or just β5i, in accordance with the rules of cooperative immunoproteasome assembly (38). The authors of that study were unable to detect the presence of mixed proteasomes containing β2i, as all of the β2i subunits were associated with immunoproteasomes. Cooperative assembly rules should preclude formation of mixed proteasomes containing β2i, because both β1i and β5i are required for its inclusion in the immunoproteasome. It is possible that β5i could compensate (perhaps partially or inefficiently) for β1i in the assembly process, or that β2i could interact with the standard β1 subunit in the complete absence of β1i (as in β1i$^{-/-}$ mice). This may explain the seemingly contradictory presence of mixed β2i-β5i proteasomes in β1i$^{-/-}$ mice. It is doubtful that mixed proteasomes containing β2i exist in wild-type mice, although this has not been formally analyzed in all tissues or cell types. Mixed proteasomes (containing β1i-β5i or β5i alone) are highly expressed in human immature and mature DCs. Human monocytes also contain a particularly high abundance of mixed proteasomes, up to 50% of the total proteasome content. The mixed proteasome content of B and T cells is

unknown. However, the finding that mixed proteasomes are expressed at high levels in some cell types, particularly APCs, suggests that they may play an important role in shaping CD8 T cell responses. Indeed, work from Zanker et al. using mice deficient in β1i, β2i or β5i/β2i demonstrated that mixed proteasomes increase viral peptide diversity and broaden antiviral CD8 T cell responses to influenza virus (157).

Mice deficient in β2i have ~20% lower numbers of CD8 T cells in the spleen and reduced response to some LCMV-derived epitopes. This is not due to impaired generation or presentation of these epitopes, but rather to either decreased precursor frequency or reduced expansion of the epitope-specific T cells, further supporting a role for the immunoproteasome in T cell survival or expansion rather than just antigen presentation (152). One strategy that has been employed to study mice lacking all immunoproteasome activity has been to use β1i/β2i double knockout mice treated with the β5i-specific inhibitor ONX 0914 (146). Although these mice have reduced CD8 T cells in the spleen, and CD8 T cell responses to several LCMV-specific MHC class I epitopes are changed (two are increased and others are decreased), these double knockout mice mount largely normal CD8 T cell responses to LCMV infection. Spleen viral titers at 4 dpi were unchanged in immunoproteasome-deficient mice treated with ONX 0914, although it remains to be seen whether viral titers at later times (such as at 8 dpi, when CD8 T cell responses were analyzed) would be affected by lack of immunoproteasome activity. Splenocytes isolated from these mice and stimulated with LPS or α-CD3/CD28 had reduced production of IL-6, TNF-α and

IFN-γ. However, this defect was observed in stimulated splenocytes from wild-type mice treated with ONX 0914 alone (and has been observed previously by the same group (158)), suggesting a specialized function of β5i in promoting cytokine production that is not shared by the other immunosubunits. Because the cytokine studies in mice lacking immunoproteasome activity were performed in splenocytes stimulated *ex vivo* or in other models, it is unknown whether these mice display defects in cytokine production in response to LCMV or other viruses *in vivo.* The relatively modest effect of impaired immunoproteasome activity on the generation of LCMV-specific IFN-γ^+ CD8 T cells suggests that overall IFN-γ production may be unaffected. However, these mice may still have defects in production of other cytokines, such as IL-6 or TNF-α, in response to LCMV or other viruses.

Immunoproteasome subunits are transcriptionally induced in the brain following LCMV infection (159). Mature immunoproteasome assembly is almost exclusively restricted to microglial-like cells, while only immunoproteasome precursors exist in astrocytes and do not exist at all in neurons or oligodendrocytes. LCMV-induced meningitis is delayed and less severe in $\beta5i^{-/-}$ mice, suggesting a role for microglial immunoproteasomes in exacerbating immunopathology. The lack of mature immunoproteasome assembly in astrocytes may be due to a posttranslational mechanism that prevents excess immunoproteasome assembly in the brain. Since cells in the central nervous system (CNS) regenerate poorly or not at all, inhibition of immunoproteasome

assembly might be a strategy to protect these cells from immunopathological destruction.

The above studies demonstrate subtle and possible organ- or virus-specific roles for the immunoproteasome during viral infection using mice deficient in only one or two immunosubunits. To assess the role of complete immunoproteasome deficiency, a recent study generated mice deficient in all three immunoproteasome subunits (triply deficient mice) (160). This had not been performed previously because the *LMP2* and *LMP7* genes (encoding β1i and β5i, respectively) are closely linked on the same chromosome and flank the *TAP1* transporter gene, so that breeding $\beta1i^{-/-}$ and $\beta5i^{-/-}$ mice with each other would not likely result in a double knockout and leave *TAP1* unaffected. However, Kincaid et al. used a sequential deletion strategy to first generate β1i/β5i doubly deficient mice, which were then bred to $\beta2i^{-/-}$ mice to generate the triply deficient mice. APCs from these mice display profound defects in MHC class I antigen presentation, defects that are much more severe than those previously described in β1i, β2i, or β5i single knockout mice. These findings suggest that there may be functional overlap between the immunosubunits, and that the crucial role of immunoproteasomes in MHC class I antigen presentation has been obscured or underestimated by the use of mice deficient in only one immunosubunit. Triply deficient mice have an approximately 50% reduction in surface levels of MHC class I (160). This is likely due to a reduction in the supply of peptides available to bind to MHC class I molecules within the cell, rather than a defect in MHC class I expression itself. Of note, a similar 50% reduction of

MHC class I surface expression is also observed in $\beta5i^{-/-}$ mice, but not mice lacking either $\beta1i$ or $\beta2i$, probably because $\beta5i^{-/-}$ mice have a more severe defect in immunoproteasome assembly than $\beta1i^{-/-}$ or $\beta2i^{-/-}$ mice (161). Presentation of nearly all MHC class I epitopes examined is significantly decreased in immunosubunit triply deficient mice both *in vitro* and *in vivo*. During LCMV infection, triply deficient mice display substantially weaker CD8 T cell responses than wild-type mice. This is due to defects in antigen presentation (and not to pleiotropic effects on T cells), because weaker T cell responses are also observed in wild-type T cells transferred into triply deficient mice. MHC class II epitope presentation and $CD4^+$ T cell responses are similar in wild-type and triply deficient mice, suggesting that the immunoproteasome does not affect processing of MHC class II antigens. It remains to be seen whether complete immunoproteasome deficiency (and the resulting substantially weaker CD8 T cell response) affects viral replication or other virus-induced inflammatory responses, such as cytokine production.

In addition to defects in antigen presentation, triply deficient mice have a peptide repertoire that substantially differs from wild-type or singly deficient mice (160). Only about 50% of the peptides presented on MHC class I molecules are shared between wild-type and triply deficient mice. This difference is significant enough that wild-type cells are rejected when transplanted into triply deficient mice, but not vice versa, suggesting that the triply deficient mice are not tolerant of epitopes generated by immunoproteasomes in wild-type mice. Although the

finding is intriguing, this study was not the first to demonstrate rejection of wild-type cells in immunoproteasome-deficient mice.

Two previous studies made similar findings in mice missing only one or two immunosubunits. Toes et al. analyzed the peptides generated by proteasomes from wild-type and $\beta5i^{-/-}$ B cells using the protein enolase-1 as an unmodified substrate (162). In comparing peptides from the two mouse strains, the authors concluded that approximately 50% of cleavage fragments were produced by the standard proteasome alone, and only 25% of peptides were produced by both standard proteasomes and immunoproteasomes. When these mice were used in skin grafting experiments, $\beta5i^{-/-}$ mice rejected skin transplants from wild-type mice, but not vice versa. This indicates that wild-type cells, which express both standard proteasomes and immunoproteasomes, trigger a CD8 T cell response in the $\beta5i^{-/-}$ mice, which express standard proteasomes only (or possibly also a minor population of mixed proteasomes). Transplanting $\beta5i^{-/-}$ cells into wild-type mice does not trigger the same response, however, because all of the peptides presented by $\beta5i^{-/-}$ cells are shared by wild-type cells. Expanding on these findings, de Verteuil et al. performed an analysis of peptides presented on MHC class I molecules of DCs from wild-type and $\beta2i^{-/-}\beta5i^{-/-}$ mice (163). Their results indicate that approximately 15% of MHC class I peptides are completely dependent on the immunoproteasome. When $\beta2i^{-/-}\beta5i^{-/-}$ mice were immunized with wild-type DCs, they generated wild-type-specific CD8 T cells. This again suggests that immunoproteasomes generate a unique set of peptides that direct CD8 T cell responses.

The finding that standard proteasomes and immunoproteasomes generate such vastly different peptide repertoires has important implications. Under non-inflammatory conditions, the peptides presented on DCs (which constitutively express both standard proteasomes and immunoproteasomes) will be significantly different from the peptides displayed on nonimmune parenchymal cells (which express only standard proteasomes). This implies that CD8 T cells stimulated by DCs may not efficiently recognize peptides displayed by nonimmune cells until immunoproteasomes are induced in those cells by IFN. In cells that do not respond to IFN-γ and/or do not express immunoproteasomes, such as cells infected with a virus that inhibits IFN-γ signaling, this could suppress CD8 T cell responses and contribute to immune evasion. The different peptide repertoires observed between standard proteasomes and immunoproteasomes also have implications for acute inflammatory responses and vaccine design. During LCMV or *Listeria monocytogenes* infection, standard proteasomes in the liver are almost completely replaced by immunoproteasomes within the first 7 days of infection, leading to strongly altered proteasome activity (164). This suggests that CD8 T cell responses during the acute phase of viral and bacterial infection are primarily directed at immunoproteasome-dependent epitopes. Vaccines directed against epitopes that are poorly processed by the immunoproteasome would likely exhibit a less robust CD8 T cell response and not generate optimal protection against a particular pathogen.

Interestingly, immunoproteasomes assemble approximately four times faster than, and show greatly reduced stability relative to standard proteasomes

(165). This suggests that immunoproteasome induction is a tightly regulated process, in which cytokines induced during the first few days of a viral infection signal a pressing need for immunoproteasome activity in the infected tissue. The relative instability of immunoproteasomes would provide a means for infected cells and tissues to quickly return to a normal state once immunoproteasomes are no longer needed, and it may suggest that ongoing or long-term immunoproteasome expression could actually be detrimental.

The role of the immunoproteasome during viral infection is still largely undefined, and there is evidence for organ-, virus- and mouse strain-specific effects. Further studies are needed, especially with the newly-generated triply deficient mice in which immunoproteasome activity is completely absent. Most studies examining immunoproteasome function during viral infection have focused almost exclusively on the effect of immunoproteasome subunits in shaping the repertoire of peptides available for MHC class I processing, and thus the hierarchy of CD8 T cell responses. However, the main function of the immunoproteasome during viral infection may actually be independent of the MHC class I antigen processing pathway. This is supported by the fact that B and T cells, which do not generally have a significant role as antigen-presenting cells (via MHC class I), express immunoproteasomes. A number of studies have suggested major roles for the immunoproteasome in T cell proliferation and survival, and there are hints from $\beta 1i^{-/-}$ mice that the immunoproteasome is also important for B cell development, as described above.

Accumulating evidence suggests that the immunoproteasome is critical for the removal of oxidized proteins and adaptation to oxidative stress (56, 72, 166-169). During coxsackievirus B3 (CVB3)-induced myocarditis, $\beta5i^{-/-}$ mice developed more severe myocardial tissue damage compared to wild-type mice (143). This was not due to a direct effect on viral replication. It is interesting to note that CD8 T cell responses in the heart, as measured by flow cytometry and immunohistochemistry, were equivalent or even slightly enhanced in $\beta5i^{-/-}$ mice after CVB3 infection, suggesting that severe tissue damage in $\beta5i^{-/-}$ mice was not due to an alteration in the CD8 T cell response. Rather, cardiomyocytes and inflammatory cells from $\beta5i^{-/-}$ mice showed increased accumulation of poly-ubiquitinated protein conjugates and oxidant-damaged proteins following treatment with IFN-γ. Hearts from CVB3-infected $\beta5i^{-/-}$ showed significant apoptotic cell death compared to infected wild-type mice. These findings suggest that the immunoproteasome protects cells from cytokine-induced proteotoxic stress by removing polyubiquitinated or oxidant-damaged proteins. Whether this role for the immunoproteasome is unique to CVB3-induced myocarditis or can be applied to other viral infections and disease states is unknown.

A recent study has suggested a new role for immunoproteasomes in maintaining cellular homeostasis (130). Raule et al. demonstrated that 26S immunoproteasomes degrade basic proteins at 4-6-fold higher rates compared to 26S standard proteasomes. This effect is observed specifically for proteins with a basic isoelectric point (high content in lysine and arginine residues), and not for neutral proteins. Histones, in particular, are extremely basic. Stimulation of cells

with proinflammatory cytokines induces transcription of hundreds of genes through multiple regulatory pathways (170, 171). Accumulation of free histones released from these sites of transcription could result in genomic instability and transcriptional inhibition (172). The ability of immunoproteasomes to remove excess free histones more efficiently than standard proteasomes could be an important mechanism by which immunoproteasomes maintain cellular homeostasis under conditions of stress and inflammation. This also suggests an additional reason for why CVB3-infected $\beta5i^{-/-}$ mice display increased cellular damage and apoptotic cell death in heart tissue compared to wild-type mice. Perhaps $\beta5i^{-/-}$ mice are unable to cope with the combined accumulation of oxidant-damage proteins and excess free histones in response to cytokine-induced stress and transcriptional activation.

Few studies have examined the effect of immunoproteasome deficiency on inflammation and protection of cells from virus- or cytokine-induced death during viral infection. It would be interesting to extend studies with influenza, MCMV, LCMV, or other viruses to assess the role of the immunoproteasome in other aspects of the inflammatory response besides the generation of virus-specific epitopes for CD8 T cell responses.

Pathogen Interaction with the Immunoproteasome

Components of many pathogens have been shown to interact with the immunoproteasome pathway. Perhaps not surprisingly, many of these pathogens establish chronic or persistent infections. Interference with the

immunoproteasome pathway may be a common mechanism by which these pathogens inhibit CD8 T cell responses, either during acute infection to establish persistence or during long-term infection to evade the immune system.

HIV-1 inhibits immunoproteasome function, likely by a number of mechanisms (41). Expression of viral p24 downregulates PA28β, β2i, and β5i in a DC line (JAWS II) and primary DCs. Exposure of those cell lines to HIV-1 p24 leads to a decrease in antigen presentation that can be overcome by pretreatment of cells with IFN-γ (such that the immunoproteasome is already upregulated by the time of p24 addition) (173). HIV-1 Tat protein interacts with six β subunits of the standard 20S proteasome, as well as the immunosubunits β2i and β5i, to decrease catalytic activity (174). Tat also binds to two α subunits, α4 and α7, preventing interaction of PA28 with the 20S core (175).

The HCV non-structural protein NS3 directly binds to β5i and reduces immunoproteasome activity (176). Downregulation of immunoproteasome protease activity has been suggested as a mechanism by which HCV could interfere with processing of viral antigens for presentation on MHC class I and could avoid host immune surveillance during persistent infection.

Human adenovirus E1A interacts with the immunoproteasome subunit β2i, but not its constitutive counterpart β2. E1A expression (either through adenovirus infection or transient transfection) prevents IFN-γ-induced upregulation of immunoproteasome subunit expression by interfering with STAT1 phosphorylation (177). Adenoviruses have developed many other pre- and post-translational strategies to interfere with MHC class I processing and presentation

that are independent of direct interactions of viral proteins and immunoproteasome subunits (reviewed in (178)).

Both HCMV and MCMV inhibit IFN-γ-induced immunoproteasome formation in fibroblasts *in vitro* (179). Inhibition of immunoproteasome formation occurs at a pretranscriptional level, because transcriptional upregulation of PA28α/β, as well as all three immunosubunits, is impaired. When cells are infected with an MCMV virus lacking M27, a gene that encodes a STAT2 inhibitor that interferes with IFN-γ receptor signaling, immunoproteasome expression is no longer inhibited.

Infection of HeLa cells with the protozoan *Trypanosoma cruzi* downregulates IFN-γ-induced biosynthesis of virtually all components of the MHC class I pathway, including all three immunosubunits, the immunoproteasome regulatory subunit PA28β, plus TAP1 and MHC class I. *T cruzi* infection also decreases proteolytic activity of the immunoproteasome. This was attributed to an unknown posttranscriptional mechanism that inhibits expression of components of the MHC class I pathway, probably a parasite component that inhibits IFN signaling (180). However, an earlier study concluded that *T. cruzi* reduces IFN-γ-mediated immunoproteasome expression in macrophages through release of reactive oxygen species (ROS), which leads to inhibition of protein tyrosine phosphatase activity (181). This in turn activates c-Jun/AP-1 signaling, which has been previously shown to negatively regulate MHC class I expression (182). It therefore seems possible that *T. cruzi* has developed multiple ways to

inhibit IFN-γ-induced immunoproteasome formation, or that mechanisms of inhibition vary between cell types.

Conclusions

CD8 T cells often play significant roles during viral infection. In endogenous antigen presentation, the proteasome is crucial for the generation of antigenic peptides for binding to MHC class I and promoting CD8 T cell responses. The immunoproteasome is a specialized type of proteasome with altered peptide cleavage properties that is constitutively expressed in hematopoietic cells and induced in nonimmune cells under conditions of inflammation. Evidence suggests that the immunoproteasome may play an important role during viral infection through regulation of CD8 T cell responses, activation of the NF-κB pathway, and management of oxidative stress. Many pathogens have mechanisms of interfering with MHC class I processing, including direct interaction with immunoproteasome subunits. It is essential to better understand the role of the immunoproteasome in different cell types, tissues, and hosts in the context of diverse inflammatory states. An improved understanding of the mechanisms of immunoproteasome function could aid in the development of vaccines and treatment strategies for viral infections.

References

1. **Falk K, Rötzschke O, Stevanović S, Jung G, Rammensee HG.** 1991. Allele-specific motifs revealed by sequencing of self-peptides eluted from MHC molecules. Nature **351:**290-296.
2. **Rock KL, Gramm C, Rothstein L, Clark K, Stein R, Dick L, Hwang D, Goldberg AL.** 1994. Inhibitors of the proteasome block the degradation of most cell proteins and the generation of peptides presented on MHC class I molecules. Cell **78:**761-771.
3. **Stoltze L, Schirle M, Schwarz G, Schröter C, Thompson MW, Hersh LB, Kalbacher H, Stevanovic S, Rammensee HG, Schild H.** 2000. Two new proteases in the MHC class I processing pathway. Nat Immunol **1:**413-418.
4. **Snyder HL, Yewdell JW, Bennink JR.** 1994. Trimming of antigenic peptides in an early secretory compartment. J Exp Med **180:**2389-2394.
5. **Craiu A, Akopian T, Goldberg A, Rock KL.** 1997. Two distinct proteolytic processes in the generation of a major histocompatibility complex class I-presented peptide. Proc Natl Acad Sci USA **94:**10850-10855.
6. **Neefjes JJ, Momburg F, Hämmerling GJ.** 1993. Selective and ATP-dependent translocation of peptides by the MHC-encoded transporter. Science **261:**769-771.
7. **Garbi N, Tan P, Diehl AD, Chambers BJ, Ljunggren HG, Momburg F, Hämmerling GJ.** 2000. Impaired immune responses and altered peptide repertoire in tapasin-deficient mice. Nat Immunol **1:**234-238.
8. **Ortmann B, Copeman J, Lehner PJ, Sadasivan B, Herberg JA, Grandea AG, Riddell SR, Tampé R, Spies T, Trowsdale J, Cresswell P.** 1997. A critical role for tapasin in the assembly and function of multimeric MHC class I-TAP complexes. Science **277:**1306-1309.
9. **Dick TP, Bangia N, Peaper DR, Cresswell P.** 2002. Disulfide bond isomerization and the assembly of MHC class I-peptide complexes. Immunity **16:**87-98.
10. **Tanaka K.** 1995. Molecular biology of proteasomes. Mol Biol Rep **21:**21-26.
11. **Groettrup M, Soza A, Kuckelkorn U, Kloetzel PM.** 1996. Peptide antigen production by the proteasome: complexity provides efficiency. Immunol Today **17:**429-435.
12. **Craiu A, Gaczynska M, Akopian T, Gramm CF, Fenteany G, Goldberg AL, Rock KL.** 1997. Lactacystin and clasto-lactacystin beta-lactone modify multiple proteasome beta-subunits and inhibit intracellular protein degradation and major histocompatibility complex class I antigen presentation. J Biol Chem **272:**13437-13445.
13. **Unno M, Mizushima T, Morimoto Y, Tomisugi Y, Tanaka K, Yasuoka N, Tsukihara T.** 2002. The structure of the mammalian 20S proteasome at 2.75 A resolution. Structure **10:**609-618.

14. **Groll M, Ditzel L, Löwe J, Stock D, Bochtler M, Bartunik HD, Huber R.** 1997. Structure of 20S proteasome from yeast at 2.4 A resolution. Nature **386:**463-471.
15. **DeMartino GN, Slaughter CA.** 1999. The proteasome, a novel protease regulated by multiple mechanisms. J Biol Chem **274:**22123-22126.
16. **Glynne R, Powis SH, Beck S, Kelly A, Kerr LA, Trowsdale J.** 1991. A proteasome-related gene between the two ABC transporter loci in the class II region of the human MHC. Nature **353:**357-360.
17. **Kelly A, Powis SH, Glynne R, Radley E, Beck S, Trowsdale J.** 1991. Second proteasome-related gene in the human MHC class II region. Nature **353:**667-668.
18. **Ortiz-Navarrete V, Seelig A, Gernold M, Frentzel S, Kloetzel PM, Hämmerling GJ.** 1991. Subunit of the '20S' proteasome (multicatalytic proteinase) encoded by the major histocompatibility complex. Nature **353:**662-664.
19. **Aki M, Shimbara N, Takashina M, Akiyama K, Kagawa S, Tamura T, Tanahashi N, Yoshimura T, Tanaka K, Ichihara A.** 1994. Interferon-gamma induces different subunit organizations and functional diversity of proteasomes. J Biochem **115:**257-269.
20. **Tanaka K.** 1994. Role of proteasomes modified by interferon-gamma in antigen processing. J Leukoc Biol **56:**571-575.
21. **Groettrup M, Kraft R, Kostka S, Standera S, Stohwasser R, Kloetzel PM.** 1996. A third interferon-gamma-induced subunit exchange in the 20S proteasome. Eur J Immunol **26:**863-869.
22. **Nandi D, Jiang H, Monaco JJ.** 1996. Identification of MECL-1 (LMP-10) as the third IFN-gamma-inducible proteasome subunit. J Immunol **156:**2361-2364.
23. **Hisamatsu H, Shimbara N, Saito Y, Kristensen P, Hendil KB, Fujiwara T, Takahashi E, Tanahashi N, Tamura T, Ichihara A, Tanaka K.** 1996. Newly identified pair of proteasomal subunits regulated reciprocally by interferon gamma. J Exp Med **183:**1807-1816.
24. **Namiki S, Nakamura T, Oshima S, Yamazaki M, Sekine Y, Tsuchiya K, Okamoto R, Kanai T, Watanabe M.** 2005. IRF-1 mediates upregulation of LMP7 by IFN-gamma and concerted expression of immunosubunits of the proteasome. FEBS Lett **579:**2781-2787.
25. **Chatterjee-Kishore M, Kishore R, Hicklin DJ, Marincola FM, Ferrone S.** 1998. Different requirements for signal transducer and activator of transcription 1alpha and interferon regulatory factor 1 in the regulation of low molecular mass polypeptide 2 and transporter associated with antigen processing 1 gene expression. J Biol Chem **273:**16177-16183.
26. **Foss GS, Prydz H.** 1999. Interferon regulatory factor 1 mediates the interferon-gamma induction of the human immunoproteasome subunit multicatalytic endopeptidase complex-like 1. J Biol Chem **274:**35196-35202.

27. **Brucet M, Marqués L, Sebastián C, Lloberas J, Celada A.** 2004. Regulation of murine Tap1 and Lmp2 genes in macrophages by interferon gamma is mediated by STAT1 and IRF-1. Genes and Immunity **5:**26-35.
28. **Freudenburg W, Gautam M, Chakraborty P, James J, Richards J, Salvatori AS, Baldwin A, Schriewer J, Buller RML, Corbett JA, Skowyra D.** 2013. Immunoproteasome Activation During Early Antiviral Response in Mouse Pancreatic β-cells: New Insights into Auto-antigen Generation in Type I Diabetes? J Clin Cell Immunol **4**.
29. **Freudenburg W, Gautam M, Chakraborty P, James J, Richards J, Salvatori AS, Baldwin A, Schriewer J, Buller RML, Corbett JA, Skowyra D.** 2013. Reduction in ATP levels triggers immunoproteasome activation by the 11S (PA28) regulator during early antiviral response mediated by IFNβ in mouse pancreatic β-cells. PLoS ONE **8:**e52408.
30. **Shin E-C, Seifert U, Kato T, Rice CM, Feinstone SM, Kloetzel P-M, Rehermann B.** 2006. Virus-induced type I IFN stimulates generation of immunoproteasomes at the site of infection. J Clin Invest **116:**3006-3014.
31. **Murata S, Sasaki K, Kishimoto T, Niwa S-I, Hayashi H, Takahama Y, Tanaka K.** 2007. Regulation of CD8+ T cell development by thymus-specific proteasomes. Science **316:**1349-1353.
32. **Nitta T, Murata S, Sasaki K, Fujii H, Ripen AM, Ishimaru N, Koyasu S, Tanaka K, Takahama Y.** 2010. Thymoproteasome shapes immunocompetent repertoire of CD8+ T cells. Immunity **32:**29-40.
33. **Xing Y, Jameson SC, Hogquist KA.** 2013. Thymoproteasome subunit-β5T generates peptide-MHC complexes specialized for positive selection. Proc Natl Acad Sci USA **110:**6979-6984.
34. **Griffin TA, Nandi D, Cruz M, Fehling HJ, Kaer LV, Monaco JJ, Colbert RA.** 1998. Immunoproteasome assembly: cooperative incorporation of interferon gamma (IFN-gamma)-inducible subunits. J Exp Med **187:**97-104.
35. **Groettrup M, Standera S, Stohwasser R, Kloetzel PM.** 1997. The subunits MECL-1 and LMP2 are mutually required for incorporation into the 20S proteasome. Proc Natl Acad Sci USA **94:**8970-8975.
36. **De M, Jayarapu K, Elenich L, Monaco JJ, Colbert RA, Griffin TA.** 2003. Beta 2 subunit propeptides influence cooperative proteasome assembly. J Biol Chem **278:**6153-6159.
37. **Kingsbury DJ, Griffin TA, Colbert RA.** 2000. Novel propeptide function in 20 S proteasome assembly influences beta subunit composition. J Biol Chem **275:**24156-24162.
38. **Guillaume B, Chapiro J, Stroobant V, Colau D, Van Holle B, Parvizi G, Bousquet-Dubouch M-P, Théate I, Parmentier N, Van den Eynde BJ.** 2010. Two abundant proteasome subtypes that uniquely process some antigens presented by HLA class I molecules. Proc Natl Acad Sci USA **107:**18599-18604.
39. **Ebstein F, Kloetzel P-M, Krüger E, Seifert U.** 2012. Emerging roles of immunoproteasomes beyond MHC class I antigen processing. Cell Mol Life Sci **69:**2543-2558.

40. **Noda C, Tanahashi N, Shimbara N, Hendil KB, Tanaka K.** 2000. Tissue distribution of constitutive proteasomes, immunoproteasomes, and PA28 in rats. Biochem Biophys Res Commun **277:**348-354.
41. **Haorah J, Heilman D, Diekmann C, Osna N, Donohue TM, Ghorpade A, Persidsky Y.** 2004. Alcohol and HIV decrease proteasome and immunoproteasome function in macrophages: implications for impaired immune function during disease. Cell Immunol **229:**139-148.
42. **Frisan T, Levitsky V, Masucci MG.** 2000. Variations in proteasome subunit composition and enzymatic activity in B-lymphoma lines and normal B cells. Int J Cancer **88:**881-888.
43. **Frisan T, Levitsky V, Polack A, Masucci MG.** 1998. Phenotype-dependent differences in proteasome subunit composition and cleavage specificity in B cell lines. J Immunol **160:**3281-3289.
44. **Altun M, Galardy PJ, Shringarpure R, Hideshima T, LeBlanc R, Anderson KC, Ploegh HL, Kessler BM.** 2005. Effects of PS-341 on the activity and composition of proteasomes in multiple myeloma cells. Cancer Res **65:**7896-7901.
45. **Macagno A, Gilliet M, Sallusto F, Lanzavecchia A, Nestle FO, Groettrup M.** 1999. Dendritic cells up-regulate immunoproteasomes and the proteasome regulator PA28 during maturation. Eur J Immunol **29:**4037-4042.
46. **Macagno A, Kuehn L, de Giuli R, Groettrup M.** 2001. Pronounced up-regulation of the PA28alpha/beta proteasome regulator but little increase in the steady-state content of immunoproteasome during dendritic cell maturation. Eur J Immunol **31:**3271-3280.
47. **Ossendorp F, Fu N, Camps M, Granucci F, Gobin SJP, van den Elsen PJ, Schuurhuis D, Adema GJ, Lipford GB, Chiba T, Sijts A, Kloetzel P-M, Ricciardi-Castagnoli P, Melief CJM.** 2005. Differential expression regulation of the alpha and beta subunits of the PA28 proteasome activator in mature dendritic cells. J Immunol **174:**7815-7822.
48. **Li J, Schuler-Thurner B, Schuler G, Huber C, Seliger B.** 2001. Bipartite regulation of different components of the MHC class I antigen-processing machinery during dendritic cell maturation. Int Immunol **13:**1515-1523.
49. **Ebstein F, Lange N, Urban S, Seifert U, Krüger E, Kloetzel P-M.** 2009. Maturation of human dendritic cells is accompanied by functional remodelling of the ubiquitin-proteasome system. Int J Biochem Cell Biol **41:**1205-1215.
50. **Lee CK, Gimeno R, Levy DE.** 1999. Differential regulation of constitutive major histocompatibility complex class I expression in T and B lymphocytes. J Exp Med **190:**1451-1464.
51. **Barton LF, Cruz M, Rangwala R, Deepe GS, Monaco JJ.** 2002. Regulation of immunoproteasome subunit expression in vivo following pathogenic fungal infection. J Immunol **169:**3046-3052.
52. **Chatterjee-Kishore M, Wright KL, Ting JP, Stark GR.** 2000. How Stat1 mediates constitutive gene expression: a complex of unphosphorylated

Stat1 and IRF1 supports transcription of the LMP2 gene. EMBO J **19:**4111-4122.

53. **Hallermalm K, Seki K, Wei C, Castelli C, Rivoltini L, Kiessling R, Levitskaya J.** 2001. Tumor necrosis factor-alpha induces coordinated changes in major histocompatibility class I presentation pathway, resulting in increased stability of class I complexes at the cell surface. Blood **98:**1108-1115.
54. **Singh S, Awasthi N, Egwuagu CE, Wagner BJ.** 2002. Immunoproteasome expression in a nonimmune tissue, the ocular lens. Archives of Biochemistry and Biophysics **405:**147-153.
55. **Piccinini M, Mostert M, Croce S, Baldovino S, Papotti M, Rinaudo MT.** 2003. Interferon-gamma-inducible subunits are incorporated in human brain 20S proteasome. J Neuroimmunol **135:**135-140.
56. **Ferrington DA, Hussong SA, Roehrich H, Kapphahn RJ, Kavanaugh SM, Heuss ND, Gregerson DS.** 2008. Immunoproteasome responds to injury in the retina and brain. J Neurochem **106:**158-169.
57. **Baumeister W, Walz J, Zühl F, Seemüller E.** 1998. The proteasome: paradigm of a self-compartmentalizing protease. Cell **92:**367-380.
58. **Navon A, Goldberg AL.** 2001. Proteins are unfolded on the surface of the ATPase ring before transport into the proteasome. Mol Cell **8:**1339-1349.
59. **Benaroudj N, Tarcsa E, Cascio P, Goldberg AL.** 2001. The unfolding of substrates and ubiquitin-independent protein degradation by proteasomes. Biochimie **83:**311-318.
60. **Rivett AJ, Bose S, Brooks P, Broadfoot KI.** 2001. Regulation of proteasome complexes by gamma-interferon and phosphorylation. Biochimie **83:**363-366.
61. **Groll M, Bajorek M, Köhler A, Moroder L, Rubin DM, Huber R, Glickman MH, Finley D.** 2000. A gated channel into the proteasome core particle. Nat Struct Biol **7:**1062-1067.
62. **Köhler A, Cascio P, Leggett DS, Woo KM, Goldberg AL, Finley D.** 2001. The axial channel of the proteasome core particle is gated by the Rpt2 ATPase and controls both substrate entry and product release. Mol Cell **7:**1143-1152.
63. **Whitby FG, Masters EI, Kramer L, Knowlton JR, Yao Y, Wang CC, Hill CP.** 2000. Structural basis for the activation of 20S proteasomes by 11S regulators. Nature **408:**115-120.
64. **Coux O, Tanaka K, Goldberg AL.** 1996. Structure and functions of the 20S and 26S proteasomes. Annu Rev Biochem **65:**801-847.
65. **Osmulski PA, Hochstrasser M, Gaczynska M.** 2009. A tetrahedral transition state at the active sites of the 20S proteasome is coupled to opening of the alpha-ring channel. Structure **17:**1137-1147.
66. **Osmulski PA, Gaczynska M.** 2002. Nanoenzymology of the 20S proteasome: proteasomal actions are controlled by the allosteric transition. Biochemistry **41:**7047-7053.

67. **Osmulski PA, Gaczynska M.** 2000. Atomic force microscopy reveals two conformations of the 20 S proteasome from fission yeast. J Biol Chem **275:**13171-13174.
68. **Raule M, Cerruti F, Benaroudj N, Migotti R, Kikuchi J, Bachi A, Navon A, Dittmar G, Cascio P.** 2014. PA28αβ Reduces Size and Increases Hydrophilicity of 20S Immunoproteasome Peptide Products. Chemistry & Biology.
69. **Cascio P, Hilton C, Kisselev AF, Rock KL, Goldberg AL.** 2001. 26S proteasomes and immunoproteasomes produce mainly N-extended versions of an antigenic peptide. EMBO J **20:**2357-2366.
70. **Ciechanover A.** 1994. The ubiquitin-proteasome proteolytic pathway. Cell **79:**13-21.
71. **Davies KJ.** 2001. Degradation of oxidized proteins by the 20S proteasome. Biochimie **83:**301-310.
72. **Pickering AM, Koop AL, Teoh CY, Ermak G, Grune T, Davies KJA.** 2010. The immunoproteasome, the 20S proteasome and the PA28αβ proteasome regulator are oxidative-stress-adaptive proteolytic complexes. Biochem J **432:**585-594.
73. **Reinheckel T, Sitte N, Ullrich O, Kuckelkorn U, Davies KJ, Grune T.** 1998. Comparative resistance of the 20S and 26S proteasome to oxidative stress. Biochem J **335 (Pt 3):**637-642.
74. **Teoh CY, Davies KJA.** 2004. Potential roles of protein oxidation and the immunoproteasome in MHC class I antigen presentation: the 'PrOxI' hypothesis. Arch Biochem Biophys **423:**88-96.
75. **Yewdell JW.** 2001. Not such a dismal science: the economics of protein synthesis, folding, degradation and antigen processing. Trends in cell biology **11:**294-297.
76. **Schimke RT, Doyle D.** 1970. Control of enzyme levels in animal tissues. Annu Rev Biochem **39:**929-976.
77. **Goldberg AL, St John AC.** 1976. Intracellular protein degradation in mammalian and bacterial cells: Part 2. Annu Rev Biochem **45:**747-803.
78. **Yewdell JW, Schubert U, Bennink JR.** 2001. At the crossroads of cell biology and immunology: DRiPs and other sources of peptide ligands for MHC class I molecules. J Cell Sci **114:**845-851.
79. **Yewdell JW, Antón LC, Bennink JR.** 1996. Defective ribosomal products (DRiPs): a major source of antigenic peptides for MHC class I molecules? J Immunol **157:**1823-1826.
80. **Esquivel F, Yewdell J, Bennink J.** 1992. RMA/S cells present endogenously synthesized cytosolic proteins to class I-restricted cytotoxic T lymphocytes. J Exp Med **175:**163-168.
81. **Khan S, De Giuli R, Schmidtke G, Bruns M, Buchmeier M, Van Den Broek M, Groettrup M.** 2001. Cutting edge: neosynthesis is required for the presentation of a T cell epitope from a long-lived viral protein. J Immunol **167:**4801-4804.

82. **Reits EA, Vos JC, Grommé M, Neefjes J.** 2000. The major substrates for TAP in vivo are derived from newly synthesized proteins. Nature **404:**774-778.
83. **Schild H, Rammensee HG.** 2000. Perfect use of imperfection. Nature **404:**709-710.
84. **Reits E, Griekspoor A, Neijssen J, Groothuis T, Jalink K, van Veelen P, Janssen H, Calafat J, Drijfhout JW, Neefjes J.** 2003. Peptide diffusion, protection, and degradation in nuclear and cytoplasmic compartments before antigen presentation by MHC class I. Immunity **18:**97-108.
85. **Princiotta MF, Finzi D, Qian S-B, Gibbs J, Schuchmann S, Buttgereit F, Bennink JR, Yewdell JW.** 2003. Quantitating protein synthesis, degradation, and endogenous antigen processing. Immunity **18:**343-354.
86. **Yewdell JW, Reits E, Neefjes J.** 2003. Making sense of mass destruction: quantitating MHC class I antigen presentation. Nat Rev Immunol **3:**952-961.
87. **Ben-Shahar S, Komlosh A, Nadav E, Shaked I, Ziv T, Admon A, DeMartino GN, Reiss Y.** 1999. 26 S proteasome-mediated production of an authentic major histocompatibility class I-restricted epitope from an intact protein substrate. J Biol Chem **274:**21963-21972.
88. **Fruci D, Lauvau G, Saveanu L, Amicosante M, Butler RH, Polack A, Ginhoux F, Lemonnier F, Firat H, van Endert PM.** 2003. Quantifying recruitment of cytosolic peptides for HLA class I presentation: impact of TAP transport. J Immunol **170:**2977-2984.
89. **Pamer E, Cresswell P.** 1998. Mechanisms of MHC class I--restricted antigen processing. Annu Rev Immunol **16:**323-358.
90. **Villanueva MS, Fischer P, Feen K, Pamer EG.** 1994. Efficiency of MHC class I antigen processing: a quantitative analysis. Immunity **1:**479-489.
91. **Driscoll J, Brown MG, Finley D, Monaco JJ.** 1993. MHC-linked LMP gene products specifically alter peptidase activities of the proteasome. Nature **365:**262-264.
92. **Gaczynska M, Rock KL, Goldberg AL.** 1993. Gamma-interferon and expression of MHC genes regulate peptide hydrolysis by proteasomes. Nature **365:**264-267.
93. **Gaczynska M, Goldberg AL, Tanaka K, Hendil KB, Rock KL.** 1996. Proteasome subunits X and Y alter peptidase activities in opposite ways to the interferon-gamma-induced subunits LMP2 and LMP7. J Biol Chem **271:**17275-17280.
94. **Früh K, Gossen M, Wang K, Bujard H, Peterson PA, Yang Y.** 1994. Displacement of housekeeping proteasome subunits by MHC-encoded LMPs: a newly discovered mechanism for modulating the multicatalytic proteinase complex. EMBO J **13:**3236-3244.
95. **Kisselev AF, Akopian TN, Woo KM, Goldberg AL.** 1999. The sizes of peptides generated from protein by mammalian 26 and 20 S proteasomes. Implications for understanding the degradative mechanism and antigen presentation. J Biol Chem **274:**3363-3371.

96. **Niedermann G, Butz S, Ihlenfeldt HG, Grimm R, Lucchiari M, Hoschützky H, Jung G, Maier B, Eichmann K.** 1995. Contribution of proteasome-mediated proteolysis to the hierarchy of epitopes presented by major histocompatibility complex class I molecules. Immunity **2:**289-299.
97. **Lucchiari-Hartz M, van Endert PM, Lauvau G, Maier R, Meyerhans A, Mann D, Eichmann K, Niedermann G.** 2000. Cytotoxic T lymphocyte epitopes of HIV-1 Nef: Generation of multiple definitive major histocompatibility complex class I ligands by proteasomes. J Exp Med **191:**239-252.
98. **Niedermann G, Geier E, Lucchiari-Hartz M, Hitziger N, Ramsperger A, Eichmann K.** 1999. The specificity of proteasomes: impact on MHC class I processing and presentation of antigens. Immunol Rev **172:**29-48.
99. **Emmerich NP, Nussbaum AK, Stevanovic S, Priemer M, Toes RE, Rammensee HG, Schild H.** 2000. The human 26 S and 20 S proteasomes generate overlapping but different sets of peptide fragments from a model protein substrate. J Biol Chem **275:**21140-21148.
100. **Beninga J, Rock KL, Goldberg AL.** 1998. Interferon-gamma can stimulate post-proteasomal trimming of the N terminus of an antigenic peptide by inducing leucine aminopeptidase. J Biol Chem **273:**18734-18742.
101. **Tanahashi N, Yokota K, Ahn JY, Chung CH, Fujiwara T, Takahashi E, DeMartino GN, Slaughter CA, Toyonaga T, Yamamura K, Shimbara N, Tanaka K.** 1997. Molecular properties of the proteasome activator PA28 family proteins and gamma-interferon regulation. Genes Cells **2:**195-211.
102. **Ahn JY, Tanahashi N, Akiyama K, Hisamatsu H, Noda C, Tanaka K, Chung CH, Shibmara N, Willy PJ, Mott JD.** 1995. Primary structures of two homologous subunits of PA28, a gamma-interferon-inducible protein activator of the 20S proteasome. FEBS Lett **366:**37-42.
103. **Rechsteiner M, Realini C, Ustrell V.** 2000. The proteasome activator 11 S REG (PA28) and class I antigen presentation. Biochem J **345 Pt 1:**1-15.
104. **Realini C, Dubiel W, Pratt G, Ferrell K, Rechsteiner M.** 1994. Molecular cloning and expression of a gamma-interferon-inducible activator of the multicatalytic protease. J Biol Chem **269:**20727-20732.
105. **Jiang H, Monaco JJ.** 1997. Sequence and expression of mouse proteasome activator PA28 and the related autoantigen Ki. Immunogenetics **46:**93-98.
106. **Honoré B, Leffers H, Madsen P, Celis JE.** 1993. Interferon-gamma up-regulates a unique set of proteins in human keratinocytes. Molecular cloning and expression of the cDNA encoding the RGD-sequence-containing protein IGUP I-5111. Eur J Biochem **218:**421-430.
107. **Ahn K, Erlander M, Leturcq D, Peterson PA, Früh K, Yang Y.** 1996. In vivo characterization of the proteasome regulator PA28. J Biol Chem **271:**18237-18242.
108. **Dubiel W, Pratt G, Ferrell K, Rechsteiner M.** 1992. Purification of an 11 S regulator of the multicatalytic protease. J Biol Chem **267:**22369-22377.

109. **Ma CP, Slaughter CA, DeMartino GN.** 1992. Identification, purification, and characterization of a protein activator (PA28) of the 20 S proteasome (macropain). J Biol Chem **267:**10515-10523.
110. **Cascio P, Call M, Petre BM, Walz T, Goldberg AL.** 2002. Properties of the hybrid form of the 26S proteasome containing both 19S and PA28 complexes. EMBO J **21:**2636-2645.
111. **Hendil KB, Khan S, Tanaka K.** 1998. Simultaneous binding of PA28 and PA700 activators to 20 S proteasomes. Biochem J **332 (Pt 3):**749-754.
112. **Kopp F, Dahlmann B, Kuehn L.** 2001. Reconstitution of hybrid proteasomes from purified PA700-20 S complexes and PA28alphabeta activator: ultrastructure and peptidase activities. J Mol Biol **313:**465-471.
113. **Tanahashi N, Murakami Y, Minami Y, Shimbara N, Hendil KB, Tanaka K.** 2000. Hybrid proteasomes. Induction by interferon-gamma and contribution to ATP-dependent proteolysis. J Biol Chem **275:**14336-14345.
114. **Yang C, Schmidt M.** 2014. Cutting through Complexity: The Proteolytic Properties of Alternate Immunoproteasome Complexes. Chemistry & Biology **21:**435-436.
115. **Groettrup M, Soza A, Eggers M, Kuehn L, Dick TP, Schild H, Rammensee HG, Koszinowski UH, Kloetzel PM.** 1996. A role for the proteasome regulator PA28alpha in antigen presentation. Nature **381:**166-168.
116. **Schwarz K, Van Den Broek M, Kostka S, Kraft R, Soza A, Schmidtke G, Kloetzel PM, Groettrup M.** 2000. Overexpression of the proteasome subunits LMP2, LMP7, and MECL-1, but not PA28 alpha/beta, enhances the presentation of an immunodominant lymphocytic choriomeningitis virus T cell epitope. J Immunol **165:**768-778.
117. **Sun Y, Sijts AJAM, Song M, Janek K, Nussbaum AK, Kral S, Schirle M, Stevanovic S, Paschen A, Schild H, Kloetzel P-M, Schadendorf D.** 2002. Expression of the proteasome activator PA28 rescues the presentation of a cytotoxic T lymphocyte epitope on melanoma cells. Cancer Res **62:**2875-2882.
118. **van Hall T, Sijts A, Camps M, Offringa R, Melief C, Kloetzel PM, Ossendorp F.** 2000. Differential influence on cytotoxic T lymphocyte epitope presentation by controlled expression of either proteasome immunosubunits or PA28. J Exp Med **192:**483-494.
119. **Murata S, Udono H, Tanahashi N, Hamada N, Watanabe K, Adachi K, Yamano T, Yui K, Kobayashi N, Kasahara M, Tanaka K, Chiba T.** 2001. Immunoproteasome assembly and antigen presentation in mice lacking both PA28alpha and PA28beta. EMBO J **20:**5898-5907.
120. **Pickering AM, Davies KJA.** 2012. Differential roles of proteasome and immunoproteasome regulators Pa28αβ, Pa28γ and Pa200 in the degradation of oxidized proteins. Archives of Biochemistry and Biophysics **523:**181-190.
121. **Corbett JA, Wang JL, Hughes JH, Wolf BA, Sweetland MA, Lancaster JR, McDaniel ML.** 1992. Nitric oxide and cyclic GMP formation induced

by interleukin 1 beta in islets of Langerhans. Evidence for an effector role of nitric oxide in islet dysfunction. Biochem J **287 (Pt 1):**229-235.
122. **Collier JJ, Fueger PT, Hohmeier HE, Newgard CB.** 2006. Pro- and antiapoptotic proteins regulate apoptosis but do not protect against cytokine-mediated cytotoxicity in rat islets and beta-cell lines. Diabetes **55:**1398-1406.
123. **Muchamuel T, Basler M, Aujay MA, Suzuki E, Kalim KW, Lauer C, Sylvain C, Ring ER, Shields J, Jiang J, Shwonek P, Parlati F, Demo SD, Bennett MK, Kirk CJ, Groettrup M.** 2009. A selective inhibitor of the immunoproteasome subunit LMP7 blocks cytokine production and attenuates progression of experimental arthritis. Nat Med **15:**781-787.
124. **Parlati F, Lee SJ, Aujay M, Suzuki E, Levitsky K, Lorens JB, Micklem DR, Ruurs P, Sylvain C, Lu Y, Shenk KD, Bennett MK.** 2009. Carfilzomib can induce tumor cell death through selective inhibition of the chymotrypsin-like activity of the proteasome. Blood **114:**3439-3447.
125. **Ho YK, Bargagna-Mohan P, Wehenkel M, Mohan R, Kim K-B.** 2007. LMP2-specific inhibitors: chemical genetic tools for proteasome biology. Chem Biol **14:**419-430.
126. **Wehenkel M, Ban J-O, Ho Y-K, Carmony KC, Hong JT, Kim KB.** 2012. A selective inhibitor of the immunoproteasome subunit LMP2 induces apoptosis in PC-3 cells and suppresses tumour growth in nude mice. Br J Cancer **107:**53-62.
127. **Miller Z, Ao L, Kim KB, Lee W.** 2013. Inhibitors of the immunoproteasome: current status and future directions. Curr Pharm Des **19:**4140-4151.
128. **Kuhn DJ, Hunsucker SA, Chen Q, Voorhees PM, Orlowski M, Orlowski RZ.** 2009. Targeted inhibition of the immunoproteasome is a potent strategy against models of multiple myeloma that overcomes resistance to conventional drugs and nonspecific proteasome inhibitors. Blood **113:**4667-4676.
129. **Kisselev AF, Callard A, Goldberg AL.** 2006. Importance of the different proteolytic sites of the proteasome and the efficacy of inhibitors varies with the protein substrate. J Biol Chem **281:**8582-8590.
130. **Raule M, Cerruti F, Cascio P.** 2014. Enhanced rate of degradation of basic proteins by 26S immunoproteasomes. Biochimica et biophysica acta **1843:**1942-1947.
131. **Huber Eva M, Basler M, Schwab R, Heinemeyer W, Kirk Christopher J, Groettrup M, Groll M.** 2012. Immuno- and Constitutive Proteasome Crystal Structures Reveal Differences in Substrate and Inhibitor Specificity. Cell **148:**727-738.
132. **Vallabhapurapu S, Karin M.** 2009. Regulation and function of NF-kappaB transcription factors in the immune system. Annu Rev Immunol **27:**693-733.
133. **Hayden MS, Ghosh S.** 2008. Shared principles in NF-kappaB signaling. Cell **132:**344-362.

134. **Traenckner EB, Wilk S, Baeuerle PA.** 1994. A proteasome inhibitor prevents activation of NF-kappa B and stabilizes a newly phosphorylated form of I kappa B-alpha that is still bound to NF-kappa B. EMBO J **13:**5433-5441.
135. **Palombella VJ, Rando OJ, Goldberg AL, Maniatis T.** 1994. The ubiquitin-proteasome pathway is required for processing the NF-kappa B1 precursor protein and the activation of NF-kappa B. Cell **78:**773-785.
136. **Hayashi T, Faustman D.** 1999. NOD mice are defective in proteasome production and activation of NF-kappaB. Mol Cell Biol **19:**8646-8659.
137. **Runnels HA, Watkins WA, Monaco JJ.** 2000. LMP2 expression and proteasome activity in NOD mice. Nat Med **6:**1064-1065; author reply 1065-1066.
138. **Kessler BM, Lennon-Duménil AM, Shinohara ML, Lipes MA, Ploegh HL.** 2000. LMP2 expression and proteasome activity in NOD mice. Nat Med **6:**1064; author reply 1065-1066.
139. **Hayashi T, Faustman D.** 2000. Essential role of human leukocyte antigen-encoded proteasome subunits in NF-kappaB activation and prevention of tumor necrosis factor-alpha-induced apoptosis. J Biol Chem **275:**5238-5247.
140. **Maldonado M, Kapphahn RJ, Terluk MR, Heuss ND, Yuan C, Gregerson DS, Ferrington DA.** 2013. Immunoproteasome Deficiency Modifies the Alternative Pathway of NFκB Signaling. PLoS ONE **8:**e56187.
141. **Hensley SE, Zanker D, Dolan BP, David A, Hickman HD, Embry AC, Skon CN, Grebe KM, Griffin TA, Chen W, Bennink JR, Yewdell JW.** 2010. Unexpected role for the immunoproteasome subunit LMP2 in antiviral humoral and innate immune responses. J Immunol **184:**4115-4122.
142. **Jang ER, Lee N-R, Han S, Wu Y, Sharma LK, Carmony KC, Marks J, Lee D-M, Ban J-O, Wehenkel M, Hong JT, Kim KB, Lee W.** 2012. Revisiting the role of the immunoproteasome in the activation of the canonical NF-κB pathway. Mol. BioSyst. **8:**2295-2302.
143. **Opitz E, Koch A, Klingel K, Schmidt F, Prokop S, Rahnefeld A, Sauter M, Heppner FL, Völker U, Kandolf R, Kuckelkorn U, Stangl K, Krüger E, Kloetzel PM, Voigt A.** 2011. Impairment of Immunoproteasome Function by β5i/LMP7 Subunit Deficiency Results in Severe Enterovirus Myocarditis. PLoS Pathog **7:**e1002233.
144. **Morel S, Lévy F, Burlet-Schiltz O, Brasseur F, Probst-Kepper M, Peitrequin AL, Monsarrat B, Van Velthoven R, Cerottini JC, Boon T, Gairin JE, Van den Eynde BJ.** 2000. Processing of some antigens by the standard proteasome but not by the immunoproteasome results in poor presentation by dendritic cells. Immunity **12:**107-117.
145. **Van den Eynde BJ, Morel S.** 2001. Differential processing of class-I-restricted epitopes by the standard proteasome and the immunoproteasome. Curr Opin Immunol **13:**147-153.

146. **Basler M, Beck U, Kirk CJ, Groettrup M.** 2011. The antiviral immune response in mice devoid of immunoproteasome activity. J Immunol **187:**5548-5557.
147. **Van Kaer L, Ashton-Rickardt PG, Eichelberger M, Gaczynska M, Nagashima K, Rock KL, Goldberg AL, Doherty PC, Tonegawa S.** 1994. Altered peptidase and viral-specific T cell response in LMP2 mutant mice. Immunity **1:**533-541.
148. **Basler M, Kirk CJ, Groettrup M.** 2013. The immunoproteasome in antigen processing and other immunological functions. Curr Opin Immunol **25:**74-80.
149. **Chen W, Norbury CC, Cho Y, Yewdell JW, Bennink JR.** 2001. Immunoproteasomes shape immunodominance hierarchies of antiviral CD8(+) T cells at the levels of T cell repertoire and presentation of viral antigens. J Exp Med **193:**1319-1326.
150. **Caudill CM, Jayarapu K, Elenich L, Monaco JJ, Colbert RA, Griffin TA.** 2006. T cells lacking immunoproteasome subunits MECL-1 and LMP7 hyperproliferate in response to polyclonal mitogens. J Immunol **176:**4075-4082.
151. **Zaiss DMW, De Graaf N, Sijts AJAM.** 2008. The proteasome immunosubunit multicatalytic endopeptidase complex-like 1 is a T-cell-intrinsic factor influencing homeostatic expansion. Infection and Immunity **76:**1207-1213.
152. **Basler M, Moebius J, Elenich L, Groettrup M, Monaco JJ.** 2006. An altered T cell repertoire in MECL-1-deficient mice. J Immunol **176:**6665-6672.
153. **Moebius J, Van Den Broek M, Groettrup M, Basler M.** 2010. Immunoproteasomes are essential for survival and expansion of T cells in virus-infected mice. Eur J Immunol **40:**3439-3449.
154. **Hutchinson S, Sims S, O'hara G, Silk J, Gileadi U, Cerundolo V, Klenerman P.** 2011. A dominant role for the immunoproteasome in CD8+ T cell responses to murine cytomegalovirus. PLoS ONE **6:**e14646.
155. **Robek MD, Garcia ML, Boyd BS, Chisari FV.** 2007. Role of immunoproteasome catalytic subunits in the immune response to hepatitis B virus. J Virol **81:**483-491.
156. **Pang KC, Sanders MT, Monaco JJ, Doherty PC, Turner SJ, Chen W.** 2006. Immunoproteasome subunit deficiencies impact differentially on two immunodominant influenza virus-specific CD8+ T cell responses. J Immunol **177:**7680-7688.
157. **Zanker D, Waithman J, Yewdell JW, Chen W.** 2013. Mixed Proteasomes Function To Increase Viral Peptide Diversity and Broaden Antiviral CD8+ T Cell Responses. J Immunol.
158. **Kalim KW, Basler M, Kirk CJ, Groettrup M.** 2012. Immunoproteasome subunit LMP7 deficiency and inhibition suppresses Th1 and Th17 but enhances regulatory T cell differentiation. J Immunol **189:**4182-4193.
159. **Kremer M, Henn A, Kolb C, Basler M, Moebius J, Guillaume B, Leist M, Van Den Eynde BJ, Groettrup M.** 2010. Reduced

Immunoproteasome Formation and Accumulation of Immunoproteasomal Precursors in the Brains of Lymphocytic Choriomeningitis Virus-Infected Mice. J Immunol **185:**5549-5560.

160. **Kincaid EZ, Che JW, York I, Escobar H, Reyes-Vargas E, Delgado JC, Welsh RM, Karow ML, Murphy AJ, Valenzuela DM, Yancopoulos GD, Rock KL.** 2012. Mice completely lacking immunoproteasomes show major changes in antigen presentation. Nat Immunol **13:**129-135.
161. **Fehling HJ, Swat W, Laplace C, Kühn R, Rajewsky K, Müller U, von Boehmer H.** 1994. MHC class I expression in mice lacking the proteasome subunit LMP-7. Science **265:**1234-1237.
162. **Toes RE, Nussbaum AK, Degermann S, Schirle M, Emmerich NP, Kraft M, Laplace C, Zwinderman A, Dick TP, Müller J, Schönfisch B, Schmid C, Fehling HJ, Stevanovic S, Rammensee HG, Schild H.** 2001. Discrete cleavage motifs of constitutive and immunoproteasomes revealed by quantitative analysis of cleavage products. J Exp Med **194:**1-12.
163. **de Verteuil D, Muratore-Schroeder TL, Granados DP, Fortier M-H, Hardy M-P, Bramoullé A, Caron E, Vincent K, Mader S, Lemieux S, Thibault P, Perreault C.** 2010. Deletion of immunoproteasome subunits imprints on the transcriptome and has a broad impact on peptides presented by major histocompatibility complex I molecules. Molecular & Cellular Proteomics **9:**2034-2047.
164. **Khan S, van den Broek M, Schwarz K, de Giuli R, Diener PA, Groettrup M.** 2001. Immunoproteasomes largely replace constitutive proteasomes during an antiviral and antibacterial immune response in the liver. J Immunol **167:**6859-6868.
165. **Heink S, Ludwig D, Kloetzel P-M, Krüger E.** 2005. IFN-gamma-induced immune adaptation of the proteasome system is an accelerated and transient response. Proc Natl Acad Sci USA **102:**9241-9246.
166. **Ethen CM, Hussong SA, Reilly C, Feng X, Olsen TW, Ferrington DA.** 2007. Transformation of the proteasome with age-related macular degeneration. FEBS Lett **581:**885-890.
167. **Hussong SA, Kapphahn RJ, Phillips SL, Maldonado M, Ferrington DA.** 2010. Immunoproteasome deficiency alters retinal proteasome's response to stress. J Neurochem **113:**1481-1490.
168. **Ferrington DA, Husom AD, Thompson LV.** 2005. Altered proteasome structure, function, and oxidation in aged muscle. FASEB J **19:**644-646.
169. **Kotamraju S, Matalon S, Matsunaga T, Shang T, Hickman-Davis JM, Kalyanaraman B.** 2006. Upregulation of immunoproteasomes by nitric oxide: potential antioxidative mechanism in endothelial cells. Free Radic Biol Med **40:**1034-1044.
170. **Boehm U, Klamp T, Groot M, Howard JC.** 1997. Cellular responses to interferon-gamma. Annu Rev Immunol **15:**749-795.
171. **Schroder K, Hertzog PJ, Ravasi T, Hume DA.** 2004. Interferon-gamma: an overview of signals, mechanisms and functions. J Leukoc Biol **75:**163-189.

172. **Singh RK, Kabbaj M-HM, Paik J, Gunjan A.** 2009. Histone levels are regulated by phosphorylation and ubiquitylation-dependent proteolysis. Nat Cell Biol **11:**925-933.
173. **Steers NJ, Peachman KK, McClain SR, Alving CR, Rao M.** 2009. Human immunodeficiency virus type 1 Gag p24 alters the composition of immunoproteasomes and affects antigen presentation. J Virol **83:**7049-7061.
174. **Apcher GS, Heink S, Zantopf D, Kloetzel P-M, Schmid H-P, Mayer RJ, Krüger E.** 2003. Human immunodeficiency virus-1 Tat protein interacts with distinct proteasomal alpha and beta subunits. FEBS Lett **553:**200-204.
175. **Huang X, Seifert U, Salzmann U, Henklein P, Preissner R, Henke W, Sijts AJ, Kloetzel PM, Dubiel W.** 2002. The RTP site shared by the HIV-1 Tat protein and the 11S regulator subunit alpha is crucial for their effects on proteasome function including antigen processing. J Mol Biol **323:**771-782.
176. **Khu Y-L, Tan Y-J, Lim SG, Hong W, Goh P-Y.** 2004. Hepatitis C virus non-structural protein NS3 interacts with LMP7, a component of the immunoproteasome, and affects its proteasome activity. Biochem J **384:**401-409.
177. **Berhane S, Aresté C, Ablack JN, Ryan GB, Blackbourn DJ, Mymryk JS, Turnell AS, Steele JC, Grand RJA.** 2011. Adenovirus E1A interacts directly with, and regulates the level of expression of, the immunoproteasome component MECL1. Virology.
178. **Blair GE, Blair-Zajdel ME.** 2004. Evasion of the immune system by adenoviruses. Curr Top Microbiol Immunol **273:**3-28.
179. **Khan S, Zimmermann A, Basler M, Groettrup M, Hengel H.** 2004. A cytomegalovirus inhibitor of gamma interferon signaling controls immunoproteasome induction. J Virol **78:**1831-1842.
180. **Camargo R, Faria LO, Kloss A, Favali CBF, Kuckelkorn U, Kloetzel P-M, de Sá CM, Lima BD.** 2014. Trypanosoma cruzi Infection Down-Modulates the Immunoproteasome Biosynthesis and the MHC Class I Cell Surface Expression in HeLa Cells. PLoS ONE **9:**e95977.
181. **Bergeron M, Blanchette J, Rouleau P, Olivier M.** 2008. Abnormal IFN-gamma-dependent immunoproteasome modulation by Trypanosoma cruzi-infected macrophages. Parasite Immunol **30:**280-292.
182. **Howcroft TK, Richardson JC, Singer DS.** 1993. MHC class I gene expression is negatively regulated by the proto-oncogene, c-jun. EMBO J **12:**3163-3169.

Chapter 4:
Prostaglandin E_2 Induction During Mouse Adenovirus Type 1 Respiratory Infection Regulates Inflammatory Mediator Generation but Does not Affect Viral Pathogenesis

Abstract

Respiratory viruses cause substantial disease and are a significant healthcare burden. Virus-induced inflammation can be detrimental to the host, causing symptoms during acute infection and leading to damage that contributes to long-term residual lung disease. Prostaglandin E_2 (PGE_2) is a lipid mediator that is increased in response to many viral infections, and inhibition of PGE_2 production during respiratory viral infection often leads to a decreased inflammatory response. We tested the hypothesis that PGE_2 promotes inflammatory responses to mouse adenovirus type 1 (MAV-1) respiratory infection. Acute MAV-1 infection increased COX-2 expression and PGE_2 production in wild type mice. Deficiency of the E prostanoid 2 receptor had no apparent effect on MAV-1 pathogenesis. Virus-induced induction of PGE_2, IFN-γ, CXCL1, and CCL5 was reduced in mice deficient in microsomal PGE synthase-1 (mPGES-$1^{-/-}$ mice). However, there were no differences between mPGES-$1^{+/+}$ and mPGES-$1^{-/-}$ mice in viral replication, recruitment of leukocytes to airways or lung inflammation. Infection of both mPGES-$1^{+/+}$ and mPGES-$1^{-/-}$ mice led to protection against reinfection. Thus, while PGE_2 promotes the expression of a

variety of cytokines in response to acute MAV-1 infection, PGE_2 synthesis does not appear to be essential for generating pulmonary immunity.

Introduction

Eicosanoids are lipid mediators generated by the release of arachidonic acid from cell membrane phospholipids in response to diverse stimuli. Prostaglandins (PGs) are derived from the oxidation of arachidonic acid by cyclooxygenase (COX) enzymes. Modification of arachidonic acid by COX forms the unstable intermediate molecule PGH_2, which is converted by specific synthases to form various PGs such as thromboxane, PGD_2, PGE_2, $PGF_{2\alpha}$, and prostacyclin (PGI_2). At least three different synthases have been shown to catalyze the conversion of PGH_2 to PGE_2 *in vitro*: microsomal prostaglandin E_2 synthase (mPGES)-1, mPGES-2, and cytosolic PGES (cPGES/p23) (1-3). However, neither mPGES-2 nor cPGES is required for *in vivo* PGE_2 synthesis (4-6) and mPGES-1 is solely responsible for both basal and inducible PGE_2 levels *in vivo* (7, 8).

PGE_2 regulates immune function in many ways that are likely to affect viral pathogenesis ((reviewed in ref. 9)). For example, PGE_2 promotes inflammation through vasodilatory mechanisms, leading to edema and facilitating passive leukocyte recruitment. Additionally, PGE_2 augments production of the proinflammatory cytokine IL-6 by leukocytes (10) and airway epithelial cells (11). In regard to adaptive immunity, PGE_2 exerts an immunosuppressive effect at high concentrations by inhibiting production of the Th1 cytokines interferon

(IFN)-γ and IL-12 (12, 13). However, nanomolar concentrations of PGE_2 enhance Th1 cytokine secretion and differentiation *in vivo* (14, 15). PGE_2 plays an important role in optimal antibody synthesis. COX inhibitors suppress antibody production in activated human B lymphocytes (16, 17), and PGE_2 can act on uncommitted B lymphocytes to promote isotype switching to IgE or IgG1 (18-20). PGE_2 production increases *in vitro* and *in vivo* in response to many respiratory viruses, including respiratory syncytial virus (RSV) (21-24), influenza (25-27), human cytomegalovirus (28) and rhinovirus (29). During RSV or influenza infection, pharmacologic inhibition of COX enzymes or a genetic deficiency of COX-2 decreases virus induction of pro-inflammatory cytokine production and pulmonary inflammation (22, 30).

Adenoviruses are non-enveloped double-stranded DNA viruses that are common causes of respiratory infection (31). HAdV-5 and recombinant HAdV-5-based vectors induce COX-2 expression and PGE_2 release in murine fibroblasts (32) and in human primary synovial fibroblasts (33) *in vitro*, respectively. However, little else is known about the role of PGE_2 in the pathogenesis of adenoviruses or other viruses that commonly cause respiratory infection. Since species-specificity of adenoviruses complicates animal studies with a human adenovirus, we previously established mouse adenovirus type 1 (MAV-1, also known as MAdV-1) as a model to study the pathogenesis of adenovirus respiratory infection in the natural host of the virus (34-40). Antibodies have a crucial role in preventing severe disseminated MAV-1 infection. Mice lacking B cells or Bruton's tyrosine kinase (Btk) have increased susceptibility to MAV-1,

and antiserum from immune $Btk^{+/+}$ mice protects $Btk^{-/-}$ mice (41). T cells cause acute immunopathology and are required for long-term host survival following intraperitoneal (i.p.) MAV-1 infection. We previously demonstrated that lung viral loads in mice rechallenged with MAV-1 28 days following primary infection remain at or below the limit of detection (35), indicating that adaptive immune responses to MAV-1 are protective.

Because previous studies of other respiratory viruses used COX-deficient animals or COX inhibition, their results could be attributed to deficiency of PGE_2 or other COX-derived mediators. We hypothesized that PGE_2 production is necessary for the appropriate coordination of inflammatory responses after adenovirus respiratory infection. To test this hypothesis, we evaluated the role of PGE_2 after MAV-1 respiratory infection using mice deficient in the terminal PGE_2 synthase, mPGES-1. Consistent with our hypothesis, induction of pro-inflammatory cytokines was reduced in mPGES-1-deficient mice following MAV-1 infection compared to mPGES-$1^{+/+}$ mice. However, PGE_2 deficiency did not affect virus-induced lung inflammation, viral replication, or the development of protective immunity in this model.

Results

Induction of COX-2 expression and PGE_2 production by MAV-1 in vivo

To investigate whether MAV-1 respiratory infection induces COX-2 expression and PGE_2 production *in vivo*, we infected wild-type (mPGES-$1^{+/+}$) mice intranasally (i.n.) with MAV-1 and harvested bronchoalveolar lavage (BAL)

cells and lung tissue at times corresponding to early infection (4 days post infection, dpi), the peak of viral replication at 7 dpi (34, 35), and later times (14 and 21 dpi) corresponding to clearance of virus from the lungs. Because inflammatory stimuli, including infection with a variety of pathogens, are frequently associated with upregulated COX-2 expression (42-46), we first used reverse transcriptase quantitative real-time PCR (RT-qPCR) to measure COX-2 mRNA levels following MAV-1 infection. COX-2 mRNA was significantly increased in the lungs and BAL cells of infected mice compared to mock infected mice at 7 dpi and decreased to baseline levels seen in mock infected mice by 14 dpi (Figure 4-1A,B). Although it was detected in both mock infected and infected mice, COX-1 expression was not upregulated by MAV-1 infection (data not shown). PGE_2 concentrations measured in lung homogenates steadily increased after infection, with significantly elevated levels at 14 and 21 dpi (Figure 4-1C, mPGES-$1^{+/+}$ mice). These data demonstrate that acute MAV-1 infection increases COX-2 mRNA and induces PGE_2 production in the lung.

Effects of EP2 deficiency on MAV-1 respiratory infection

The physiological effects of PGE_2 depend on its activation of four distinct cell membrane-associated G protein-coupled E prostanoid (EP) receptors (47). PGE_2 inhibits alveolar macrophage (AM) phagocytosis via EP2 activation and subsequent increases in cAMP (48), and PGE_2 also inhibits bacterial killing by AMs and reactive oxygen intermediate generation by AMs in an EP2/EP4- and cAMP-dependent manner (49). The inhibitory effects of PGE_2 on host

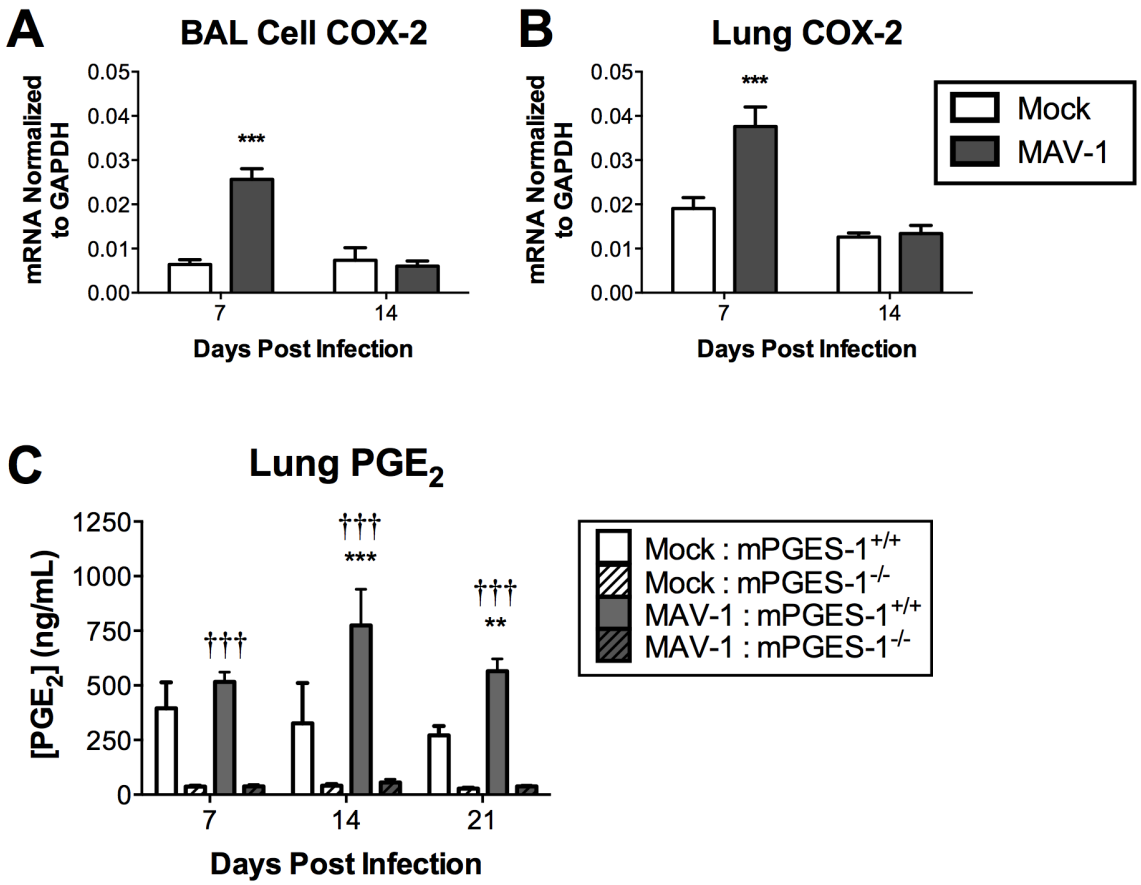

Figure 4-1. Induction of lung COX-2 expression and PGE_2 production.

Mice were infected i.n. with MAV-1 (grey bars) or mock infected (white bars) with conditioned media. A-B) RNA was extracted from BAL cells or lungs harvested at the indicated time points and RT-qPCR was used to quantify COX-2 expression, which is expressed in arbitrary units. C) ELISA was used to quantify PGE_2 concentrations in lung homogenates from both mPGES-$1^{+/+}$ and mPGES-$1^{-/-}$ mice at the indicated time points. Combined data from n=8-9 (for BAL COX-2), n=5-23 (for lung COX-2) and n=3-5 (for ELISA) mice per group are presented as means ± S.E.M. Statistical comparisons were made using two-way ANOVA followed by Bonferroni's multiple comparison tests. *P<0.05, **P<0.01 and ***P<0.001, comparing mock to MAV-1 for a given genotype. †††P< 0.001, comparing genotypes within the same condition.

inflammatory responses have been linked to signaling through EP2 and EP4 (50), and PGE_2 signaling through EP2 suppresses clearance from the lungs of *Pseudomonas aeruginosa* (45) and *Streptococcus pneumoniae* (47). To determine whether PGE_2 has a similar effect on control of MAV-1 infection or modulation of MAV-1-induced lung inflammation, we first studied acute MAV-1 respiratory infection in EP2-deficient ($EP2^{-/-}$) mice. Following i.n. infection with MAV-1, no deaths occurred in either $EP2^{-/-}$ or $EP2^{+/+}$ controls. Lung viral loads were comparable in $EP2^{-/-}$ and $EP2^{+/+}$ mice at 7 dpi (Figure 4-2A), which we have previously described as the peak of viral replication in the lungs (34, 35). Viral loads were substantially less in both $EP2^{-/-}$ and $EP2^{+/+}$ mice at 14 dpi, with no significant differences between the groups at this time point.

Acute MAV-1 respiratory infection induced a moderate pneumonitis in $EP2^{+/+}$ mice, with the accumulation of inflammatory cells around airways and hypercellularity in alveolar walls by 7 dpi that decreased somewhat by 14 dpi (Figure 4-2C,D). We observed similar patterns of MAV-1-induced inflammation in the lungs of $EP2^{-/-}$ mice at both 7 and 14 dpi (Figure 4-2E,F). Pathology index scores (Table 4-1) quantifying lung inflammation confirmed that there was not a significant difference between $EP2^{+/+}$ and $EP2^{-/-}$ mice at either time point (Figure 4-2B).

Effects of mPGES-1 deficiency on MAV-1-induced lung inflammation

It is possible that redundancy of function between EP2 and EP4, which both mediate PGE_2-induced increases in cAMP, accounted for the lack of

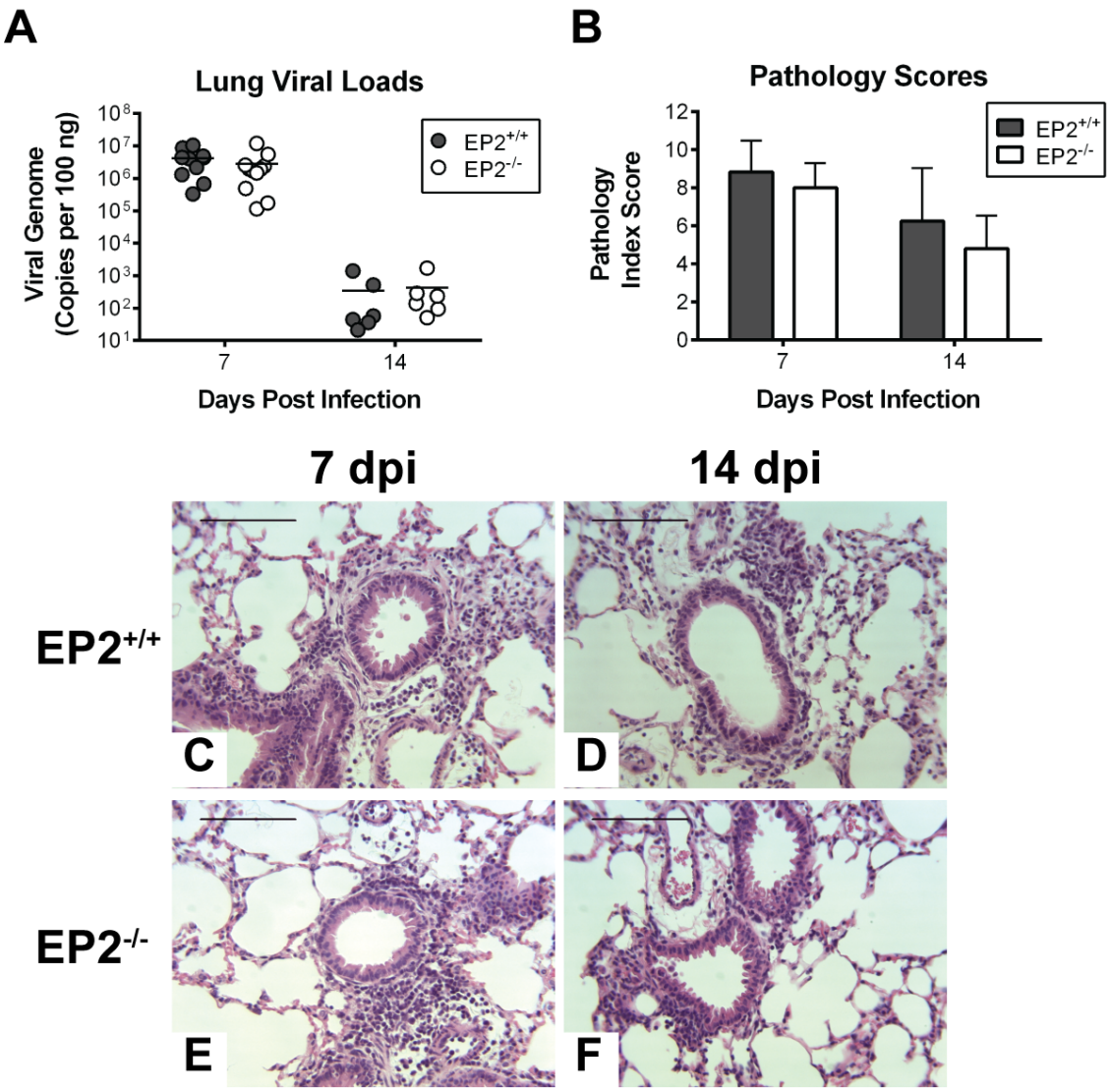

Figure 4-2. Effects of EP2 deficiency on MAV-1 respiratory infection.

Mice were infected i.n. with MAV-1. A) DNA was extracted from lungs from $EP2^{+/+}$ and $EP2^{-/-}$ mice at the indicated time points. qPCR was used to quantify DNA viral loads, which are expressed as copies of MAV-1 genome per 100 ng of input DNA. Individual circles represent values for individual mice and horizontal bars represent means for each group. B) Pathology index scores were generated to quantify cellular inflammation. Combined data from 4 to 6 mice per group are presented as means ± S.E.M. C-F) Hematoxylin and eosin-stained sections were prepared from paraffin-embedded sections (bottom panels). Scale bars, 100 μm.

differences seen between $EP2^{+/+}$ and $EP2^{-/-}$ mice. To capture the possible contributions of PGE_2 to MAV-1 pathogenesis without regard to individual receptors, we used mice deficient in mPGES-1. This enzyme is responsible for the majority of the conversion of PGH_2 to PGE_2, so mPGES-1-deficient ($mPGES\text{-}1^{-/-}$) mice are almost completely PGE_2-deficient (Figure IV-1C and refs. 7, 51)). This strategy also allows us to assess whether PGE_2 may influence MAV-1 infection via interactions with EP1 or EP3 receptors as well. Consistent with this, PGE_2 levels in lung homogenates from $mPGES\text{-}1^{-/-}$ mice were substantially lower than in $mPGES\text{-}1^{+/+}$ control mice and remained unchanged after MAV-1 infection (Figure 4-1C). We did not detect any compensatory increase in mRNA levels of mPGES-2 or cPGES in $mPGES\text{-}1^{-/-}$ mice compared to $mPGES\text{-}1^{+/+}$ controls at baseline before infection or at any time after infection (data not shown).

Decreased PGE_2 production is associated with decreased virus-induced cytokine production following influenza virus infection of $COX\text{-}2^{-/-}$ mice or mice treated with the COX-2 inhibitor celecoxib (30, 52). We hypothesized that PGE_2 promotes virus-induced cytokine and chemokine production following MAV-1 infection. To determine whether PGE_2 deficiency in $mPGES\text{-}1^{-/-}$ mice affected MAV-1-induced cytokine responses, we measured mRNA and protein levels of cytokines and chemokines that are commonly induced by MAV-1 infection (34, 35). At 7 dpi, IFN-γ mRNA was significantly increased in lungs of infected mice compared to mock-infected mice, although induction did not differ between $mPGES\text{-}1^{+/+}$ and $mPGES\text{-}1^{-/-}$ mice (Figure 4-3A). MAV-1 infection induced similar

increases of TNF-α mRNA in mPGES-1$^{+/+}$ and mPGES-1$^{-/-}$ mice at 7 and 14 dpi (Figure 4-3B). At 7 and 14 dpi, lung CCL5 mRNA was significantly increased after infection, although the magnitude of induction was similar in mPGES-1$^{+/+}$ and mPGES-1$^{-/-}$ mice (Figure 4-3C). The kinetics and magnitude of CXCL1 mRNA were similar in infected mPGES-1$^{+/+}$ and mPGES-1$^{-/-}$ mice, with maximal induction occurring at 7 dpi (Figure 4-3D).

For each cytokine examined, peak induction of protein in BALF occurred at 7 dpi and protein levels then decreased over time, returning to baseline by 21 dpi. Peak IFN-γ protein concentrations were detected at 7 dpi in BALF from both infected mPGES-1$^{+/+}$ and mPGES-1$^{-/-}$ mice, but the amount of IFN-γ protein was significantly less in mPGES-1$^{-/-}$ mice than in mPGES-1$^{+/+}$ mice (Figure 4-3E). By 14 dpi, IFN-γ in both mPGES-1$^{+/+}$ and mPGES-1$^{-/-}$ mice decreased to baseline levels. We did not detect changes of IL-4 protein in BALF at any time point (data not shown), suggesting that PGE_2 deficiency did not result in Th2 skewing following MAV-1 infection. Concentrations of TNF-α protein in BALF were also less in infected mPGES-1$^{-/-}$ mice than in mPGES-1$^{+/+}$ mice at 7 dpi, although this difference was not statistically significant (Figure 4-3F). TNF-α protein concentrations in BALF returned to baseline by 14 dpi. CCL5 protein induction was also lower in infected mPGES-1$^{-/-}$ mice compared to infected mPGES-1$^{+/+}$ mice at 7 and 14 dpi, although the difference was only statistically significant at 7 dpi (Figure 4-3G). At 7 dpi, concentrations of CXCL1 protein in BALF were less in infected mPGES-1$^{-/-}$ mice than in mPGES-1$^{+/+}$ mice (Figure 4-3H). By 14 dpi, CXCL1 decreased to baseline levels in both mPGES-1$^{+/+}$ and mPGES-1$^{-/-}$ mice.

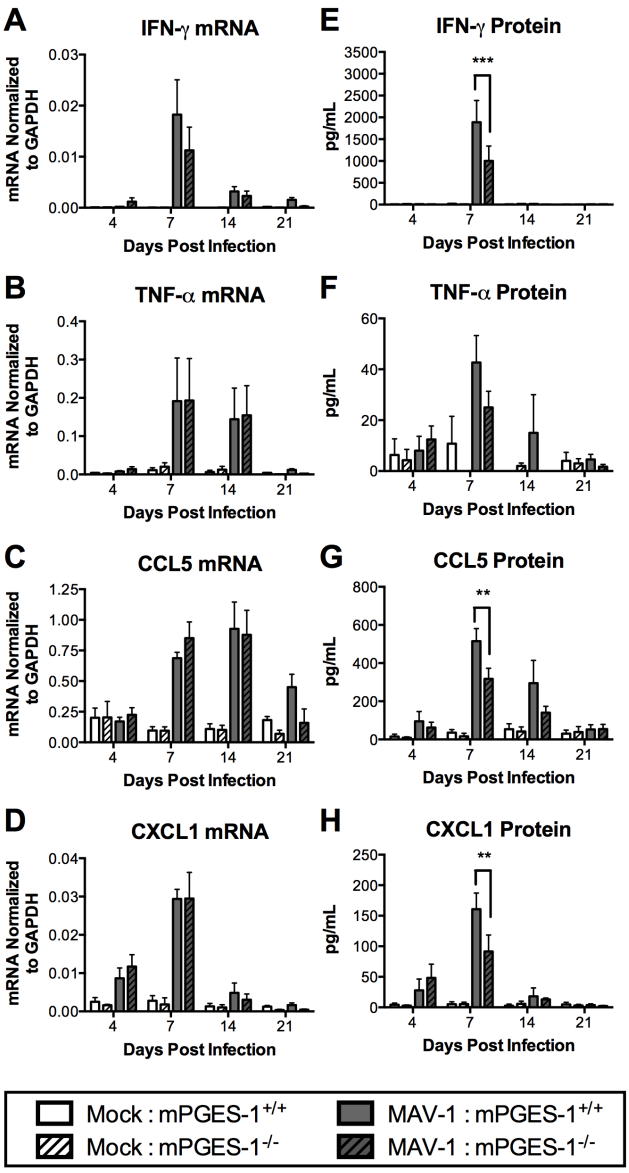

Figure 4-3. Effects of mPGES-1 deficiency on MAV-1-induced cytokine production.

mPGES-$1^{+/+}$ and mPGES-$1^{-/-}$ mice were infected i.n. with MAV-1 or mock infected with conditioned media. A-D) RNA was extracted from lungs harvested at the indicated time points and RT-qPCR was used to quantify cytokine expression, which is shown in arbitrary units. E-H) ELISA was used to quantify cytokine concentrations in BALF at the indicated time points. Combined data from 3 to 5 mice per group are presented as means ± S.E.M. Statistical comparisons were made using two-way ANOVA followed by Bonferroni's multiple comparison tests. $^{**}P<0.01$

To determine whether these effects on proinflammatory cytokines and chemokines correlated with changes in other measures of virus-induced lung inflammation, we enumerated leukocytes in BALF obtained from mPGES-$1^{+/+}$ and mPGES-$1^{-/-}$ mice after infection. There were no statistically significant differences between infected mPGES-$1^{+/+}$ and mPGES-$1^{-/-}$ mice in the numbers or types of leukocytes in BALF at any time point examined (data not shown). Next, we evaluated MAV-1-induced cellular inflammation in the lungs of mPGES-$1^{+/+}$ and mPGES-$1^{-/-}$ mice. As we have previously described (34, 35), we observed focal areas of inflammation surrounding medium and large airways, accompanied by scattered interstitial infiltrates in both mPGES-$1^{+/+}$ and mPGES-$1^{-/-}$ mice (Figure 4-4A). Lung inflammation peaked at 7 dpi and became somewhat less pronounced by 14 dpi. By 21 dpi, cellular inflammation had largely resolved in both mPGES-$1^{+/+}$ and mPGES-$1^{-/-}$ mice. We used pathology index scores (Table 4-1) to quantify lung inflammation. Pathology scores were greater in infected mice than in mock infected controls at 7 and 14 dpi, when inflammation was greatest (Figure 4-4B). There were no statistically significant differences in pathology index scores measured in mPGES-$1^{+/+}$ and mPGES-$1^{-/-}$ mice at any time.

It is possible that mPGES-1 deficiency could result in shunting of the COX-derived intermediate PGH_2 to other synthases such as the prostaglandin I_2 (PGI_2) synthase, leading to increased production of the next most abundant COX pathway product, PGI_2. Because PGI_2 signaling through the IP receptor also involves increases in intracellular cAMP, PGI_2 overproduction could potentially

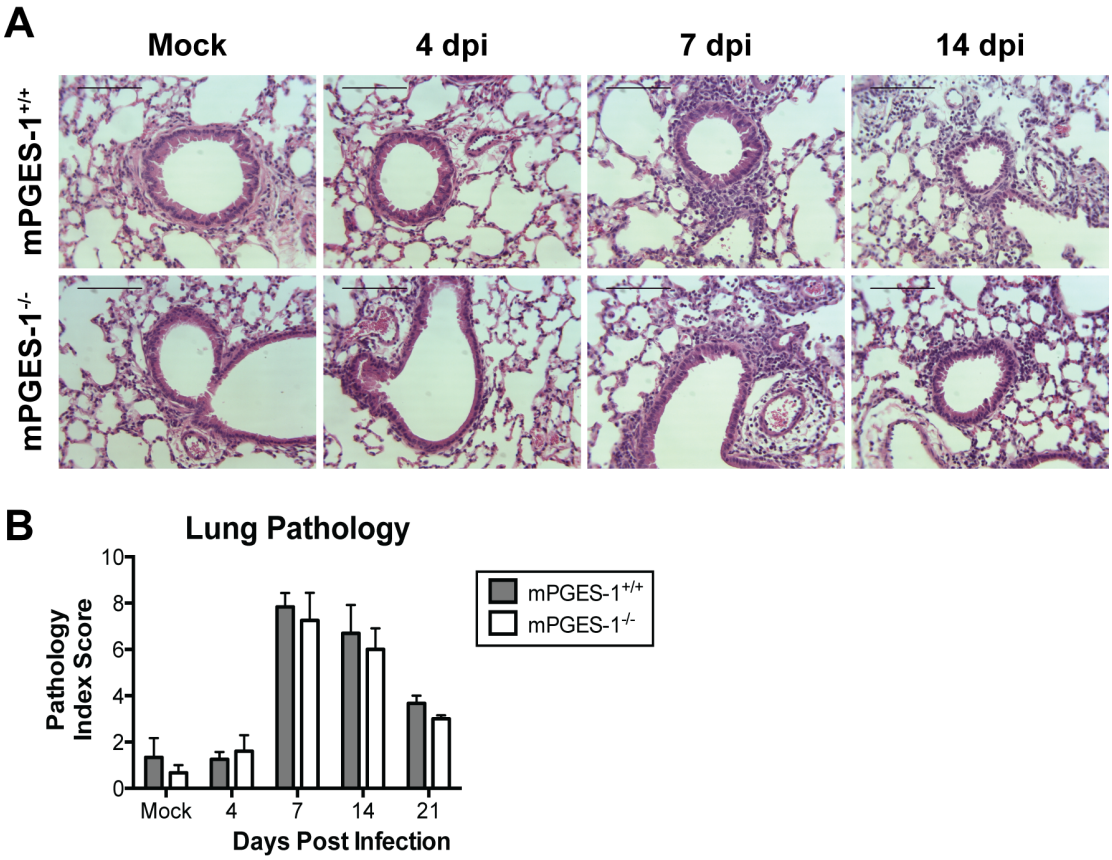

Figure 4-4. Effects of mPGES-1 deficiency on MAV-1-induced lung inflammation.

mPGES-1$^{+/+}$ and mPGES-1$^{-/-}$ mice were infected i.n. with MAV-1 or mock infected with conditioned media. Lungs were harvested at the indicated time points. A) Hematoxylin and eosin-stained sections were prepared from paraffin-embedded sections. Scale bars, 100 μm. B) Pathology index scores were generated to quantify cellular inflammation. Combined data from 3 to 6 mice per group are presented as means ± S.E.M.

compensate for PGE_2 deficiency in our model. To determine whether this was the case, we measured concentrations of the PGI_2 metabolite 6-keto-PGF1α in lung homogenates before and after infection. We observed small but insignificant increases of 6-keto-PGF1α in both mPGES-$1^{+/+}$ and mPGES-$1^{-/-}$ mice after infection compared to mock infected mice. However, there were no significant differences between 6-keto-PGF1α concentrations in mPGES-$1^{+/+}$ and mPGES-$1^{-/-}$ mice at any time point (data not shown). This suggests that PGI_2 overproduction does not substantially compensate for any effect of PGE_2 deficiency in mPGES-$1^{-/-}$ mice infected with MAV-1.

Effects of mPGES-1 deficiency on susceptibility to MAV-1

PGE_2 deficiency in mPGES-$1^{-/-}$ mice was associated with less production of IFN-γ and other cytokines in the airways of infected mice (Figure 4-3). To determine whether these differences correlated with increased susceptibility to MAV-1 infection, we used qPCR to quantify viral loads in the lungs and other target organs. Virus was detectable in the lungs by 4 dpi, and viral loads peaked at 7 dpi in both mPGES-$1^{+/+}$ and mPGES-$1^{-/-}$ mice (Figure 4-5). Lung viral loads decreased substantially in both mPGES-$1^{+/+}$ and mPGES-$1^{-/-}$ mice at 14 and 21 dpi, consistent with clearance of virus from the lungs in both groups (Figure 4-5). There were no statistically significant differences in lung viral loads measured in mPGES-$1^{+/+}$ mice compared to mPGES-$1^{-/-}$ mice at any time point. Likewise, there were no statistically significant differences in viral loads measured in the brains and spleens of mPGES-$1^{+/+}$ mice compared to mPGES-$1^{-/-}$ mice at any

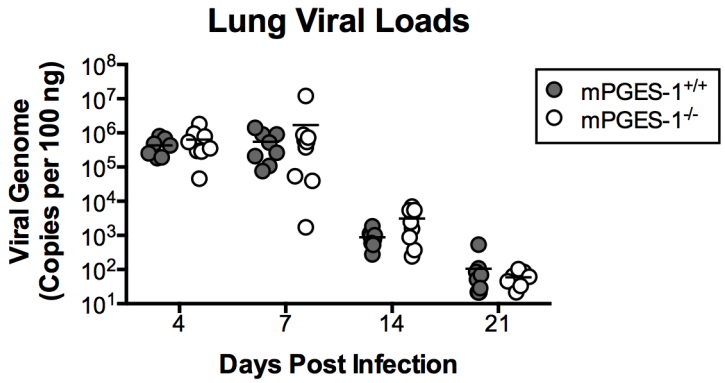

Figure 4-5. Effects of mPGES-1 deficiency on MAV-1 viral loads.

mPGES-$1^{+/+}$ and mPGES-$1^{-/-}$ mice were infected i.n. with MAV-1 or mock infected with conditioned media. DNA was extracted from lungs harvested at the indicated time points. qPCR was used to quantify MAV-1 genome copies in lung DNA. DNA viral loads are expressed as copies of MAV-1 genome per 100 ng of input DNA. Individual circles represent values for individual mice and horizontal bars represent means for each group.

time point (data not shown). Collectively, these data suggest that PGE_2 deficiency does not affect the control of viral replication in the lungs during acute infection, clearance of virus from the lungs, or dissemination of virus to other target organs.

Effect of the nonselective COX inhibitor indomethacin on MAV-1 infection

To determine whether COX-derived products other than PGE_2 contribute to MAV-1-induced inflammatory responses, we infected mice i.n. with 10^5 pfu MAV-1 and treated mice daily with an i.p. injection of indomethacin as previously described (53) and then harvested samples at 7 d.p.i. Indomethacin treatment reduced lung PGE_2 concentrations by approximately 30% in infected mice (data not shown). Unlike our findings in mPGES-$1^{-/-}$ mice, treatment of MAV-1-infected mice with indomethacin did not affect virus-induced production of IFN-γ, CXCL1, CCL5, or TNF-α (Figure 4-6A and data not shown). Likewise, indomethacin did not affect the development of lung pathology after MAV-1 infection (Figure 4-6B) or MAV-1 lung viral loads (Figure 4-6C).

Adaptive immunity to MAV-1 is not substantially affected by PGE_2 deficiency

PGE_2 has a variety of effects on T and B cell function that are likely to affect the development of adaptive immunity and subsequent protection from secondary infection. Because of the various effects of PGE_2 on T and B lymphocyte function, we reasoned that PGE_2 deficiency might inhibit appropriate adaptive immune responses to MAV-1 infection. To examine this, we infected or

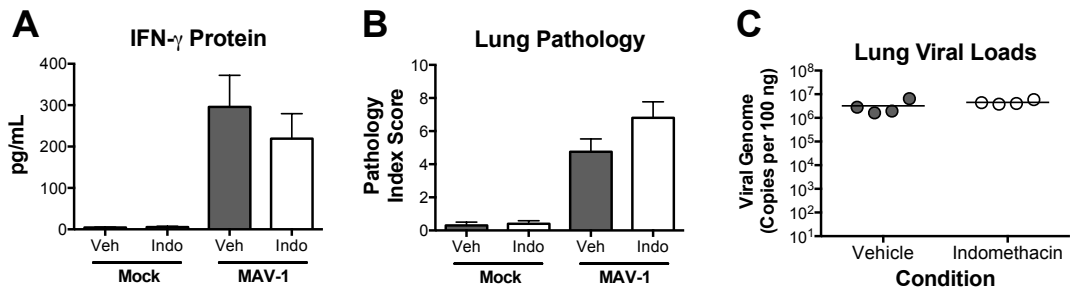

Figure 4-6. Effects of COX inhibition on MAV-1 respiratory infection.

Wild type mice were infected i.n. with MAV-1 or mock infected with conditioned media. Mice were treated daily with indomethacin (1.2 mg/kg given i.p.) or vehicle control until samples were harvested at 7 d.p.i. A) ELISA was used to quantify IFN-γ concentrations in BALF. Combined data from 4 to 5 mice per group are presented as means ± S.E.M. B) Pathology index scores were generated to quantify cellular inflammation in lungs. Combined data from 4 to 5 mice per group are presented as means ± S.E.M. C) DNA was extracted from lungs and qPCR was used to quantify MAV-1 genome copies in lung DNA. DNA viral loads are expressed as copies of MAV-1 genome per 100 ng of input DNA. Individual circles represent values for individual mice and horizontal bars represent means for each group.

mock infected mPGES-1$^{+/+}$ and mPGES-1$^{-/-}$ mice i.n. with 10^5 p.f.u. of MAV-1 and then rechallenged them with virus or conditioned media at 28 dpi. We measured lung viral loads at 7 days after the second challenge, using protection (lower lung viral loads following rechallenge) as a marker of adaptive immune function. Virus was readily detectable in mPGES-1$^{+/+}$ mice that were originally mock infected and then infected with virus 28 days later (Figure 4-7A). mPGES-1$^{+/+}$ mice that were initially infected with virus and then rechallenged with virus at 28 dpi had viral loads that were significantly lower than viral loads measured in mice that were initially mock infected and then infected with virus 28 days later (Figure 4-7A). This suggests that mPGES-1$^{+/+}$ mice were capable of generating a protective adaptive immune response. When we rechallenged mPGES-1$^{-/-}$ mice, we observed protection equivalent to that observed in mPGES-1$^{+/+}$ mice (Figure 4-7A).

To verify that this experimental design could demonstrate a difference in adaptive immune responses, we performed a similar rechallenge experiment using Aβ$^{-/-}$ (MHC II-deficient) mice. Following primary infection, lung viral loads in Aβ$^{-/-}$ mice were approximately 1 log unit higher than in Aβ$^{+/+}$ mice at 7 dpi (Figure 4-7B). While lung viral loads were slightly lower in Aβ$^{-/-}$ mice rechallenged with virus than in Aβ$^{-/-}$ mice following primary infection, this difference was substantially less than the corresponding difference in Aβ$^{+/+}$ mice (Figure 4-7B). As expected, the data from these rechallenge experiments indicate that MHC II (and thus CD4 T cells) are required for the development of protective immunity to MAV-1. Although subtle effects of PGE_2 deficiency on specific aspects of T or B

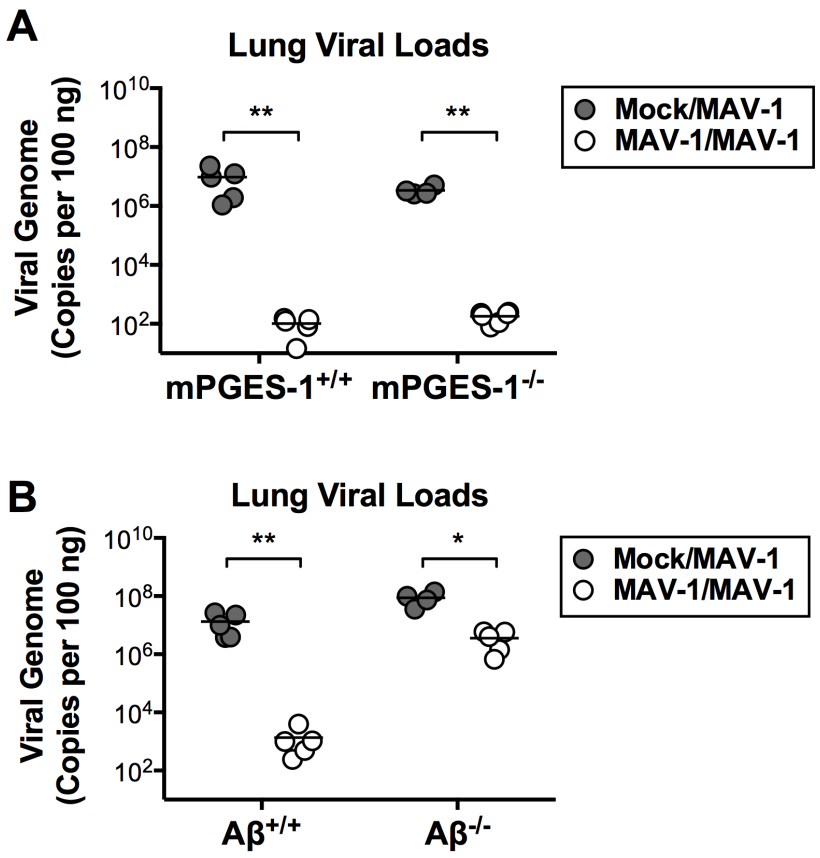

Figure 4-7. Protective immunity to MAV-1 infection.

A) mPGES-$1^{-/-}$ and B) Aβ$^{-/-}$ mice, along with appropriate mPGES-$1^{+/+}$ and Aβ$^{+/+}$ controls, were infected i.n. with MAV-1 or mock infected with conditioned media. At 28 dpi, mice were re-infected i.n. with MAV-1 and lungs were harvested at 7 dpi. DNA was extracted from lungs and qPCR was used to quantify DNA viral loads, which are expressed as copies of MAV-1 genome per 100 ng of input DNA. Individual circles represent values for individual mice and horizontal bars represent means for each group. Statistical comparisons were made using the Mann-Whitney rank sum test for differences between conditions within a given genotype. *P<0.05 and **P<0.01

lymphocyte function remain possible, these data suggest that PGE_2 does not make substantial contributions to adaptive immune responses that are required for protection against MAV-1 respiratory infection.

Discussion

The expression of COX-2 and production of PGE_2 increases in response to acute respiratory infection with several viruses (21-29). Previous studies have typically used COX inhibition or COX-deficient animals to study contributions of PGE_2 to viral pathogenesis. Because these strategies affect all COX-derived mediators, specific roles played by PGE_2 during viral respiratory infection remain unclear. In this study, we demonstrate that acute MAV-1 respiratory infection also induces COX-2 expression and PGE_2 production in the lungs. PGE_2 regulates immune function in many ways that could potentially affect viral pathogenesis. Inhibition of PGE_2 production during respiratory viral infection with RSV or influenza leads to decreased pro-inflammatory cytokine production and decreased pulmonary inflammation (22, 30). Based on these previous studies, we hypothesized that PGE_2 coordinates inflammatory responses during adenovirus respiratory infection. Using mPGES-1-deficient mice, we demonstrated that PGE_2 promoted the production of some inflammatory cytokines during MAV-1 infection. However, we were surprised to find no evidence that PGE_2 regulated viral replication, inflammatory cell accumulation, inflammatory cell composition, or development of protective adaptive immune responses.

Our results differ from what has been observed with other respiratory viruses. For example, inhibition of PGE_2 production during influenza or RSV infection has significant effects on virus-induced inflammatory responses. During influenza infection, treatment of mice with the COX-2 inhibitor celecoxib suppresses virus-induced production of proinflammatory cytokines in the lungs, although it does not affect viral titers or disease severity (52). Treatment of influenza-infected mice with COX inhibitors results in improved lung function and reduced immunopathology (54). In our study, treatment with the nonselective COX inhibitor indomethacin did not affect virus-induced lung pathology or cytokine production (Figure 4-6A,B), despite decreasing PGE_2 levels. This lack of effect again suggest differences between the role of PGE_2 and other COX-derived mediators in MAV-1 pathogenesis compared to other viruses, although it may also reflect an incomplete suppression of PGE_2 production by drug treatment. Genetic COX-2 deficiency has a more pronounced effect on influenza-induced disease than does pharmacologic inhibition, because COX-$2^{-/-}$ mice have reduced mortality, inflammation and cytokine responses after influenza infection compared to wild-type control mice (30). Treatment of RSV-infected airway epithelial cells with the COX-2 inhibitors NS-398 or celecoxib reduces production of virus particles and proinflammatory cytokines *in vitro* (21), although COX inhibition does not appear to significantly affect RSV replication *in vivo*. Similar to the effects of COX inhibition in influenza-infected mice, COX inhibition results in decreased lung pathology in RSV-infected cotton rats (22).

Our results showing reduced production of proinflammatory cytokines after MAV-1 infection of mPGES-1-deficient mice are similar to the effects of COX inhibition during influenza or RSV infection. This supports a role for PGE_2 in promoting proinflammatory cytokine production in the lung during viral infection. However, unlike studies using COX inhibition during influenza or RSV infection, we did not observe a substantial effect of PGE_2 deficiency on MAV-1-induced lung pathology. This suggests that the effects on lung pathology observed with COX inhibition during influenza or RSV infection could be due to decreased production of another COX-derived eicosanoid such as thromboxane, PGD_2, PGF_2, and PGI_2. Interestingly, levels of PGE_2 in influenza-infected COX-$2^{-/-}$ mice are equivalent to levels measured in infected COX-$2^{+/+}$ control mice (30), further supporting the possibility that the effects of COX-2 deficiency on influenza pathogenesis may not be solely due to decreased production of PGE_2. We typically observe host responses to acute MAV-1 respiratory infection that are generally similar to those seen with RSV and influenza infection. However, RNA viruses such as RSV and influenza are likely to interact with different pattern recognition receptors than a DNA virus such as MAV-1 or the human adenoviruses. It is possible that subtle differences in the mechanisms underlying the induction of inflammatory responses by these viruses, along with differential effects of PGE_2 or other eicosanoids on those responses, could account for differences between our results with MAV-1 and those with RSV and influenza.

We used mice deficient in mPGES-1 to specifically characterize the effects of reduced PGE_2 production on viral replication and host responses to

primary MAV-1 infection. Although overproduction of other prostaglandins in the absence of mPGES-1 occurs in some models using mPGES-1-deficient mice (7, 51, 55, 56), we did not detect significant overproduction of PGI_2 metabolites in mPGES-$1^{-/-}$ mice at baseline or following infection with MAV-1. Therefore, we do not believe that overproduction of other prostaglandins compensated for PGE_2 deficiency in our experiments, reducing any potential effect on MAV-1 pathogenesis. It is possible that other mediators not measured, such as leukotrienes, could be compensating for PGE_2 deficiency in our model. The use of mPGES-$1^{-/-}$ mice instead of pharmacologic inhibition of PGE_2 production allowed us to study the effects of almost complete PGE_2 deficiency. COX or mPGES-1 inhibitors do not achieve complete inhibition of enzymatic activity by COX or mPGES-1, whereas mPGES-$1^{-/-}$ mice have a complete loss of mPGES-1 activity and are therefore more completely PGE_2-deficient (7, 51). It is possible that mice genetically deficient in mPGES-1 could have functional differences in the development of the immune system that we have not defined in our experiments, possibly establishing compensatory pathways to overcome any defects that would have been the result of PGE_2 deficiency.

We have previously demonstrated that MAV-1 induces a Th1 response in the lungs of infected mice, with significant upregulation of IFN-γ that peaks at 7 dpi (35). Some reports have suggested that PGE_2 promotes a Th2-polarized environment by suppressing production of the Th1 cytokines IFN-γ and IL-12 *in vitro* (12, 13). However, nanomolar concentrations of PGE_2 enhance Th1 cytokine secretion and differentiation *in vivo* (14, 15). We demonstrated less

induction of IFN-γ in mPGES-1$^{-/-}$ mice infected with MAV-1, supporting the notion that PGE_2 could contribute to an appropriate Th1 response to MAV-1 infection. The decreased IFN-γ response observed in mPGES-1$^{-/-}$ mice is likely due to a decrease in IFN-γ production by $CD4^+$ and $CD8^+$ T cells, as these cell types are the major producers of IFN-γ during MAV-1 respiratory infection (Mary McCarthy and Jason Weinberg, unpublished data). Viral loads in mPGES-1$^{-/-}$ mice did not differ from those of mPGES-1$^{+/+}$ mice at 7 dpi despite less induction of IFN-γ in mPGES-1$^{-/-}$ mice. We have previously demonstrated that IFN-γ does play some role in the control of viral replication (35), but results from that study and from the present experiments suggest that other factors are likely able to compensate for IFN-γ deficiency to control MAV-1 replication in the lung

In addition to its contributions to T cell polarization, PGE_2 plays an important role in promoting antibody synthesis and isotype switching (16-20). Due to the potential effects of PGE_2 on T cell polarization and B cell antibody responses, we hypothesized that PGE_2 deficiency might inhibit appropriate adaptive immune responses to MAV-1 infection. Total serum IgG levels were similar in mPGES-1$^{+/+}$ and mPGES-1$^{-/-}$ mice (data not shown), suggesting that total antibody production in response to MAV-1 infection is unaffected by the absence of PGE_2. It is possible that virus-specific antibody production and virus-specific T cell functions were altered by PGE_2 deficiency. However, the results of our rechallenge experiments, in which both mPGES-1$^{+/+}$ and mPGES-1$^{-/-}$ mice were protected by prior infection, suggest that PGE_2 is not likely to substantially affect the development of protective immune responses to MAV-1.

COX inhibitors such as acetaminophen and ibuprofen are frequently used to alleviate fever and other symptoms in patients with respiratory infections. Decreases in RSV- and influenza-induced inflammation in animals treated with COX inhibitors or genetically deficient in COX-2 suggest that modulation of virus-induced PGE_2 production may have other benefits for patients with infections caused by some viruses. Our results with MAV-1 infection of PGE_2-deficient mice suggest that PGE_2 promotes MAV-1-induced cytokine production but does not have a dramatic effect on MAV-1-induced lung inflammation or control of viral replication. A more generalized inhibition of eicosanoids in addition to PGE_2 may be necessary to achieve more pronounced effects on virus-induced inflammatory responses. Ultimately, this may provide an attractive approach to limiting damage caused by virus-induced inflammation without having a substantial effect on the control of viral infection by host immune responses.

Materials and Methods

Ethics Statement

All animal work was conducted according to relevant national and international guidelines. All animal studies were approved by the University of Michigan Committee on Use and Care of Animals (Protocol Number 9054).

Mice

mPGES-1 heterozygous mice on a DBA1lac/J background (6) were originally obtained from Pfizer, Inc. (Groton, CT) and then backcrossed onto a

C57BL/6 background. Homozygous mPGES-1$^{-/-}$ mice and homozygous wild type mPGES-1$^{+/+}$ mice derived from the same heterozygous mPGES-1$^{+/-}$ parents were bred at the University of Michigan. MHC class II deficient mice (Aβ$^{-/-}$) (57) were purchased from Taconic and bred at the University of Michigan. Adult (4 to 6 weeks of age) males were used in all experiments. All mice were maintained under specific pathogen-free conditions.

Virus and Infections

MAV-1 was grown and passaged in NIH 3T6 fibroblasts, and titers of viral stocks were determined by plaque assay on 3T6 cells as previously described (58). Adult mice were anesthetized with ketamine and xylazine and infected intranasally (i.n.) with 10^5 plaque forming units (p.f.u.) of MAV-1 in 40 μl of sterile phosphate-buffered saline (PBS). Control mice were mock infected i.n. with conditioned media at an equivalent dilution in sterile PBS. Mice were euthanized by pentobarbital overdose at the indicated time points. Lungs were harvested, snap frozen in dry ice, and stored at -80°C until processed further. In separate experiments, mice received an i.p. injection of indomethacin (1.2 mg/kg in PBS) or vehicle control (DMSO similarly diluted in PBS) starting on the day of infection and then on each day thereafter.

Histology

Lungs were harvested from a subset of mice and fixed in 10% formalin. Prior to fixation, lungs were gently inflated with PBS via the trachea to maintain

lung architecture. After fixation, organs were embedded in paraffin, and 5 μm sections were obtained for histopathology. Sections were stained with hematoxylin and eosin to evaluate cellular infiltrates. All sectioning and staining was performed by the Pathology Cores for Animal Research in the University of Michigan Unit for Laboratory Management. Slides were viewed through a Laborlux 12 microscope (Leitz). Digital images were obtained with an EC3 digital imaging system (Leica Microsystems) using Leica Acquisition Suite software (Leica Microsystems). Final images were assembled using Adobe Illustrator (Adobe Systems). Adjustments to the color balance of digital images were applied in Adobe Illustrator equally to all experimental and control images.

To quantify cellular inflammation in the lungs, slides were examined in a blinded fashion to determine a pathology index as previously described (35), generating separate scores for the severity of cellular infiltrates around airway lumens and interstitial infiltrates (Table 4-1). Each score was multiplied by a number reflecting the extent of involvement in the lung (5% to 25% = 1, >25% to 50% = 2, >50% = 3). The final pathology index was obtained by adding together the values for cellular infiltrates around airway lumens and for interstitial infiltrates.

Isolation of DNA and RNA

DNA was extracted from the middle lobe of the right lung using the DNeasy® Tissue Kit (Qiagen Inc.). DNA was extracted from approximately one-fifth of the spleen using the DNeasy® Tissue Kit. For DNA extraction from brain,

half of each brain was homogenized using a sterile razor blade, and a portion of the homogenate was used to extract DNA using the DNeasy® Tissue Kit. Total RNA was extracted from lungs as previously described (38).

Analysis of Viral Loads

MAV-1 viral loads were measured in organs using quantitative real-time polymerase chain reaction (qPCR) as previously described (35, 38). Primers and probe used to detect a 59-bp region of the MAV-1 E1A gene are detailed in Table 4-2. Five µl of extracted DNA were added to reactions containing TaqMan II Universal PCR Mix with UNG (Applied Biosystems), forward and reverse primers (each at 200 nM final concentration), and probe (200 nM final concentration) in a 25 µl reaction volume. Analysis on an ABI Prism 7300 machine (Applied Biosystems) consisted of 40 cycles of 15 s at 90°C and 60 s at 60°C. Standard curves generated using known amounts of plasmid containing the MAV-1 EIA gene were used to convert cycle threshold values for experimental samples to copy numbers of EIA DNA. Results were standardized to the nanogram (ng) amount of input DNA. Each sample was assayed in triplicate. The limit of detection of this assay is typically between 10^1 and 10^2 copies of MAV-1 genome per 100 ng input DNA.

Analysis of Host Gene Expression

Cytokine gene expression was quantified using reverse transcriptase (RT)-qPCR. First, 2.5 µg of RNA were reverse transcribed using MMLV reverse

transcriptase (Invitrogen) in 20 µl reactions according to the manufacturer's instructions. Water was added to the cDNA product to bring the total volume to 50 µl. cDNA was amplified using duplexed gene expression assays for mouse CCL5, CXCL1 and GAPDH (Applied Biosystems). Five µl of cDNA were added to reactions containing TaqMan Universal PCR Mix and 1.25 µl each of 20X gene expression assays for the target cytokine and GAPDH. Primers used to detect IFN-γ, TNF-α, COX-1, and COX-2 are described in Table 4-2. For these measurements, 5 µl of cDNA were added to reactions containing Power SYBR Green PCR Mix (Applied Biosystems) and forward and reverse primers (each at 200 nM final concentration) in a 25 µl reaction volume. When SYBR green was used to quantify cytokine gene expression, separate reactions were prepared with primers for mouse GAPDH (Table 4-2, used at 200 nM each). In all cases, RT-qPCR analysis consisted of 40 cycles of 15 s at 90°C and 60 s at 60°C. Quantification of target gene mRNA was normalized to GAPDH and expressed in arbitrary units as $2^{-\Delta Ct}$, where Ct is the threshold cycle and $\Delta Ct = Ct(target) - Ct(GAPDH)$.

Analysis of Inflammatory Cells in Bronchoalveolar Lavage Fluid

Mice were euthanized via pentobarbital overdose at the indicated time points. Lungs were lavaged three times with the same aliquot of 1 mL sterile PBS containing protease inhibitor (complete, Mini, EDTA-free tablets; Roche Applied Science). Cells in bronchoalveolar lavage fluid (BALF) were counted using a hemocytometer. When RNA was extracted from cells in BALF, the cells pelleted

in a tabletop microcentrifuge at 17,000 x g for 10 min at 4°C and then resuspended in 0.5 mL of TRIzol® (Invitrogen). RNA was subsequently isolated according to the manufacturer's protocol.

Analysis of Cytokine Protein in Bronchoalveolar Lavage Fluid

The remaining cells in BALF were pelleted by centrifugation and supernatant was stored at -80°C. Cytokine protein concentrations in supernatant were determined by ELISA (Duoset Kits, R&D Systems) according to the manufacturer's protocol.

Lung PGE_2 Measurements

Lung tissue was suspended in CelLytic MT (Sigma-Aldrich) containing protease inhibitor (complete, Mini, EDTA-free tablets; Roche Applied Science) and 10 mM indomethacin (Sigma-Aldrich) at a concentration of 100 mg lung tissue per 1 mL homogenization buffer. Tissue was homogenized (MagNA Lyser, Roche Applied Science) in 2 x 60 s cycles at high speed (6,000) with 90 s cooling between cycles. After homogenization, tissue was spun twice at 17,000 x g for 10 min at 4°C and supernatant was stored at -80°C until assayed. Samples were diluted in PGE_2 enzyme immunoassay buffer and quantity of PGE_2 was determined using PGE_2 ELISA Kit (Enzo Life Sciences) according to the manufacturer's protocol.

Statistics

Analysis of data for statistical significance was conducted using Prism 3 for Macintosh (GraphPad Software, Incorporated). Differences between groups at multiple time points were analyzed using two-way analysis of variance (ANOVA) followed by Bonferroni's multiple comparison tests. Comparisons between two groups at a single time point were made using the Mann-Whitney rank sum test. *P* values less than 0.05 were considered statistically significant.

Table 4-1. Quantification of cellular inflammation in histologic specimens.

Score[a]	Cellular Infiltrates Around Airway Lumens	Interstitial Infiltrates
0	No infiltrates	No infiltrates
1	1 to 3 cell diameters thick	Increased cells visible only at high power
2	4 to 10 cell diameters thick	Easily seen cellular infiltrates
3	>10 cell diameters thick	Extensive consolidation by inflammatory cells

[a]A score from 0 to 3 was given for each of the two categories. The score for each category was multiplied by a number reflecting the extent of involvement in the specimen (5% to 25% = 1, >25% to 50% = 2, >50% = 3). The final pathology index score was obtained by adding together values for each category, resulting in a total score that could range from 0 to 18.

Table 4-2. Primers and probes used for real-time PCR analysis

Target	Oligonucleotide	Sequence (5′ to 3′)
MAV-1 E1A	Forward primer	GCACTCCATGGCAGGATTCT
	Reverse primer	GGTCGAAGCAGACGGTTCTTC
	Probe	TACTGCCACTTCTGC
IFN-γ	Forward primer	AAAGAGATAATCTGGCTCTGC
	Reverse primer	GCTCTGAGACAATGAACGCT
COX-1	Forward primer	CTTCTTAGGGAATCCCATCTG
	Reverse primer	CTTCAGTGAGGCTGTGTTGACAAG
COX-2	Forward primer	TGACCCCCAAGGCTCAAAT
	Reverse primer	GAACCCAGGTCCTCGCTTATG
TNF-α	Forward primer	CCACCACGCTCTTCTGTCTAC
	Reverse primer	AGGGTCTGGGCCATAGAACT
GAPDH	Forward primer	TGCACCACCAACTGCTTAG
	Reverse primer	GGATGCAGGGATGATGTTC

References

1. **Tanikawa N, Ohmiya Y, Ohkubo H, Hashimoto K, Kangawa K, Kojima M, Ito S, Watanabe K.** 2002. Identification and characterization of a novel type of membrane-associated prostaglandin E synthase. Biochem Biophys Res Commun **291:**884-889.
2. **Tanioka T, Nakatani Y, Semmyo N, Murakami M, Kudo I.** 2000. Molecular identification of cytosolic prostaglandin E2 synthase that is functionally coupled with cyclooxygenase-1 in immediate prostaglandin E2 biosynthesis. J Biol Chem **275:**32775-32782.
3. **Jakobsson PJ, Thorén S, Morgenstern R, Samuelsson B.** 1999. Identification of human prostaglandin E synthase: a microsomal, glutathione-dependent, inducible enzyme, constituting a potential novel drug target. Proc Natl Acad Sci USA **96:**7220-7225.
4. **Jania LA, Chandrasekharan S, Backlund MG, Foley NA, Snouwaert J, Wang I-M, Clark P, Audoly LP, Koller BH.** 2009. Microsomal prostaglandin E synthase-2 is not essential for in vivo prostaglandin E2 biosynthesis. Prostaglandins Other Lipid Mediat **88:**73-81.
5. **Lovgren AK, Kovarova M, Koller BH.** 2007. cPGES/p23 is required for glucocorticoid receptor function and embryonic growth but not prostaglandin E2 synthesis. Mol Cell Biol **27:**4416-4430.
6. **Trebino CE, Stock JL, Gibbons CP, Naiman BM, Wachtmann TS, Umland JP, Pandher K, Lapointe J-M, Saha S, Roach ML, Carter D, Thomas NA, Durtschi BA, McNeish JD, Hambor JE, Jakobsson P-J, Carty TJ, Perez JR, Audoly LP.** 2003. Impaired inflammatory and pain responses in mice lacking an inducible prostaglandin E synthase. Proc Natl Acad Sci USA **100:**9044-9049.
7. **Boulet L, Ouellet M, Bateman KP, Ethier D, Percival MD, Riendeau D, Mancini JA, Méthot N.** 2004. Deletion of microsomal prostaglandin E2 (PGE2) synthase-1 reduces inducible and basal PGE2 production and alters the gastric prostanoid profile. J Biol Chem **279:**23229-23237.
8. **Murakami M, Naraba H, Tanioka T, Semmyo N, Nakatani Y, Kojima F, Ikeda T, Fueki M, Ueno A, Oh S, Kudo I.** 2000. Regulation of prostaglandin E2 biosynthesis by inducible membrane-associated prostaglandin E2 synthase that acts in concert with cyclooxygenase-2. J Biol Chem **275:**32783-32792.
9. **McCarthy MK, Weinberg JB.** 2012. Eicosanoids and Respiratory Viral Infection: Coordinators of Inflammation and Potential Therapeutic Targets. Mediators of Inflammation **2012:**1-13.
10. **McCoy JM, Wicks JR, Audoly LP.** 2002. The role of prostaglandin E2 receptors in the pathogenesis of rheumatoid arthritis. J Clin Invest **110:**651-658.
11. **Tavakoli S, Cowan MJ, Benfield T, Logun C, Shelhamer JH.** 2001. Prostaglandin E(2)-induced interleukin-6 release by a human airway epithelial cell line. Am J Physiol Lung Cell Mol Physiol **280:**L127-133.

12. **Betz M, Fox BS.** 1991. Prostaglandin E2 inhibits production of Th1 lymphokines but not of Th2 lymphokines. J Immunol **146:**108-113.
13. **Snijdewint FG, Kaliński P, Wierenga EA, Bos JD, Kapsenberg ML.** 1993. Prostaglandin E2 differentially modulates cytokine secretion profiles of human T helper lymphocytes. J Immunol **150:**5321-5329.
14. **Bloom D, Jabrane-Ferrat N, Zeng L, Wu A, Li L, Lo D, Turck CW, An S, Goetzl EJ.** 1999. Prostaglandin E2 enhancement of interferon-gamma production by antigen-stimulated type 1 helper T cells. Cell Immunol **194:**21-27.
15. **Yao C, Sakata D, Esaki Y, Li Y, Matsuoka T, Kuroiwa K, Sugimoto Y, Narumiya S.** 2009. Prostaglandin E2-EP4 signaling promotes immune inflammation through Th1 cell differentiation and Th17 cell expansion. Nat Med **15:**633-640.
16. **Bancos S, Bernard MP, Topham DJ, Phipps RP.** 2009. Ibuprofen and other widely used non-steroidal anti-inflammatory drugs inhibit antibody production in human cells. Cell Immunol **258:**18-28.
17. **Ryan EP, Pollock SJ, Pollack SJ, Murant TI, Bernstein SH, Felgar RE, Phipps RP.** 2005. Activated human B lymphocytes express cyclooxygenase-2 and cyclooxygenase inhibitors attenuate antibody production. J Immunol **174:**2619-2626.
18. **Roper RL, Brown DM, Phipps RP.** 1995. Prostaglandin E2 promotes B lymphocyte Ig isotype switching to IgE. J Immunol **154:**162-170.
19. **Fedyk ER, Phipps RP.** 1996. Prostaglandin E2 receptors of the EP2 and EP4 subtypes regulate activation and differentiation of mouse B lymphocytes to IgE-secreting cells. Proc Natl Acad Sci USA **93:**10978-10983.
20. **Roper RL, Graf B, Phipps RP.** 2002. Prostaglandin E2 and cAMP promote B lymphocyte class switching to IgG1. Immunol Lett **84:**191-198.
21. **Liu T, Zaman W, Kaphalia BS, Ansari GAS, Garofalo RP, Casola A.** 2005. RSV-induced prostaglandin E2 production occurs via cPLA2 activation: role in viral replication. Virology **343:**12-24.
22. **Richardson JY, Ottolini MG, Pletneva L, Boukhvalova M, Zhang S, Vogel SN, Prince GA, Blanco JCG.** 2005. Respiratory syncytial virus (RSV) infection induces cyclooxygenase 2: a potential target for RSV therapy. J Immunol **174:**4356-4364.
23. **Radi ZA, Meyerholz DK, Ackermann MR.** 2010. Pulmonary cyclooxygenase-1 (COX-1) and COX-2 cellular expression and distribution after respiratory syncytial virus and parainfluenza virus infection. Viral Immunol **23:**43-48.
24. **Sznajer Y, Westcott JY, Wenzel SE, Mazer B, Tucci M, Toledano BJ.** 2004. Airway eicosanoids in acute severe respiratory syncytial virus bronchiolitis. J Pediatr **145:**115-118.
25. **Lee Suki MY, Cheung CY, Nicholls John M, Hui Kenrie PY, Leung Connie YH, Uiprasertkul M, Tipoe George L, Lau YL, Poon Leo LM, Ip Nancy Y, Guan Y, Peiris JSM.** 2008. Hyperinduction of Cyclooxygenase‐2‐Mediated Proinflammatory Cascade: A Mechanism

for the Pathogenesis of Avian Influenza H5N1 Infection. J Infect Dis **198:**525-535.
26. **Woo PCY, Tung ETK, Chan K-H, Lau CCY, Lau SKP, Yuen K-Y.** 2010. Cytokine profiles induced by the novel swine-origin influenza A/H1N1 virus: implications for treatment strategies. J Infect Dis **201:**346-353.
27. **Darwish I, Mubareka S, Liles WC.** 2011. Immunomodulatory therapy for severe influenza. Expert Rev Anti Infect Ther **9:**807-822.
28. **Zhu H, Cong J-P, Yu D, Bresnahan WA, Shenk TE.** 2002. Inhibition of cyclooxygenase 2 blocks human cytomegalovirus replication. Proc Natl Acad Sci USA **99:**3932-3937.
29. **Seymour ML, Gilby N, Bardin PG, Fraenkel DJ, Sanderson G, Penrose JF, Holgate ST, Johnston SL, Sampson AP.** 2002. Rhinovirus infection increases 5-lipoxygenase and cyclooxygenase-2 in bronchial biopsy specimens from nonatopic subjects. J Infect Dis **185:**540-544.
30. **Carey MA, Bradbury JA, Seubert JM, Langenbach R, Zeldin DC, Germolec DR.** 2005. Contrasting effects of cyclooxygenase-1 (COX-1) and COX-2 deficiency on the host response to influenza A viral infection. J Immunol **175:**6878-6884.
31. **Knipe D, Howley P, Griffin D, Lamb R, Martin M, Roizman B, Straus S.** 2007. Adenoviridae: The Viruses and Their Replication, p. 2355-2436, Fields Virology, vol. 1.
32. **Culver CA, Laster SM.** 2007. Adenovirus type 5 exerts multiple effects on the expression and activity of cytosolic phospholipase A2, cyclooxygenase-2, and prostaglandin synthesis. J Immunol **179:**4170-4179.
33. **Crofford LJ, McDonagh KT, Guo S, Mehta H, Bian H, Petruzelli LM, Roessler BJ.** 2005. Adenovirus binding to cultured synoviocytes triggers signaling through MAPK pathways and induces expression of cyclooxygenase-2. J Gene Med **7:**288-296.
34. **Weinberg JB, Stempfle GS, Wilkinson JE, Younger JG, Spindler KR.** 2005. Acute respiratory infection with mouse adenovirus type 1. Virology **340:**245-254.
35. **Procario MC, Levine RE, McCarthy MK, Kim E, Zhu L, Chang C-H, Hershenson MB, Weinberg JB.** 2012. Susceptibility to acute mouse adenovirus type 1 respiratory infection and establishment of protective immunity in neonatal mice. J Virol **86:**4194-4203.
36. **Weinberg JB, Lutzke ML, Efstathiou S, Kunkel SL, Rochford R.** 2002. Elevated chemokine responses are maintained in lungs after clearance of viral infection. J Virol **76:**10518-10523.
37. **Anderson VE, Nguyen Y, Weinberg JB.** 2009. Effects of allergic airway disease on mouse adenovirus type 1 respiratory infection. Virology **391:**25-32.
38. **Nguyen Y, McGuffie BA, Anderson VE, Weinberg JB.** 2008. Gammaherpesvirus modulation of mouse adenovirus type 1 pathogenesis. Virology **380:**182-190.

39. **Weinberg JB, Jensen DR, Gralinski LE, Lake AR, Stempfle GS, Spindler KR.** 2007. Contributions of E1A to mouse adenovirus type 1 pathogenesis following intranasal inoculation. Virology **357:**54-67.
40. **Nguyen Y, Procario MC, Ashley SL, O'Neal WK, Pickles RJ, Weinberg JB.** 2011. Limited effects of Muc1 deficiency on mouse adenovirus type 1 respiratory infection. Virus Res **160:**351-359.
41. **Moore ML, McKissic EL, Brown CC, Wilkinson JE, Spindler KR.** 2004. Fatal disseminated mouse adenovirus type 1 infection in mice lacking B cells or Bruton's tyrosine kinase. J Virol **78:**5584-5590.
42. **Steer SA, Corbett JA.** 2003. The role and regulation of COX-2 during viral infection. Viral Immunol **16:**447-460.
43. **Natarajan G, Glibetic M, Raykova V, Ofenstein JP, Thomas RL, Aranda JV.** 2007. Nitric oxide and prostaglandin response to group B streptococcal infection in the lung. Ann Clin Lab Sci **37:**170-176.
44. **Xu F, Xu Z, Zhang R, Wu Z, Lim J-H, Koga T, Li J-D, Shen H.** 2008. Nontypeable Haemophilus influenzae induces COX-2 and PGE2 expression in lung epithelial cells via activation of p38 MAPK and NF-kappa B. Respir Res **9:**16.
45. **Sadikot RT, Zeng H, Azim AC, Joo M, Dey SK, Breyer RM, Peebles RS, Blackwell TS, Christman JW.** 2007. Bacterial clearance of Pseudomonas aeruginosa is enhanced by the inhibition of COX-2. Eur. J. Immunol. **37:**1001-1009.
46. **Rangel Moreno J, Estrada García I, De La Luz García Hernández M, Aguilar Leon D, Marquez R, Hernández Pando R.** 2002. The role of prostaglandin E2 in the immunopathogenesis of experimental pulmonary tuberculosis. Immunology **106:**257-266.
47. **Aronoff DM, Bergin IL, Lewis C, Goel D, O'brien E, Peters-Golden M, Mancuso P.** 2012. E-prostanoid 2 receptor signaling suppresses lung innate immunity against Streptococcus pneumoniae. Prostaglandins Other Lipid Mediat **98:**23-30.
48. **Aronoff DM, Canetti C, Peters-Golden M.** 2004. Prostaglandin E2 inhibits alveolar macrophage phagocytosis through an E-prostanoid 2 receptor-mediated increase in intracellular cyclic AMP. J Immunol **173:**559-565.
49. **Serezani CH, Chung J, Ballinger MN, Moore BB, Aronoff DM, Peters-Golden M.** 2007. Prostaglandin E2 suppresses bacterial killing in alveolar macrophages by inhibiting NADPH oxidase. Am J Respir Cell Mol Biol **37:**562-570.
50. **Serezani CH, Ballinger MN, Aronoff DM, Peters-Golden M.** 2008. Cyclic AMP: master regulator of innate immune cell function. Am J Respir Cell Mol Biol **39:**127-132.
51. **Kapoor M, Kojima F, Qian M, Yang L, Crofford LJ.** 2006. Shunting of prostanoid biosynthesis in microsomal prostaglandin E synthase-1 null embryo fibroblasts: regulatory effects on inducible nitric oxide synthase expression and nitrite synthesis. FASEB J **20:**2387-2389.

52. **Carey MA, Bradbury JA, Rebolloso YD, Graves JP, Zeldin DC, Germolec DR.** 2010. Pharmacologic inhibition of COX-1 and COX-2 in influenza A viral infection in mice. PLoS ONE **5:**e11610.
53. **Coomes SM, Wilke CA, Moore TA, Moore BB.** 2010. Induction of TGF-beta 1, not regulatory T cells, impairs antiviral immunity in the lung following bone marrow transplant. J Immunol **184:**5130-5140.
54. **Lauder SN, Taylor PR, Clark SR, Evans RL, Hindley JP, Smart K, Leach H, Kidd EJ, Broadley KJ, Jones SA, Wise MP, Godkin AJ, O'Donnell V, Gallimore AM.** 2011. Paracetamol reduces influenza-induced immunopathology in a mouse model of infection without compromising virus clearance or the generation of protective immunity. Thorax **66:**368-374.
55. **Monrad SU, Kojima F, Kapoor M, Kuan EL, Sarkar S, Randolph GJ, Crofford LJ.** 2011. Genetic deletion of mPGES-1 abolishes PGE2 production in murine dendritic cells and alters the cytokine profile, but does not affect maturation or migration. Prostaglandins Leukot Essent Fatty Acids **84:**113-121.
56. **Wang M, Zukas AM, Hui Y, Ricciotti E, Puré E, FitzGerald GA.** 2006. Deletion of microsomal prostaglandin E synthase-1 augments prostacyclin and retards atherogenesis. Proc Natl Acad Sci USA **103:**14507-14512.
57. **Grusby MJ, Johnson RS, Papaioannou VE, Glimcher LH.** 1991. Depletion of CD4+ T cells in major histocompatibility complex class II-deficient mice. Science **253:**1417-1420.
58. **Cauthen A, Welton A, Spindler KR.** 2007. Construction of mouse adenovirus type 1 mutants. Methods Mol Med **130:**41-59.

Notes

This chapter was reprinted and modified from McCarthy, MK, Levine, RE, Procario, MC, McDonnell, PJ, Zhu, L, Aronoff, DA, Crofford, LE, and Weinberg, JB. 2013. Prostaglandin E_2 induction during mouse adenovirus type 1 respiratory infection regulates inflammatory mediator generation but does not affect viral pathogenesis. *PLOS One*. 8:e77628. DOI: 10.1371/journal.pone.0077628

Chapter 5:
Increased susceptibility to mouse adenovirus type 1 infection following bone marrow transplant correlates with defective T cell response that is not mediated by exaggerated prostaglandin E_2 production

Abstract

Adenovirus infections are an important complication following hematopoietic stem cell transplantation. We used mouse adenovirus type 1 (MAV-1) respiratory infection in an allogeneic bone marrow transplant (BMT) mouse model, and demonstrated that BMT mice displayed significantly delayed clearance of virus from the lungs. CD4 and CD8 T cell function was impaired in BMT mice compared to untransplanted controls. Lung viral loads in untransplanted CD8-deficient mice were higher than CD8$\alpha^{+/+}$ control mice, suggesting that delayed MAV-1 clearance in BMT mice may be due to defective CD8 T cell function. Baseline PGE_2 levels were higher in bronchoalveolar lavage fluid (BALF) from BMT mice than in non-BMT controls, and PGE_2 levels in BALF from BMT mice were dramatically higher than in non-BMT controls after MAV-1 infection. Allogeneic BMT using PGE_2-deficient mice as donors or recipients failed to correct the defect in viral clearance, and treatment of untransplanted mice with the PGE_2 analog misoprostol was not associated with increased lung viral loads. Thus, although PGE_2 production is exaggerated in the lungs of BMT mice infected with MAV-1, PGE_2 overproduction is not directly responsible for

delayed viral clearance. Instead, our data suggest that PGE_2-independent effects on CD8 T cell function may contribute to the inability of BMT mice to clear virus from the lungs.

Introduction

Hematopoietic stem cell transplant (HSCT), including bone marrow transplant (BMT), is a common therapy for management of a variety of malignant and autoimmune diseases. However, its use is limited by a number of complications, particularly in the lung. Pulmonary complications may be caused by multiple factors, including the conditioning regimen prior to transplantation and the development of graft-versus-host disease (GVHD) in allogeneic transplantation, where the donor and recipient are not genetically identical (1, 2). Viral infection is an important complication in both allogeneic and autologous BMT (3-5).

Human adenoviruses (HAdVs) cause considerable morbidity and mortality in BMT patients (6-8). Depending on the assay used, HAdVs have been detected in up to 29% of BMT patients during weekly surveillance screening (9, 10). Disease rates as high as 6.5% have been reported, with >50% mortality rates in BMT patients with HAdV disease in some studies (10, 11). Pediatric patients are at a higher risk for adenovirus disease (8, 12), likely due to higher infection rates in this population and a relative lack of species cross-reactive T and B cell responses compared to adults, in whom some adenovirus-specific immunity has been established (13). Severe GVHD (14), T-cell-depleted grafts, and leukopenia (15) are additional risk factors for adenovirus infection following BMT.

A number of studies have reported profound defects in both innate and adaptive immune function following BMT (reviewed in (2)). Prostaglandin E_2 (PGE_2) is a lipid mediator that has a variety of effects on immune function. PGE_2 can be immunosuppressive *in vitro,* inhibiting production of the Th1 cytokines IFN-γ and IL-12 (16, 17). Alveolar macrophage and neutrophil phagocytosis and bacterial killing is inhibited by PGE_2 (18, 19). Levels of circulating PGE_2 are elevated in BMT patients (20). PGE_2 contributes to the suppression of lymphocyte function observed in human BMT patients (21). Other groups have demonstrated exaggerated PGE_2 production and increased susceptibility to *Pseudomonas aeruginosa* and *Staphylococcus aureus* infection in syngeneic BMT mice (22-24). The inability of mice to effectively control bacterial infections in the lung is directly linked to the immunosuppressive effects of PGE_2 on macrophage and neutrophil function. Syngeneic BMT mice display defective control of viral replication in a mouse model of respiratory virus infection using murine gammaherpesvirus-68 (γHV-68) (25). This model is characterized by impaired CD4 T cell proliferation and Th1 responses due to overproduction of TGF-β1 in BMT mice.

Because adenovirus infections are an important complication following allogeneic BMT, we chose to study pulmonary immunity to adenovirus infection post-BMT using mouse adenovirus type 1 (MAV-1, also known as MAdV-1) as a model (26-32). Following intranasal (i.n.) MAV-1 infection, virus clearance from the lungs was significantly delayed in mice that received allogeneic BMT compared to untransplanted control mice. Our data suggest that activation of

both CD4 and CD8 T cells is impaired in BMT mice. Delayed virus clearance was not related to exaggerated PGE_2 production, as allogeneic BMT using PGE_2-deficient mice as donors or recipients failed to correct the defect in viral clearance.

Results

Delayed viral clearance from lungs of mice after allogeneic BMT

To determine whether mice were more susceptible to adenovirus infection following allogeneic BMT, we infected control (BALB/c and C57BL/6) and allogeneic (BALB/c donor, C57BL/6 recipient) BMT mice with MAV-1 at 5 weeks post-BMT, when numbers of hematopoietic cells are fully reconstituted and the majority of hematopoietic cells are donor-derived (33). We assessed viral loads in the lung at times corresponding to the peak of viral replication (7 dpi) and clearance of virus from the lungs (14 and 21 dpi). Peak lung viral loads at 7 dpi were comparable between control and BMT mice (Figure 5-1). Viral loads were substantially less in control mice at 14 and 21 dpi, as virus was cleared from the lungs. However, viral loads at 14 dpi in BMT mice were approximately two log units higher than in control mice and were equivalent to those at 7 dpi. By 21 dpi, viral loads in BMT mice were decreased, but they were still significantly higher than those in either control group. These data indicate that peak viral replication is equivalent in control and BMT mice, but viral clearance from lungs of BMT mice was significantly delayed.

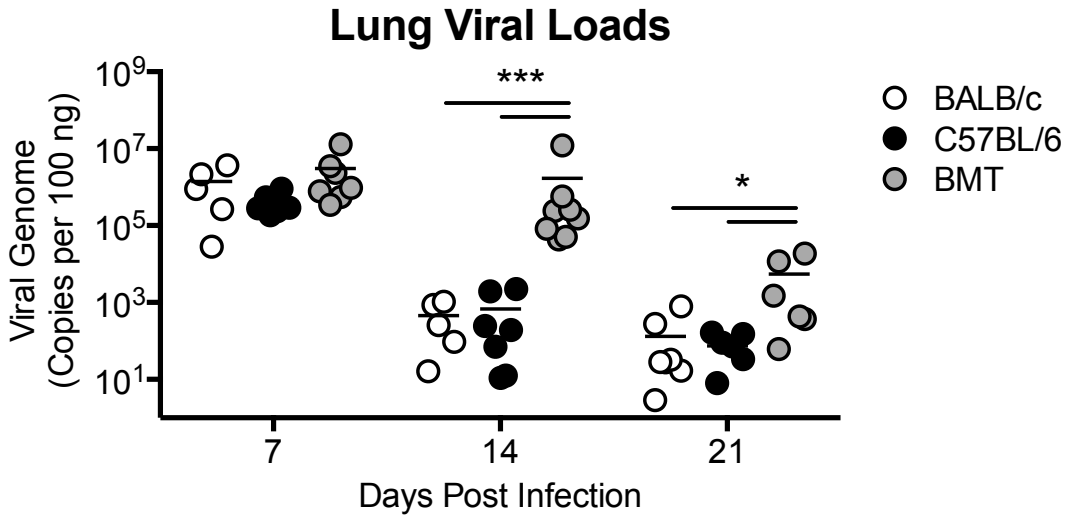

Figure 5-1. Delayed viral clearance from lungs of mice after allogeneic BMT.

BMT mice and untransplanted BALB/c and C57BL/6 controls were infected intranasally (i.n.) with MAV-1. DNA was extracted from lungs harvested at the indicated time points. qPCR was used to quantify MAV-1 genome copies in lung DNA. DNA viral loads are expressed as copies of MAV-1 genome per 100 ng of input DNA. Individual circles represent values for individual mice and horizontal bars represent means for each group. Statistical comparisons were made using two-way ANOVA followed by Bonferroni's multiple comparison tests. ***P<0.001, *P<0.05.

BMT mice have a defect in T cell recruitment and activation

T cells can play both inflammatory and cytolytic roles during viral infection, either by release of cytokines such as IFN-γ or TNF-α, or through secretion of cytolytic granules such as granzyme B (GzmB), that lyse virus-infected cells. During acute MAV-1 encephalomyelitis following intraperitoneal inoculation, mice deficient in α/β T cells fail to control MAV-1 replication and succumb 9 to 16 weeks after the initial infection, indicating that either CD4 or CD8 T cells are required for long-term host survival of MAV-1 intraperitoneal (i.p.) infection (34). We hypothesized that the inability of BMT mice to efficiently clear virus from the lungs could be due to differences in T cell recruitment or activation after infection. To assess whether T cell activation is reduced in BMT mice, we measured mRNA levels of IFN-γ and GzmB. At 7 dpi, both IFN-γ and GzmB expression were increased in BALB/c and C57BL/6 infected groups compared to mock infected controls (Figure 5-2A,B). However, IFN-γ and GzmB induction were substantially reduced in BMT mice. At 14 dpi, both IFN-γ and GzmB were slightly upregulated in all three infected groups of mice, although upregulation was not statistically significant compared to the mock infected groups and did not differ between BMT and control groups (data not shown).

The reduction in IFN-γ and GzmB transcripts in BMT mice could be due to defective T cell recruitment, activation, or both. To assess overall CD4 and CD8 T cell recruitment and activation, we isolated lung lymphocytes from BALB/c and BMT mice (in which hematopoietic cells were derived from the BALB/c donor

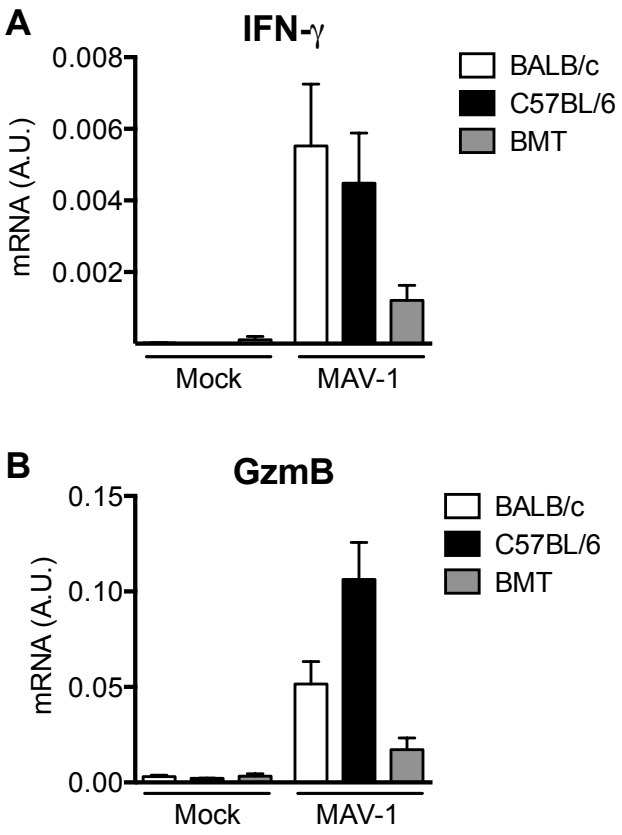

Figure 5-2. Reduced IFN-γ and GzmB induction in lungs of BMT mice.

BMT mice and untransplanted BALB/c and C57BL/6 controls were infected i.n. with MAV-1 or mock infected with conditioned media. RNA was extracted from lungs harvested at 7 dpi and RT-qPCR was used to quantify A) IFN-g mRNA and B) GzmB mRNA, which are expressed in arbitrary units. Combined data from n=2-4 (mock condition), n=5-8 (MAV-1 condition) mice per group are presented as means ± S.E.M.

strain) at 7 dpi and performed intracellular cytokine staining. We used TCRβ as a marker for T cells. The total number of TCRβ$^+$ cells increased slightly in untransplanted BALB/c mice after infection, but not in BMT mice (Figure 5-3A). There were fewer TCRβ$^+$CD4$^+$ T cells in the lungs of BMT mice compared to BALB/c mice both before and after infection, although this difference was not statistically significant (Figure 5-3B). BALB/c and BMT mice had equivalent numbers of TCRβ$^+$CD8$^+$ T cells in the lungs after infection (Figure 5-3C). We next performed intracellular staining on lung lymphocytes at 7 dpi to evaluate T cell activation. In BALB/c mice, there was a significant accumulation of CD4 and CD8 T cells producing IFN-γ or GzmB after MAV-1 infection (Figure 5-3D, E). However, the accumulation of IFN-γ$^+$ and GzmB$^+$ CD4 and CD8 T cells was markedly diminished in infected BMT mice. These data indicate that CD4 T cell recruitment, but not CD8 T cell recruitment, is slightly impaired in BMT mice. Moreover, BMT mice have significantly fewer CD4 and CD8 T cells producing IFN-γ or GzmB after infection.

T cells from BMT mice respond poorly when stimulated

We observed a slight defect in CD4 T cell recruitment to the lungs of BMT mice after infection, which could account for the lower number of IFN-γ$^+$ and GzmB$^+$ CD4 T cells overall in these mice. To address T cell activation in BMT mice directly, we isolated lung lymphocytes at 7 dpi and restimulated T cells overnight with anti-CD3 antibody. We measured production of IL-2, IFN-γ, IL-4, and IL-17 in the supernatant as a marker for T cell polarization and activation. T

cells isolated from infected BALB/c mice produced significantly more IL-2, IFN-γ, and IL-17 upon restimulation than T cells isolated from mock infected BALB/c mice (Figure 5-4A, B and D). We observed slightly higher IL-4 production in stimulated T cells from infected BALB/c mice, but this was not significantly different from T cells from mock infected BALB/c mice (Figure 5-4C). Although T cells from infected BMT mice did produce somewhat more IL-2, IFN-γ, and IL-17 compared to those from mock-infected BMT mice, their production was substantially lower than that observed in infected BALB/c mice. This indicates that even when equal numbers of T cells from the lungs of BALB/c or BMT mice are restimulated, T cells from BMT mice are impaired in activation. Therefore, even though we observed a slight defect in recruitment of CD4 T cells in BMT mice, the significant reduction in IFN-γ^+ and GzmB$^+$ T cells in the lungs of BMT mice is more likely due to an overall activation defect rather than a defect in recruitment.

Delayed viral clearance in untransplanted mice lacking CD8 T cells

We observed a reduction in IFN-γ expression and IFN-γ-expressing cells in BMT mice, most likely due to impaired activation of CD4 and CD8 T cells. To assess the effect of complete IFN-γ deficiency on virus clearance, we infected IFN-$\gamma^{+/+}$ and IFN-$\gamma^{-/-}$ mice on a C57BL/6 background and measured lung viral loads at 14 dpi. Viral loads were equivalent in IFN-$\gamma^{+/+}$ and IFN-$\gamma^{-/-}$ mice (Figure 5-5A), suggesting that IFN-γ does not play a significant role in viral clearance. We have previously shown that IFN-γ deficiency on a BALB/c background leads to a

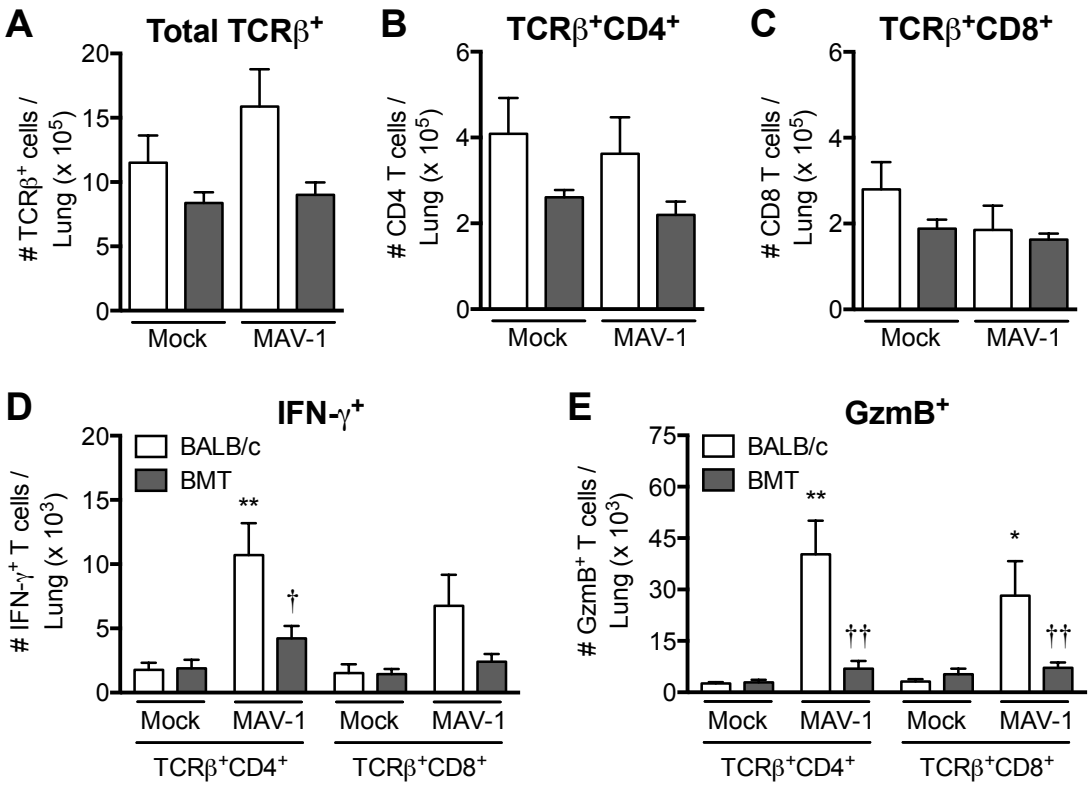

Figure 5-3. Reduced numbers of IFN-γ- and GzmB-producing CD4 and CD8 T cells in lungs of BMT mice.

BMT mice and untransplanted BALB/c controls were infected i.n. with MAV-1 or mock infected with conditioned media, and lung leukocytes were isolated at 7 dpi. Lung leukocytes were stimulated with PMA/ionomycin and stained to quantify the number of A) total TCRβ$^+$ cells, B) TCRβ$^+$CD4$^+$ T cells, C) TCRβ$^+$CD8$^+$ T cells, D) IFN-γ$^+$ T cells, and E) GzmB$^+$ T cells per lung. Combined data from n=3-4 mice per group are presented as means ± S.E.M. Statistical comparisons were made using one-way ANOVA followed by Bonferroni's multiple comparison tests. ***P*<0.01 and **P*<0.05 comparing mock to MAV-1. ††*P*<0.01 and †*P*<0.05 comparing BALB/c to BMT mice.

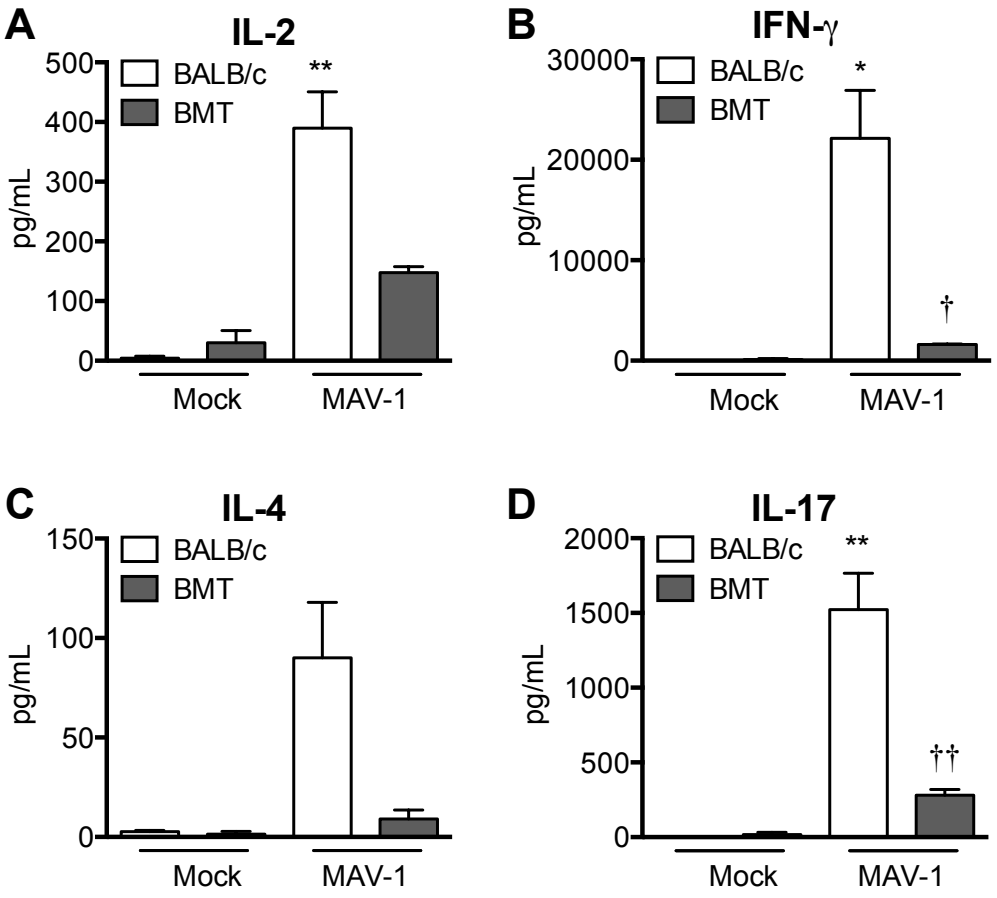

Figure 5-4. T cells from BMT mice respond poorly when stimulated.

BMT mice and untransplanted BALB/c controls were infected i.n. with MAV-1 or mock infected with conditioned media, and lung leukocytes were isolated at 7 dpi. Lung leukocytes were stimulated overnight with anti-CD3 antibody and ELISA was used to measure A) IL-2, B) IFN-γ, C) IL-4, and D) IL-17 production in the supernatant. Combined data from n=3-8 mice per group are presented as means ± S.E.M. Statistical comparisons were made using one-way ANOVA followed by Bonferroni's multiple comparison tests. ***P*<0.01 and **P*<0.05 comparing mock to MAV-1. ††*P*<0.01 and †*P*<0.05 comparing BALB/c to BMT mice.

modest (<1 log) increase in viral loads at 14 dpi (27). Together, these results suggest that IFN-γ deficiency does not significantly affect viral clearance in the context of either a BALB/c or C57BL/6 background.

Although IFN-γ does not substantially contribute to viral clearance, other aspects of T cell activation, namely GzmB production, were clearly impaired in BMT mice and could be responsible for the delayed viral clearance that we observed. We next infected $CD8\alpha^{+/+}$ and $CD8\alpha^{-/-}$ mice, which lack CD8 T cells, with MAV-1 and measured lung viral loads at 14 dpi. Viral loads were significantly greater in $CD8\alpha^{-/-}$ mice compared to $CD8\alpha^{+/+}$ mice (Figure 5-5B). The difference was similar in magnitude to that observed in BMT mice compared to untransplanted controls at 14 dpi (Figure 5-1). These results suggest that CD8 T cells are one of the major contributors to clearance of virus-infected cells from the lung during MAV-1 infection.

PGE_2 is overproduced in BMT mice

Other groups have demonstrated exaggerated PGE_2 production and increased susceptibility to bacterial infections in syngeneic BMT mice (22, 23). This increased susceptibility was directly linked to exaggerated PGE_2 production in BMT mice and the immunosuppressive effects of PGE_2 on macrophages and neutrophils. High concentrations of PGE_2 exert an immunosuppressive effect on Th1 responses by inhibiting production of IFN-γ and IL-12 *in vitro* (16, 17). We hypothesized that excess PGE_2 production in BMT mice was responsible for impaired T cell activation and delayed viral clearance. PGE_2 concentrations

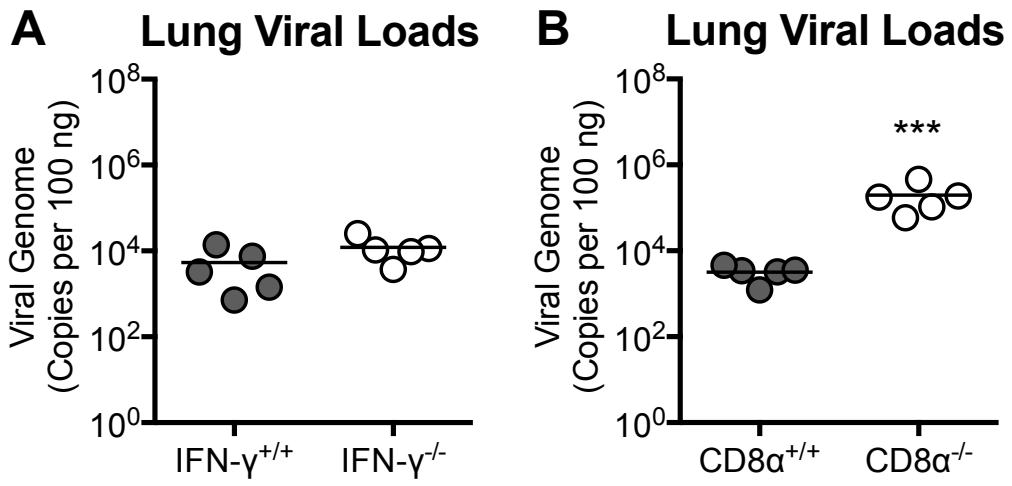

Figure 5-5. Delayed viral clearance in untransplanted mice lacking CD8 T cells.

A) IFN-$\gamma^{+/+}$ and IFN-$\gamma^{-/-}$ mice and B) CD8$\alpha^{+/+}$ and CD8$\alpha^{-/-}$ were infected i.n. with MAV-1. DNA was extracted from lungs harvested at 14 dpi. qPCR was used to quantify MAV-1 genome copies in lung DNA. DNA viral loads are expressed as copies of MAV-1 genome per 100 ng of input DNA. Individual circles represent values for individual mice and horizontal bars represent means for each group. Statistical comparisons were made using Mann-Whitney test. ***P<0.001, comparing CD8$\alpha^{+/+}$ to CD8$\alpha^{-/-}$.

measured in bronchoalveolar lavage fluid (BALF) were slightly higher in BMT mice at baseline prior to infection (5 weeks post-BMT) (Figure 5-6). PGE_2 levels increased after infection in both untransplanted control groups, with a slight delay observed in BALB/c mice. PGE_2 levels in BMT mice increased dramatically after infection, and PGE_2 production was significantly higher in BMT mice than either control group at 14 and 21 dpi (Figure 5-6).

PGE_2 does not contribute to delayed viral clearance in BMT mice

To determine whether excess PGE_2 contributes to the delayed viral clearance in BMT mice, we performed allogeneic BMT with various combinations of mice deficient in microsomal prostaglandin E synthase-1 (mPGES-1) as donors and recipients. mPGES-1 is an enzyme that is responsible for the majority of the conversion of PGH_2 to PGE_2, so that mPGES-1-deficient mice on a C57BL/6 background (indicated as mPGES-$1^{-/-}$/B6) are almost completely PGE_2-deficient (35, 36). We infected these mice with MAV-1 at 5 weeks post-BMT and measured lung viral loads and BALF PGE_2 at 14 dpi. PGE_2 was overproduced following infection compared to untransplanted BALB/c and C57BL/6 control groups when wild-type C57BL/6 mice were used as recipients in the BMT, as we observed previously (Figure 5-6 and Figure 5-7A). When wild-type BALB/c bone marrow was transferred into mPGES-$1^{-/-}$/B6 recipients, PGE_2 levels were equivalent to those of wild-type C57BL/6 recipients. This suggests that hematopoietic cells from the BALB/c donor strain (which is not PGE_2-deficient) were the major source of PGE_2 in the BMT.

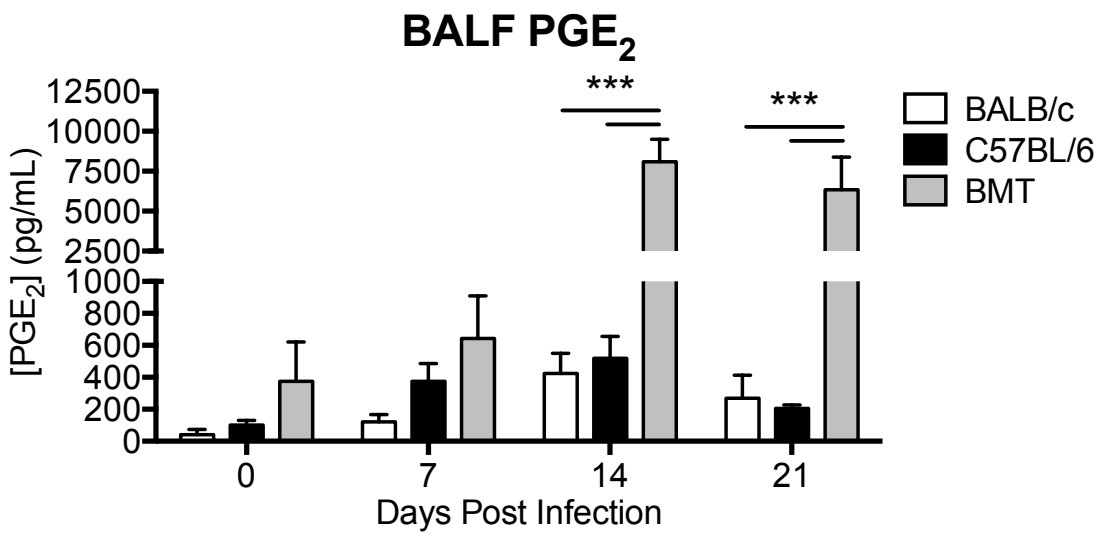

Figure 5-6. PGE_2 is overproduced in BMT mice.

BMT mice and untransplanted BALB/c and C57BL/6 controls were infected i.n. with MAV-1 or mock infected with conditioned media. ELISA was used to quantify PGE_2 concentrations in BALF at the indicated time points. Combined data from n=3-4 mice per group are presented as means ± S.E.M. Statistical comparisons were made using two-way ANOVA followed by Bonferroni's multiple comparison tests. ***P<0.001.

In order to create mice in which the immune cell compartment was deficient in PGE_2, we reversed the order of the BMT, this time using wild-type C57BL/6 or mPGES-$1^{-/-}$/B6 mice as donors and wild-type BALB/c mice as recipients. Compared to BMT with wild-type BALB/c donors and wild-type C57BL/6 recipients, we observed significantly less PGE_2 production at 14 dpi following BMT using C57BL/6 mice as donors and BALB/c mice as recipients. When mPGES-$1^{-/-}$/B6 bone marrow was transferred into wild-type BALB/c mice, PGE_2 production was equivalent to that of either control group, indicating that normal PGE_2 production was restored (Figure 5-7A, far right side). The differing amounts of PGE_2 observed between the BMT combinations using wild-type C57BL/6 mice and wild-type BALB/c mice as recipients likely relate to differing amounts of irradiation received at the time of transplant (1400 rad for C57BL/6 versus 1000 rad for BALB/c, due to higher sensitivity of BALB/c mice to radiation (37)).

Despite varying levels of PGE_2 production, all combinations of BMT using PGE_2-deficient mice as donors or recipients had significantly higher lung viral loads at 14 dpi than either control group (Figure 5-7B). Furthermore, in the two BMT combinations in which we observed the lowest PGE_2 concentrations (recipient strain was BALB/c), we still observed defective IFN-γ and GzmB expression at 7 dpi (Figure 5-7C, D). These results suggest that although PGE_2 is produced in excess in the BALF of BMT mice, it does not contribute to delayed viral clearance or affect T cell activation.

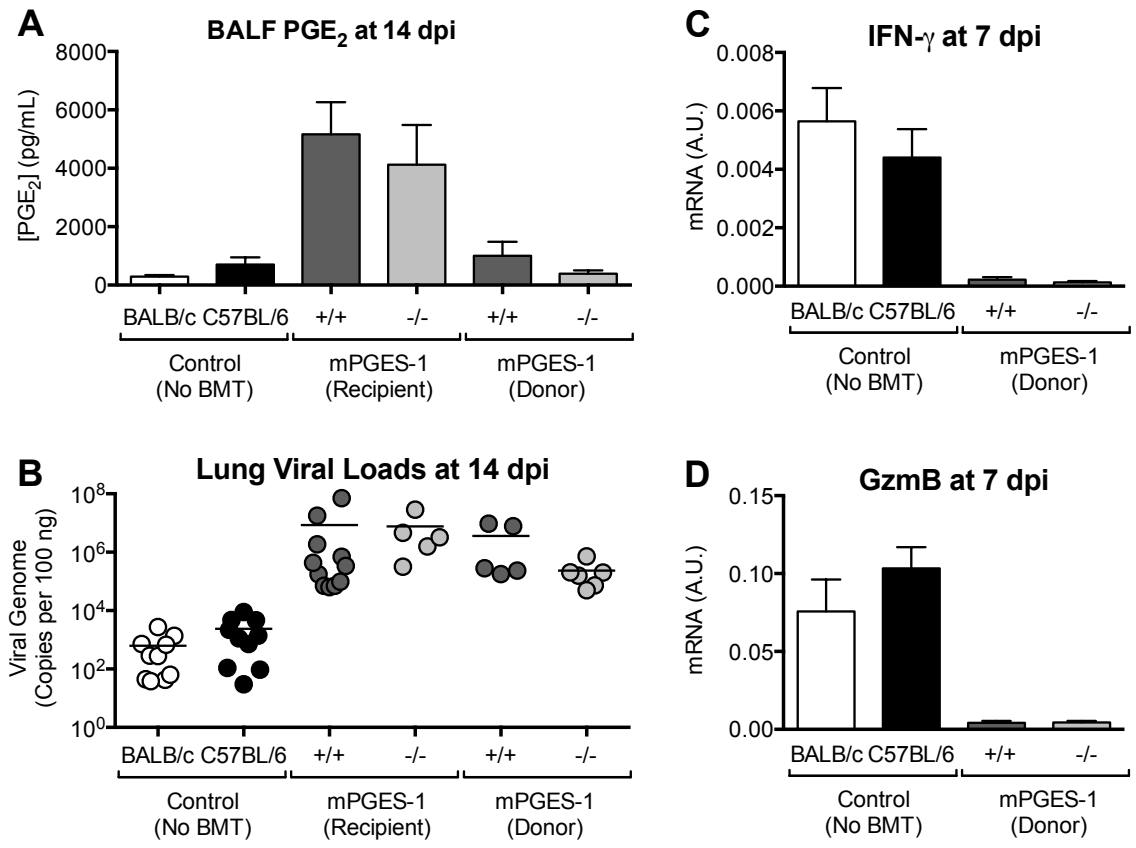

Figure 5-7. Restoration of normal PGE_2 levels fails to correct viral clearance defect in BMT mice.

BMT mice and untransplanted BALB/c and C57BL/6 controls were infected i.n. with MAV-1 or mock infected with conditioned media. A) ELISA was used to quantify PGE_2 concentrations in BALF at the indicated time points. Combined data from n=5-15 mice per group are presented as means ± S.E.M. B) DNA was extracted from lungs harvested at 14 dpi. qPCR was used to quantify MAV-1 genome copies in lung DNA. DNA viral loads are expressed as copies of MAV-1 genome per 100 ng of input DNA. Individual circles represent values for individual mice and horizontal bars represent means for each group. RNA was extracted from lungs harvested at 7 dpi and RT-qPCR was used to quantify C) IFN-γ mRNA and D) GzmB mRNA, which are expressed in arbitrary units. Combined data from n=5-11 mice per group are presented as means ± S.E.M.

Excess PGE_2 in untransplanted mice does not affect viral clearance

To examine the role of excess PGE_2 outside of the context of BMT, we treated untransplanted C57BL/6 mice with misoprostol, a PGE_2 analog, starting the day of infection. Mice treated with misoprostol produced significantly more IFN-γ after infection compared to vehicle-treated mice, indicating that excess PGE_2 increased T cell responses to MAV-1 infection, rather than playing a suppressive role (Figure 5-8A). Misoprostol treatment did not affect peak viral replication at 7 dpi or viral clearance from the lungs at 14 dpi (Figure 5-8B). This indicates that excess PGE_2 does not affect viral clearance in untransplanted mice, providing further support for the lack of an effect of PGE_2 overproduction on MAV-1 clearance following BMT.

Discussion

We have shown that mice that underwent allogeneic BMT displayed significant defects in clearance of MAV-1 from the lungs. BMT mice had significantly fewer IFN-γ- and GzmB-producing CD4 and CD8 T cells in the lungs compared to untransplanted controls. Cytokine production by restimulated T cells was dramatically less in T cells isolated from BMT mice compared to controls. Lung viral loads in untransplanted CD8-deficient mice were higher than wild-type mice, suggesting that delayed MAV-1 clearance in BMT mice may be due to defective CD8 T cell function. Levels of the immunomodulatory lipid mediator PGE_2 were dramatically higher in BALF from BMT mice than in controls after

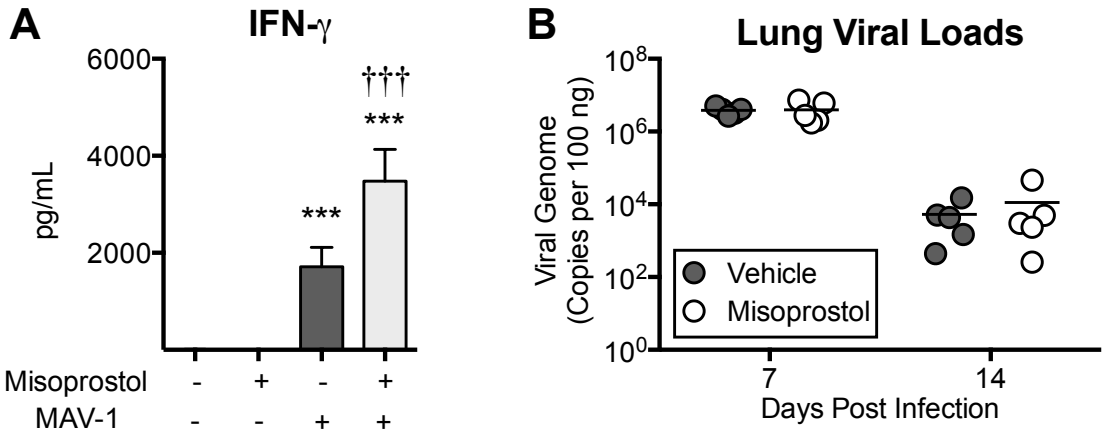

Figure 5-8. Excess PGE_2 in untransplanted mice does not affect viral clearance.

C57BL/6 mice were infected i.n. with MAV-1 and treated once daily with 20 μg misoprostol or vehicle (DMSO). A) ELISA was used to quantify IFN-γ concentrations in BALF from mice at 7 dpi. Combined data from n=5 mice per group are presented as means ± S.E.M. ****P*<0.001 comparing mock to MAV-1. †††*P*<0.001 comparing misoprostol- to vehicle-treated group. B) DNA was extracted from lungs harvested at the indicated time points. qPCR was used to quantify MAV-1 genome copies in lung DNA. DNA viral loads are expressed as copies of MAV-1 genome per 100 ng of input DNA. Individual circles represent values for individual mice and horizontal bars represent means for each group.

MAV-1 infection. However, allogeneic BMT using PGE_2-deficient mice as donors or recipients failed to correct the defect in viral clearance, and treatment of untransplanted mice with the PGE_2 analog misoprostol was not associated with increased lung viral loads.

Our results are in agreement with other studies demonstrating impaired immunity following BMT (reviewed in (2)). Syngeneic BMT mice infected with γHV-68 display a defect in the ability to clear lytic virus from the lungs (25). In that study, the number of IFN-γ-producing CD4 T cells was significantly reduced and the number of IL-17-producing CD4 T cells was enhanced in lungs of BMT mice after γHV-68 infection. We also observed defective Th1 responses in BMT mice after MAV-1 infection. However, we did not observe an increase in IL-17 production from BMT T cells, indicating that Th responses were not skewed toward a Th17 phenotype in MAV-1-infected BMT mice. Rather, T cells from BMT mice were impaired in their ability to produce both IFN-γ and IL-17 in MAV-1 infected mice. We have previously demonstrated that IL-17 produced by CD4 and γδ-T cells during MAV-1 infection contributes to neutrophil recruitment to the lungs, but IL-17 deficiency does not affect peak viral replication or viral clearance (38). Therefore, it is unlikely that decreased IL-17 from T cells was responsible for delayed clearance of MAV-1 in BMT mice.

CD4 T cell-derived IFN-γ is critical for control of γHV-68 replication (39), and defective Th1 responses are probably a major contributor to increased γHV-68 susceptibility observed in BMT mice. However, we show that decreased IFN-γ is unlikely to be responsible for defective clearance of MAV-1 after BMT,

because untransplanted IFN-$\gamma^{-/-}$ mice had equivalent viral loads at 14 dpi compared to wild-type mice. Similarly, we have previously shown that IFN-γ makes only minor contributions to control of MAV-1 replication in another mouse strain background, BALB/c (27). Rather, the delayed viral clearance in BMT mice was likely due to decreased production of cytolytic effectors such as GzmB by CD4 and CD8 T cells.

It is possible that decreased generation of MAV-1-specific antibodies by B cells contributed to delayed viral clearance in BMT mice. B cells are important for survival in mice with systemic MAV-1 infection (40). However, neutralizing antibodies do not appear until at least 14 dpi in the sera of mice infected i.p. with MAV-1 (41). Therefore, B cells would be unlikely to make substantial contributions to viral clearance until after 14 dpi. While B cells may play a role in control of viral replication between 14 and 21 dpi, our results strongly suggest that immune deficiencies occurring before 14 dpi were responsible for the delayed viral clearance in BMT mice. Mice deficient in CD8 T cells had similar viral loads to BMT mice at 14 dpi, suggesting that CD8 T cell function is a critical factor involved in MAV-1 clearance from the lungs.

DCs are important antigen presenting cells that function as initiators of the adaptive immune response. Coomes et al. showed that DCs isolated from BMT mice are able to upregulate MHC class II and costimulatory molecules as well as untransplanted mice do, and DCs are efficient stimulators of T cell proliferation in a mixed lymphocyte reaction (MLR) (25). DCs derived from peripheral blood of HSCT patients are also efficient stimulators in MLR (42). In our work, T cells

produced similar amounts of IFN-γ when stimulated with MAV-1-infected APCs from either BALB/c or BMT mice (data not shown). This suggests that APC function, at least in terms of promoting Th1 cytokines, in BMT mice is not impaired.

A number of studies have reported that PGE_2 suppresses production of Th1 cytokines (16, 17), an effect that is observed when local PGE_2 concentrations are greater than 1 nM (43). Others have demonstrated PGE_2 inhibition of T cell proliferation in MLR (44). PGE_2 inhibits T cell recruitment and delays the induction of virus-specific T cell responses in the lungs of influenza virus-infected mice (45). We hypothesized that overproduction of PGE_2 in BMT mice was responsible for suppression of T cell responses that normally clear virus from the lung. BMT using PGE_2-deficient mice as donors or recipients did not correct the defect in viral clearance or restore T cell activation (by measurement of IFN-γ and GzmB levels). Mice treated with the PGE_2 analog misoprostol cleared virus as efficiently as controls. This suggests that while PGE_2 is overproduced after BMT and suppresses T cell responses in other settings, it does not contribute to delayed viral clearance post-BMT.

Immune recovery appears to play a significant role in HAdV infections post-transplant. A number of studies have documented a positive correlation between lymphocyte count (both absolute lymphocyte count and CD4 count) and clearance of HAdV and survival (15, 46, 47). In adult and pediatric HSCT patients, clearance of HAdV from peripheral blood is associated with the emergence of HAdV-specific CD4 and CD8 T cell responses (48). Clearance of

HAdV is also associated with an increase in titers of serotype-specific antibodies (46), indicating that both B and T cell function may be important for control of HAdV post-transplant. *Ex vivo* generation and adoptive transfer of virus-specific CD4 or CD8 T cells has been explored as immunotherapy for HSCT patients with disease caused by HAdV and other viruses. This strategy has already been successfully used in transplant patients with Epstein Barr virus (EBV)-induced lymphoproliferative disease (49-51). It has also been used with some success in pediatric transplant patients with HAdV viremia (52) or prophylactically to prevent HAdV disease (53). A number of studies have demonstrated *ex vivo* generation of HAdV-specific cytotoxic CD4 and CD8 T cells, some of which were cross-reactive against multiple HAdV serotypes (54-59). These studies show promise for the effective treatment of HAdV infections post-BMT. Further insight into the mechanisms of immune dysfunction post-BMT may assist in the development of treatment strategies for HAdV-infected patients.

Materials and Methods

Mice

BALB/c, C57BL/6, CD8$\alpha^{-/-}$ [B6.129S2-*Cd8a*^{tm1Mak}/J], and IFN-$\gamma^{-/-}$ [B6.129S7-*Ifng*^{tm1Ts}/J] mice (all knockouts backcrossed onto a C57BL/6 background) were obtained from the Jackson Laboratory. mPGES-1 heterozygous mice on a DBA1lac/J background (60) were originally obtained from Pfizer, Inc. (Groton, CT) and then backcrossed onto a C57BL/6 background. Homozygous mPGES-1$^{-/-}$ mice and homozygous wild type mPGES-1$^{+/+}$ mice

derived from the same heterozygous mPGES-1$^{+/-}$ parents were bred at the University of Michigan. Adult males were used in all experiments. All mice were maintained under specific pathogen-free conditions.

Bone Marrow Transplantation

Bone marrow transplantation was performed as previously described (22, 25). Recipient C57BL/6 mice received 1400 rad of total body irradiation using a ^{137}Cs irradiator, delivered in two doses 3 hours apart. In experiments in which C57BL/6 mice were used as donors in the allogeneic transplant, recipient BALB/c mice received 1000 rad of total body irradiation delivered in two doses 3 hours apart. Bone marrow cells (5 x 10^6) harvested from donor mice were injected into the tail vein of irradiated recipient mice. Mice were given acidified water (pH 3.3) for the first 3 weeks after BMT. Total hematopoietic cell numbers are fully reconstituted in the lung and spleen at 5 weeks post-BMT (25, 33). All infections were carried out 5-6 weeks post-BMT.

Virus and Infections

MAV-1 was grown and passaged in NIH 3T6 fibroblasts, and titers of viral stocks were determined by plaque assay on 3T6 cells as previously described (61). Adult mice were anesthetized with ketamine and xylazine and infected intranasally (i.n.) with 10^5 plaque forming units (p.f.u.) of MAV-1 in 40 μl of sterile phosphate-buffered saline (PBS). Control mice were mock infected i.n. with conditioned media at an equivalent dilution in sterile PBS. Mice were euthanized

by pentobarbital overdose at the indicated time points. Lungs were harvested, snap frozen in dry ice, and stored at -80°C until processed further.

Misoprostol treatment

Mice were injected intraperitoneally with 20 μg misoprostol once daily starting on the day of infection, a dosing regimen adapted from (62).

Isolation of DNA and RNA

DNA was extracted from the middle lobe of the right lung using the DNeasy® Tissue Kit (Qiagen Inc.). Total RNA was extracted from lungs using TRIzol® (Invitrogen) as previously described (30).

Analysis of Viral Loads

MAV-1 viral loads were measured in organs using quantitative real-time polymerase chain reaction (qPCR) as previously described (27, 30). Primers and probe used to detect a 59-bp region of the MAV-1 E1A gene are detailed in Table 2. Five μl of extracted DNA were added to reactions containing TaqMan II Universal PCR Mix with UNG (Applied Biosystems), forward and reverse primers (each at 200 nM final concentration), and probe (20 nM final concentration) in a 25 μl reaction volume. Analysis on an ABI Prism 7300 machine (Applied Biosystems) consisted of 40 cycles of 15 s at 90°C and 60 s at 60°C. Standard curves generated using known amounts of plasmid containing the MAV-1 EIA gene were used to convert cycle threshold values for experimental samples to

copy numbers of EIA DNA. Results were standardized to the nanogram (ng) amount of input DNA. Each sample was assayed in triplicate. The limit of detection of this assay is typically between 10^1 and 10^2 copies of MAV-1 genome per 100 ng input DNA.

Analysis of Host Gene Expression

Cytokine gene expression was quantified using reverse transcriptase (RT)-qPCR. First, 2.5 μg of RNA were reverse transcribed using MMLV reverse transcriptase (Invitrogen) in 20 μl reactions according to the manufacturer's instructions. Water was added to the cDNA product to bring the total volume to 50 μl. Primers used to detect IFN-γ and GzmB (PrimerBankID 7305123a1 (63)) are described in Table 5-1. For these measurements, 5 μl of cDNA were added to reactions containing Power SYBR Green PCR Mix (Applied Biosystems) and forward and reverse primers (each at 200 nM final concentration) in a 25 μl reaction volume. When SYBR green was used to quantify cytokine gene expression, separate reactions were prepared with primers for mouse GAPDH (Table 5-1, used at 200 nM each). In all cases, RT-qPCR analysis consisted of 40 cycles of 15 s at 90°C and 60 s at 60°C. Quantification of target gene mRNA was normalized to GAPDH and expressed in arbitrary units as $2^{-\Delta Ct}$, where Ct is the threshold cycle and $\Delta Ct = Ct(target) – Ct(GAPDH)$.

Analysis of Cytokine or PGE_2 Levels in Bronchoalveolar Lavage Fluid

Mice were euthanized via pentobarbital overdose at the indicated time points. Lungs were lavaged three times with the same aliquot of 1 mL sterile PBS containing protease inhibitor (complete, Mini, EDTA-free tablets; Roche Applied Science). Cells in bronchoalveolar lavage fluid (BALF) were pelleted by centrifugation and supernatant was stored at -80°C until assayed. Cytokine protein concentrations in supernatant were determined by ELISA (Duoset Kits, R&D Systems) according to the manufacturer's protocol. BALF supernatants were diluted in PGE_2 enzyme immunoassay buffer and quantity of PGE_2 was determined using PGE_2 ELISA Kit (Enzo Life Sciences) according to the manufacturer's protocol.

Isolation of Cells from Lungs

In some experiments, left lungs were excised and cut into small pieces before digestion for 30 min at 37°C in a 1 mg/ml solution of collagenase A (Sigma). The digested tissue was then pushed through a syringe with a 1.5-in 22-gauge needle and pelleted at 3,000 rpm (402 x g) for 5 min. After lysis of red blood cells in 1X lysing buffer (BD PharMingen) for 3 min, tissue debris was removed by a brief spin (~5 to 10 s) at 1,000 rpm (45 x g). The remaining cells were pelleted at 1,200 rpm (64 x g) for 6 min prior to staining.

Intracellular Cytokine Staining

Cells isolated from lungs were plated at 10^6 cells/ml and stimulated with 50 ng/ml PMA and 1.5 µM ionomycin (Calbiochem) for 5 h at 37°C. Cells were preincubated with anti-FcγR mAb 2.4G2 to block nonspecific binding before they were stained with the following PE-Cy7-, APC-H7, and V450-conjugated antibodies: CD4 (RM4-5), CD8 (53-6.7), and TCR-β (H57-597) (BD Biosciences). Cells were then fixed in 4% paraformaldehyde for 10 min at room temperature, and permeabilized with 0.2% saponin (Sigma). Finally, cells were stained with FITC- and AF-647-labeled IFN-γ (XMG1.2) and GzmB (GB11) antibodies (BD Biosciences) and analyzed by flow cytometry. Events were acquired on a FACSCanto (BD) flow cytometer, and data were analyzed with FlowJo software (Tree Star). Cells were classified as $CD4^+$ T cells ($TCR\beta^+CD4^+$) and $CD8^+$ T cells ($TCR\beta^+CD8^+$).

Lymphocyte Stimulation

Lymphocytes were seeded at a concentration of 3×10^5 cells/well in 96-well plates coated with anti-CD3 antibody (BioLegend, 5 µg/ml) and incubated for 24 h. Supernatants were then collected for ELISA. Cytokine protein concentrations in supernatant were determined by ELISA (Duoset Kits, R&D Systems) according to the manufacturer's protocol.

Statistics

Analysis of data for statistical significance was conducted using Prism 6 for Macintosh (GraphPad Software, Incorporated). Differences between groups at multiple time points were analyzed using two-way analysis of variance (ANOVA) followed by Bonferroni's multiple comparison tests. Comparisons between two groups at a single time point were made using the Mann-Whitney rank sum test. *P* values less than 0.05 were considered statistically significant.

Table 5-1. Primers and probes used for real-time PCR analysis

Target	Oligonucleotide	Sequence (5′ to 3′)
MAV-1 E1A	Forward primer	GCACTCCATGGCAGGATTCT
	Reverse primer	GGTCGAAGCAGACGGTTCTTC
	Probe	TACTGCCACTTCTGC
IFN-γ	Forward primer	AAAGAGATAATCTGGCTCTGC
	Reverse primer	GCTCTGAGACAATGAACGCT
GzmB	Forward primer	CCACTCTCGACCCTACATGG
	Reverse primer	GGCCCCCAAAGTGACATTTATT
GAPDH	Forward primer	TGCACCACCAACTGCTTAG
	Reverse primer	GGATGCAGGGATGATGTTC

References

1. **Soubani AO, Miller KB, Hassoun PM.** 1996. Pulmonary complications of bone marrow transplantation. Chest **109:**1066-1077.
2. **Coomes SM, Hubbard LLN, Moore BB.** 2010. Impaired pulmonary immunity post-bone marrow transplant. Immunol Res.
3. **Martín-Peña A, Aguilar-Guisado M, Espigado I, Parody R, Miguel Cisneros J.** 2011. Prospective study of infectious complications in allogeneic hematopoietic stem cell transplant recipients. Clin Transplant **25:**468-474.
4. **Gil L, Styczynski J, Komarnicki M.** 2007. Infectious complication in 314 patients after high-dose therapy and autologous hematopoietic stem cell transplantation: risk factors analysis and outcome. Infection **35:**421-427.
5. **Auner HW, Sill H, Mulabecirovic A, Linkesch W, Krause R.** 2002. Infectious complications after autologous hematopoietic stem cell transplantation: comparison of patients with acute myeloid leukemia, malignant lymphoma, and multiple myeloma. Annals of Hematology **81:**374-377.
6. **Walls T, Shankar AG, Shingadia D.** 2003. Adenovirus: an increasingly important pathogen in paediatric bone marrow transplant patients. Lancet Infect Dis **3:**79-86.
7. **Kojaoghlanian T, Flomenberg P, Horwitz MS.** 2003. The impact of adenovirus infection on the immunocompromised host. Rev Med Virol **13:**155-171.
8. **Baldwin A, Kingman H, Darville M, Foot AB, Grier D, Cornish JM, Goulden N, Oakhill A, Pamphilon DH, Steward CG, Marks DI.** 2000. Outcome and clinical course of 100 patients with adenovirus infection following bone marrow transplantation. Bone Marrow Transplantation **26:**1333-1338.
9. **Runde V, Ross S, Trenschel R, Lagemann E, Basu O, Renzing-Köhler K, Schaefer UW, Roggendorf M, Holler E.** 2001. Adenoviral infection after allogeneic stem cell transplantation (SCT): report on 130 patients from a single SCT unit involved in a prospective multi center surveillance study. Bone Marrow Transplantation **28:**51-57.
10. **Flomenberg P, Babbitt J, Drobyski WR, Ash RC, Carrigan DR, Sedmak GV, McAuliffe T, Camitta B, Horowitz MM, Bunin N.** 1994. Increasing incidence of adenovirus disease in bone marrow transplant recipients. J Infect Dis **169:**775-781.
11. **Hierholzer JC.** 1992. Adenoviruses in the immunocompromised host. Clin Microbiol Rev **5:**262-274.
12. **Howard DS, Phillips II GL, Reece DE, Munn RK, Henslee-Downey J, Pittard M, Barker M, Pomeroy C.** 1999. Adenovirus infections in hematopoietic stem cell transplant recipients. Clin Infect Dis **29:**1494-1501.

13. **Leen AM, Bollard CM, Myers GD, Rooney CM.** 2006. Adenoviral infections in hematopoietic stem cell transplantation. Biol Blood Marrow Transplant **12:**243-251.
14. **Shields AF, Hackman RC, Fife KH, Corey L, Meyers JD.** 1985. Adenovirus infections in patients undergoing bone-marrow transplantation. N Engl J Med **312:**529-533.
15. **Chakrabarti S, Mautner V, Osman H, Collingham KE, Fegan CD, Klapper PE, Moss PAH, Milligan DW.** 2002. Adenovirus infections following allogeneic stem cell transplantation: incidence and outcome in relation to graft manipulation, immunosuppression, and immune recovery. Blood **100:**1619-1627.
16. **Betz M, Fox BS.** 1991. Prostaglandin E2 inhibits production of Th1 lymphokines but not of Th2 lymphokines. J Immunol **146:**108-113.
17. **Snijdewint FG, Kaliński P, Wierenga EA, Bos JD, Kapsenberg ML.** 1993. Prostaglandin E2 differentially modulates cytokine secretion profiles of human T helper lymphocytes. J Immunol **150:**5321-5329.
18. **Aronoff DM, Canetti C, Peters-Golden M.** 2004. Prostaglandin E2 inhibits alveolar macrophage phagocytosis through an E-prostanoid 2 receptor-mediated increase in intracellular cyclic AMP. J Immunol **173:**559-565.
19. **Serezani CH, Chung J, Ballinger MN, Moore BB, Aronoff DM, Peters-Golden M.** 2007. Prostaglandin E2 suppresses bacterial killing in alveolar macrophages by inhibiting NADPH oxidase, p. 562-570, Am J Respir Cell Mol Biol, vol. 37.
20. **Cayeux SJ, Beverley PC, Schulz R, Dörken B.** 1993. Elevated plasma prostaglandin E2 levels found in 14 patients undergoing autologous bone marrow or stem cell transplantation. Bone marrow transplantation **12:**603-608.
21. **Klingemann HG, Tsoi MS, Storb R.** 1986. Inhibition of prostaglandin E2 restores defective lymphocyte proliferation and cell-mediated lympholysis in recipients after allogeneic marrow grafting. Blood **68:**102-107.
22. **Ballinger MN, Aronoff DM, McMillan TR, Cooke KR, Olkiewicz K, Toews GB, Peters-Golden M, Moore BB.** 2006. Critical role of prostaglandin E2 overproduction in impaired pulmonary host response following bone marrow transplantation. J Immunol **177:**5499-5508.
23. **Hubbard LLN, Ballinger MN, Thomas PE, Wilke CA, Standiford TJ, Kobayashi KS, Flavell RA, Moore BB.** 2010. A role for IL-1 Receptor-associated kinase-M in Prostaglandin E(2)-induced immunosuppression post-bone marrow transplantation. J Immunol **184:**6299-6308.
24. **Domingo-Gonzalez R, Katz S, Serezani CH, Moore TA, Levine AM, Moore BB.** 2013. Prostaglandin E2-Induced Changes in Alveolar Macrophage Scavenger Receptor Profiles Differentially Alter Phagocytosis of Pseudomonas aeruginosa and Staphylococcus aureus Post-Bone Marrow Transplant. J Immunol.

25. **Coomes SM, Wilke CA, Moore TA, Moore BB.** 2010. Induction of TGF-beta 1, not regulatory T cells, impairs antiviral immunity in the lung following bone marrow transplant. J Immunol **184:**5130-5140.
26. **Weinberg JB, Stempfle GS, Wilkinson JE, Younger JG, Spindler KR.** 2005. Acute respiratory infection with mouse adenovirus type 1. Virology **340:**245-254.
27. **Procario MC, Levine RE, McCarthy MK, Kim E, Zhu L, Chang C-H, Hershenson MB, Weinberg JB.** 2012. Susceptibility to acute mouse adenovirus type 1 respiratory infection and establishment of protective immunity in neonatal mice. J Virol **86:**4194-4203.
28. **Weinberg JB, Lutzke ML, Efstathiou S, Kunkel SL, Rochford R.** 2002. Elevated chemokine responses are maintained in lungs after clearance of viral infection. J Virol **76:**10518-10523.
29. **Anderson VE, Nguyen Y, Weinberg JB.** 2009. Effects of allergic airway disease on mouse adenovirus type 1 respiratory infection. Virology **391:**25-32.
30. **Nguyen Y, McGuffie BA, Anderson VE, Weinberg JB.** 2008. Gammaherpesvirus modulation of mouse adenovirus type 1 pathogenesis. Virology **380:**182-190.
31. **Weinberg JB, Jensen DR, Gralinski LE, Lake AR, Stempfle GS, Spindler KR.** 2007. Contributions of E1A to mouse adenovirus type 1 pathogenesis following intranasal inoculation. Virology **357:**54-67.
32. **Nguyen Y, Procario MC, Ashley SL, O'Neal WK, Pickles RJ, Weinberg JB.** 2011. Limited effects of Muc1 deficiency on mouse adenovirus type 1 respiratory infection. Virus Res **160:**351-359.
33. **Hubbard LLN, Ballinger MN, Wilke CA, Moore BB.** 2008. Comparison of Conditioning Regimens for Alveolar Macrophage Reconstitution and Innate Immune Function Post Bone Marrow Transplant. Exp Lung Res **34:**263-275.
34. **Moore ML, Brown CC, Spindler KR.** 2003. T cells cause acute immunopathology and are required for long-term survival in mouse adenovirus type 1-induced encephalomyelitis. J Virol **77:**10060-10070.
35. **Kapoor M, Kojima F, Qian M, Yang L, Crofford LJ.** 2006. Shunting of prostanoid biosynthesis in microsomal prostaglandin E synthase-1 null embryo fibroblasts: regulatory effects on inducible nitric oxide synthase expression and nitrite synthesis. FASEB J **20:**2387-2389.
36. **Boulet L, Ouellet M, Bateman KP, Ethier D, Percival MD, Riendeau D, Mancini JA, Méthot N.** 2004. Deletion of microsomal prostaglandin E2 (PGE2) synthase-1 reduces inducible and basal PGE2 production and alters the gastric prostanoid profile. J Biol Chem **279:**23229-23237.
37. **Duran-Struuck R, Dysko RC.** 2009. Principles of bone marrow transplantation (BMT): providing optimal veterinary and husbandry care to irradiated mice in BMT studies. JAALAS **48:**11-22.
38. **McCarthy MK, Zhu L, Procario MC, Weinberg JB.** 2014. IL-17 contributes to neutrophil recruitment but not to control of viral replication

during acute mouse adenovirus type 1 respiratory infection. Virology **456-457:**259-267.

39. **Sparks-Thissen RL, Braaten DC, Hildner K, Murphy TL, Murphy KM, Virgin HW.** 2005. CD4 T cell control of acute and latent murine gammaherpesvirus infection requires IFNgamma. Virology **338:**201-208.
40. **Moore ML, McKissic EL, Brown CC, Wilkinson JE, Spindler KR.** 2004. Fatal disseminated mouse adenovirus type 1 infection in mice lacking B cells or Bruton's tyrosine kinase. J Virol **78:**5584-5590.
41. **van der Veen J, Mes A.** 1973. Experimental infection with mouse adenovirus in adult mice. Arch Gesamte Virusforsche **42:**235-241.
42. **Avigan D, Wu Z, Joyce R, Elias A, Richardson P, McDermott D, Levine J, Kennedy L, Giallombardo N, Hurley D, Gong J, Kufe D.** 2000. Immune reconstitution following high-dose chemotherapy with stem cell rescue in patients with advanced breast cancer. Bone marrow transplantation **26:**169-176.
43. **Yao C, Sakata D, Esaki Y, Li Y, Matsuoka T, Kuroiwa K, Sugimoto Y, Narumiya S.** 2009. Prostaglandin E2-EP4 signaling promotes immune inflammation through Th1 cell differentiation and Th17 cell expansion. Nat Med **15:**633-640.
44. **Nataraj C, Thomas DW, Tilley SL, Nguyen MT, Mannon R, Koller BH, Coffman TM.** 2001. Receptors for prostaglandin E(2) that regulate cellular immune responses in the mouse. J Clin Invest **108:**1229-1235.
45. **Coulombe F, Jaworska J, Verway M, Tzelepis F, Massoud A, Gillard J, Wong G, Kobinger G, Xing Z, Couture C, Joubert P, Fritz JH, Powell WS, Divangahi M.** 2014. Targeted Prostaglandin E2 Inhibition Enhances Antiviral Immunity through Induction of Type I Interferon and Apoptosis in Macrophages. Immunity **40:**554-568.
46. **Heemskerk B, Lankester AC, van Vreeswijk T, Beersma MFC, Claas ECJ, Veltrop-Duits LA, Kroes ACM, Vossen JMJJ, Schilham MW, van Tol MJD.** 2005. Immune reconstitution and clearance of human adenovirus viremia in pediatric stem-cell recipients. J Infect Dis **191:**520-530.
47. **Van Tol MJD, Claas ECJ, Heemskerk B, Veltrop-Duits LA, De Brouwer CS, Van Vreeswijk T, Sombroek CC, Kroes ACM, Beersma MFC, De Klerk EPA, Egeler RM, Lankester AC, Schilham MW.** 2005. Adenovirus infection in children after allogeneic stem cell transplantation: diagnosis, treatment and immunity. Bone Marrow Transplantation **35 Suppl 1:**S73-76.
48. **Zandvliet ML, Falkenburg JHF, van Liempt E, Veltrop-Duits LA, Lankester AC, Kalpoe JS, Kester MGD, van der Steen DM, van Tol MJ, Willemze R, Guchelaar H-J, Schilham MW, Meij P.** 2010. Combined CD8+ and CD4+ adenovirus hexon-specific T cells associated with viral clearance after stem cell transplantation as treatment for adenovirus infection. Haematologica **95:**1943-1951.
49. **Rooney CM, Smith CA, Ng CY, Loftin SK, Sixbey JW, Gan Y, Srivastava DK, Bowman LC, Krance RA, Brenner MK, Heslop HE.**

1998. Infusion of cytotoxic T cells for the prevention and treatment of Epstein-Barr virus-induced lymphoma in allogeneic transplant recipients. Blood **92:**1549-1555.

50. **Heslop HE, Ng CY, Li C, Smith CA, Loftin SK, Krance RA, Brenner MK, Rooney CM.** 1996. Long-term restoration of immunity against Epstein-Barr virus infection by adoptive transfer of gene-modified virus-specific T lymphocytes. Nat Med **2:**551-555.
51. **Rooney CM, Smith CA, Ng CY, Loftin S, Li C, Krance RA, Brenner MK, Heslop HE.** 1995. Use of gene-modified virus-specific T lymphocytes to control Epstein-Barr-virus-related lymphoproliferation. Lancet **345:**9-13.
52. **Geyeregger R, Freimüller C, Stemberger J, Artwohl M, Witt V, Lion T, Fischer G, Lawitschka A, Ritter J, Hummel M, Holter W, Fritsch G, Matthes-Martin S.** 2014. First-in-man clinical results with good manufacturing practice (GMP)-compliant polypeptide-expanded adenovirus-specific T cells after haploidentical hematopoietic stem cell transplantation. J Immunotherapy **37:**245-249.
53. **Leen AM, Christin A, Myers GD, Liu H, Cruz CR, Hanley PJ, Kennedy-Nasser AA, Leung KS, Gee AP, Krance RA, Brenner MK, Heslop HE, Rooney CM, Bollard CM.** 2009. Cytotoxic T lymphocyte therapy with donor T cells prevents and treats adenovirus and Epstein-Barr virus infections after haploidentical and matched unrelated stem cell transplantation. Blood **114:**4283-4292.
54. **Smith CA, Woodruff LS, Rooney C, Kitchingman GR.** 1998. Extensive cross-reactivity of adenovirus-specific cytotoxic T cells. Hum Gene Ther **9:**1419-1427.
55. **Smith CA, Woodruff LS, Kitchingman GR, Rooney CM.** 1996. Adenovirus-pulsed dendritic cells stimulate human virus-specific T-cell responses in vitro. J Virol **70:**6733-6740.
56. **Heemskerk B, Veltrop-Duits LA, van Vreeswijk T, ten Dam MM, Heidt S, Toes REM, van Tol MJD, Schilham MW.** 2003. Extensive cross-reactivity of CD4+ adenovirus-specific T cells: implications for immunotherapy and gene therapy. J Virol **77:**6562-6566.
57. **Feuchtinger T, Lang P, Hamprecht K, Schumm M, Greil J, Jahn G, Niethammer D, Einsele H.** 2004. Isolation and expansion of human adenovirus-specific CD4+ and CD8+ T cells according to IFN-gamma secretion for adjuvant immunotherapy. Exp Hematol **32:**282-289.
58. **Chakupurakal G, Onion D, Bonney S, Cobbold M, Mautner V, Moss P.** 2013. HLA-peptide multimer selection of adenovirus-specific T cells for adoptive T-cell therapy. J Immunotherapy **36:**423-431.
59. **Leen AM, Sili U, Savoldo B, Jewell AM, Piedra PA, Brenner MK, Rooney CM.** 2004. Fiber-modified adenoviruses generate subgroup cross-reactive, adenovirus-specific cytotoxic T lymphocytes for therapeutic applications. Blood **103:**1011-1019.
60. **Trebino CE, Stock JL, Gibbons CP, Naiman BM, Wachtmann TS, Umland JP, Pandher K, Lapointe J-M, Saha S, Roach ML, Carter D, Thomas NA, Durtschi BA, McNeish JD, Hambor JE, Jakobsson P-J,**

Carty TJ, Perez JR, Audoly LP. 2003. Impaired inflammatory and pain responses in mice lacking an inducible prostaglandin E synthase. Proc Natl Acad Sci USA **100:**9044-9049.

61. **Cauthen A, Welton A, Spindler KR.** 2007. Construction of mouse adenovirus type 1 mutants. Methods Mol Med **130:**41-59.
62. **Zaslona Z, Serezani CH, Okunishi K, Aronoff DM, Peters-Golden M.** 2012. Prostaglandin E2 restrains macrophage maturation via E prostanoid receptor 2/protein kinase A signaling. Blood **119:**2358-2367.
63. **Spandidos A, Wang X, Wang H, Seed B.** 2010. PrimerBank: a resource of human and mouse PCR primer pairs for gene expression detection and quantification. Nucleic Acids Res **38:**D792-799.

Chapter 6:
IL-17 contributes to neutrophil recruitment but not to control of viral replication during acute mouse adenovirus type 1 respiratory infection

Abstract

IL-17-producing $CD4^+$ helper T cells (Th17 cells) promote inflammatory responses to many pathogens. We used mouse adenovirus type 1 (MAV-1) to determine contributions of IL-17 to adenovirus pathogenesis. MAV-1 infection of C57BL/6 mice upregulated lung expression of IL-17 and the Th17-associated factors IL-23 and RORγt. Only $CD4^+$ T cells were associated with virus-specific IL-17 production. Fewer neutrophils were recruited to airways of IL-$17^{-/-}$ mice following MAV-1 infection, but there were no other differences in pulmonary inflammation between IL-$17^{+/+}$ and IL-$17^{-/-}$ mice. Mice depleted of neutrophils using anti-Gr-1 antibody had greater lung viral loads than controls. Despite impaired neutrophil recruitment, there were no differences between IL-$17^{+/+}$ and IL-$17^{-/-}$ mice in peak lung viral loads, clearance of virus from the lungs, or establishment of protective immunity. We demonstrate robust Th17 responses during MAV-1 respiratory infection, but these responses are not essential for control of virus infection or for virus-induced pulmonary inflammation.

Introduction

The human adenoviruses (HAdV) are common causes of acute respiratory infection (1). Adenovirus respiratory infections can present with a wide range of clinical syndromes ranging from mild upper respiratory tract infections to more severe manifestations such as necrotizing pneumonitis and bronchiolitis obliterans (2). Immunocompromised patients, such as those who have undergone bone marrow transplantation, are at risk for greatly increased morbidity and mortality from adenovirus infection (3, 4).

The strict species specificity of the adenoviruses complicates animal studies with a HAdV. We have established mouse adenovirus type 1 (MAV-1) as a model to study the pathogenesis of adenovirus respiratory infection in the natural host of the virus. Using this model, we have shown that acute MAV-1 respiratory infection is associated with cellular inflammation and increased production of multiple cytokines and chemokines in the lungs (5-7). In particular, the marked induction of IFN-γ expression without induction of IL-4 production (6) is consistent with T helper type 1 (Th1) polarization in the lungs following MAV-1 infection. IFN-γ deficiency is associated with small increases in MAV-1 lung viral loads (6), while Th2 polarization using cockroach antigen sensitization in an allergic airways disease model has no effect on MAV-1 replication in the lungs (5).

Th1 $CD4^+$ T cells are classically characterized by their production of IFN-γ, and Th2 $CD4^+$ T cells are characterized by production of cytokines such as IL-4, IL-5, and IL-13 (8). An additional lineage of T cells, Th17 T cells, is defined by the

production by cytokines such as IL-17A and IL-17F (9, 10). Th17 cell differentiation from naïve $CD4^+$ T cells is promoted by IL-1β, IL-6, TGF-β and IL-23 and occurs under the control of the transcriptional regulators RORγt and RORα, while it is negatively regulated by IFN-γ, IL-4, and IL-13 (11). Th17-associated cytokines have been implicated in a variety of inflammatory and autoimmune diseases, and animals deficient in IL-17 or its receptor, IL-17RA, are more susceptible to a variety of bacterial and fungal infections (11).

Less information is available regarding the role of Th17 immune function in the pathogenesis of respiratory viral infections. IL-17 expression in the lungs is induced by infection with viruses such as respiratory syncytial virus (RSV), influenza virus, and pneumonia virus of mice, an RNA virus in the same family (*Paramyxoviridae*) and genus (*Pneumovirus*) as RSV (12-15). IL-17 promotes pulmonary inflammation and viral replication during RSV infection and negatively regulates the generation of RSV-specific $CD8^+$ T cells (14). Signaling through IL-17RA is necessary for weight loss and neutrophil migration to the lungs following influenza infection, although IL-17RA signaling is not necessary for recruitment of virus-specific $CD8^+$ T cells or viral clearance (12). Th17 function may play a role in an effective memory response to influenza, as antibody neutralization of IL-17 decreased protection from challenge with a different subtype of influenza virus (16). Importantly, Th17 responses to adenovirus respiratory infection have not been characterized. In this study, we used MAV-1 to characterize Th17 responses to adenovirus respiratory infection and to test the

hypothesis that IL-17 is required for control of MAV-1 replication during acute respiratory infection.

Results

MAV-1 induces IL-17 production in lungs of infected mice.

Acute MAV-1 respiratory infection increases production of the Th1 cytokine IFN-γ in the lungs but not Th2 cytokines such as IL-4 and IL-13 (5, 6, 17). To investigate whether MAV-1 respiratory infection induces lung IL-17 production, C57BL/6 mice were infected intranasally (i.n.) with MAV-1 and bronchoalveolar lavage fluid (BALF) and lung tissue were harvested at times corresponding to early infection (4 days post infection, dpi), the peak of viral replication at 7 dpi (6, 7), and a later time corresponding to clearance of virus from the lungs (14 dpi). Reverse transcriptase quantitative real-time PCR (RT-qPCR) was used to measure IL-17A mRNA levels following MAV-1 infection (Figure 6-1A). IL-17A mRNA levels were increased in the lungs of infected mice compared to mock infected controls. IL-17A expression peaked at 7 dpi and then decreased by 14 dpi. The concentration of IL-17A protein (hereafter referred to as IL-17) was also increased in BALF at 7 dpi (Figure 6-1B), the time corresponding to the peak of IL-17A mRNA levels and the typical peak of MAV-1 replication in the lungs (6, 7, 17). Likewise, the protein concentration of IL-23 was significantly increased in BALF at 7 dpi (Figure 6-1C). At the same time, the mRNA level of RORγt, a key regulator of Th17 differentiation (18), was

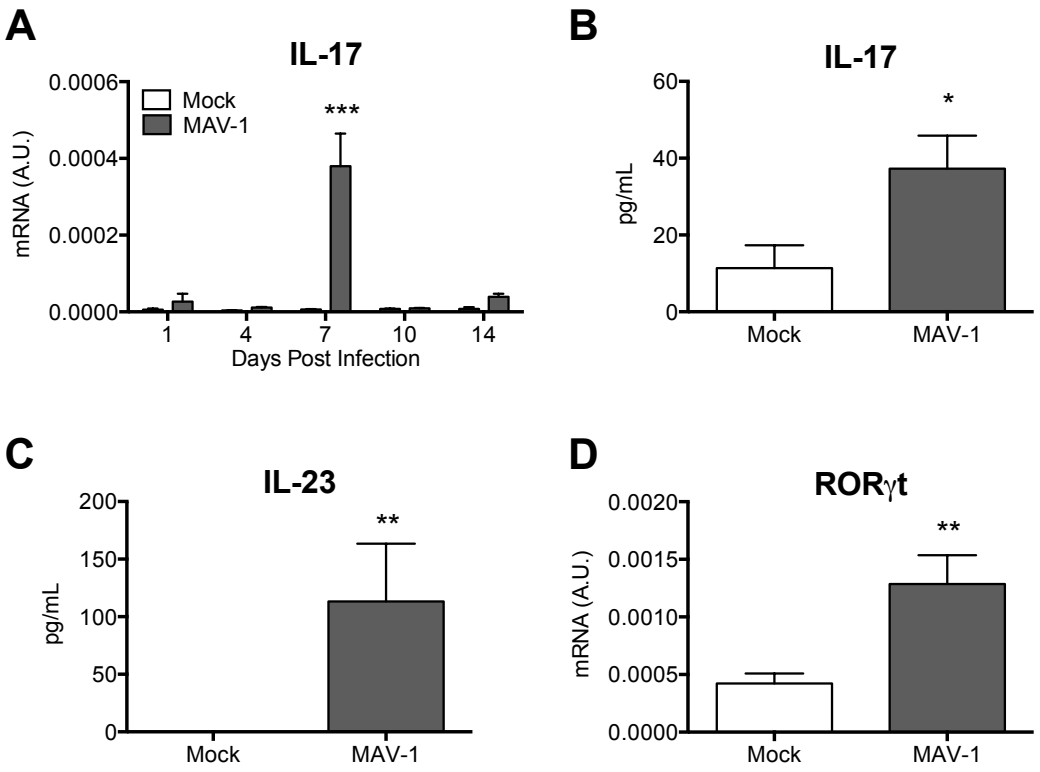

Figure 6-1. MAV-1-induced IL-17 responses in the lung.

Mice were infected i.n. with MAV-1 or mock infected with conditioned media. A) RNA was extracted from lungs harvested at the indicated time points and RT-qPCR was used to quantify IL-17A mRNA, which is expressed in arbitrary units. B-C) ELISA was used to quantify IL-17 and IL-23 concentrations in BALF from mice at 7 dpi. D) RT-qPCR was used to quantify lung RORγt expression at 7 dpi. Combined data from n=3-13 (A), n=10 (B and D) and n=5 (C) mice per group are presented as means ± S.E.M. Statistical comparisons were made using two-way ANOVA followed by Bonferroni's multiple comparison tests (A) or Mann-Whitney test (B-D). **P*<0.05, ***P*<0.01 and ****P*<0.001, comparing mock to MAV-1.

significantly greater in lungs of infected mice than in mock infected controls (Figure 6-1D).

Th17 cells and γδ T cells are the main contributors to IL-17A production following MAV-1 infection.

To determine the source of IL-17 production in the lung, we isolated lung lymphocytes at 7 dpi and used intracellular cytokine staining to define the extent of Th1, Th2, and Th17 polarization following MAV-1 infection. Consistent with cytokine induction in the lungs (Figure 6-1), the percentage of IL-17$^+$CD4$^+$ T cells was significantly increased in the lungs of infected mice compared to mock infected controls (Figure 6-2A). As we have previously demonstrated (6), the percentage of IFN-γ$^+$CD4$^+$ T cells was also significantly increased (Figure 6-2B), whereas we detected a corresponding very small but statistically significant decrease in the percentage of IL-4$^+$CD4$^+$ T cells (Figure 6-2C). When stimulated *ex vivo* with anti-CD3 antibody, lymphocytes isolated from the lungs of infected mice produced significantly more IL-17 (Figure 6-2D) and IFN-γ (Figure 6-2E) than cells isolated from mock infected controls. T cells isolated from the MLN of mock infected and infected mice produced equivalent amounts of IL-17 (Figure 6-2F), although T cells from MLN of infected mice produced more IFN-γ than cells isolated from mock infected controls (Figure 6-2G).

Next, we isolated lymphocytes from the lungs of mice at 7 dpi and used intracellular cytokine staining following stimulation with phorbol-12-myristate-13-acetate (PMA) and ionomycin to more specifically determine the lymphocyte

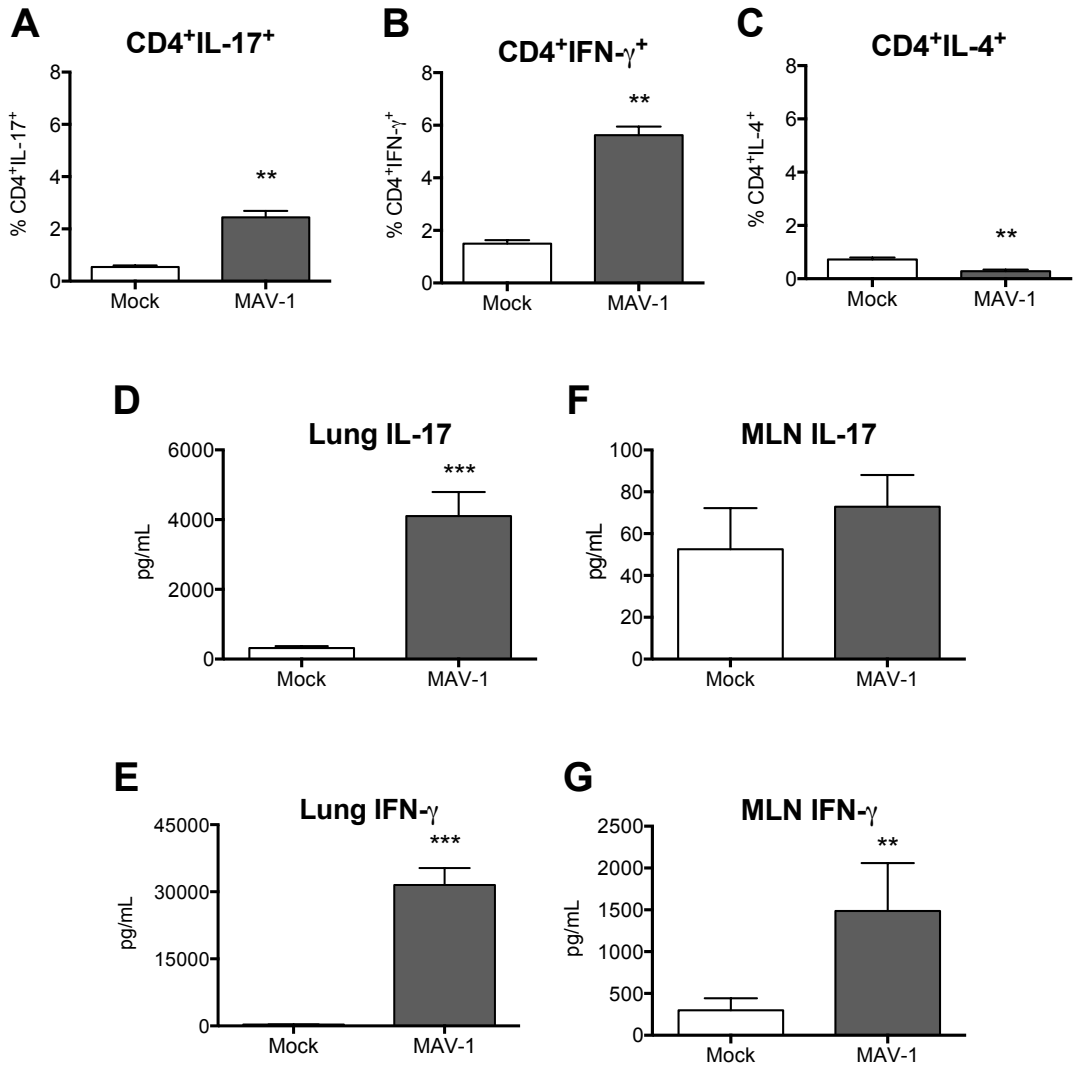

Figure 6-2. T cell polarization in lungs after MAV-1 infection.

Mice were infected i.n. with MAV-1 or mock infected with conditioned media and lung lymphocytes were isolated at 7 dpi. A-C) Intracellular cytokine staining was used to quantify the percentage of $CD4^+$ T cells that were IL-17^+, IFN-γ^+, or IL-4^+. D-G) Lung leukocytes or mediastinal lymph node cells were stimulated overnight with anti-CD3 antibody and ELISA was used to measure IL-17 or IFN- γ production in the supernatant. Combined data from n=5 (A-C) and n=10 (D-G) mice per group are presented as means ± S.E.M. Statistical comparisons were made using Mann-Whitney test. $^{**}P<0.01$ and $^{***}P<0.001$, comparing mock to MAV-1.

type(s) responsible for IL-17 production. The percentages of IL-17^{+}CD4^{+} T cells and IL-17^{+} γδ T cells were significantly increased in the lungs of infected mice compared to mock infected controls (Figure 6-3A). In contrast, we observed no difference in IL-17^{+} (NK), natural killer T (NKT), or CD8 T cell populations obtained from mock infected and infected mice. In order to determine whether the IL-17-producing cell populations were antigen-specific, we stimulated lung lymphocytes with antigen presenting cells (APCs) exposed to MAV-1. We detected significantly more virus-specific IL-17^{+}CD4^{+} T cells in lymphocytes obtained from infected mice compared to mock infected controls (Figure 6-3B). Virus-specific IL-17 production was not noted in other lymphocyte populations, suggesting that only the classical Th17 cells (IL-17^{+}CD4^{+} T cells) are antigen-specific. In contrast, virus-specific IFN-γ production was observed in both CD4^{+} and CD8^{+} T cells (Figure 6-3C). Together, these data demonstrate that both CD4^{+} and γδ T cells are major contributors to IL-17 production in the lungs following MAV-1 infection, but only IL-17 production by CD4^{+} T cells is virus-specific.

IL-17 contributes to neutrophil recruitment to the airways of mice infected with MAV-1.

To investigate contributions of IL-17 to MAV-1 pathogenesis, we infected IL-17$^{+/+}$ and IL-17$^{-/-}$ mice with MAV-1. No MAV-1-associated mortality occurred in IL-17$^{+/+}$ or IL-17$^{-/-}$ animals (data not shown). Acute MAV-1 respiratory infection induced histological changes in the lungs of both IL-17$^{+/+}$ and IL-17$^{-/-}$ mice at 7

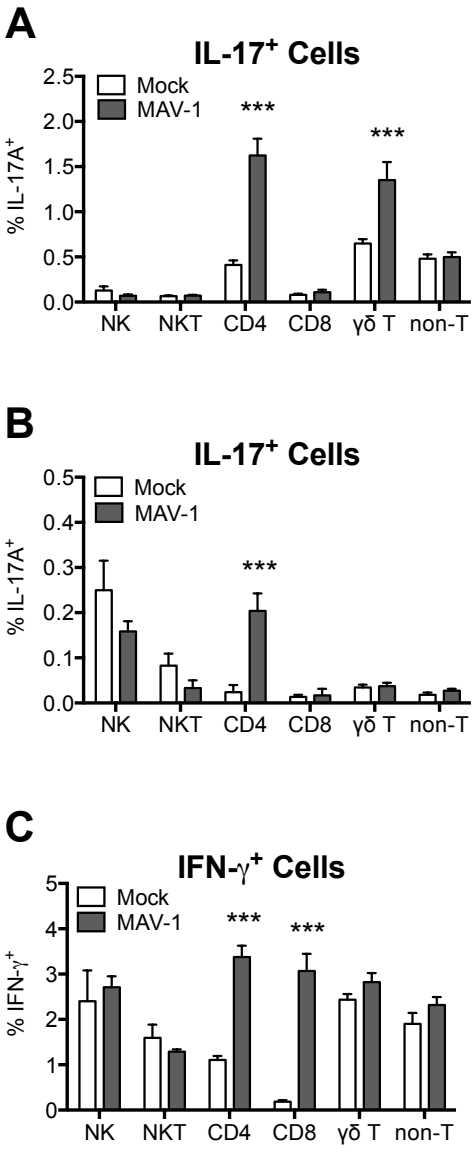

Figure 6-3. Cell types contributing to IL-17 and IFN-γ production after MAV-1 infection.

Mice were infected i.n. with MAV-1 or mock infected with conditioned media and lung lymphocytes were isolated at 7 dpi. A) Lung leukocytes were stimulated with PMA/ionomycin and intracellular cytokine staining was used to quantify the percentage of each cell type that was IL-17$^+$. B) Lung leukocytes were stimulated overnight with MAV-1-infected APCs and intracellular cytokine staining was used to quantify the percent of each cell type that was IL-17$^+$. C) Lung leukocytes were stimulated with PMA/ionomycin and intracellular cytokine staining was used to quantify the percentage of each cell type that was IFN-γ$^+$. Combined data from n=5 mice per group are presented as means ± S.E.M. Statistical comparisons were made using two-way ANOVA followed by Bonferroni's multiple comparison tests. ***P<0.001, comparing mock to MAV-1.

dpi that were characterized by bronchopneumonia and interstitial infiltrates (Figure 6-4A). Minimal residual inflammation was present in the lungs of IL-17$^{+/+}$ and IL-17$^{-/-}$ mice at 21 dpi. Next, we isolated cells from airways of IL-17$^{+/+}$ and IL-17$^{-/-}$ mice by BAL. Following infection, fewer cells overall were recruited to the airways of IL-17$^{-/-}$ mice than IL-17$^{+/+}$ mice at 7 dpi, the peak of histologically apparent inflammation (Figure 6-4B). Differential counting revealed that fewer neutrophils were recruited to the airways of IL-17$^{-/-}$ mice compared to IL-17$^{+/+}$ mice, with a corresponding increase in the percentage of macrophages that were recruited to airways of IL-17$^{+/+}$ mice (Figure 6-4C).

IL-17 deficiency has little effect on T cell polarization in the lungs of MAV-1-infected mice.

To determine whether IL-17 deficiency altered T cell polarization in the lungs following MAV-1 infection, we isolated lung lymphocytes from IL-17$^{+/+}$ and IL-17$^{-/-}$ mice at various times following infection and measured cytokine production following *ex vivo* stimulation with anti-CD3 antibody. As expected, T cells harvested from the lungs of IL-17$^{-/-}$ mice did not produce IL-17 (Figure 6-5A). IFN-γ was produced in equivalent amounts by lung T cells harvested from IL-17$^{+/+}$ and IL-17$^{-/-}$ mice at 7 dpi (Figure 6-5B), while very little IL-4 was produced by stimulated T cells from IL-17$^{+/+}$ or IL-17$^{-/-}$ mice at any time point (Figure 6-5C). We detected no IL-17A mRNA in the lungs or IL-17 protein in the airways of IL-17$^{-/-}$ mice following MAV-1 infection (data not shown). In addition, we did not observe increases in mRNA levels of other members of the IL-17

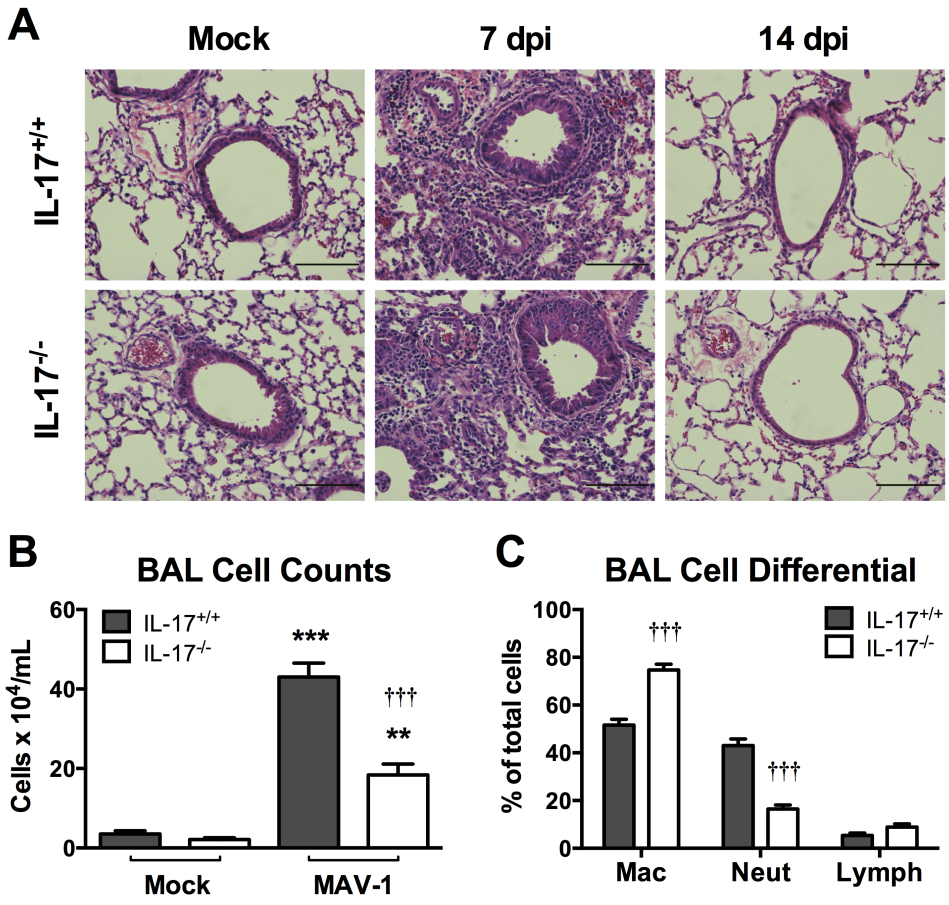

Figure 6-4. Effect of IL-17 deficiency on MAV-1-induced inflammation.

Wild type (IL-17$^{+/+}$) and IL-17$^{-/-}$ mice were infected i.n. with MAV-1 or mock infected with conditioned media and lung tissue was harvested at 7 and 21 dpi. A) Hematoxylin and eosin-stained sections were prepared from paraffin-embedded sections. Scale bars, 100 µm. B) Total numbers of inflammatory cells in BALF at 7 dpi were quantified using a hemocytometer. C) Differential counting of macrophages/monocytes (Mac), neutrophils (Neut) and lymphocytes (Lymph) was performed on cytospin preparations of BALF cells obtained at 7 dpi. Combined data from n=8-14 (B), and n=12-13 (C) mice per group are presented as means ± S.E.M. Statistical comparisons were made using two-way ANOVA followed by Bonferroni's multiple comparison tests. **P<0.01 and ***P<0.001, comparing mock to MAV-1. †††P<0.001, comparing IL-17$^{+/+}$ to IL-17$^{-/-}$ mice.

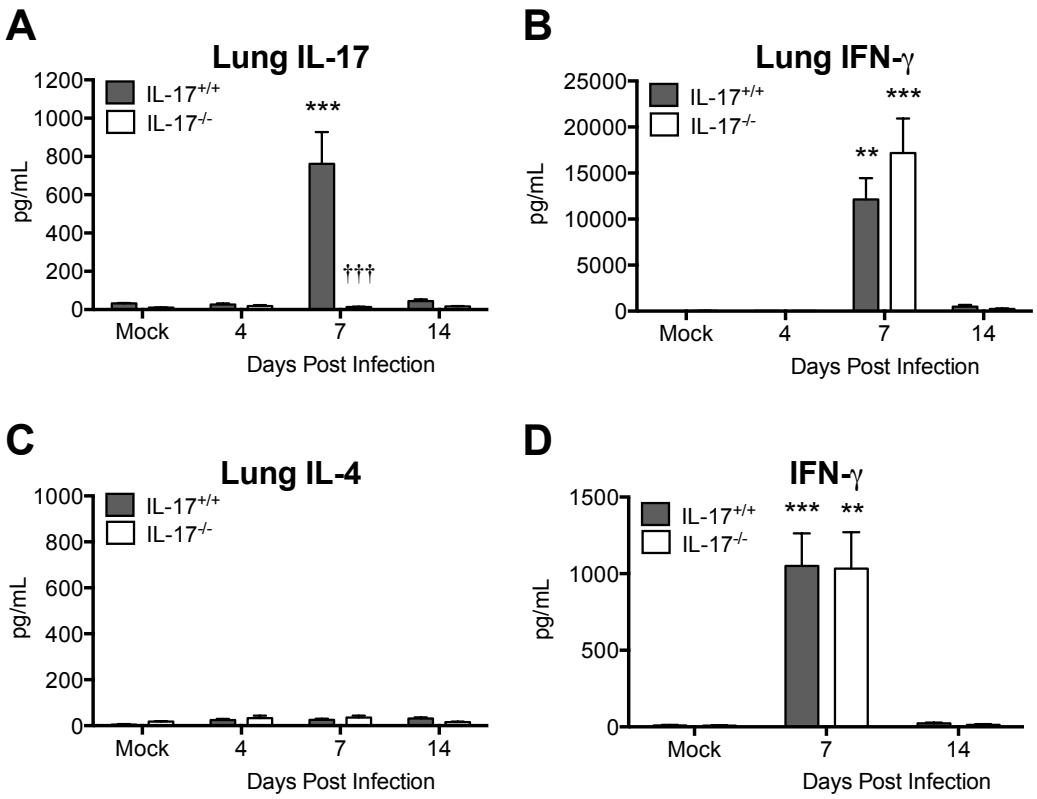

Figure 6-5. Effect of IL-17 deficiency on MAV-1-induced Th1, Th2, and Th17 cytokine production.

Wild type (IL-17$^{+/+}$) and IL-17$^{-/-}$ mice were infected i.n. with MAV-1 or mock infected with conditioned media. A-C) Lung leukocytes isolated from mice at the indicated time points were stimulated overnight with anti-CD3 antibody and ELISA was used to measure IL-17, IFN-γ, and IL-4 production. D) ELISA was used to quantify IFN-γ concentrations in BALF at the indicated time points. Combined data from n=3-5 (A-C) and n=8-21 (D) mice per group are presented as means ± S.E.M. Statistical comparisons were made using two-way ANOVA followed by Bonferroni's multiple comparison tests. ** P<0.01 and *** P<0.001, comparing mock to MAV-1. ††† P<0.001, comparing IL-17$^{+/+}$ to IL-17$^{-/-}$ mice.

family, such as IL-17C, IL-17D or IL-17F, in IL-17$^{-/-}$ mice after infection that would suggest compensatory expression of these IL-17 subtypes (data not shown). IFN-γ concentrations were similar in BALF of IL-17$^{+/+}$ and IL-17$^{-/-}$ mice at 7 and 14 dpi (Figure 6-5D).

IL-17 is not essential for control of viral replication.

IL-17 deficiency was associated with decreased neutrophil recruitment to the airways during acute MAV-1 respiratory infection. To determine whether IL-17 deficiency and the associated defect in neutrophil recruitment could have an effect on control of viral replication in the lungs, we first depleted neutrophils from C57BL/6 mice using an anti-Gr-1 antibody. Antibody depletion decreased the total number of cells recruited to the airways of infected mice (Figure 6-6A), and no neutrophils were detected in the airways of depleted mice (Figure 6-6B). It is important to consider that the anti-Gr-1 antibody is also capable of depleting other types of cells including dendritic cells and monocytes (19), although we did not observe a significant decrease in the absolute number of monocytes recruited to the airways in anti-Gr-1-treated mice (Figure 6-6B). All anti-Gr-1-treated and control animals survived infection (data not shown). Lung viral loads were significantly higher in the lungs of anti-Gr-1-treated mice than in control mice at 7 dpi, the peak of viral replication in the lungs (Figure 6-6C). This difference suggests that neutrophils contribute to the control of viral replication to some extent. In contrast, there were no statistically significant differences

between lung viral loads measured in IL-17$^{+/+}$ and IL-17$^{-/-}$ mice at any time point (Figure 6-7A).

To assess whether IL-17 affects the development of an adaptive immune response, we infected IL-17$^{-/-}$ and IL-17$^{+/+}$ mice with MAV-1 and rechallenged with MAV-1 28 days after the first infection. In both IL-17$^{+/+}$ and IL-17$^{-/-}$ mice, lung viral loads were substantially lower at 7 days following rechallenge (Figure 6-7B) than they were at 7 days following primary infection (Figure 6-7A), suggesting that protective immunity developed following primary infection. Lung viral loads did not differ between IL-17$^{-/-}$ and IL-17$^{+/+}$ mice 7 days following rechallenge (Figure 6-7B). Thus, while MAV-1-induced IL-17 production in the lungs promotes recruitment of neutrophils to the lungs during acute MAV-1 respiratory infection, our data demonstrate that IL-17 is not essential for the control of viral replication in the lungs or for clearance of virus from the lungs during acute respiratory infection. In addition, IL-17 is not essential for the establishment of protective immunity following primary infection.

Discussion

IL-17 and related components of Th17 immune function are increasingly identified as contributors to the pathogenesis of many infections, including respiratory infections caused by viruses. Induction of IL-17 expression has been described in studies using recombinant HAdV-based vectors in mice or rats (20, 21), but no data exist that describe IL-17 induction in the context of respiratory infection by an adenovirus in its natural host. Our results clearly demonstrate

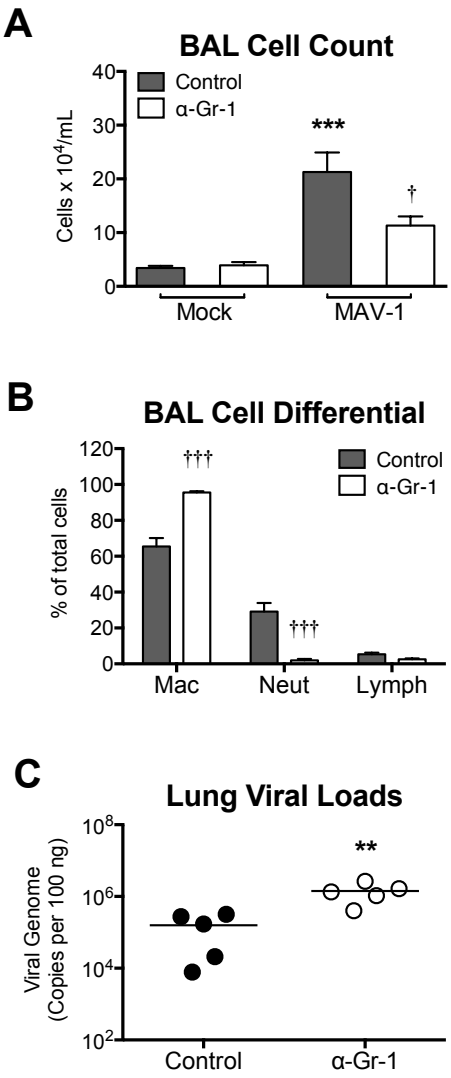

Figure 6-6. Effect of neutrophil depletion on acute MAV-1 infection.

Wild type mice were infected i.n. with MAV-1 or mock infected with conditioned media. Mice were treated every other day with anti-Gr-1 antibody (100 μg/dose given i.p.) or control serum until samples were harvested at 7 dpi. A) Total numbers of inflammatory cells in BALF were quantified using a hemocytometer. B) Differential counting of monocytes (Mono), macrophages (Mac), neutrophils (Neut) and lymphocytes (Lymph) was performed on cytospin preparations of BALF cells. C) DNA was extracted from lungs and qPCR was used to quantify MAV-1 genome copy number. Lung DNA viral loads are expressed as copies of MAV-1 genome per 100 ng of input DNA. Individual circles represent values for individual mice and horizontal bars represent means for each group. Combined data from n=3-5 (A-B) mice per group are presented as means ± S.E.M. Statistical comparisons were made using two-way ANOVA followed by Bonferroni's multiple comparison tests (A-B) or Mann-Whitney test (C). ** P<0.01 and *** P<0.001, comparing mock to MAV-1. ††† P<0.001, comparing Control to α-Gr-1.

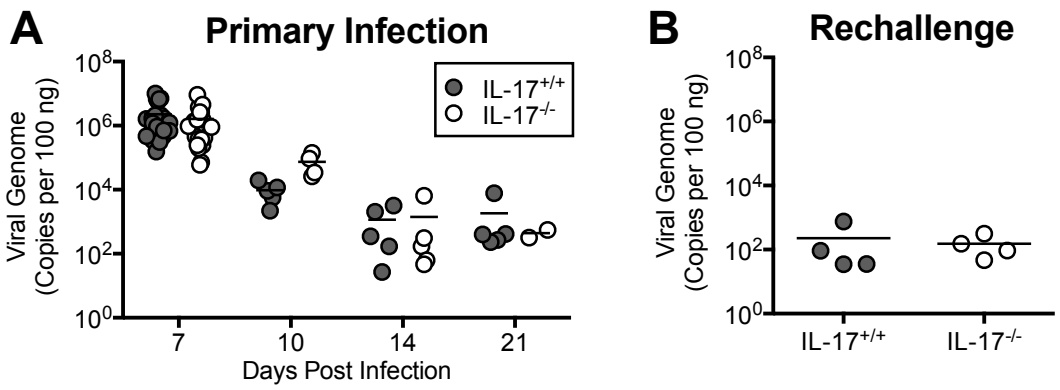

Figure 6-7. Effect of IL-17 deficiency on control of MAV-1 replication in lungs.

A) Wild type (IL-17$^{+/+}$) and IL-17$^{-/-}$ mice were infected i.n. with MAV-1 or mock infected with conditioned media and lungs were harvested at the indicated time points. B) IL-17$^{+/+}$ and IL-17$^{-/-}$ mice were infected i.n. with MAV-1 and then rechallenged with MAV-1 28 days after the primary infection. Lungs were harvested at 7 days post rechallenge. DNA was extracted from lungs and qPCR was used to quantify MAV-1 genome copy number. DNA viral loads are expressed as copies of MAV-1 genome per 100 ng of input DNA. Individual circles represent values for individual mice and horizontal bars represent means for each group. Statistical comparisons were made using two-way ANOVA followed by Bonferroni's multiple comparison tests.

robust induction of IL-17A mRNA and protein in the lungs of mice infected with MAV-1.

Although $\alpha\beta^+$ $CD4^+$ T cells are often considered to be the primary source of IL-17 production, other cell types are also capable of producing IL-17 (18). For instance, $\gamma\delta$ T cells have been identified as the source of early, non-antigen specific IL-17 production in some circumstances (22, 23). IL-17 production by $CD8^+$ T cells, NKT cells, neutrophils and macrophages has also been described (18). In this study, we detected IL-17 production by $CD4^+$ T cells and $\gamma\delta$ T cells but not in $CD8^+$ T cells, NK cells, or NKT cells isolated from lungs of MAV-1 infected mice (Figure 6-3A). Only $CD4^+$ T cell production of IL-17 was virus-specific (Figure 6-3B), consistent with nonspecific IL-17 production by $\gamma\delta$ T cells observed in other studies (22). IL-17-producing $CD8^+$ (Tc17) T cells can be detected in the lung as early as 4 days following influenza infection (16). We did not detect IL-17 production by $CD8^+$ T cells at 7 days following MAV-1 infection, suggesting that the development of Tc17 responses may not be a universal feature of respiratory viral infections. We may have missed Tc17 responses that develop later during the course of MAV-1 infection. However, we detected typical Th1 and Th17 responses in the lungs of MAV-1-infected mice at 7 dpi, and Tc17 responses develop with kinetics similar to those of Th1 and Th17 responses following influenza infection (16). It therefore seems unlikely that Tc17 responses are induced by MAV-1 respiratory infection.

IL-17 stimulates the production of growth factors such as G-CSF (24, 25) and chemokines such as CXCL1 (26, 27), which in turn lead to increased

neutrophil production and recruitment of neutrophils to sites of inflammation. Consistent with these functions of IL-17, we detected neutrophil recruitment to the airways of MAV-1-infected IL-17$^{+/+}$ mice that was significantly less in IL-17$^{-/-}$ mice (Figure 6-4). Similar effects of IL-17 deficiency or IL-17 blockade on virus-induced neutrophil recruitment have been reported in studies of influenza and RSV infection (12, 14). In addition, IL-17 deficiency is associated with overall decreases in pulmonary inflammation and lung injury following infection with RSV (14) or influenza (13). Other than decreased neutrophil recruitment to the airways, IL-17 deficiency had no substantial effect on the extent of MAV-1-induced pulmonary inflammation at its peak, 7 dpi, or on the resolution of pulmonary inflammation by 21 dpi. This suggests that MAV-1 induces a variety of other proinflammatory cytokines and chemokines not affected by IL-17 that are more important contributors to pulmonary inflammation in our model.

Because neutrophil recruitment was impaired in IL-17$^{-/-}$ mice, we sought to characterize the effects of neutrophils on MAV-1 infection by depleting neutrophils with anti-Gr-1 antibody. Our results suggest that neutrophils do contribute to the control of viral replication in the lungs, although we are unable to rule out the possibility that depletion of other cell types by the anti-Gr-1 antibody, which recognizes Ly6G on peripheral neutrophils but also on dendritic cell and monocyte populations (19), may have been responsible for higher viral loads detected in animals treated with anti-Gr-1 antibody. Even though we detected fewer neutrophils in the airways of IL-17$^{-/-}$ mice following infection, there were no differences in lung viral loads between IL-17$^{+/+}$ and IL-17$^{-/-}$ mice at any time point.

Neutrophil recruitment was impaired but not absent in IL-17$^{-/-}$ mice, potentially mitigating the effect in IL-17$^{-/-}$ mice compared to mice treated with anti-Gr-1 antibody, in which neutrophils were almost completely absent. It is also likely that IL-17 deficiency does not have a substantial effect on other host factors that are important for control of viral replication in our model. For instance, IFN-γ has some suppressive effect on MAV-1 replication *in vitro* (28), and we have shown that lung viral loads are higher in IFN-γ-deficient mice on a BALB/c background (6). IFN-γ production in response to MAV-1 infection did not differ between IL-17$^{+/+}$ and IL-17$^{-/-}$ mice (Fig. 5), suggesting that IFN-γ may continue to provide a protective effect even in the absence of IL-17 production. IL-17 signaling through IL-17RA is also dispensable for control of influenza replication during acute infection (12), and decreased instead of increased RSV viral loads were noted in mice treated with anti-IL-17 antibody (14). Using MAV-1, we therefore provide additional evidence that IL-17 is not crucial for control of viral replication in the lungs during acute infection.

IL-17 may be important for the establishment of effective adaptive immune responses to respiratory viruses. IL-17-secreting CD4$^+$ and CD8$^+$ effector T cells can be detected in the lung in response to influenza infection, antibody-mediated neutralization of IL-17 diminishes the protection resulting from priming with heterosubtypic influenza virus, and transfer of *ex vivo*-generated IL-17$^+$ CD8$^+$ T cells (Tc17 effectors) to naïve mice protects against subsequent lethal challenge with influenza, (16). Interestingly, the protective effect of Tc17 cells was associated with early recruitment of neutrophils to the lungs of mice challenged

with influenza, again providing some evidence that neutrophils could contribute to control of respiratory virus infection. This does not seem to be a universal response to respiratory virus infection, as we did not detect IL-17^{+} CD8^{+} T cells in the lungs of mice infected with MAV-1 (Figure 6-3). However, IL-17$^{-/-}$ mice cleared virus from the lungs by 21 dpi as effectively as IL-17$^{+/+}$ mice (Figure 6-7A), suggesting that adaptive immune responses to MAV-1 are likely to be preserved in the absence of IL-17. Consistent with this, IL-17$^{-/-}$ mice controlled viral replication just as well as IL-17$^{+/+}$ mice after MAV-1 rechallenge (Figure 6-7B).

In summary, acute MAV-1 respiratory infection induces the production of IL-17 in the lungs. CD4^{+} T cells are the major source of IL-17 production in the lungs and MLN of MAV-1-infected mice. Although IL-17 facilitates the recruitment of neutrophils to the airways, and neutrophils may contribute to control of MAV-1 replication, IL-17 is not essential for the control of viral MAV-1 replication in the lungs or for clearance of MAV-1 from the lungs during acute infection. In addition, IL-17 is not essential for the establishment of protective immunity following primary infection. Immunomodulation by targeting IL-17 may prove to be an appealing therapeutic target in situations in which IL-17-mediated inflammation plays a substantial role in the pathogenesis of virus-associated lung injury, as it may with pathogens such as influenza and RSV. Our results suggest that IL-17 neutralization would have a small impact on adenovirus-induced lung injury, although it would likely not have a negative impact on host control of adenovirus replication in the lung.

Materials and Methods

Mice

All animal studies were approved by the University of Michigan Committee on Use and Care of Animals. C57BL/6J mice were obtained from The Jackson Laboratory. IL-17$^{-/-}$ mice on a C57BL/6 background (29) were obtained from Bethany Moore (University of Michigan) with the permission of Yoichiro Iwakura (Tokyo University of Science, Japan) and bred at the University of Michigan. All mice were maintained under specific-pathogen-free conditions.

Virus and Infections

MAV-1 was grown and passaged in NIH 3T6 fibroblasts, and titers of viral stocks were determined by plaque assay on 3T6 cells as previously described (11). Mice (4 to 6 weeks of age) were anesthetized with ketamine and xylazine and infected i.n. with 10^5 plaque-forming units (PFU) of MAV-1 in 40 µl of sterile phosphate-buffered saline (PBS). Control mice were mock infected i.n. with conditioned medium at an equivalent dilution in sterile PBS. To assess protective immunity, a subset of mice was rechallenged i.n. with 10^5 pfu of MAV-1 28 days following primary infection. Mice were euthanized by pentobarbital overdose at the indicated time points. Lungs were harvested, snap frozen in dry ice, and stored at -80°C until processed further.

Histology

Lungs were harvested from a subset of mice and fixed in 10% formalin. Prior to fixation, lungs were gently inflated with PBS via the trachea to maintain lung architecture. After fixation, organs were embedded in paraffin, and 5 μm sections were obtained for histopathology. Sections were stained with hematoxylin and eosin to evaluate cellular infiltrates. All sectioning and staining was performed by the Pathology Cores for Animal Research in the University of Michigan Unit for Laboratory Management. Slides were viewed through an Olympus BX41 microscope and digital images were processed using Olympus DP Manager software. Final images were assembled using Adobe Illustrator (Adobe Systems). Adjustments to the color balance of digital images were applied in Adobe Illustrator equally to all experimental and control images.

Isolation of RNA and DNA

DNA was extracted from the middle lobe of the right lung using the DNeasy Tissue Kit (Qiagen Inc.). Total RNA was extracted from lungs using TRIzol (Invitrogen) as previously described (30).

Analysis of Viral Loads

MAV-1 viral loads were measured in organs using quantitative real-time polymerase chain reaction (qPCR) as previously described (6, 30). Primers and probe used in this assay to detect a 59 bp region of the MAV-1 E1A gene are

described in Table 6-1. Results were standardized to the nanogram (ng) amount of input DNA.

Analysis of Host Gene Expression

Cytokine gene expression was quantified using RT-qPCR. First, 2.5 µg of RNA were reverse transcribed using MMLV reverse transcriptase (Invitrogen) in 20 µl reactions according to the manufacturer's instructions. Water was added to the cDNA product to bring the total volume to 50 µl. Primers used to detect IL-17A, RORγt, and IFN-γ are described in Table 6-1. For these measurements, 5 µl of cDNA were added to reactions containing Power SYBR Green PCR Mix (Applied Biosystems) and forward and reverse primers (each at 200 nM final concentration) in a 25 µl reaction volume. Separate reactions were prepared with primers for mouse GAPDH (Table 6-1, used at 200 nM each). In all cases, RT-qPCR analysis consisted of 40 cycles of 15 s at 90°C and 60 s at 60°C. Quantification of target gene mRNA was normalized to GAPDH and expressed in arbitrary units as $2^{-\Delta Ct}$, where Ct is the threshold cycle and ΔCt = Ct(target) – Ct(GAPDH).

Analysis of Inflammatory Cells in Bronchoalveolar Lavage Fluid

Mice were euthanized via pentobarbital overdose at the indicated time points. Lungs were lavaged three times with the same aliquot of 1 mL sterile PBS containing protease inhibitor (complete, Mini, EDTA-free tablets; Roche Applied Science). Cells in BALF were counted using a hemocytometer. Samples were

centrifuged at 13,500 rpm for 10 min at 4°C, after which the supernatant was removed and the cell pellet was resuspended in 125 µL sterile PBS containing protease inhibitor. The remaining BALF was stored at -80°C. The cells were centrifuged in a Shandon Cytospin (Shandon Elliot) and differential cell counting was performed after staining with Hema 3 Stain Set (Fisher Scientific).

Isolation of Cells from Lungs and Mediastinal Lymph Nodes

In some experiments, left lungs were excised and cut into small pieces before digestion for 30 min at 37°C in a 1 mg/ml solution of collagenase A (Sigma). The digested tissue was then pushed through a syringe with a 1.5-in 22-gauge needle and pelleted at 3,000 rpm (402 x g) for 5 min. After lysis of red blood cells in 1X lysing buffer (BD PharMingen) for 3 min, tissue debris was removed by a brief spin (~5 to 10 s) at 1,000 rpm (45 x g). The remaining cells were pelleted at 1,200 rpm (64 x g) for 6 min prior to staining.

Single cell suspensions from mediastinal lymph nodes were prepared by grinding the tissue gently between glass slides and passing cells through a 64 µm cell strainer. The cells were pelleted at 1,200 rpm (64 x g) for 6 min prior to staining.

Intracellular Cytokine Staining

Cells isolated from lungs or MLN were plated at 10^6 cells/ml and stimulated with 50 ng/ml PMA and 1.5 µM ionomycin (Calbiochem) for 5 h at 37°C. For antigen presenting cell (APC) stimulation, 5 x 10^5 cells were cocultured

overnight in 96-well plates with MAV-1-pulsed APCs (10^6 cells/well). APCs were prepared by depleting T cells from single cell suspensions of splenocytes using anti-CD3 microbeads (Miltenyi Biotech). Prior to coculture with cells isolated from lungs or MLN, APCs were exposed to MAV-1 at a multiplicity of infection of 5 for 48 h and then irradiated with 3000 rads. Monensin (Sigma) was added at 3 μM during the last 3 h of coculture. Cells were preincubated with anti-FcγR mAb 2.4G2 to block nonspecific binding before they were stained with the following Per-CP-, APC-, FITC-, biotin- and PE-Cy7-conjugated antibodies: CD4 (L3T4), CD8 (53-6.7), TCR-β (H57-597), TCR-γδ (GL3), and NK1.1 (PK136) antibodies (BD Biosciences). Cells were then fixed in 4% paraformaldehyde for 10 min at room temperature, and permeabilized with 0.2% saponin (Sigma). Finally, cells were stained with APC-Cy7- and PE-labeled IL17A (TC11-18H10) and IFN-γ (XMG1.2) antibodies (BD Biosciences) and analyzed by flow cytometry. Events were acquired on a FACSCanto (BD) flow cytometer, and data were analyzed with FlowJo software (Tree Star). Cells were classified as $CD4^+$ T cells ($TCR\beta^+CD4^+$), $CD8^+$ T cells ($TCR\beta^+CD8^+$), NK cells ($NK1.1^+TCR\beta^-$), NKT cells ($NK1.1^+TCR\beta^+$), γδ T cells ($TCR\delta^+TCR\beta^-$), and non-T cells ($TCR\beta^-TCR\delta$-$NK1.1^-$).

Lymphocyte Stimulation

Lymphocytes were seeded at a concentration of 3 x 10^5 cells/well in 96-well plates coated with anti-CD3 antibody (BioLegend, 5 μg/ml) and incubated for 24 h. Supernatant was then collected for ELISA.

Analysis of Cytokine Protein

Cytokine protein concentrations in BALF and cell culture supernatant were determined by ELISA (Duoset Kits, R&D Systems) according to the manufacturer's protocol.

Neutrophil Depletion

Mice were pretreated intraperitoneally (i.p.) with 100 μg of anti-Gr-1 antibody (clone RB6-8C5), a generous gift from Dr. Gary Huffnagle, beginning 24 h before MAV-1 infection and then every other day until day 6. The control group received an equivalent amount of pre-immune mouse serum (Sigma) in sterile PBS.

Statistics

Analysis of data for statistical significance was conducted using Prism 6 for Macintosh (GraphPad Software, Incorporated). Differences between groups at multiple time points were analyzed using two-way analysis of variance (ANOVA) followed by Bonferroni's multiple comparison tests. Comparisons between two groups at a single time point were made using the Mann-Whitney rank sum test. *P* values less than 0.05 were considered statistically significant.

Table 6-1. Primers and probes used for real-time PCR analysis

Target	Oligonucleotide	Sequence (5′ to 3′)
MAV-1 E1A	Forward primer	GCACTCCATGGCAGGATTCT
	Reverse primer	GGTCGAAGCAGACGGTTCTTC
	Probe	TACTGCCACTTCTGC
IL-17A	Forward primer	GGGTCTTCATTGCGGTGG
	Reverse primer	CTCCAGAAGGCCCTCAGACTAC
RORγt	Forward primer	CCGCTGAGAGGGCTTCAC
	Reverse primer	TGCAGGAGTAGGCCACATTACA
IFN-γ	Forward primer	AAAGAGATAATCTGGCTCTGC
	Reverse primer	GCTCTGAGACAATGAACGCT
GAPDH	Forward primer	TGCACCACCAACTGCTTAG
	Reverse primer	GGATGCAGGGATGATGTTC

References

1. **Stempel HE, Martin ET, Kuypers J, Englund JA, Zerr DM.** 2009. Multiple viral respiratory pathogens in children with bronchiolitis. Acta Paediatr **98:**123-126.
2. **Horwitz MS.** 2001. Adenoviruses, p. 2301-2327. *In* Knipe DM, Howley PM (ed.), Fields Virology, vol. 2. Lippincott Williams & Wilkins, Philadelphia.
3. **Hale GA, Heslop HE, Krance RA, Brenner MA, Jayawardene D, Srivastava DK, Patrick CC.** 1999. Adenovirus infection after pediatric bone marrow transplantation. Bone Marrow Transplant **23:**277-282.
4. **Walls T, Shankar AG, Shingadia D.** 2003. Adenovirus: an increasingly important pathogen in paediatric bone marrow transplant patients. Lancet Infect Dis **3:**79-86.
5. **Anderson VE, Nguyen Y, Weinberg JB.** 2009. Effects of allergic airway disease on mouse adenovirus type 1 respiratory infection. Virology **391:**25-32.
6. **Procario MC, Levine RE, McCarthy MK, Kim E, Zhu L, Chang CH, Hershenson MB, Weinberg JB.** 2012. Susceptibility to acute mouse adenovirus type 1 respiratory infection and establishment of protective immunity in neonatal mice. J Virol **86:**4194-4203.
7. **Weinberg JB, Stempfle GS, Wilkinson JE, Younger JG, Spindler KR.** 2005. Acute respiratory infection with mouse adenovirus type 1. Virology **340:**245-254.
8. **Mosmann TR, Coffman RL.** 1989. TH1 and TH2 cells: different patterns of lymphokine secretion lead to different functional properties. Annual review of immunology **7:**145-173.
9. **Harrington LE, Hatton RD, Mangan PR, Turner H, Murphy TL, Murphy KM, Weaver CT.** 2005. Interleukin 17-producing CD4+ effector T cells develop via a lineage distinct from the T helper type 1 and 2 lineages. Nat Immunol **6:**1123-1132.
10. **Park H, Li Z, Yang XO, Chang SH, Nurieva R, Wang YH, Wang Y, Hood L, Zhu Z, Tian Q, Dong C.** 2005. A distinct lineage of CD4 T cells regulates tissue inflammation by producing interleukin 17. Nat Immunol **6:**1133-1141.
11. **Korn T, Bettelli E, Oukka M, Kuchroo VK.** 2009. IL-17 and Th17 Cells. Annual review of immunology **27:**485-517.
12. **Crowe CR, Chen K, Pociask DA, Alcorn JF, Krivich C, Enelow RI, Ross TM, Witztum JL, Kolls JK.** 2009. Critical role of IL-17RA in immunopathology of influenza infection. J Immunol **183:**5301-5310.
13. **Li C, Yang P, Sun Y, Li T, Wang C, Wang Z, Zou Z, Yan Y, Wang W, Wang C, Chen Z, Xing L, Tang C, Ju X, Guo F, Deng J, Zhao Y, Yang P, Tang J, Wang H, Zhao Z, Yin Z, Cao B, Wang X, Jiang C.** 2012. IL-17 response mediates acute lung injury induced by the 2009 pandemic influenza A (H1N1) virus. Cell research **22:**528-538.
14. **Mukherjee S, Lindell DM, Berlin AA, Morris SB, Shanley TP, Hershenson MB, Lukacs NW.** 2011. IL-17-induced pulmonary

pathogenesis during respiratory viral infection and exacerbation of allergic disease. Am J Pathol **179:**248-258.

15. **Spolski R, Wang L, Wan CK, Bonville CA, Domachowske JB, Kim HP, Yu Z, Leonard WJ.** 2012. IL-21 promotes the pathologic immune response to pneumovirus infection. J Immunol **188:**1924-1932.
16. **Hamada H, Garcia-Hernandez Mde L, Reome JB, Misra SK, Strutt TM, McKinstry KK, Cooper AM, Swain SL, Dutton RW.** 2009. Tc17, a unique subset of CD8 T cells that can protect against lethal influenza challenge. J Immunol **182:**3469-3481.
17. **McCarthy MK, Levine RE, Procario MC, McDonnell PJ, Zhu L, Mancuso P, Crofford LJ, Aronoff DM, Weinberg JB.** 2013. Prostaglandin E2 induction during mouse adenovirus type 1 respiratory infection regulates inflammatory mediator generation but does not affect viral pathogenesis. PLoS One **8:**e77628.
18. **Xu S, Cao X.** 2010. Interleukin-17 and its expanding biological functions. Cell Mol Immunol **7:**164-174.
19. **Egan CE, Sukhumavasi W, Bierly AL, Denkers EY.** 2008. Understanding the multiple functions of Gr-1(+) cell subpopulations during microbial infection. Immunologic research **40:**35-48.
20. **Hou L, Jie Z, Desai M, Liang Y, Soong L, Wang T, Sun J.** 2013. Early IL-17 production by intrahepatic T cells is important for adaptive immune responses in viral hepatitis. J Immunol **190:**621-629.
21. **Vavrincova-Yaghi D, Deelman LE, Goor H, Seelen M, Kema IP, Smit-van Oosten A, Zeeuw D, Henning RH, Sandovici M.** 2011. Gene therapy with adenovirus-delivered indoleamine 2,3-dioxygenase improves renal function and morphology following allogeneic kidney transplantation in rat. J Gene Med **13:**373-381.
22. **Martin B, Hirota K, Cua DJ, Stockinger B, Veldhoen M.** 2009. Interleukin-17-producing gammadelta T cells selectively expand in response to pathogen products and environmental signals. Immunity **31:**321-330.
23. **Shibata K, Yamada H, Hara H, Kishihara K, Yoshikai Y.** 2007. Resident Vdelta1+ gammadelta T cells control early infiltration of neutrophils after Escherichia coli infection via IL-17 production. J Immunol **178:**4466-4472.
24. **Fossiez F, Djossou O, Chomarat P, Flores-Romo L, Ait-Yahia S, Maat C, Pin JJ, Garrone P, Garcia E, Saeland S, Blanchard D, Gaillard C, Das Mahapatra B, Rouvier E, Golstein P, Banchereau J, Lebecque S.** 1996. T cell interleukin-17 induces stromal cells to produce proinflammatory and hematopoietic cytokines. J Exp Med **183:**2593-2603.
25. **Laan M, Prause O, Miyamoto M, Sjostrand M, Hytonen AM, Kaneko T, Lotvall J, Linden A.** 2003. A role of GM-CSF in the accumulation of neutrophils in the airways caused by IL-17 and TNF-alpha. Eur Respir J **21:**387-393.
26. **Ye P, Rodriguez FH, Kanaly S, Stocking KL, Schurr J, Schwarzenberger P, Oliver P, Huang W, Zhang P, Zhang J, Shellito JE, Bagby GJ, Nelson S, Charrier K, Peschon JJ, Kolls JK.** 2001.

Requirement of interleukin 17 receptor signaling for lung CXC chemokine and granulocyte colony-stimulating factor expression, neutrophil recruitment, and host defense. J Exp Med **194:**519-527.
27. **Witowski J, Pawlaczyk K, Breborowicz A, Scheuren A, Kuzlan-Pawlaczyk M, Wisniewska J, Polubinska A, Friess H, Gahl GM, Frei U, Jorres A.** 2000. IL-17 stimulates intraperitoneal neutrophil infiltration through the release of GRO alpha chemokine from mesothelial cells. J Immunol **165:**5814-5821.
28. **Kajon AE, Spindler KR.** 2000. Mouse adenovirus type 1 replication in vitro is resistant to interferon. Virology **274:**213-219.
29. **Nakae S, Komiyama Y, Nambu A, Sudo K, Iwase M, Homma I, Sekikawa K, Asano M, Iwakura Y.** 2002. Antigen-specific T cell sensitization is impaired in IL-17-deficient mice, causing suppression of allergic cellular and humoral responses. Immunity **17:**375-387.
30. **Nguyen Y, McGuffie BA, Anderson VE, Weinberg JB.** 2008. Gammaherpesvirus modulation of mouse adenovirus type 1 pathogenesis. Virology **380:**182-190.

Notes

This chapter was reprinted and modified from McCarthy, MK, Zhu, L, Procario, MC, and Weinberg, JB. 2014. IL-17A contributes to neutrophil recruitment but not to control of viral replication during acute mouse adenovirus type 1 respiratory infection. *Virology.* 456-457:259-267. DOI: 10.1016/j.virol.2014.04.008

Chapter 7:
Proinflammatory effects of interferon gamma in mouse adenovirus type 1 myocarditis

Abstract

Adenoviruses are frequent causes of pediatric myocarditis. Little is known about the pathogenesis of adenovirus myocarditis, and the species-specificity of human adenoviruses has limited the development of animal models, which is a significant barrier to strategies for prevention or treatment. We have developed a mouse model of myocarditis following mouse adenovirus type 1 (MAV-1) infection to study the pathogenic mechanisms of this important cause of pediatric myocarditis. Following intranasal infection of neonatal C57BL/6 mice, we detected viral replication and induction of interferon-gamma (IFN-γ) in the hearts of infected mice. MAV-1 caused myocyte necrosis and induced substantial cellular inflammation that was predominantly composed of $CD3^+$ T lymphocytes. Depletion of IFN-γ during acute infection reduced cardiac inflammation in MAV-1-infected mice without affecting viral replication. We observed decreased contractility during acute infection of neonatal mice, and persistent viral infection in the heart was associated with cardiac remodeling and hypertrophy in adulthood. IFN-γ is a proinflammatory mediator during adenovirus-induced myocarditis, and persistent adenovirus infection may contribute to ongoing cardiac dysfunction.

Importance

Studying the pathogenesis of myocarditis caused by different viruses is essential in order to characterize both virus-specific and generalized factors that contribute to disease. Very little is known about the pathogenesis of adenovirus myocarditis, which is a significant impediment to the development of treatment or prevention strategies. We used MAV-1 to establish a mouse model of human adenovirus myocarditis, providing the means to study host and pathogen factors contributing to adenovirus-induced cardiac disease during acute and persistent infection. The MAV-1 model will enable fundamental studies of viral myocarditis, including IFN-γ modulation, as a therapeutic strategy.

Introduction

Acute myocarditis is a significant cause of morbidity and mortality in childhood. Myocarditis has been identified in 16 to 21% of sudden deaths in children (1). The course of viral myocarditis is often more severe in neonates and infants than in older patients, with up to 67% mortality in newborns and 55% in infants less than 1 year of age compared to 20 to 25% in older children and 38% in adults (2, 3). Associations between myocarditis and adenovirus infection are well established (3-5). Persistent human adenovirus (HAdV) infections of the myocardium have been implicated in the development of dilated cardiomyopathy and cardiac dysfunction (6-8). Detection of HAdV genomes in myocardial biopsies of pediatric heart transplant recipients is predictive of coronary artery

vasculopathy and transplant loss (9). The histopathology of hearts in patients with HAdV myocarditis can be milder than that in patients with myocarditis caused by other viruses (3), suggesting that mechanisms underlying HAdV-mediated disease may differ from those involved in myocarditis caused by other viruses.

Much of what is known about viral myocarditis has come from the study of myocarditis resulting from coxsackievirus B3 (CVB3) and reovirus. The pathogenesis of viral myocarditis involves many interrelated processes. Direct damage to cardiac myocytes can occur by viral lysis, inhibition of host protein synthesis, or cleavage of host proteins such as dystrophin by viral proteases (10). Immune responses to acute infection contribute to the clearance of virus but can also cause further damage, either directly or due to cross-reaction between viral and cardiac antigens that leads to autoimmune myocardial injury (11). Interferon (IFN)-α and IFN-β, the type I IFNs, are essential for limiting viral replication in cardiac myocytes and are protective in a neonatal mouse model of reovirus myocarditis (12). IFN-γ, the type II IFN, is upregulated and is often protective in models of viral myocarditis (12-14), although other reports suggest that it can promote myocarditis associated with CVB3 (15, 16), and prolonged expression of IFN-γ may lead to a chronic inflammatory cardiomyopathy (17). Myocyte apoptosis induced by viral infection and virus-induced inflammation can also contribute to progressive cardiac damage (18). Ongoing injury can lead to myocardial remodeling and fibrosis accompanied by ventricular dilation and cardiac dysfunction.

We have previously established intranasal MAV-1 infection of C57BL/6 and BALB/c mice as a model to study the pathogenesis of adenovirus respiratory infection (19). One previous report demonstrated that intraperitoneal (i.p.) MAV-1 infection of neonatal outbred Swiss Webster mice led to cardiac inflammation, myocardial fibrosis, and calcification (20), and a related virus (MAV-3) was detected in the heart following intravenous infection of adult C57BL/6N mice (21). However, MAV-1 and MAV-3 have yet to be used in detailed studies of myocarditis pathogenesis. Here, we demonstrate that intranasal MAV-1 infection of neonatal mice led to viral replication and induction of IFN-γ expression in the heart that correlated with cellular inflammation and acute myocyte necrosis. Depletion of IFN-γ during acute infection reduced cardiac inflammation in MAV-1-infected mice without affecting viral replication. Long-term persistence of viral DNA was associated with increased heart mass and cellular hypertrophy.

Results

MAV-1 infects primary cardiac myocytes ex vivo and hearts in vivo.

To determine whether MAV-1 can productively infect cardiac myocytes, we isolated cardiac myocytes from adult mice and inoculated them with MAV-1. We used RT-qPCR to quantify the expression of the MAV-1 E1A and hexon genes and qPCR to quantify viral DNA in infected myocytes. Expression of E1A, a nonstructural gene expressed early in infection, and hexon, a virion structural protein expressed late, increased between 24 and 48 hpi (Figure 7-1A). Likewise, viral DNA increased between 24 and 48 hpi (Figure 7-1B), further suggesting

productive viral replication in these cells. To confirm that infectious progeny were produced from cardiac myocytes, we performed plaque assays with supernatants of infected cardiac myocyte cultures. Viral titers in the supernatants of infected cells increased slightly over time (Figure 7-1C), further indicating that cardiac myocytes were productively infected by MAV-1.

To verify that MAV-1 replicates in hearts *in vivo*, we infected 7-day old C57BL/6 mice i.n. with MAV-1. We harvested hearts at multiple time points and used qPCR to quantify DNA viral loads. MAV-1 DNA was readily detectable at 4 dpi (Figure 7-1D). Viral loads in the heart increased to peak levels between 7 and 10 dpi and were reduced at 21 dpi. We also detected expression of MAV-1 E1A and hexon genes in the hearts of infected mice using RT-qPCR (Figure 7-1E, F). Expression of both E1A and hexon peaked at 7 and 10 dpi and then decreased over time, although we detected persistent expression at 21 dpi. The presence of viral gene expression and the logarithmic increases and subsequent decreases in heart viral loads over the time course suggest that MAV-1 replicates in the hearts of mice following i.n. infection.

MAV-1 induces cellular inflammation in the heart.

Cardiac inflammation was reported following i.p. MAV-1 infection of neonatal outbred Swiss Webster mice (20), but this inflammatory response was not characterized in detail. We evaluated the histologic appearance of hearts obtained from inbred mice at various times post infection. We observed no differences between hearts of mock-infected and infected mice at 4 dpi (data not

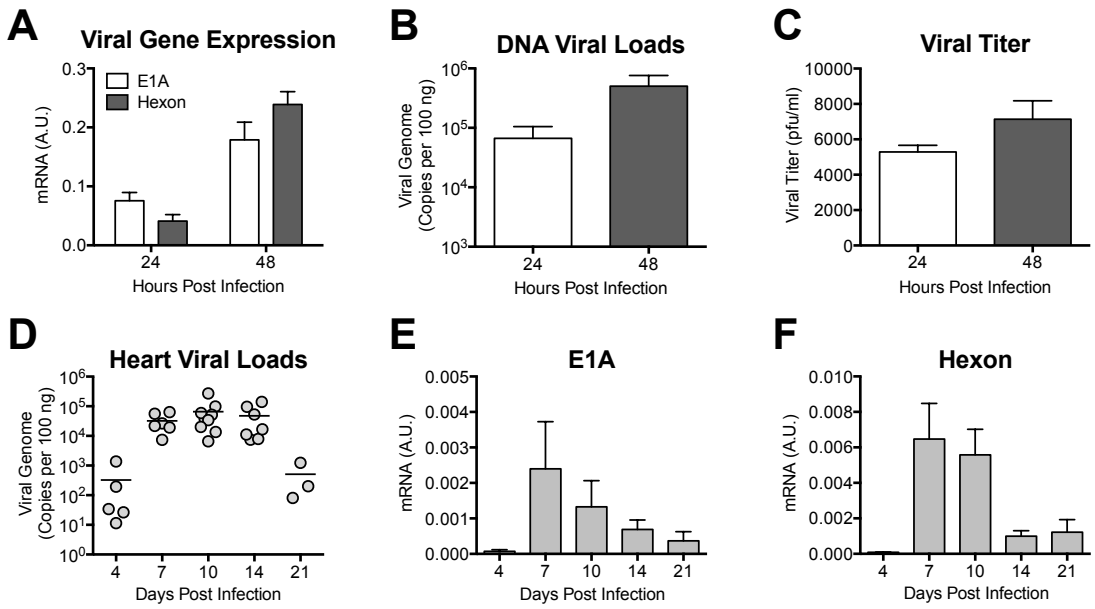

Figure 7-1. MAV-1 infects cardiac myocytes *ex vivo* and neonatal hearts *in vivo*.

A) Primary cardiac myocytes from adult C57BL/6 mice were infected with MAV-1 (MOI=5) and expression of the viral E1A and hexon genes was measured by RT-qPCR, shown standardized to GAPDH in arbitrary units (A.U.). B) DNA was extracted from primary cardiac myocytes and qPCR was used to quantify copies of MAV-1 genome. C) Supernatants harvested from infected primary cardiac myocytes and viral titers measured by plaque assay. Error bars represent means ± S.E.M of three samples per time point. D) Neonatal mice were infected with MAV-1. qPCR was used to quantify viral loads in hearts. DNA viral loads are expressed as copies of MAV-1 genome per 100 ng of input DNA. Individual circles represent values for individual mice and horizontal bars represent means for each group. Expression of the viral genes E) E1A and F) hexon were measured in the heart by RT-qPCR, shown in arbitrary units and standardized to GAPDH. Combined data from 4 to 9 mice per group are presented as means ± S.E.M.

shown) or at 7 dpi (Figure 7-2A). By 10 dpi, numerous focal accumulations of inflammatory cells were present, scattered throughout the myocardium (Figure 7-2A). In many areas, these foci were associated with necrotic cardiac myocytes. Cellular inflammation was less severe at 14 and 21 dpi, although hearts of infected mice contained scattered focal accumulations of mononuclear inflammatory cells and necrotic cardiac myocytes (Figure 7-2A and data not shown).

We used immunohistochemistry to evaluate and quantify recruitment of inflammatory cells to hearts following MAV-1 infection. Increased numbers of $CD3^+$ T lymphocytes were first detected in hearts of infected mice at 7 dpi (Figure 7-2B). By 10 dpi, we observed further increases in the number of $CD3^+$ cells. At this time, recruited $CD3^+$ cells were clustered around blood vessels and distributed throughout the myocardium (Figure 7-2A, B). Fewer $CD3^+$ cells were detected at later times, but they were still present in greater numbers in the hearts of infected mice than mock infected mice at 14 and 21 dpi (Figure 7-2B). Both $CD4^+$ and $CD8^+$ cells were detected in the hearts of infected mice at 10 dpi, although $CD8^+$ cells were more abundant than $CD4^+$ cells (Figure 7-2C). We also observed recruitment of $F4/80^+$ macrophages to the heart after MAV-1 infection (data not shown).

Histological evaluation suggested that MAV-1 infection and/or MAV-1-induced cardiac inflammation induces myocyte necrosis. To determine whether the histological findings described above correlated with other markers of cardiac injury during acute infection, we measured cardiac troponin I (cTnI) in the serum

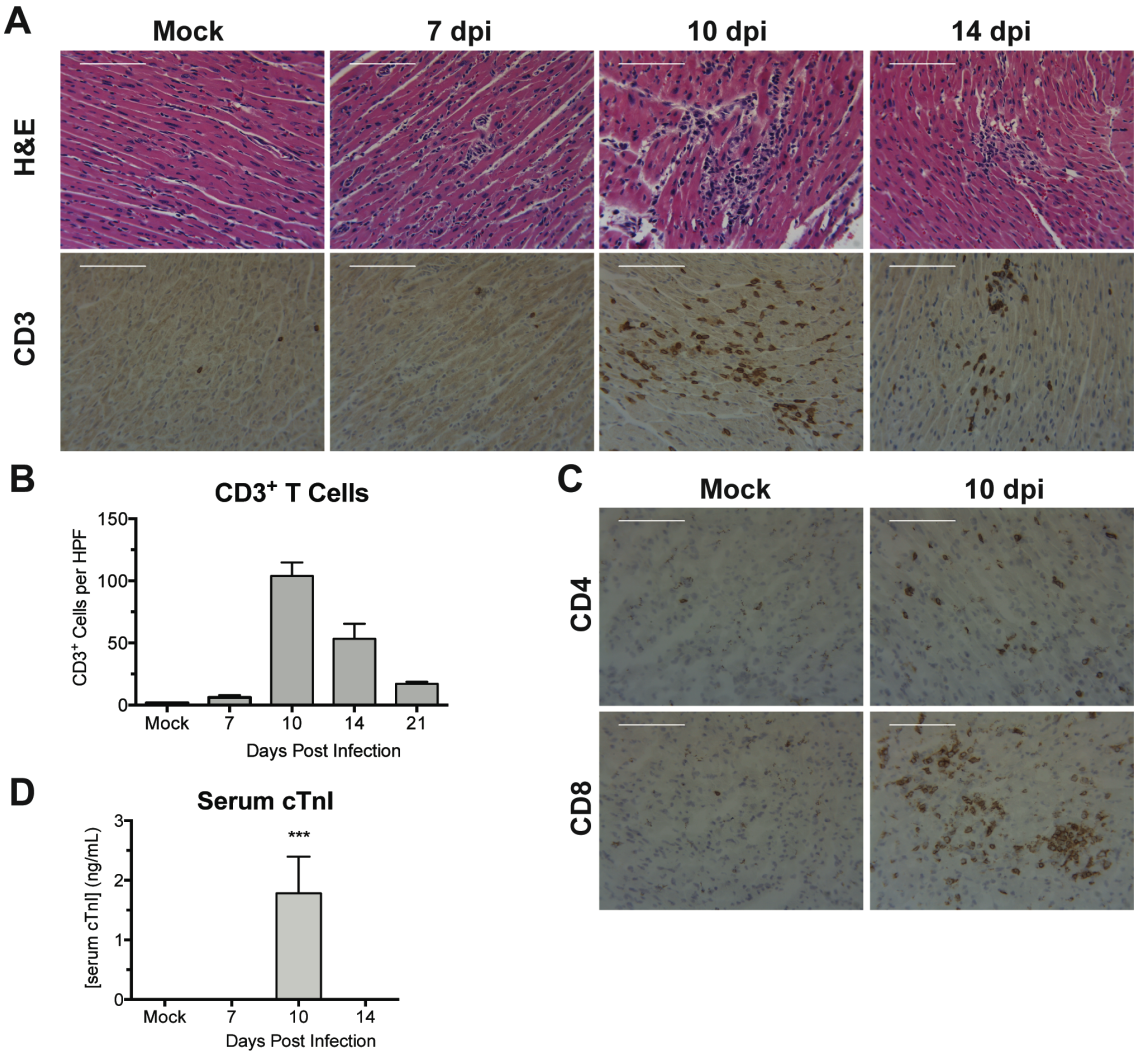

Figure 7-2. Cellular inflammation in hearts of infected neonatal mice.

Mice were infected with MAV-1 or mock infected with conditioned media. A) Hematoxylin and eosin-stained or CD3-stained sections were prepared from paraffin-embedded sections. Scale bars, 100 μm. B) CD3 staining was quantified by counting the number of $CD3^+$ cells per high power field, averaging three fields per individual mouse. Combined data from 3 to 5 mice per group are presented as means ± S.E.M. C) CD4- and CD8-stained sections were prepared from hearts of infected neonatal mice at 10 dpi. Scale bars, 100 μm. D) Serum cTnI levels were measured by ELISA. Combined data from 4 to 6 mice per group are presented as means ± S.E.M. ***P<0.001, comparing Mock to MAV-1.

of mice after infection. We detected increased concentrations of cTnI in the serum of infected mice at 10 dpi (Figure 7-2D) but not at other times or in mock infected mice.

IFN-γ and other proinflammatory cytokines are upregulated in hearts of infected neonatal mice.

Because we observed recruitment of T cells to the heart following MAV-1 infection, we used RT-qPCR to measure expression of proinflammatory chemokines and cytokines in the heart. We detected increased expression of IFN-γ in the hearts of infected mice beginning at 7 dpi (Figure 7-3A). IFN-γ upregulation peaked at 10 dpi and decreased in magnitude, but persisted in infected mice at 21 dpi. We observed no significant changes in expression of IFN-β, IL-4 or IL-17 (data not shown). We detected increased expression of the chemokine CCL5 starting at 10 dpi that persisted in infected mice until 21 dpi (Figure 7-3B). Expression of TNF-α (Figure 7-3C) and IL-1β (Figure 7-3D) was also increased in infected mice, whereas we detected no significant changes in expression of IL-6 (data not shown).

MAV-1-induced cardiac disease is less pronounced in adult mice.

We have previously described increased susceptibility to MAV-1 respiratory infection and blunted lung IFN-γ responses in neonatal mice compared to adults (22). To determine whether this is also the case in the heart,

we compared viral loads and inflammatory responses in the hearts of neonates and adult mice. We detected peak viral loads in the hearts of adults at 10 dpi (Figure 7-4A). There were no statistically significant differences between heart viral loads in neonates and adults at any time point. There was substantially less cellular inflammation and evidence of myocyte necrosis (data not shown) and fewer CD3+ cells in adult hearts (Figure 7-4B). cTnI was not detected in the serum of infected adult mice at any time point (data not shown). IFN-γ (Figure 7-4C), CCL5 (Figure 7-4D), and TNF-α (Figure 7-4E) were upregulated in the hearts of infected adult mice, but the magnitudes of these responses were substantially lower and the kinetics were delayed compared to those in neonates, in contrast to our previous findings in the lungs (22). We detected marked increases in the expression of both IL-1β (Figure 7-4F) and IL-6 (Figure 7-4G) in adult mice at 14 dpi, but expression of both had decreased to baseline levels by 21 dpi. Peak levels of IL-1β and IL-6 were greater in adults than in neonates at 14 dpi. However, there was minimal difference between neonates and adults when comparing the fold change in mRNA levels relative to mock infected animals at 14 dpi for IL-1β (neonates, 1.83 ± 0.29; adults, 4.64 ± 2.26; P=0.44) or IL-6 (neonates, 1.56 ± 0.67; adults, 4.92 ± 2.67; P=0.34).

MAV-1 infection is associated with cardiac dysfunction in neonatal mice.

Acute viral myocarditis often results in decreased cardiac function (23, 24). To determine whether our histological observations correlated with measurements of cardiac function, we assessed heart function by

echocardiography. In mice infected as neonates, there were no differences in left ventricular ejection fraction or cardiac output between mock- and MAV-1-infected mice at 5 dpi (Figure 7-5A,B). However, left ventricular ejection fraction and cardiac output were significantly lower in infected neonates compared to mock-infected controls at 10 dpi. MAV-1 infection of neonatal mice did not cause left ventricle dilation (Figure 7-5C), and heart rate did not differ between groups (Figure 7-5D). MAV-1 infection of adult mice had no effect on left ventricular ejection fraction, cardiac output, left ventricle dilation, or heart rate at 10 dpi (Figure 7-5E-H).

IFN-γ is proinflammatory during MAV-1 myocarditis

Type I IFN (IFN-α and IFN-β) and type II IFN (IFN-γ) are upregulated and are often protective in other models of viral myocarditis (12-14). Although we did not observe virus-induced changes in IFN-β expression (data not shown), we did detect significant upregulation of IFN-γ in hearts after MAV-1 infection (Figure 7-3A). To further define the role of IFN-γ during MAV-1 myocarditis, we depleted IFN-γ beginning on the day after infection. Due to accelerated mortality in the infected IFN-γ -depleted mice beginning at 9 days after infection (Figure 7-6A), mice were euthanized at 9 dpi. Heart viral loads did not differ between IFN-γ-depleted and control mice at 9 dpi (Figure 7-6B). The severity of myocarditis was quantified by blinded scoring of histological sections of hearts. As before,

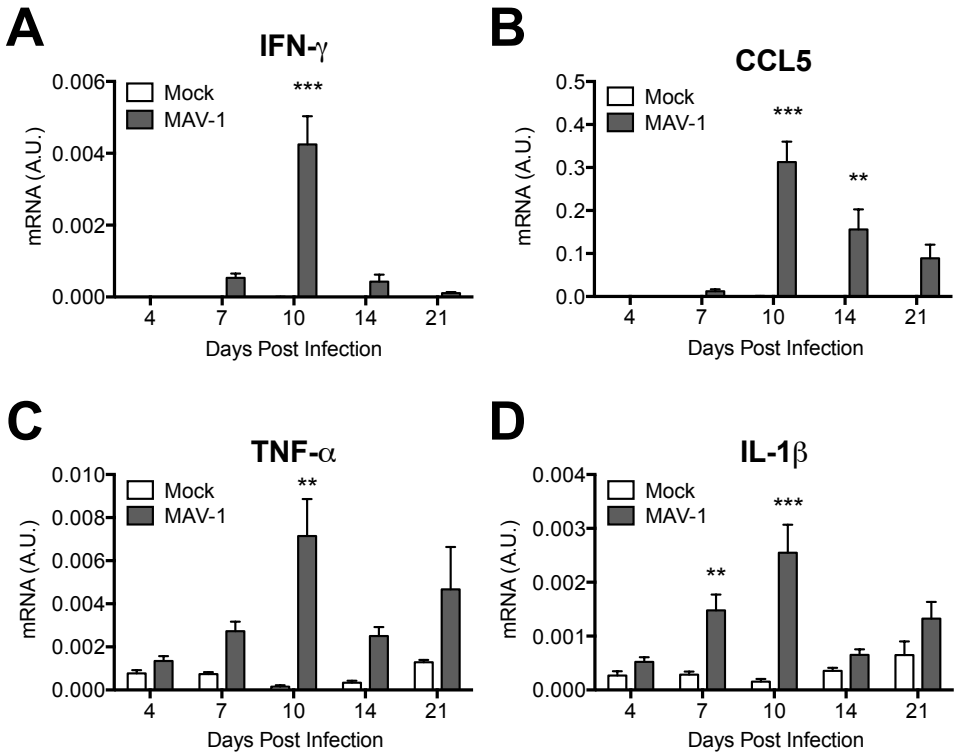

Figure 7-3. Induction of cytokines in hearts.

Mice were infected with MAV-1 or mock infected with conditioned media. RT-qPCR was used to quantify A) IFN-γ, B) CCL5, and C) TNF-α, and D) IL-1β expression, shown and standardized to GAPDH in arbitrary units (A.U.). Combined data from 4 to 13 mice per group are presented as means ± S.E.M. ****P*<0.001, ***P*<0.01 comparing Mock to MAV-1 at a given timepoint.

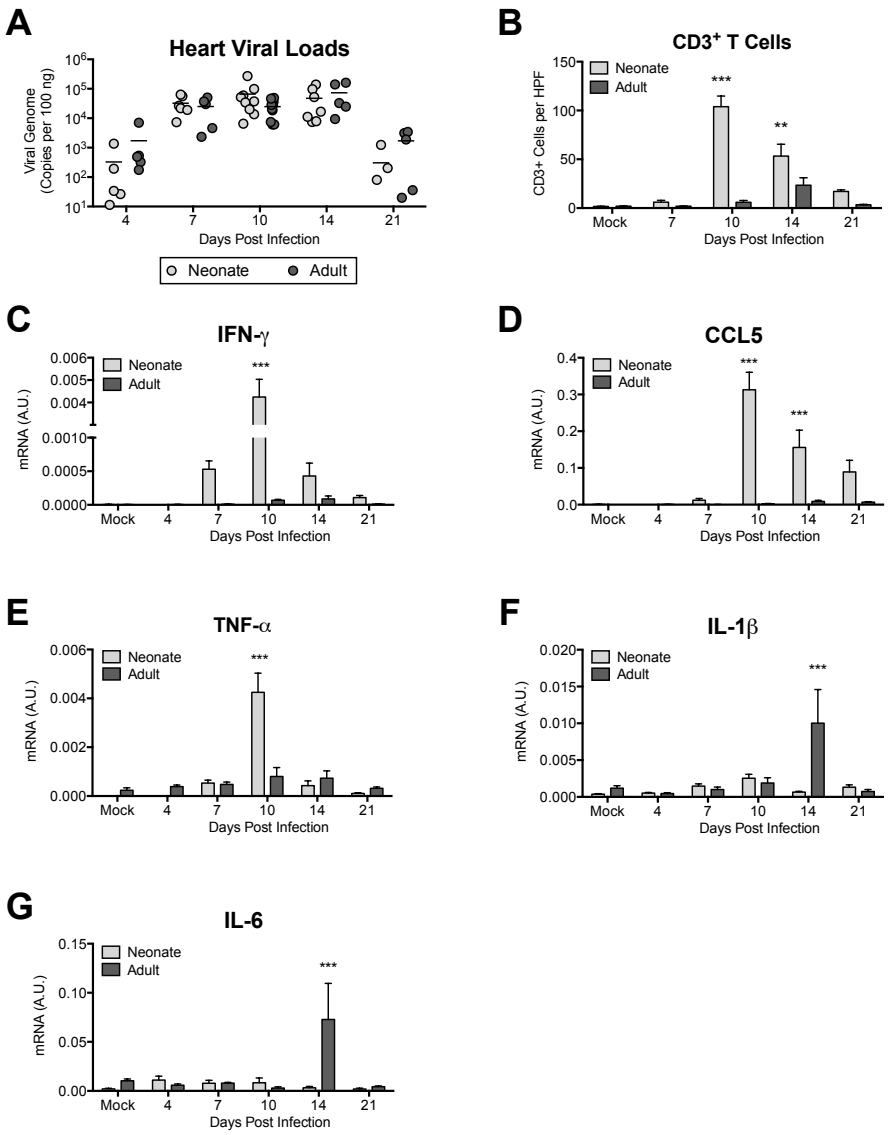

Figure 7-4. Age-based differences in MAV-1 myocarditis.

Adult and neonatal mice were infected with MAV-1. A) qPCR was used to quantify MAV-1 genome copies in heart DNA. DNA viral loads are expressed as copies of MAV-1 genome per 100 ng of input DNA. Individual circles represent values for individual mice and horizontal bars represent means for each group. B) CD3 staining was quantified by counting the number of CD3+ cells per high power field, averaging three fields per individual mouse. Combined data from 2 to 5 mice per group are presented as means ± S.E.M. ***P<0.001, **P<0.01 comparing neonate to adult at a given time point. RT-qPCR was used to quantify expression of C) IFN-γ, D) CCL5, E) TNF-α, F) IL-1β, and G) IL-6,, all shown standardized to GAPDH in arbitrary units (A.U.). Combined data from 4 to 13 mice per group are presented as means ± S.E.M. Neonatal data from Figures 1D, 2B, and 3A-D are included in A, B, and C-F, respectively, for reference.

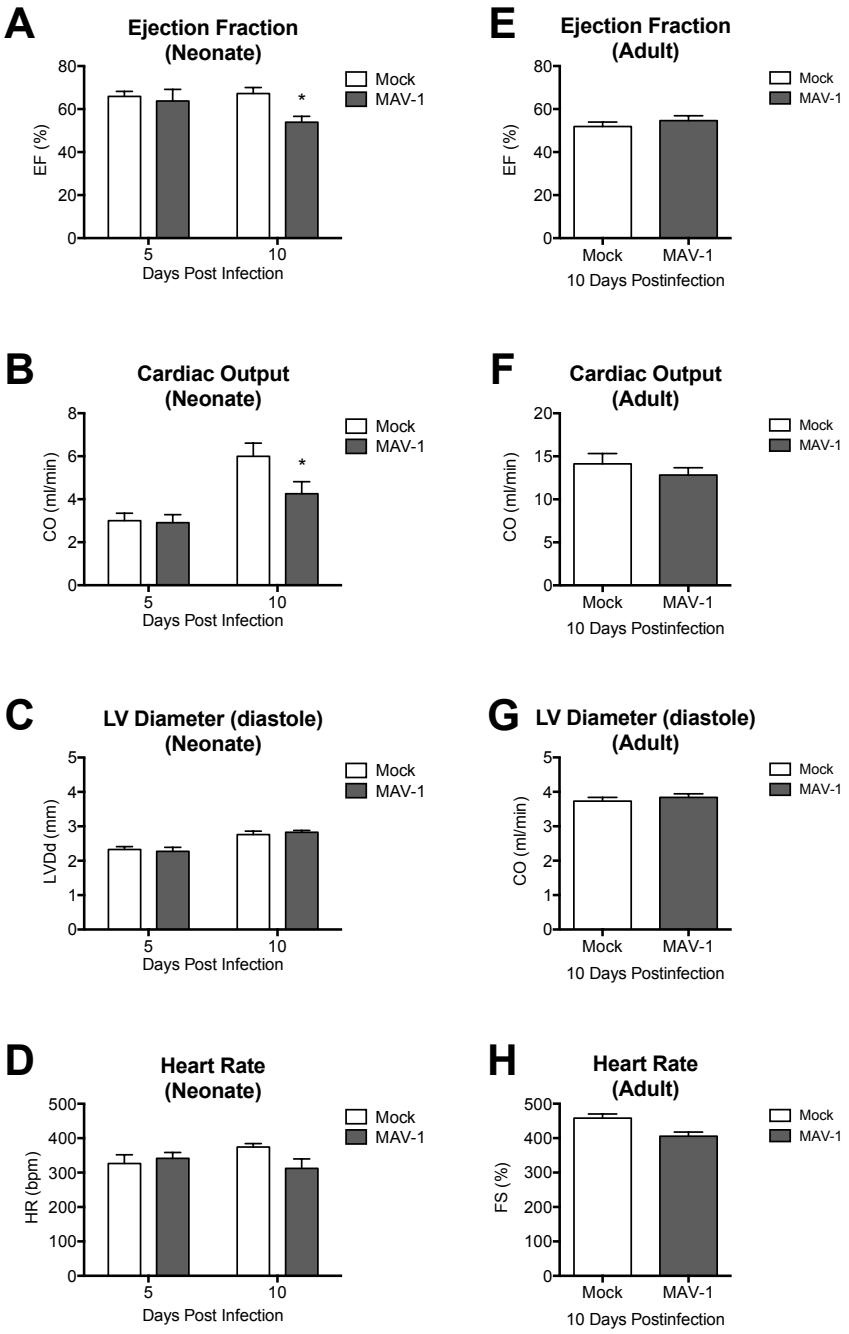

Figure 7-5. Cardiac dysfunction following MAV-1 infection.

Neonatal and adult mice were infected with MAV-1 and echocardiography was performed to measure A,E) ejection fraction, B,F) cardiac output, C,G) left ventricle internal diameter, and D,H) heart rate. Combined data from 4 to 11 mice per group are presented as means ± S.E.M. *P<0.05 comparing Mock to MAV-1 at a given time point.

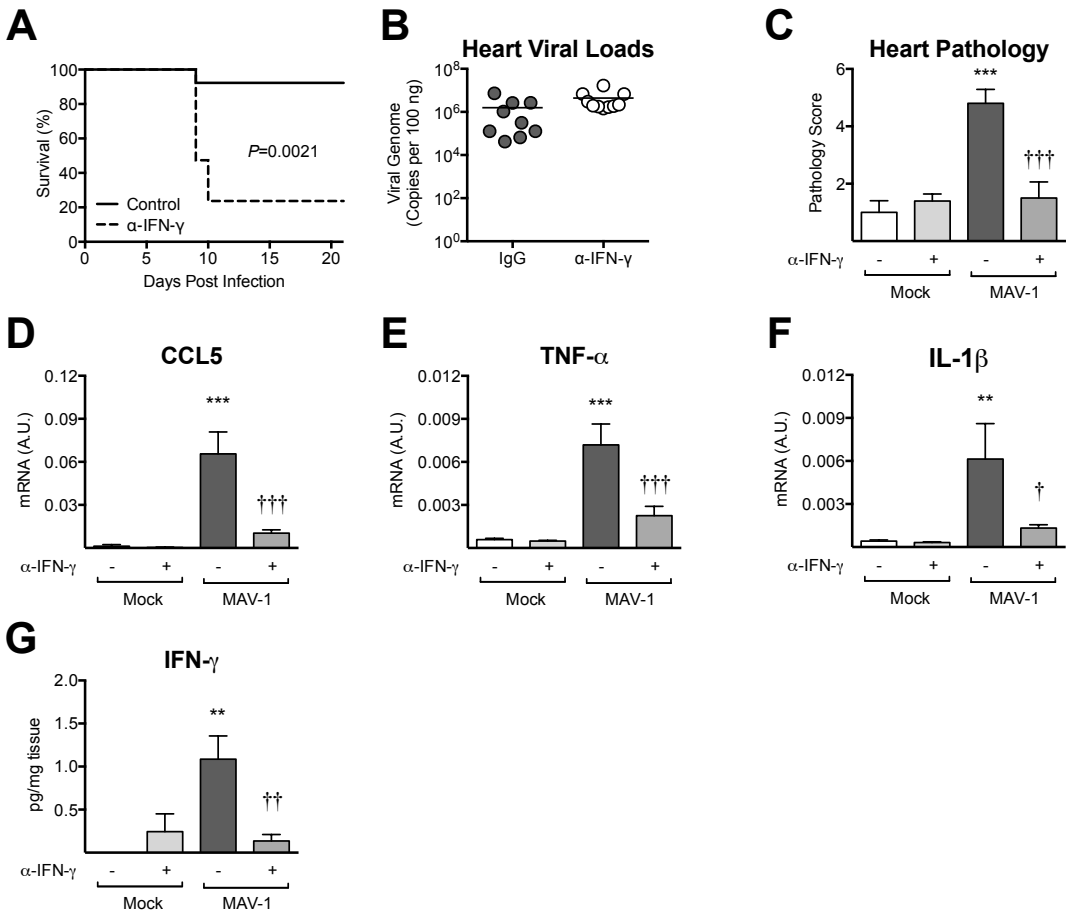

Figure 7-6. Role of IFN-γ in MAV-1 myocarditis.

Mice were infected with MAV-1 or mock infected with conditioned media and treated every other day with control IgG or anti-IFN-γ antibody beginning at 1 dpi. A) Survival of infected animals was compared using the log-rank (Mantel-Cox) test. B) qPCR was used to quantify MAV-1 genome copies in heart DNA. Viral loads are expressed as copies of MAV-1 genome per 100 ng of input DNA. Individual circles represent values for individual mice and horizontal bars represent means for each group. C) Pathology index scores were generated to quantify cellular inflammation. RT-qPCR was used to quantify D) CCL5, E) TNF-α, and F) IL-1β expression, shown standardized to GAPDH in arbitrary units (A.U.). Combined data from 4 to 6 mice per group are presented as means ± S.E.M. G) ELISA was used to measure IFN-γ protein in heart homogenate. IFN-γ data from 3 to 5 mice per group are standardized to mg of heart tissue and presented as means ± S.E.M. ***P<0.001, **P<0.01, and *P<0.05 comparing Mock to MAV-1 within a given condition. †††P<0.001, ††P<0.001, and †P<0.05 comparing MAV-1-infected control IgG- to anti-IFN-γ-treated mice.

substantial cellular inflammation was present in the hearts of control mice infected with MAV-1. In contrast, virus-induced cardiac inflammation was significantly lower in IFN-γ-depleted mice, equivalent to that in mock-infected animals (Figure 7-6C). Likewise, IFN-γ depletion reduced virus-induced CCL5, TNF-α, and IL-1β upregulation (Figure 7-6D-F). We confirmed IFN-γ depletion using ELISA to measure IFN-γ protein in heart homogenate (Figure 7-6G).

Persistent MAV-1 infection is associated with cardiac hypertrophy.

Both HAdV and MAV-1 establish persistent infections (25, 26). To determine whether MAV-1 persists in the heart, we infected mice at 7 days of age and harvested hearts from surviving mice at approximately 9 weeks post infection, when the mice had grown into adulthood. We detected viral genome in all infected mice by both nested PCR (Figure 7-7A) and qPCR (data not shown). To determine whether persistent MAV-1 infection affects cardiac function, we performed echocardiography at 9 weeks post infection. Although there was a trend toward lower left ventricle ejection fraction in mice that were infected as neonates compared to mock-infected mice (data not shown), the difference was not statistically significant, suggesting that the acute functional deficits of MAV-1 infection were at least partially recovered. We observed a significant increase in the left ventricle mass (as measured by echocardiography) to tibia length ratio in MAV-1-infected mice compared to mock-infected mice (Figure 7-7B). There were no statistically significant differences between groups in tibia length (data not shown). To further assess long-term effects of infection, we quantified

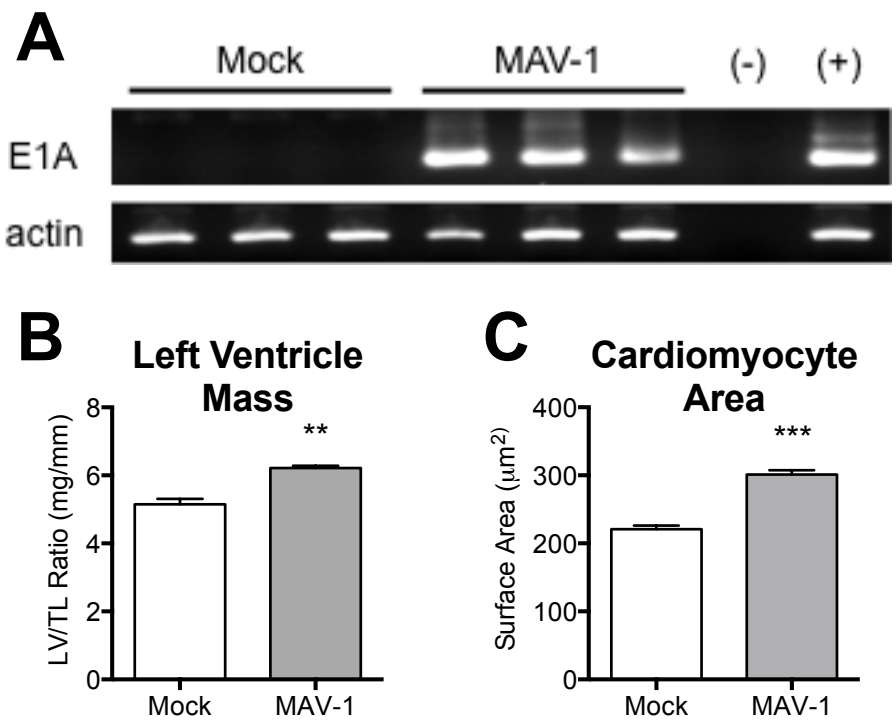

Figure 7-7. MAV-1 persistence and cardiac hypertrophy.

Mice were infected with MAV-1 and hearts harvested at 9 weeks post infection. A) Nested PCR was used to evaluate the presence of MAV-1 DNA (top) and β-actin (bottom). B) Left ventricular mass (LV) was measured by echocardiography and normalized to tibia length (TL). C) Heart sections were stained with FITC-conjugated wheat germ agglutinin to outline cell borders. Cardiomyocyte cross-sectional area was measured from digital images using NIH ImageJ software. Combined data from >350 cells for each condition are presented as means ± S.E.M. ***P<0.001, **P<0.01 comparing Mock to MAV-1.

cardiomyocyte cross-sectional area in cardiac sections stained with wheat germ agglutinin. Mice that were infected as neonates displayed a significant increase in cardiomyocyte size, consistent with cellular hypertrophy (Figure 7-7C).

Discussion

HAdV are common causes of viral myocarditis (3, 4). They are implicated in the development of dilated cardiomyopathy (27) and cardiac dysfunction (28, 29). The present study is the first to examine the pathogenesis of adenovirus myocarditis in detail, using MAV-1 to study an adenovirus in its natural host. We demonstrated that i.n. MAV-1 infection of neonatal C57BL/6 mice caused myocardial inflammation and tissue damage. Maximal viral loads, induction of IFN-γ and recruitment of $CD3^+$ T cells correlated with markers of cardiomyocyte damage and cardiac dysfunction. Neutralization of IFN-γ during acute MAV-1 infection reduced cardiac inflammation without affecting viral replication. Long-term persistence of MAV-1 in hearts was associated with increased LV mass and cellular hypertrophy.

Although it is possible that virus present in residual blood in hearts harvested from mice contributed to measured viral loads in our study, increases in viral gene expression and logarithmic increases in viral loads between 4 and 7 dpi strongly suggest that MAV-1 replicates in hearts of mice after infection. Further, our *in vitro* data showing MAV-1 replication in primary cardiac myocytes suggest that cardiac myocytes are a likely cellular target of the virus *in vivo*, consistent with a previous report demonstrating the presence of MAV-1 in

cardiac myocytes using electron microscopy (20). In that study, virions appeared to be present in other cell types as well, including cardiac fibroblasts and endothelial cells. Cardiac fibroblasts may serve as another target of MAV-1 replication *in vivo*, and we are currently investigating this possibility. HAdV DNA is often detected at high levels in lymphocytes of human tonsillar and adenoid tissue (30), and MAV-1 has been reported to replicate in macrophages (31), raising the possibility that MAV-1 could also infect resident or recruited immune cells in the heart.

$CD3^+$ T cells and $F4/80^+$ macrophages were recruited to the hearts of neonatal mice after MAV-1 infection. This is consistent with observations that hearts of patients with HAdV myocarditis are infiltrated with T cells and macrophages (28, 32). The T cell infiltrates following MAV-1 infection were mainly $CD8^+$ T cells, although $CD4^+$ T cells were also present. Following i.p. MAV-1 infection of adult mice, either $CD4^+$ or $CD8^+$ T cells are required for viral clearance from brain, and perforin (Pfn) contributes to signs of acute encephalomyelitis (33). A previous study demonstrated a role for both $CD4^+$ and $CD8^+$ T cells in the development of CVB3 myocarditis (34), and Pfn is a major contributor to severe tissue damage during CVB3 myocarditis (35). T cells likely contribute to both tissue damage and control of viral replication in the heart during acute MAV-1 infection. Specific mechanisms regulating the effects of T cells in the heart during MAV-1 myocarditis have not yet been defined.

$CD8^+$ T cells may play both inflammatory and cytolytic roles during infection, either by secretion of cytokines, such as IFN-γ or TNF-α, or through

release of cytolytic granules such as Pfn (36). Both type I and type II IFN can play protective roles in other models of viral myocarditis (12, 14, 37). IFN-γ and Pfn play antagonistic roles during chronic myocarditis caused by *Trypanosoma cruzi*, with Pfn^+CD8^+ T cells implicated in causing tissue damage and IFN-γ $^+CD8^+$ T cells preventing tissue damage (36). In the current study, we identified robust induction of IFN-γ in the heart after MAV-1 infection, consistent with previous studies showing induction of IFN-γ in MAV-1-infected lungs (22, 38). During acute MAV-1 respiratory infection of adult mice, $CD4^+$ and $CD8^+$ T cells are the primary producers of IFN-γ in the lung (39). IFN-γ induced during MAV-1 myocarditis is likely produced by infiltrating $CD4^+$ and/or $CD8^+$ T cells, because the robust IFN-γ induction that we observe correlates closely with recruitment of these cells to the myocardium. Cells not evaluated in this study, such as natural killer cells, may also contribute to early IFN-γ production in the heart during MAV-1 myocarditis.

Although IFN-γ is induced in the lung during MAV-1 respiratory infection, it is not essential for control of MAV-1 replication in the lungs or for survival of adult mice following i.n. inoculation (22). Similarly, IFN-γ does not appear to be critical for control of MAV-1 replication in the hearts of neonatal mice, since IFN-γ depletion did not lead to increased viral replication in the heart. IFN-γ-depleted mice developed significantly less cardiac inflammation after MAV-1 infection, suggesting that IFN-γ plays a proinflammatory role in the heart as it does in some reports of CVB3 myocarditis (15, 16). At the same time, IFN-γ-depleted mice became moribund sooner than controls following infection. In addition, we

detected equivalent viral loads in neonates and adults despite substantially greater IFN-γ induction in neonates. MAV-1 can be detected in many different organs following both i.n. and i.p. inoculation (40). We speculate that IFN-γ has organ-specific effects on MAV-1 pathogenesis. IFN-γ depletion might lead to increased viral loads and/or increased immunopathology in other organs, in particular the lungs, due to the inoculation route used in this study, and brain, as central nervous system disease is a cause of mortality in susceptible mouse strains following i.p. inoculation (41, 42). Our findings indicate that IFN-γ exerts an important proinflammatory effect in the heart during MAV-1 myocarditis in neonatal mice, and that inflammation induced by IFN-γ signaling rather than direct antiviral effects of IFN-γ may be important for survival. Similarly, IFN-γ overexpression (13) or administration (43) ameliorates myocarditis in CVB3 and encephalomyocarditis virus models, respectively. However, this effect is likely due to the direct suppression of viral replication by IFN-γ or IFN-γ-mediated activation of natural killer cells (44).

Acute MAV-1 infection caused cardiac dysfunction in neonatal mice, similar to decreased cardiac function seen after infection with influenza A or CVB3 (23, 24). The significantly decreased cardiac function in MAV-1-infected mice that we observed at 10 dpi correlated with the greatest degree of virus-induced IFN-γ expression and also with peak levels of viral replication and cellular inflammation. It may be that cardiac dysfunction observed during MAV-1 myocarditis is due to direct cardiomyocyte damage caused by MAV-1 infection itself or by cytotoxic effects of virus-induced immune responses. However,

because viral replication in hearts of adult mice was not associated with substantial inflammation, evidence of cardiac myocyte damage, or echocardiographic changes, it seems likely that host responses to viral infection are the most important contributors to cardiac dysfunction following MAV-1 infection. For instance, IFN-γ itself contributes to contractile dysfunction in immune-mediated myocarditis (45). Given its pronounced upregulation during MAV-1 myocarditis, it seems possible that IFN-γ contributes to the physiological abnormalities that we detected in infected mice. Other cytokines induced in the heart by MAV-1 infection, including TNF-α, IL-1β, and IL-6, have also been reported to impair cardiac contractility (46-50) and may therefore also contribute to cardiac dysfunction during MAV-1 infection.

Our results suggest that MAV-1 replicates equally well in hearts of neonatal and adult mice, but only neonatal mice are susceptible to MAV-1-induced myocarditis. Immune responses to many different pathogens differ between neonates and adults. Neonates are generally thought to mount inefficient Th1 responses (51, 52), although there is evidence that neonatal T cells can mount protective $CD8^+$ T cell responses equivalent to that of adults (53). We have recently observed susceptibility differences between neonatal and adult BALB/c mice to MAV-1 respiratory infection that correlated with less exuberant IFN-γ responses in neonatal lungs (22). Our results in the present study using neonate and adult C57BL/6 mice, however, demonstrate that neonatal mice have an exaggerated IFN-γ response in heart tissue compared to adult mice after MAV-1 infection that correlates with infiltration of $CD3^+$ T cells

and cardiac myocyte damage. This suggests that the response to acute MAV-1 infection is both age- and organ-specific. Supporting this possibility, a previous study demonstrated that susceptibility of mice to group B coxsackieviruses differs by age of mice, organ, and virus type (54).

The exuberant immune response observed in the hearts of neonatal mice, but not adult mice, after MAV-1 infection could be due to organ- and age-specific differences in cytokine receptor expression levels or function of antigen presenting cells. Age-based differences in the activity of intracellular signaling pathways could also lead to the age-specific outcomes we observe during MAV-1 myocarditis. For instance, a previous study demonstrated high expression of components of the IL-1R/TLR signaling pathway in the neonatal period that is rapidly down-regulated by 12 months of age (55). Another study demonstrated hypersensitivity of neonatal mice to TLR stimulation compared to adult mice, which may increase susceptibility of neonates to infection (56). Interestingly, we detected a different pattern in overall levels of IL-1β and IL-6 mRNA late during infection, both of which were higher in adults than in neonates at 14 dpi (Figure 7-4). Contributions of these cytokines to the control of MAV-1 replication and to MAV-1-induced disease in the heart or in other organs have not yet been described. These cytokines may serve to limit viral replication in adult mice, minimizing deleterious virus-induced inflammation and subsequent cardiac dysfunction. Our data emphasize both the complicated interplay of various immune responses that is likely to occur during MAV-1 myocarditis as well as the changes in immune function that occur with age.

Persistent HAdV infections have been implicated in the development of dilated cardiomyopathy (DCM) and cardiac dysfunction (8, 28, 29, 57). A wide range of viral genomes (enterovirus, HAdV, parvovirus B19 or human herpesvirus 6) were detected in endomyocardial biopsies from patients with clinically suspected myocarditis or dilated cardiomyopathy (29). We demonstrated that MAV-1 DNA persisted to at least 9 weeks post infection in hearts of mice infected with MAV-1 as neonates, and MAV-1 persistence was associated with cardiac hypertrophy. It is unclear whether long-term persistent MAV-1 replication occurs in the heart and in which cells MAV-1 persists. Using RT-qPCR, we were unable to detect viral gene expression in hearts at 9 weeks post infection (data not shown), although it is possible that this technique is not sensitive enough to detect isolated replication in a very small number of cells. Long-term effects of MAV-1 infection on cardiac remodeling could be due to chronic inflammation induced by persistence of virus in the absence of active replication. Long-term effects of infection on cardiac function can be caused by an autoimmune process, as occurs with autoreactive T cells that arise following CV3B infection (58). To our knowledge, no reports document this type of response during HAdV or MAV-1 infection, but we are in the process of characterizing virus-specific and autoreactive T cells in the context of MAV-1 myocarditis.

In summary, our findings demonstrate that IFN-γ is a proinflammatory mediator during adenovirus-induced myocarditis, and they suggest that persistent adenovirus infection may contribute to ongoing cardiac dysfunction

and cardiac remodeling. The MAV-1 model will enable fundamental studies of adenovirus myocarditis and facilitate investigation of therapeutic strategies such as modulation of IFN-γ and other host responses.

Materials and Methods

Cardiac myocyte primary culture and infection

Cardiac myocytes were isolated as previously described (59), plated on laminin-coated coverslips, cultured in presence of the contraction inhibitor 25 μM S-(-)-blebbistatin (Toronto Research Chemicals), and infected at a multiplicity of infection (MOI) of 5. At 24 or 48 hr, supernatant was collected and the cells were incubated in 0.5 mL of TRIzol® (Invitrogen) for 5 min. RNA and DNA were isolated according to the manufacturer's protocol and resuspended in HPLC-grade water. Infectious virus in supernatant was quantified by plaque assay as previously described (60).

Mice

All work was approved by the University of Michigan Committee on Use and Care of Animals. C57BL/6 mothers with litters of neonatal mice and male C57BL/6 mice (4-6 weeks of age) were obtained from The Jackson Laboratory. All mice were maintained under specific pathogen-free conditions.

Virus and infections

MAV-1 was grown and titered on NIH 3T6 fibroblasts as previously described (60). Neonates (7 days old) were manually restrained and infected intranasally (i.n.) with 10^5 plaque-forming units (pfu) in 10 μl of sterile phosphate-buffered saline (PBS). Adult mice were anesthetized with ketamine and xylazine and infected i.n. with 10^5 pfu of MAV-1 in 40 μl of sterile PBS. Control mice were mock infected i.n. with conditioned media at an equivalent dilution in sterile PBS. Mice were euthanized by pentobarbital overdose at the indicated time points. Blood was collected from the posterior vena cava of euthanized animals and incubated on ice for 15-30 min. Samples were centrifuged in a tabletop microcentrifuge at 17,000 x g for 10 min at 4°C. Serum was transferred to a new microcentrifuge tube and stored at -80°C until assayed. After blood collection, hearts were harvested, snap frozen in dry ice, and stored at -80°C until processed further. One third to one half of each heart (~20 mg) was homogenized in 1 mL of TRIzol® (Invitrogen) using sterile glass beads in a mini Beadbeater (Biospec Products) for 30 seconds. RNA and DNA were isolated from the homogenates according to the manufacturer's protocol.

Analysis of Viral Loads by PCR

MAV-1 viral loads were measured in organs and in cardiac myocytes infected *ex vivo* using quantitative real-time polymerase chain reaction (qPCR) as previously described (39). Primers and probe used to detect a 59-bp region of the MAV-1 E1A gene are listed in Table 7-1. Five μl of extracted DNA were

added to reactions containing TaqMan II Universal PCR Mix with UNG (Applied Biosystems), forward and reverse primers (each at 200 nM final concentration), and probe (20 nM final concentration) in a 25 µl reaction volume. Analysis on an ABI Prism 7300 machine (Applied Biosystems) consisted of 40 cycles of 15 s at 90°C and 60 s at 60°C. Standard curves generated using known amounts of plasmid containing the MAV-1 EIA gene were used to convert threshold cycle values for experimental samples to copy numbers of EIA DNA. Results were standardized to the nanogram (ng) amount of input DNA. Each sample was assayed in triplicate.

Nested PCR Detection of Viral DNA

Primers used in nested PCR to detect a final 246-bp region of MAV-1 E1A are listed in Table 7-2. Five hundred ng of extracted DNA were added to reactions containing 10X Standard Taq Buffer (New England BiosystemsBioLabs), 4 mM $MgCl_2$, 0.8 mM deoxynucleoside triphosphate (Promega), Taq polymerase (New England BioLabs), and 100 nM forward and reverse primers in a 100 µl reaction volume. The first PCR amplification was carried out with 1 cycle at 94°C for 10 min, 35 cycles of 94°C for 30 s, 55°C for 30 s, and 72°C for 30 s, followed by 1 cycle at 72°C for 7 min on an Eppendorf thermocycler. After the initial round of PCR, 20 µl of primary PCR product was added to fresh PCR mixture and amplified in a second round of PCR. The second PCR round was conducted under the same conditions with the exception of 200 nM primer concentrations instead of 100 nM, and 30 cycles instead of 35.

Real-time PCR Analysis of Gene Expression

Cytokine gene expression was quantified using reverse transcriptase (RT)-qPCR as previously described (22, 38). First, 2.5 μg of RNA were reverse transcribed using MMLV reverse transcriptase (Invitrogen) in 20 μl reactions according to the manufacturer's instructions. Water was added to the cDNA product to bring the total volume to 50 μl. cDNA was amplified using duplexed gene expression assays for mouse CCL5 and GAPDH (Applied Biosystems). Five μl of cDNA were added to reactions containing TaqMan Universal PCR Mix and 1.25 μl each of 20X gene expression assays for the target cytokine and GAPDH. Primers used to detect IFN-γ, tumor necrosis factor alpha (TNF-α), GAPDH, early region 1A (E1A), and hexon are listed in Table 7-1. For these measurements, 5 μl of cDNA were added to reactions containing Power SYBR Green PCR Mix (Applied Biosystems) and forward and reverse primers (each at 200 nM final concentration) in a 25 μl reaction volume. In all cases, RT-qPCR analysis consisted of 40 cycles of 15 s at 90°C and 60 s at 60°C. Quantification of target gene mRNA was normalized to GAPDH and expressed in arbitrary units as $2^{-\Delta Ct}$, where Ct is the threshold cycle and ΔCt = Ct(target) – Ct(GAPDH).

IFN-γ Neutralization

Rabbit anti-mouse IFN-γ (α-IFN-γ) polyclonal antibody (61) and nonimmune rabbit serum were generously provided by Dr. Steven Kunkel (University of Michigan) and purified using protein A column purification (Thermo

Scientific). Beginning on the first day post infection, mice were treated with 50 µg of α-IFN-γ antibody or nonimmune rabbit IgG given i.p. every other day beginning at 1 dpi. Neutralizing activity of α-IFN-γ was confirmed by its capacity to block IFN-γ-mediated repression of MAV-1 replication *in vitro* (data not shown).

Measurement of IFN-γ Protein

In some experiments, heart tissue (approximately half of a neonatal heart) was homogenized in PBS containing protease inhibitor (complete, Mini, EDTA-free tablets; Roche Applied Science) and 1% Triton X-100 (Fisher Scientific) at a concentration of 50 mg lung tissue per 1 mL homogenization buffer. Tissue was homogenized using sterile glass beads in a mini Beadbeater (Biospec Products) for 2 x 30 s cycles, resting on ice between cycles. After homogenization, tissue was spun twice at 17,000 x g for 15 min at 4°C and supernatant was stored at -80°C until assayed. IFN-γ protein concentrations in heart homogenates were determined by ELISA (Duoset Kits, R&D Systems) according to the manufacturer's protocol.

Histology

Hearts were fixed in 10% formalin and embedded in paraffin. Five µm sections were stained with hematoxylin and eosin to evaluate cellular infiltrates. Separate sections were stained with anti-CD3 antibody (Thermo Scientific). $CD3^+$ cells were quantified at 40X magnification, using the average of at least three independent fields per sample. Results are expressed as the number of $CD3^+$

cells per high power field (HPF). In some experiments, hearts were removed and immediately frozen in Tissue-Tek OCT Compound (Sakura Finetek), and 5 μm sections were strained with antibodies to CD4 and CD8 (Serotec and BD Pharmingen, respectively). Sectioning and immunohistochemical staining were performed by the University of Michigan Unit for Laboratory Animal Medicine Pathology Cores for Animal Research. Heart sections were viewed through a Laborlux 12 microscope (Leitz). Digital images were obtained with an EC3 digital imaging system (Leica Microsystems) using Leica Acquisition Suite software (Leica Microsystems). Images were assembled using Adobe Illustrator (Adobe Systems). To quantify cellular inflammation in the hearts, slides were examined in a blinded fashion to determine a pathology index score for the size/intensity of cellular infiltrate and the extent of involvement in the heart (Table 7-3).

To visualize cardiomyocyte cell membranes, paraffin-free left ventricular heart sections were incubated with 100 μg/ml FITC-conjugated wheat germ agglutinin (Sigma) in PBS for 2 hours and then washed 3 times with PBS. Slides were mounted using Prolong Gold Antifade reagent with DAPI (4,6-diamidine-2-phenylindole; Invitrogen). Fluorescent images were viewed through an Olympus BX41 microscope and digital images were processed using Olympus DP Manager software. Cross-sectional areas were calculated from fluorescent images using NIH ImageJ software (62).

Determination of Serum Cardiac Troponin Levels

Cardiac troponin I (cTnI) concentrations were measured using the Ultra Sensitive Mouse Cardiac Troponin-I ELISA Kit (Life Diagnostics) according to the manufacturer's instructions. Samples were assayed in duplicate.

Echocardiography

In vivo echocardiography was performed as previously described (63), consistent with guidelines of the American Society of Echocardiography. Mice were anesthetized by inhaled isoflurane, chest hair was removed with Nair^{TM} (Church & Dwight), and imaging was performed using Vevo770 Ultrasound system (Visual Sonics Inc). Transducers used were an RMV707B (15-45Mhz) for adult mice or an RMV706 (20-60Mhz) for neonatal mice. Imaging and analysis were performed by a single blinded sonographer. Left ventricular (LV) mass was calculated by measuring the LV internal diameter (LVID), the LV posterior wall thickness (LVPW), and interventricular septal thickness (IVS) in diastole (d), using the following formula: LV mass=1.053*[(LVIDd+LVPWd+IVSd)^3-LVIDd^3. LV end systolic and end diastolic dimensions (LVs and LVd), as well as systolic and diastolic wall thickness were measured from M-mode tracings to calculate fractional shortening and ejection fraction assuming a spherical LV geometry [(LVd^3-LVs^3)/LV d^{3}x100)],

Statistics

Analysis for statistical significance was conducted using Prism 6 for Macintosh (GraphPad Software, Incorporated). Differences between more than two groups at a single time point were analyzed using one-way analysis of variance (ANOVA). Differences between groups at multiple time points were analyzed using two-way analysis of variance (ANOVA) followed by Bonferroni's multiple comparison tests. For viral load data, differences between groups at a given time point in log-transformed viral loads were analyzed using the Mann-Whitney test. Survival analysis was performed using the log-rank (Mantel-Cox) test. *P* values less than 0.05 were considered statistically significant.

Table 7-1. **Primers and probes used for real-time PCR analysis**

Target	Oligonucleotide	Sequence (5′ to 3′)
MAV-1 E1A genomic	Forward primer	GCACTCCATGGCAGGATTCT
	Reverse primer	GGTCGAAGCAGACGGTTCTTC
	Probe	TACTGCCACTTCTGC
GAPDH	Forward primer	TGCACCACCAACTGCTTAG
	Reverse primer	GGATGCAGGGATGATGTTC
IFN-γ	Forward primer	AAAGAGATAATCTGGCTCTGC
	Reverse primer	GCTCTGAGACAATGAACGCT
TNF-α	Forward primer	CCACCACGCTCTTCTGTCTAC
	Reverse primer	AGGGTCTGGGCCATAGAACT
MAV-1 E1A	Forward primer	AATGGGTTTTGCAGTCTGTGTTAC
	Reverse primer	CGCCTGAGGCAGCAGATC
MAV-1 Hexon	Forward primer	GGCCAACACTACCGACACTT
	Reverse primer	TTTTGTCCTGTGGCATTTGA

Table 7-2. **Primers and probes used for nested PCR analysis**

Target	Oligonucleotide	Sequence (5′ to 3′)
MAV-1 E1A Round 1	Forward primer	ATGTCGCGGCTCCTACG
	Reverse primer	CAACGAACCATAAAAAGACATCAT
MAV-1 E1A Round 2	Forward primer	ATGGGATGGTTCGCCTACTT
	Reverse primer	CACCGCAGATCCATGTCCTCAA
Actin	Forward primer	CCTAAGGCCAACCGTGAAAAGATG
	Reverse primer	ACCGCTCGTTGCCAATAGTGATG

Table 7-3. Quantification of cellular inflammation in histologic specimens.

Severity Score*	Description	Extent Score	Description
0	no inflammatory infiltrates		
1	inflammatory cells present without discrete foci	1	mild (<25% of section involved)
2	larger foci of 10 to 100 inflammatory cells	2	moderate (~25-75% of section involved)
3	larger foci of >100 inflammatory cells	3	Severe (>75% of section involved)

*A score from 0 to 3 was given for the size/intensity of cellular infiltrates. The score was then multiplied by a number reflecting the extent of involvement in the specimen to reach a single final severity score, resulting in a total score that could range from 0 to 9.

References

1. **Grist NR, Reid D.** 1988. General pathogenicity and epidemiology, p. 241-252. *In* Bendinelli M, Friedman H (ed.), Coxsackieviruses: a General Update. Plenum, New York, NY.
2. **Amabile N, Fraisse A, Bouvenot J, Chetaille P, Ovaert C.** 2006. Outcome of acute fulminant myocarditis in children. Heart **92:**1269-1273.
3. **Bowles NE, Ni J, Kearney DL, Pauschinger M, Schultheiss H-P, McCarthy R, Hare J, Bricker JT, Bowles KR, Towbin JA.** 2003. Detection of viruses in myocardial tissues by polymerase chain reaction. evidence of adenovirus as a common cause of myocarditis in children and adults. J Am Coll Cardiol **42:**466-472.
4. **Martin AB, Webber S, Fricker FJ, Jaffe R, Demmler G, Kearney D, Zhang YH, Bodurtha J, Gelb B, Ni J.** 1994. Acute myocarditis. Rapid diagnosis by PCR in children. Circulation **90:**330-339.
5. **Feldman AM, McNamara D.** 2000. Myocarditis. N Engl J Med **343:**1388-1398.
6. **Kuhl U, Pauschinger M, Seeberg B, Lassner D, Noutsias M, Poller W, Schultheiss HP.** 2005. Viral persistence in the myocardium is associated with progressive cardiac dysfunction. Circulation **112:**1965-1970.
7. **Tatrai E, Hartyanszky I, Jr., Laszik A, Acsady G, Sotonyi P, Hubay M.** 2011. The role of viral infections in the development of dilated cardiomyopathy. Pathol Oncol Res **17:**229-235.
8. **Pauschinger M, Bowles NE, Fuentes-Garcia FJ, Pham V, Kühl U, Schwimmbeck PL, Schultheiss HP, Towbin JA.** 1999. Detection of adenoviral genome in the myocardium of adult patients with idiopathic left ventricular dysfunction. Circulation **99:**1348-1354.
9. **Shirali GS, Ni J, Chinnock RE, Johnston JK, Rosenthal GL, Bowles NE, Towbin JA.** 2001. Association of viral genome with graft loss in children after cardiac transplantation. N Engl J Med **344:**1498-1503.
10. **Dennert R, Crijns HJ, Heymans S.** 2008. Acute viral myocarditis. Eur Heart J **29:**2073-2082.
11. **Rose NR, Hill SL.** 1996. The pathogenesis of postinfectious myocarditis. Clin Immunol Immunopathol **80:**S92-99.
12. **Sherry B, Torres J, Blum MA.** 1998. Reovirus induction of and sensitivity to beta interferon in cardiac myocyte cultures correlate with induction of myocarditis and are determined by viral core proteins. J Virol **72:**1314-1323.
13. **Henke A, Jarasch N, Martin U, Zell R, Wutzler P.** 2008. Characterization of the protective capability of a recombinant coxsackievirus B3 variant expressing interferon-gamma. Viral Immunology **21:**38-48.
14. **Irvin SC, Zurney J, Ooms LS, Chappell JD, Dermody TS, Sherry B.** 2011. A Single Amino Acid Polymorphism in Reovirus Protein μ2 Determines Repression of Interferon Signaling and Modulates Myocarditis. J Virol.

15. **Frisancho-Kiss S, Nyland JF, Davis SE, Frisancho JA, Barrett MA, Rose NR, Fairweather D.** 2006. Sex differences in coxsackievirus B3-induced myocarditis: IL-12Rbeta1 signaling and IFN-gamma increase inflammation in males independent from STAT4. Brain research **1126:**139-147.
16. **Huber SA, Graveline D, Born WK, O'Brien RL.** 2001. Cytokine production by Vgamma(+)-T-cell subsets is an important factor determining CD4(+)-Th-cell phenotype and susceptibility of BALB/c mice to coxsackievirus B3-induced myocarditis. Journal of virology **75:**5860-5869.
17. **Torzewski M, Wenzel P, Kleinert H, Becker C, El-Masri J, Wiese E, Brandt M, Pautz A, Twardowski L, Schmitt E, Münzel T, Reifenberg K.** 2012. Chronic inflammatory cardiomyopathy of interferon γ-overexpressing transgenic mice is mediated by tumor necrosis factor-α. Am J Pathol **180:**73-81.
18. **DeBiasi RL, Robinson BA, Sherry B, Bouchard R, Brown RD, Rizeq M, Long C, Tyler KL.** 2004. Caspase inhibition protects against reovirus-induced myocardial injury in vitro and in vivo. J Virol **78:**11040-11050.
19. **Weinberg JB, Stempfle GS, Wilkinson JE, Younger JG, Spindler KR.** 2005. Acute respiratory infection with mouse adenovirus type 1. Virology **340:**245-254.
20. **Blailock ZR, Rabin ER, Melnick JL.** 1968. Adenovirus myocarditis in mice. An electron microscopic study. Exp Mol Pathol **9:**84-96.
21. **Klempa B, Kruger DH, Auste B, Stanko M, Krawczyk A, Nickel KF, Uberla K, Stang A.** 2009. A novel cardiotropic murine adenovirus representing a distinct species of mastadenoviruses. J Virol **83:**5749-5759.
22. **Procario MC, Levine RE, McCarthy MK, Kim E, Zhu L, Chang C-H, Hershenson MB, Weinberg JB.** 2012. Susceptibility to acute mouse adenovirus type 1 respiratory infection and establishment of protective immunity in neonatal mice. J Virol **86:**4194-4203.
23. **Pan H-Y, Yamada H, Chida J, Wang S, Yano M, Yao M, Zhu J, Kido H.** 2011. Up-regulation of ectopic trypsins in the myocardium by influenza A virus infection triggers acute myocarditis. Cardiovascular Research **89:**595-603.
24. **Cheung C, Marchant D, Walker EK-Y, Luo Z, Zhang J, Yanagawa B, Rahmani M, Cox J, Overall C, Senior RM, Luo H, McManus BM.** 2008. Ablation of matrix metalloproteinase-9 increases severity of viral myocarditis in mice. Circulation **117:**1574-1582.
25. **Horwitz MS.** 2001. Adenovirus immunoregulatory genes and their cellular targets. Virology **279:**1-8.
26. **Smith K, Brown CC, Spindler KR.** 1998. The role of mouse adenovirus type 1 early region 1A in acute and persistent infections in mice. J Virol **72:**5699-5706.

27. **Tátrai E, Hartyánszky I, Lászik A, Acsády G, Sótonyi P, Hubay M.** 2011. The role of viral infections in the development of dilated cardiomyopathy. Pathol Oncol Res **17:**229-235.
28. **Kühl U, Pauschinger M, Noutsias M, Seeberg B, Bock T, Lassner D, Poller W, Kandolf R, Schultheiss H-P.** 2005. High prevalence of viral genomes and multiple viral infections in the myocardium of adults with "idiopathic" left ventricular dysfunction. Circulation **111:**887-893.
29. **Kühl U, Pauschinger M, Seeberg B, Lassner D, Noutsias M, Poller W, Schultheiss H-P.** 2005. Viral persistence in the myocardium is associated with progressive cardiac dysfunction. Circulation **112:**1965-1970.
30. **Garnett CT, Erdman D, Xu W, Gooding LR.** 2002. Prevalence and quantitation of species C adenovirus DNA in human mucosal lymphocytes. J Virol **76:**10608-10616.
31. **Ashley SL, Welton AR, Harwood KM, Rooijen NV, Spindler KR.** 2009. Mouse adenovirus type 1 infection of macrophages. Virology **390:**307-314.
32. **Treacy A, Carr MJ, Dunford L, Palacios G, Cannon GA, O'Grady A, Moran J, Hassan J, Loy A, Connell J, Devaney D, Kelehan P, Hall WW.** 2010. First report of sudden death due to myocarditis caused by adenovirus serotype 3. J Clin Microbiol **48:**642-645.
33. **Moore ML, Brown CC, Spindler KR.** 2003. T cells cause acute immunopathology and are required for long-term survival in mouse adenovirus type 1-induced encephalomyelitis. J Virol **77:**10060-10070.
34. **Henke A, Huber S, Stelzner A, Whitton JL.** 1995. The role of CD8+ T lymphocytes in coxsackievirus B3-induced myocarditis. J Virol **69:**6720-6728.
35. **Gebhard JR, Perry CM, Harkins S, Lane T, Mena I, Asensio VC, Campbell IL, Whitton JL.** 1998. Coxsackievirus B3-induced myocarditis: perforin exacerbates disease, but plays no detectable role in virus clearance. Am J Pathol **153:**417-428.
36. **Silverio JC, Pereira IR, Cipitelli MdC, Vinagre NF, Rodrigues MM, Gazzinelli RT, Lannes-Vieira J.** 2012. CD8(+) T-cells expressing interferon gamma or perforin play antagonistic roles in heart injury in experimental trypanosoma cruzi-elicited cardiomyopathy. PLoS Pathog **8:**e1002645.
37. **Henke A, Jarasch N, Martin U, Zell R, Wutzler P.** 2008. Characterization of the protective capability of a recombinant coxsackievirus B3 variant expressing interferon-gamma. Viral Immunol **21:**38-48.
38. **McCarthy MK, Levine RE, Procario MC, McDonnell PJ, Zhu L, Mancuso P, Crofford LJ, Aronoff DM, Weinberg JB.** 2013. Prostaglandin E2 Induction during Mouse Adenovirus Type 1 Respiratory Infection Regulates Inflammatory Mediator Generation but Does Not Affect Viral Pathogenesis. PLoS ONE **8:**e77628.
39. **McCarthy MK, Zhu L, Procario MC, Weinberg JB.** 2014. IL-17 contributes to neutrophil recruitment but not to control of viral replication

during acute mouse adenovirus type 1 respiratory infection. Virology **456-457:**259-267.
40. **Kajon AE, Brown CC, Spindler KR.** 1998. Distribution of mouse adenovirus type 1 in intraperitoneally and intranasally infected adult outbred mice. J. Virol. **72:**1219-1223.
41. **Guida JD, Fejer G, Pirofski LA, Brosnan CF, Horwitz MS.** 1995. Mouse adenovirus type 1 causes a fatal hemorrhagic encephalomyelitis in adult C57BL/6 but not BALB/c mice. J. Virol. **69:**7674-7681.
42. **Spindler KR, Fang L, Moore ML, Hirsch GN, Brown CC, Kajon A.** 2001. SJL/J mice are highly susceptible to infection by mouse adenovirus type 1. J. Virol. **75:**12039-12046.
43. **Yamamoto N, Shibamori M, Ogura M, Seko Y, Kikuchi M.** 1998. Effects of intranasal administration of recombinant murine interferon-gamma on murine acute myocarditis caused by encephalomyocarditis virus. Circulation **97:**1017-1023.
44. **Godeny EK, Gauntt CJ.** 1987. Murine natural killer cells limit coxsackievirus B3 replication. J Immunol **139:**913-918.
45. **Pérez Leirós C, Goren N, Sterin-Borda L, Borda ES.** 1997. Myocardial dysfunction in an experimental model of autoimmune myocarditis: role of IFN-gamma. Neuroimmunomodulation **4:**91-97.
46. **Janssen SP, Gayan-Ramirez G, Van den Bergh A, Herijgers P, Maes K, Verbeken E, Decramer M.** 2005. Interleukin-6 causes myocardial failure and skeletal muscle atrophy in rats. Circulation **111:**996-1005.
47. **Kapadia SR, Oral H, Lee J, Nakano M, Taffet GE, Mann DL.** 1997. Hemodynamic regulation of tumor necrosis factor-alpha gene and protein expression in adult feline myocardium. Circulation research **81:**187-195.
48. **Okusawa S, Gelfand JA, Ikejima T, Connolly RJ, Dinarello CA.** 1988. Interleukin 1 induces a shock-like state in rabbits. Synergism with tumor necrosis factor and the effect of cyclooxygenase inhibition. The Journal of clinical investigation **81:**1162-1172.
49. **Van Tassell BW, Seropian IM, Toldo S, Mezzaroma E, Abbate A.** 2013. Interleukin-1beta induces a reversible cardiomyopathy in the mouse. Inflammation research : official journal of the European Histamine Research Society ... [et al.] **62:**637-640.
50. **Yokoyama T, Vaca L, Rossen RD, Durante W, Hazarika P, Mann DL.** 1993. Cellular basis for the negative inotropic effects of tumor necrosis factor-alpha in the adult mammalian heart. The Journal of clinical investigation **92:**2303-2312.
51. **Adkins B, Bu Y, Guevara P.** 2002. Murine neonatal CD4+ lymph node cells are highly deficient in the development of antigen-specific Th1 function in adoptive adult hosts. J Immunol **169:**4998-5004.
52. **Adkins B, Leclerc C, Marshall-Clarke S.** 2004. Neonatal adaptive immunity comes of age. Nat Rev Immunol **4:**553-564.
53. **Zhang J, Silvestri N, Whitton JL, Hassett DE.** 2002. Neonates mount robust and protective adult-like CD8(+)-T-cell responses to DNA vaccines. J Virol **76:**11911-11919.

54. **Khatib R, Chason JL, Silberberg BK, Lerner AM.** 1980. Age-dependent pathogenicity of group B coxsackieviruses in Swiss-Webster mice: infectivity for myocardium and pancreas. J Infect Dis **141:**394-403.
55. **Martino D, Holt P, Prescott S.** 2012. A novel role for interleukin-1 receptor signaling in the developmental regulation of immune responses to endotoxin. Pediatr Allergy Immunol **23:**567-572.
56. **Zhao J, Kim KD, Yang X, Auh S, Fu Y-X, Tang H.** 2008. Hyper innate responses in neonates lead to increased morbidity and mortality after infection. Proc Natl Acad Sci USA **105:**7528-7533.
57. **Tátrai E, Hartyánszky I, Lászik A, Acsády G, Sótonyi P, Hubay M.** 2011. The role of viral infections in the development of dilated cardiomyopathy. Pathol. Oncol. Res. **17:**229-235.
58. **Gangaplara A, Massilamany C, Brown DM, Delhon G, Pattnaik AK, Chapman N, Rose N, Steffen D, Reddy J.** 2012. Coxsackievirus B3 infection leads to the generation of cardiac myosin heavy chain-α-reactive CD4 T cells in A/J mice. Clin Immunol **144:**237-249.
59. **Kabaeva Z, Zhao M, Michele DE.** 2008. Blebbistatin extends culture life of adult mouse cardiac myocytes and allows efficient and stable transgene expression. Am J Physiol Heart Circ Physiol **294:**H1667-1674.
60. **Cauthen A, Welton A, Spindler KR.** 2007. Construction of mouse adenovirus type 1 mutants. Methods Mol Med **130:**41-59.
61. **Chensue SW, Ruth JH, Warmington K, Lincoln P, Kunkel SL.** 1995. In vivo regulation of macrophage IL-12 production during type 1 and type 2 cytokine-mediated granuloma formation. J Immunol **155:**3546-3551.
62. **Schneider CA, Rasband WS, Eliceiri KW.** 2012. NIH Image to ImageJ: 25 years of image analysis. Nature Methods **9:**671-675.
63. **Zolov SN, Bridges D, Zhang Y, Lee W-W, Riehle E, Verma R, Lenk GM, Converso-Baran K, Weide T, Albin RL, Saltiel AR, Meisler MH, Russell MW, Weisman LS.** 2012. In vivo, Pikfyve generates PI(3,5)P2, which serves as both a signaling lipid and the major precursor for PI5P. Proc Natl Acad Sci USA **109:**17472-17477.

Chapter 8:
Role of the immunoproteasome during MAV-1 myocarditis

Abstract

Adenoviruses (AdVs) are significant causes of pediatric myocarditis. Little is known about the pathogenesis of AdV myocarditis, which is a significant barrier to developing prevention or treatment strategies. The immunoproteasome is a complex induced by interferon-gamma (IFN-γ) that plays an important role during viral infection through regulation of CD8 T cell responses, activation of the NF-κB pathway, and management of oxidative stress. We used mouse adenovirus type 1 (MAV-1) to test the hypothesis that immunoproteasome activation contributes to AdV-induced myocarditis. Transcript and protein levels of the immunoproteasome subunit β5i and the immunoproteasome regulator PA28 were upregulated in infected hearts coincident with peak viral replication and IFN-γ expression. We detected an increase in β5i active subunits and a decrease in standard proteasome β5 active subunits, with an overall increase in the β5i:β5 ratio at 11 dpi. Treatment of mice with the nonspecific proteasome inhibitor bortezomib reduced proinflammatory cytokine production in infected hearts without significantly affecting mortality. However, treatment of mice with the immunoproteasome-specific inhibitor ONX 0914 did not have a substantial effect on proinflammatory cytokine induction or pathology. IFN-$\gamma^{-/-}$ mice showed less immunoproteasome induction and increased mortality after MAV-1 infection.

Brain tissue of infected IFN-$\gamma^{-/-}$ and ONX 0914-treated mice showed extensive inflammation and hemorrhage, suggesting that the immunoproteasome may play a protective role in other organs during MAV-1 infection. Inhibition of proteasome activity may provide a novel approach to decrease cardiac damage induced by AdV or other pathogens, and the role of the immunoproteasome and other inflammatory mediators may be organ-specific.

Introduction

Proteasomes play a primary role in the generation of antigenic peptides for presentation on MHC class I molecules (1-3). The 20S proteasome core is a barrel-shaped complex composed of four stacked heptameric rings: two outer alpha rings and two inner beta rings (4, 5). The catalytic activity is restricted to three of the beta subunits, β1, β2 and β5, that account for the caspase-like, trypsin-like, and chymotrypsin-like activities of the proteasome, respectively (6). Exposure of cells to IFN-γ results in the induction of three homologous β-type proteasome "immunosubunits": β1, β2i, and β5i, which form a specialized complex called the immunoproteasome (7-14).

The changes in proteasome subunit composition from standard to immunosubunits in response to IFN-γ stimulation alter the proteolytic activity of the complex. The immunoproteasome is thought to generate peptides better suited to binding to MHC class I molecules compared to the constitutive proteasome, and thus be more efficient than the constitutive proteasome at contributing to eliciting of immune responses (15, 16). Another protein complex

induced by IFN-γ is PA28, a large regulatory complex that binds the ends of the 20S proteasome core to further enhance the ability of the proteasome to degrade short peptide substrates (17, 18). The immunoproteasome plays a role in the generation of CD8 T cell epitopes from a variety of viruses, included mouse cytomegalovirus, hepatitis B virus, influenza virus, and lymphocytic choriomeningitis virus (LCMV) (19-24).

The constitutive proteasome plays a crucial role in activation of the NF-κB pathway through processing of the p105 precursor of the NF-κB p50 subunit or through the degradation of IκBα (25, 26). However, a role for the immunoproteasome in NF-κB pathway activation has been debated. Immunoproteasome inhibition or deficiency leads to decreased proinflammatory cytokine production by re-stimulated splenocytes (27, 28). Dendritic cells (DCs) from immunoproteasome-deficient mice show reduced innate cytokine production in response to influenza virus infection, possibly due to impaired NF-κB activation (29). The immunoproteasome may play a role in other host responses independent of MHC class I antigen processing or NF-κB activation. For example, accumulating evidence suggests that the immunoproteasome is critical for the removal of oxidized proteins and adaptation to oxidative stress (30-35).

Adenoviruses (AdVs) are important causes of myocarditis, and persistent AdV infections have been implicated in the development of dilated cardiomyopathy and cardiac dysfunction (36-41). We have previously demonstrated that intranasal infection of neonatal mice with mouse adenovirus type 1 (MAV-1) leads to viral replication and induction of IFN-γ expression in the

heart that correlates with recruitment of T cells, proinflammatory cytokine production, and acute myocyte necrosis (Chapter 7). We hypothesized that the immunoproteasome plays a proinflammatory role during MAV-1 myocarditis and is essential for coordinated inflammatory responses to MAV-1 infection in the heart. Nonspecific proteasome inhibition blunted proinflammatory cytokine production during MAV-1 myocarditis, but immunoproteasome inhibition did not. Mortality was increased in IFN-γ-deficient mice and mice treated with an immunoproteasome inhibitor after MAV-1 infection, possibly due to substantial inflammation and hemorrhage in the brains of these mice. Our results suggest that IFN-γ and the immunoproteasome plays organ-specific roles during MAV-1 infection.

Results

Immunoproteasome induction in hearts after MAV-1 infection.

To determine whether MAV-1 infection induces immunoproteasome activity in the heart, we infected neonatal mice i.n. with MAV-1 or mock infected with conditioned media and measured mRNA levels of β5i and PA28α at various times post infection. Both β5i and PA28α were significantly increased in hearts of infected mice compared to mock infected mice beginning at 7 dpi (Figure 8-1A, B). Levels remained elevated at 10 dpi and then decreased over time. Peak β5i and PA28α mRNA induction coincided with peak viral replication and induction of IFN-γ (Figure 7-3A).

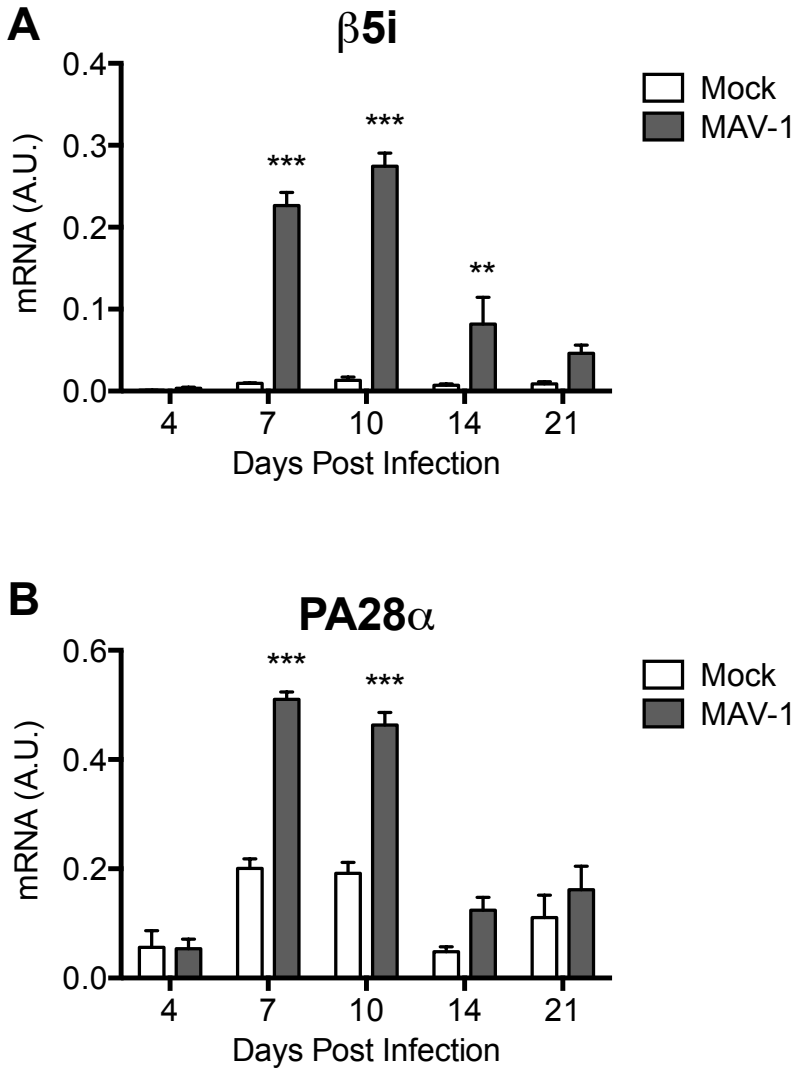

Figure 8-1. Immunoproteasome expression in the heart after MAV-1 infection.

Mice were infected i.n. with MAV-1 or mock infected with conditioned media. RT-qPCR was used to quantify A) β5i and B) PA28α expression, shown standardized to GAPDH in arbitrary units (A.U.). Combined data from 3 to 6 mice per group are presented as means ± S.E.M. ****P*<0.001, ***P*<0.01 comparing Mock to MAV-1 at a given timepoint.

To determine whether the significant increase in immunoproteasome subunit mRNA levels observed between 7 and 14 dpi resulted in an increase at the protein level, we measured β5, β5i, and PA28α/β levels in heart lysates at 11 dpi. We observed a significant increase in β5i protein and a corresponding decrease in β5 protein in heart lysates of infected mice compared to mock infected mice (Figure 8-2A and Table 8-1). Levels of the IFN-γ-induced immunoproteasome regulatory complex PA28α/β were also significantly greater in heart lysates from mice after MAV-1 infection (Figure 8-2A and Table 8-1).

We measured proteasome activity in hearts of infected and mock infected mice at 11 dpi using a proteasome constitutive immunoproteasome subunit (active site) ELISA (ProCISE) assay (42). Consistent with the western blot data, activity of β5 was significantly decreased in lysates of infected hearts compared to mock infected hearts, while activity of β5i was substantially increased (Figure 8-2B and Table 8-1). When β5i and β5 activities are expressed as a ratio of immunoproteasome/proteasome activity, the β5i:β5 activity ratio significantly increased from 0.36 ± 0.02 in mock-infected mice to 1.48 ± 0.08 in infected mice (Table 8-1), indicating that the immunoproteasome accounts for the majority of total proteasome activity in hearts at 11 dpi. These results demonstrate that immunoproteasome expression and activity are induced in the hearts of mice after MAV-1 infection.

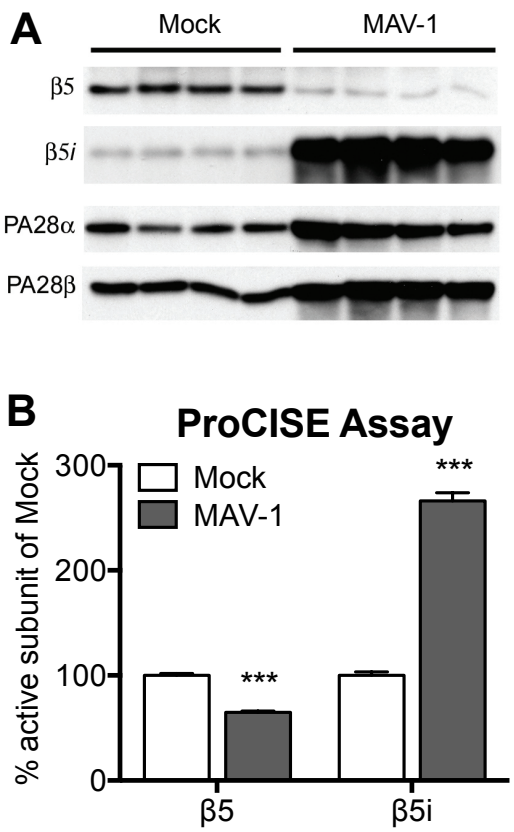

Figure 8-2. Immunoproteasome protein expression and activity in the heart after MAV-1 infection.

Mice were infected i.n. with MAV-1 and hearts were harvested at 11 dpi. A) Western blot was used to analyze expression of β5, β5i, PA28α, and PA28β in heart lysates. B) ProCISE assay was used to analyze β5 and β5i activity in heart lysates. Combined data from 4 mice per group are presented as means ± S.E.M. ****P*<0.001.

Protein Level	Subunit	Mock (% control ± SEM)	MAV-1 (% control ± SEM)	*P*
	β5	99.8 ± 3.1	17.0 ± 3.3	<0.001
	β5i	99.8 ± 12.3	1104.0 ± 101.6	<0.001
	PA28α	100.3 ± 11.6	212.8 ± 29.7	<0.001
	PA28β	100.0 ± 2.1	187.5 ± 17.0	<0.001

Active Subunits	Subunit	Mock (% control ± SEM)	MAV-1 (% control ± SEM)	*P*
	β5	100.0 ± 2.3	64.8 ± 1.7	<0.001
	β5i	100.0 ± 4.0	266.0 ± 15.9	<0.001

Activity (ratio)		Mock (active β5i:β5 ratio)	MAV-1 (active β5i:β5 ratio)	*P*
	β5i:β5 ratio	0.36 ± 0.02	1.48 ± 0.08	<0.001

Table 8-1. Quantification of immunoproteasome expression and activity in heart lysates.

Mice were infected i.n. with MAV-1 and heart tissue was harvested at 11 dpi. Western blot and ProCISE assays were used to quantify proteasome subunit expression and activity in heart lysates.

Effect of nonspecific proteasome inhibition on MAV-1 myocarditis.

To determine the effect of increased immunoproteasome activity on MAV-1 myocarditis, we used the reversible proteasome inhibitor bortezomib. Bortezomib nonspecifically inhibits both the β5 subunit of the constitutive proteasome and the β5i subunit of the immunoproteasome (43). Because immunoproteasome induction is not detected in infected hearts until after 4 dpi (Figure 8-1), and to avoid substantial inhibition of the constitutive proteasome before the immunoproteasome is induced, we treated mice with bortezomib every other day starting at 4 dpi. We harvested hearts at 10 dpi.

Bortezomib treatment did not affect survival of infected mice (data not shown). Heart viral loads were equivalent in vehicle- and bortezomib-treated mice (Figure 8-3A). MAV-1 infection results in upregulation of multiple proinflammatory cytokines and chemokines in the heart, including CCL5 and TNF-α (Figure 7-3). We used RT-qPCR to measure expression of these mediators in the heart following bortezomib treatment. CCL5 and TNF-α expression were significantly increased in hearts of vehicle-treated mice after infection compared to mock infected vehicle-treated mice (Figure 8-3B, C). However, induction of CCL5 and TNF-α was blunted in bortezomib-treated mice after infection. The size and extent of inflammatory foci present in the heart at 10 dpi were similar in vehicle- and bortezomib-treated mice (data not shown). This suggests that proteasome activity does not affect overall viral replication or pathology in the heart at 10 dpi, but it does contribute to induction of proinflammatory cytokines in the heart during MAV-1 infection.

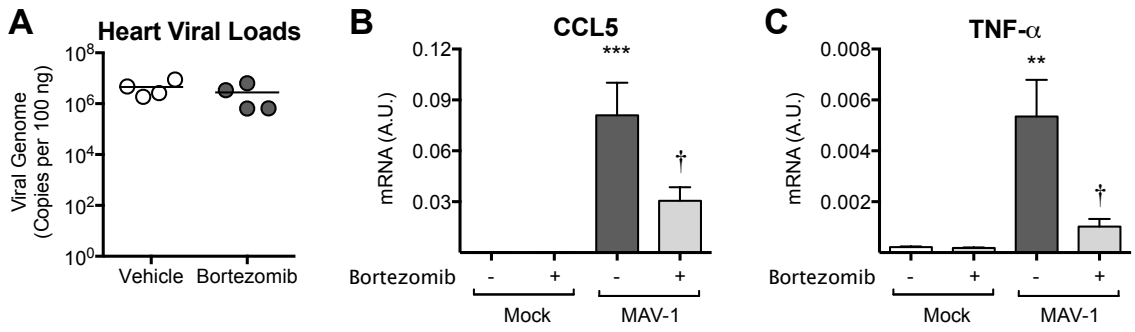

Figure 8-3. Effect of proteasome inhibition on MAV-1 myocarditis.

Mice were infected with MAV-1 or mock infected with conditioned media and treated every other day with vehicle or 0.5 mg/kg bortezomib starting at 4 dpi. Hearts were harvested at 10 dpi. A) qPCR was used to quantify MAV-1 genome copies in heart DNA. Viral loads are expressed as copies of MAV-1 genome per 100 ng of input DNA. Individual circles represent values for individual mice and horizontal bars represent means for each group. RT-qPCR was used to quantify B) CCL5 and C) TNF-α expression, shown standardized to GAPDH in arbitrary units (A.U.). Combined data from 5 mice per group are presented as means ± S.E.M. ***P<0.001, **P<0.01 comparing Mock to MAV-1 within a given condition. †P<0.05 comparing MAV-1-infected vehicle- to bortezomib-treated mice.

Effect of immunoproteasome inhibition on MAV-1 myocarditis.

Because bortezomib inhibits both the proteasome and the immunoproteasome, its effects on the induction of proinflammatory cytokines after MAV-1 infection could be due to inhibition of the standard proteasome. To determine the effect of immunoproteasome activity on MAV-1 myocarditis, we treated mice with the β5i-specific inhibitor ONX 0914 every other day starting at 1 dpi. ONX 0914 inhibits β5i with an IC_{50} value of approximately 10 nM (44). Due to increased mortality in the infected ONX 0914-treated group, we harvested heart tissue at 9 dpi. ONX 0914 treatment did not affect viral loads at 9 dpi (Figure 8-4A). CCL5 and TNF-α expression were significantly increased in vehicle-treated mice after infection compared to mock infected vehicle-treated mice (Figure 8-4B, C). CCL5 induction was blunted in mice treated with ONX 0914, but TNF-α expression was unaffected. ONX 0914 treatment did not affect the size and extent of inflammatory foci in hearts of MAV-1-infected mice (data not shown). These results suggest that immunoproteasome activity contributes less overall to virus-induced inflammation in the heart than does constitutive proteasome activity during MAV-1 infection.

Impaired immunoproteasome induction and increased mortality in IFN-γ-deficient mice after MAV-1 infection.

MAV-1 infection of neonatal mice induces IFN-γ expression in the heart (Figure 7-3A). IFN-γ depletion starting the day after infection blunted the induction of proinflammatory cytokines and reduced pathology in the heart. IFN-γ

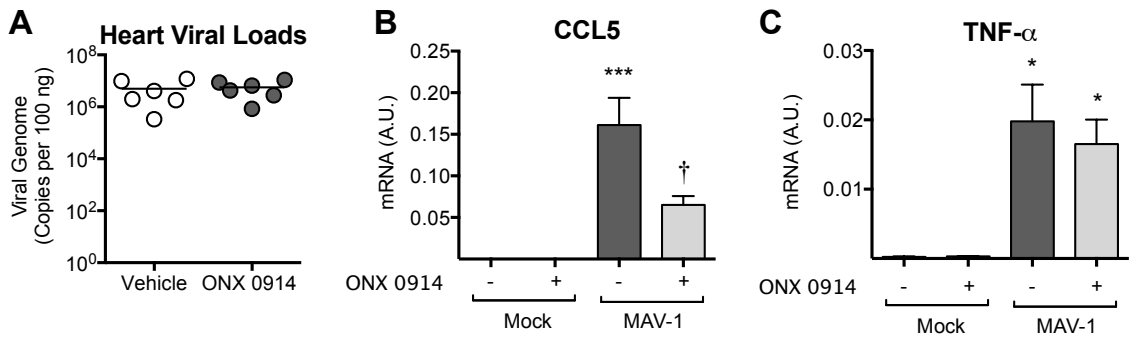

Figure 8-4. Effect of immunoproteasome inhibition on MAV-1 myocarditis.

Mice were infected with MAV-1 or mock infected with conditioned media and treated every other day with vehicle or 5 mg/kg ONX 0914 starting at 1 dpi. Hearts were harvested at 9 dpi. A) qPCR was used to quantify MAV-1 genome copies in heart DNA. Viral loads are expressed as copies of MAV-1 genome per 100 ng of input DNA. Individual circles represent values for individual mice and horizontal bars represent means for each group. RT-qPCR was used to quantify B) CCL5 and C) TNF-α expression, shown standardized to GAPDH in arbitrary units (A.U.). Combined data from 4 to 6 mice per group are presented as means ± S.E.M. ***P<0.001, *P<0.05 comparing Mock to MAV-1 within a given condition. †P<0.05 comparing MAV-1-infected vehicle- to ONX 0914-treated mice.

depletion also reduced β5i mRNA levels after infection, although not completely (data not shown). We hypothesized that the immunoproteasome would not be induced in MAV-1-infected hearts in the complete absence of IFN-γ. To assess the role of complete IFN-γ deficiency on MAV-1 myocarditis, we infected neonatal wild-type (IFN-$\gamma^{+/+}$) and IFN-γ-deficient (IFN-$\gamma^{-/-}$) mice with MAV-1. MAV-1 infection was almost uniformly lethal to IFN-$\gamma^{-/-}$ mice by 8 dpi, while approximately 50% of IFN-$\gamma^{+/+}$ mice survived (Figure 8-5A). Although heart viral loads were significantly higher in IFN-$\gamma^{-/-}$ mice compared to IFN-$\gamma^{+/+}$ mice at 7 dpi, the magnitude of this difference was small (Figure 8-5B). Therefore, the increased mortality of IFN-$\gamma^{-/-}$ mice is unlikely to be due solely to increased viral replication in the heart. Expression of β5i was significantly reduced in infected IFN-$\gamma^{-/-}$ mice compared to infected IFN-$\gamma^{+/+}$ mice at 7 dpi (Figure 8-5C) and was not different from baseline β5i expression previously observed in mock infected mice (Figure 8-1A), indicating that IFN-γ is responsible for induction of the immunoproteasome in hearts after MAV-1 infection.

To determine the effect of IFN-γ deficiency on other MAV-1-induced inflammatory responses, we used RT-qPCR to measure expression of CCL5 and TNF-α in the heart. We have previously observed that CCL5 and TNF-α expression peak in hearts of infected mice at 10 dpi, and induction is low at earlier time points (Figure 7-3). Consistent with this, overall CCL5 and TNF-α mRNA levels were low in infected IFN-$\gamma^{+/+}$ mice at 7 dpi compared to levels of expression observed at 10 dpi (Figure 7-3). CCL5 expression was not

significantly different between infected IFN-$\gamma^{+/+}$ and IFN-$\gamma^{-/-}$ mice at 7 dpi (data not shown). Expression of TNF-α was slightly reduced in IFN-$\gamma^{-/-}$ mice compared to IFN-$\gamma^{+/+}$ mice (Figure 8-5D). We observed minimal inflammation in hearts of IFN-$\gamma^{+/+}$ mice, and there was significantly less inflammation in hearts of infected IFN-$\gamma^{-/-}$ mice at 7 dpi, although the magnitude of the difference was small (Figure 8-5E). MAV-1 infection causes cardiac dysfunction in neonatal mice at 10 dpi, but not at 5 dpi (Figure 7-5). Consistent with low levels of proinflammatory cytokines and pathology present in infected hearts at 7 dpi, left ventricle ejection fraction was normal in IFN-$\gamma^{+/+}$ mice at this time (Figure 8-5F) and did not differ from values we previously observed in mock-infected mice (Figure 7-5). We observed no difference in left ventricle ejection fraction between infected IFN-$\gamma^{+/+}$ mice and IFN-$\gamma^{-/-}$ mice (Figure 8-5F), suggesting that increased mortality in IFN-$\gamma^{-/-}$ mice is not due to changes in overall cardiac function. Thus, while IFN-γ is responsible for immunoproteasome induction in heart tissue after MAV-1 infection, it does not have a substantial effect on viral replication or the early inflammatory response in the heart at 7 dpi. However, IFN-γ is critical for survival of neonatal mice after MAV-1 infection.

Unexpected role for IFN-γ-induced immunoproteasome activity in the brain.

Previous data indicate that substantial inflammatory and necrotic lesions do not develop in heart tissue until 9 or 10 dpi (Figure 7-2 and data not

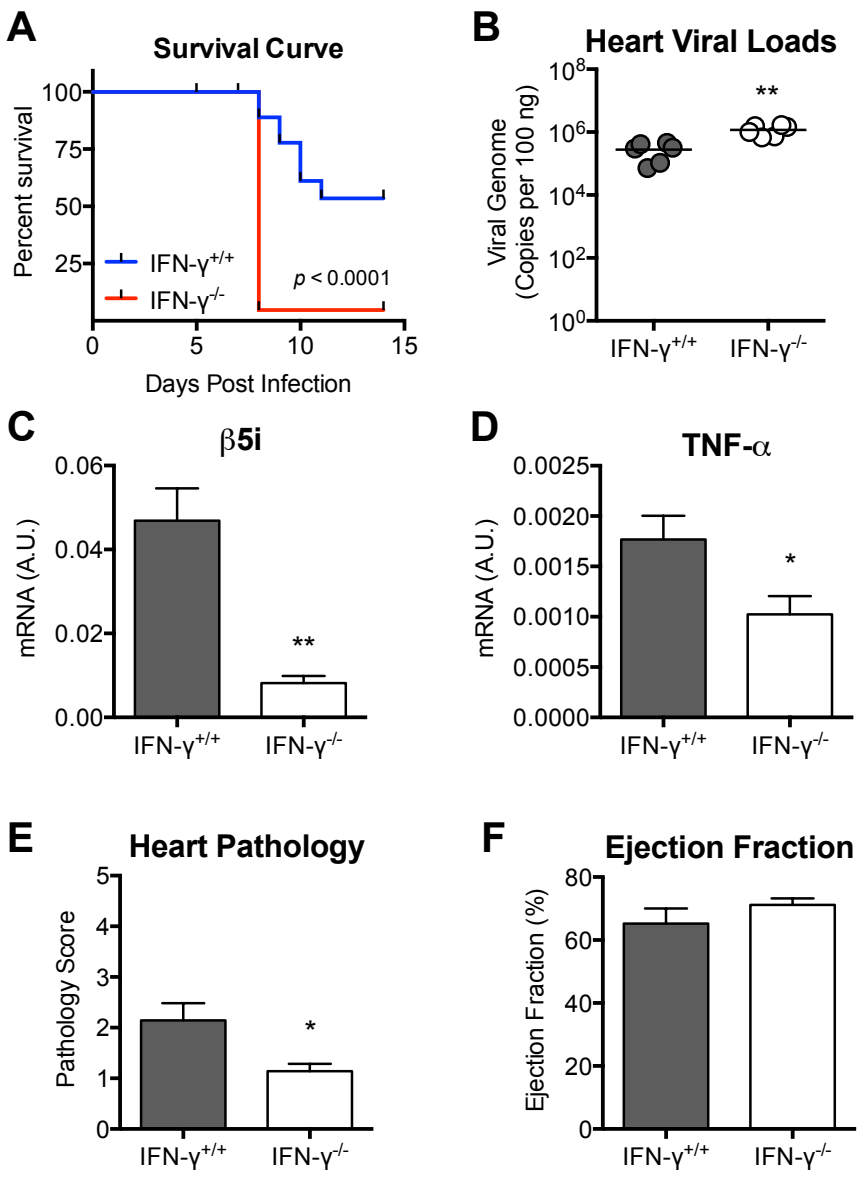

Figure 8-5. Effect of IFN-γ deficiency on MAV-1 infection.

IFN-$\gamma^{+/+}$ and IFN-$\gamma^{-/-}$ mice were infected i.n. with MAV-1 and A) monitored for survival. B) Hearts were harvested at 7 dpi and qPCR was used to quantify MAV-1 genome copies in heart DNA. DNA viral loads are expressed as copies of MAV-1 genome per 100 ng of input DNA. Individual circles represent values for individual mice and horizontal bars represent means for each group. RT-qPCR was used to quantify C) β5i and D) TNF-α expression, shown and standardized to GAPDH in arbitrary units (A.U.). E) Pathology index scores were generated to quantify cellular inflammation. F) Echocardiography was performed to measure ejection fraction. Combined data from 5 to 7 mice per group are presented as means ± S.E.M. $^{**}P<0.01$, $^{*}P<0.05$.

shown). We observed increased mortality in both ONX 0914-treated and IFN-$\gamma^{-/-}$ mice after MAV-1 infection. ONX 0914-treated mice showed only mild differences in virus-induced inflammatory responses in the heart. The increased mortality in MAV-1-infected IFN-$\gamma^{-/-}$ mice occurs prior to the development of significant cardiac inflammation and is not accompanied by defects in cardiac function. We hypothesized that the early mortality of ONX 0914-treated and IFN-$\gamma^{-/-}$ mice was independent of effects on inflammation in the heart and was due to a requirement for IFN-γ in another organ.

We examined H&E-stained sections of various organs from IFN-$\gamma^{+/+}$ and IFN-$\gamma^{-/-}$ mice at 8 dpi, when all IFN-$\gamma^{-/-}$ mice are moribund. Inflammation in the lungs and liver did not differ between the two strains of mice (data not shown). At 8 dpi, we observed scattered small foci of inflammatory cells surrounding blood vessels in the brains of IFN-$\gamma^{+/+}$ mice, largely localized to the midbrain region (Figure 8-6, black arrow). However, in the brains of IFN-$\gamma^{-/-}$ mice at 8 dpi, inflammatory foci were more abundant throughout the tissue compared to IFN-$\gamma^{+/+}$ mice. We also observed substantial areas of hemorrhage in brains of IFN-$\gamma^{-/-}$ mice (Figure 8-6). There was some degeneration of the cerebellar Purkinje layer in infected of IFN-$\gamma^{+/+}$ mice. However, there was extensive Purkinje layer damage and some hemorrhage present in the cerebella of IFN-$\gamma^{-/-}$ mice (Figure 8-6, white arrow). This suggests that IFN-$\gamma^{-/-}$ mice may be dying rapidly due to extensive inflammation and hemorrhage in the brain after MAV-1 infection. Whether this is due to uncontrolled viral replication or another effect of IFN-γ on virus-induced host responses remains to be determined.

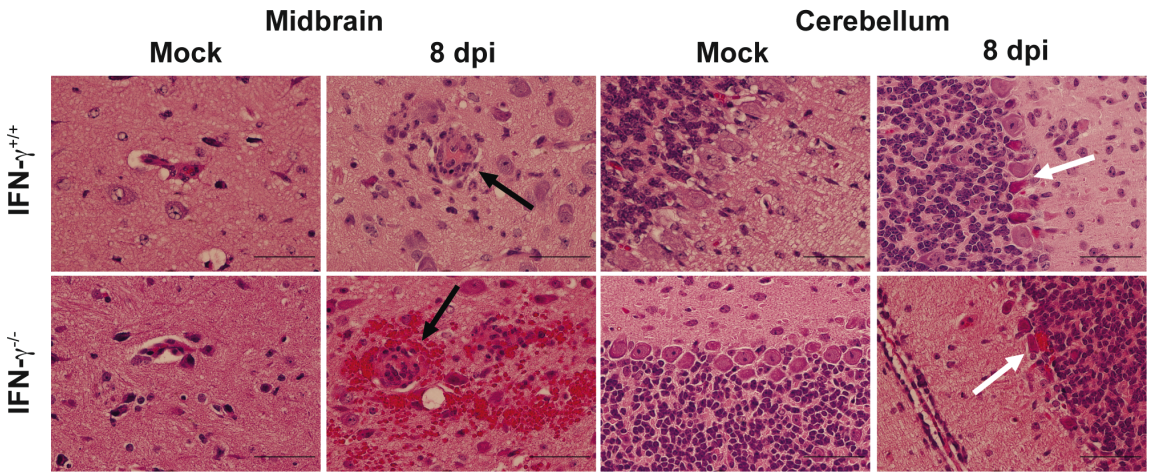

Figure 8-6. Effect of IFN-γ deficiency on cellular inflammation in brains of neonatal mice after MAV-1 infection.

IFN-$\gamma^{+/+}$ and IFN-$\gamma^{-/-}$ mice were infected i.n. with MAV-1 and brains were harvested at 8 dpi. Hematoxylin and eosin-stained sections were prepared from paraffin-embedded sections. Scale bars, 100 μm. Black arrows (left) indicate blood vessel and white arrows (right) indicate the Purkinje cell layer.

We made similar observations in vehicle- and ONX 0914-treated mice at 9 dpi, when the majority of ONX 0914-treated mice were moribund. The brains of vehicle-treated MAV-1-infected mice contained scattered foci of inflammatory cells around blood vessels, with some hemorrhage present (data not shown). However, in the brains of ONX 0914-treated mice the foci of inflammatory cells and hemorrhage were more abundant than in vehicle-treated mice (data not shown). These results suggest that infected ONX 0914-treated mice may have increased mortality because of extensive inflammation and hemorrhage in the brain. The increased inflammation in brains of ONX 0914-treated mice mirrors that of IFN-$\gamma^{-/-}$ mice, suggesting that the effects of IFN-γ on virus-induced brain inflammation may be mediated by immunoproteasome induction.

Discussion

We have shown that MAV-1 infection of neonatal mice results in induction of immunoproteasome expression and activity in the heart, coincident with peak viral loads and IFN-γ induction. Inhibition of proteasome activity using the nonspecific proteasome inhibitor bortezomib blunted the induction of proinflammatory cytokines after infection without affecting mortality. However, treatment of mice with the immunoproteasome-specific inhibitor ONX 0914 reduced CCL5 induction, but did not affect induction of other proinflammatory cytokines or heart pathology. Mortality was increased in IFN-$\gamma^{-/-}$ mice after MAV-1 infection, although immunoproteasome induction and inflammation was reduced in hearts of IFN-$\gamma^{-/-}$ mice compared to IFN-$\gamma^{+/+}$ mice at 7 dpi. Extensive

inflammation and hemorrhage were present in brain tissue of infected IFN-$\gamma^{-/-}$ and ONX 0914-treated mice, suggesting that the immunoproteasome may play a protective role in other organs during MAV-1 infection.

Immunoproteasome induction is observed in the heart during coxsackievirus B3 (CVB3)-induced myocarditis (45). Ongoing CVB3-induced myocarditis in susceptible mouse strains (A.BY/SnJ and SWR/J) is associated with increased formation and activity of immunoproteasomes in the heart. Interestingly, resistant strains of mice (C57BL/6 and DBA/J) also upregulate immunoproteasome expression after CVB3 infection, but peak expression occurs early (at 4 dpi) and is concurrent with type I IFN responses (46). Cardiomyocytes are likely the main contributors to immunoproteasome expression at early times after CVB3 infection, because there are no significant populations of inflammatory cells present in the heart at 4 dpi. In susceptible strains of mice, peak immunoproteasome expression occurs 1-2 weeks post infection and is associated with IFN-γ expression and the influx of inflammatory cells. Immunoproteasome induction is linked to enhanced CVB3 epitope generation (46). Thus, early immunoproteasome induction and enhanced generation of CVB3 epitopes coincides with less severe inflammation in resistant strains of mice, while delayed immunoproteasome induction correlates with severe inflammation and chronic infection. We observed immunoproteasome induction in the hearts of mice infected with MAV-1 that correlated with IFN-γ expression and the influx of inflammatory cells. We have not detected induction of type I IFN in heart tissue after MAV-1 infection (data not shown). Hematopoietic cells, such

as T cells and macrophages, constitutively express immunoproteasome subunits (47-50). IFN-γ induces immunoproteasome expression in non-hematopoietic cell types. Because immunoproteasome induction during MAV-1 myocarditis coincides with IFN-γ expression and inflammatory cell recruitment, it is likely that both resident heart cells (cardiomyocytes and fibroblasts) and recruited immune cells (macrophages and T cells) are contributors to immunoproteasome subunit expression and activity in MAV-1-infected hearts.

Inhibition of the proteasome using the nonspecific proteasome inhibitor bortezomib blunted induction of proinflammatory cytokines and chemokines in heart tissue after MAV-1 infection. During LCMV infection, bortezomib treatment impairs priming of naïve T cells in the spleen, leading to increased viral replication (51). Bortezomib treatment during MAV-1 infection did not affect viral loads in the heart at 10 dpi, suggesting that overall CD8 T cell responses are intact. We administered bortezomib beginning at 4 dpi in order to prevent substantial inhibition of the constitutive proteasome before the immunoproteasome is induced in heart tissue. Priming of naïve T cells in the mediastinal lymph nodes (the primary draining lymph nodes of the lungs and heart) may have already occurred by 4 dpi. This may be why bortezomib administration starting at 4 dpi in our model did not directly affect viral replication in the heart. Bortezomib treatment inhibits proinflammatory cytokine production in murine models of colitis and collagen-induced arthritis (52, 53), likely due to inhibition of IκB degradation. We observed a similar effect of bortezomib treatment on MAV-1 infection, with blunted induction of CCL5 and TNF-α,

suggesting that proteasome activity is important for the induction of proinflammatory cytokines during MAV-1 myocarditis. It is possible that we would see a greater effect of bortezomib on cardiac inflammatory responses during MAV-1 infection by altering the dose and timing of bortezomib administration.

In contrast to bortezomib, treatment of mice with the β5i-specific inhibitor ONX 0914 did not affect TNF-α induction and only slightly impaired induction of CCL5 in heart tissue after MAV-1 infection. ONX 0914 treatment also did not affect overall inflammation in infected heart tissue. This suggests that the immunoproteasome does not play a major role in proinflammatory cytokine induction or the recruitment of inflammatory cells to the heart during MAV-1 myocarditis. We chose to initiate ONX 0914 treatment at 1 dpi in order to recapitulate our time course of IFN-γ depletion after MAV-1 infection. It is possible that we may observe greater effects of immunoproteasome inhibition on heart inflammation by delaying ONX 0914 administration until there is substantial immunoproteasome induction in the heart (for example, starting at 4 dpi or later).

During CVB3-induced myocarditis, $\beta5i^{-/-}$ mice develop more severe myocardial tissue damage compared to wild-type mice (54). This is not due to a direct effect on viral replication, CD8 T cell responses, or induction of proinflammatory cytokines such as IL-6, TNF-α, or IFN-β. Rather, cardiomyocytes and inflammatory cells from $\beta5i^{-/-}$ mice have increased accumulation of poly-ubiquitinated protein conjugates and oxidant-damaged proteins following treatment with IFN-γ. Hearts from CVB3-infected $\beta5i^{-/-}$ have significant apoptotic cell death compared to infected wild-type mice. These

findings suggest that the immunoproteasome protects cells from cytokine-induced proteotoxic stress by removing polyubiquitinated or oxidant-damaged proteins. We did not observe substantial differences in cardiac inflammation in infected ONX 0914-treated mice, although we did not examine apoptosis or oxidized protein levels in hearts after infection. Since β5i is required for incorporation of β1i and β2i into newly assembled immunoproteasomes, $\beta5i^{-/-}$ mice have a severe defect in immunoproteasome assembly (55). It is possible that a greater reduction of immunoproteasome activity during MAV-1 infection, such as in $\beta5i^{-/-}$ mice, would result in a greater effect on overall inflammation in the heart. We did observe accelerated mortality in infected ONX 0914-treated mice compared to vehicle-treated mice, suggesting that immunoproteasome activity may be important for overall survival during MAV-1 infection in neonatal mice.

Mice deficient in IFN-γ did not upregulate β5i expression in heart tissue after MAV-1 infection, indicating that IFN-γ is required for immunoproteasome induction during MAV-1 myocarditis. IFN-γ deficiency did not affect viral replication in the heart. However, mortality was increased in neonatal $IFN\text{-}\gamma^{-/-}$ mice, which succumbed by 8 dpi, a time before substantial inflammation develops in the heart. We have previously shown that IFN-γ has only minor effects on viral replication in the lungs of adult mice after MAV-1 infection and does not affect mortality (56). It is surprising that there are striking age-based differences in the requirement for IFN-γ during MAV-1 infection. The early

mortality of neonatal IFN-$\gamma^{-/-}$ mice before significant cardiac inflammation suggested that IFN-γ may play an important role in another organ.

Brains of neonatal IFN-$\gamma^{-/-}$ mice showed diffuse inflammatory foci and severe hemorrhage at 8 dpi, suggesting that early mortality in these mice may be due to excess inflammation and cell damage in the brain. ONX 0914-treated mice, which also displayed accelerated mortality following MAV-1 infection, had more hemorrhage in brain tissue compared to vehicle-treated mice at 9 dpi. This suggests that the requirement of IFN-γ for survival of MAV-1 infection in neonatal mice may be mediated by immunoproteasome activity. Little is known about the role of the immunoproteasome in brain tissue. Immunoproteasome assembly is induced in microglial-like cells in the brain following LCMV infection (57). LCMV-induced meningitis is delayed and less severe in β5i$^{-/-}$ mice, suggesting a role for microglial immunoproteasomes in exacerbating immunopathology. However, our results suggest that IFN-γ-induced immunoproteasomes in the brain may play a protective role during MAV-1 infection.

In contrast, our results following IFN-γ depletion or immunoproteasome inhibition suggest that the immunoproteasome promotes some aspects of virus-induced inflammation in heart tissue. This would indicate that the role of the immunoproteasome during MAV-1 infection of neonatal mice is organ-specific, with the immunoproteasome playing a proinflammatory role in the heart and an anti-inflammatory, protective role in the brain. It is possible that the primary function of the immunoproteasome in the brain is to prevent the buildup of oxidized and damaged proteins within infected cells or neighboring cells exposed

to proinflammatory cytokines. In this case, immunoproteasome inhibition would lead to accumulation of toxic levels of damaged proteins within cells and excess cell death. This, in turn, could enhance the recruitment of inflammatory cells to the brain tissue in mice treated with an immunoproteasome inhibitor.

In summary, our findings demonstrate that the immunoproteasome is induced during MAV-1-induced myocarditis. While proteasome activity promotes the expression of some proinflammatory cytokines, immunoproteasome activity affects only some aspects of virus-induced inflammation in the heart during MAV-1 infection. IFN-γ is required for immunoproteasome induction in heart tissue, and it is also required for survival of MAV-1 infection in neonatal mice. Our results suggest that the requirement of IFN-γ for survival is independent of an affect on cardiac inflammation and instead may be due to a protective role of IFN-γ-induced immunoproteasome activity in the brain. The constitutive proteasome and the immunoproteasome likely have non-redundant functions during MAV-1 infection, and the role of the immunoproteasome may be organ-specific. The MAV-1 model will enable further studies of the role of the immunoproteasome and other inflammatory mediators during adenovirus myocarditis and disseminated adenovirus infection.

Materials and Methods

Mice

All work was approved by the University of Michigan Committee on Use and Care of Animals. IFN-$\gamma^{-/-}$ mice (originally from The Jackson Lab) on a C57BL/6 background were generously provided by Dr. Benjamin Segal (University of Michigan) and were bred at the University of Michigan. C57BL/6 mothers with litters of neonatal mice were obtained from The Jackson Laboratory. All mice were maintained under specific pathogen-free conditions.

Virus and infections

MAV-1 was grown and titered on NIH 3T6 fibroblasts as previously described (58). Neonates (7 days old) were manually restrained and infected intranasally (i.n.) with 10^5 plaque-forming units (pfu) in 10 μl of sterile phosphate-buffered saline (PBS). Control mice were mock infected i.n. with conditioned media at an equivalent dilution in sterile PBS. Mice were euthanized by pentobarbital overdose at the indicated time points. Hearts were harvested, snap frozen in dry ice, and stored at -80°C until processed further. One third to one half of each heart (~20 mg) was homogenized in 1 mL of TRIzol® (Invitrogen) using sterile glass beads in a mini Beadbeater (Biospec Products) for 30 seconds. RNA and DNA were isolated from the homogenates according to the manufacturer's protocol.

SDS-PAGE and Western Blot Analysis

Tissues were lysed using 1X loading buffer (50 mM Tris-Cl at pH 6.8, 2% SDS, and 10% glycerol) for the preparation of total proteins (59). Western blots were performed using primary antibodies against PA28α (PW 8185, Affiniti Research Products), PA28β (PW 8240, Affiniti Research Products), proteasome subunit β5 (anti-PSMB5; customized antibody from (60)), or immunoproteasome subunit β5i (anti-LMP7, Enzo Life Sciences). All SDS-PAGE and western blotting were performed as previously described (60, 61).

Measurement of proteasome and immunoproteasome activity

The ProCISE assay, performed as in (61), involves the following steps: (1) incubation of the biotinylated active site probe with activated 20S proteasomes from tissue lysates, (2) denaturation with 6 M guanidine hydrochloride, (3) addition of streptavidin-coated beads to capture probe-bound active sites, (4) extensive bead washing, (5) addition of proteasome subunit-specific primary antibody followed by a secondary HRP-conjugated antibody, and (6) luminescence-based detection.

Proteasome and Immunoproteasome inhibition

Beginning at 4 dpi, mice were treated with 0.5 mg/kg bortezomib (Thermo Fisher Scientific) or DMSO given i.p. every other day until 8 dpi. For immunoproteasome-specific inhibition, mice were treated with 5 mg/kg ONX

0914 (SelleckChem) or vehicle (Captisol®, Captisol® Ligand Technology) given subcutaneously every other day starting at one day post infection.

Analysis of Viral Loads by PCR

MAV-1 viral loads were measured in organs using quantitative real-time polymerase chain reaction (qPCR) as previously described (62). Primers and probe used to detect a 59-bp region of the MAV-1 E1A gene are listed in Table 1. Five µl of extracted DNA were added to reactions containing TaqMan II Universal PCR Mix with UNG (Applied Biosystems), forward and reverse primers (each at 200 nM final concentration), and probe (20 nM final concentration) in a 25 µl reaction volume. Analysis on an ABI Prism 7300 machine (Applied Biosystems) consisted of 40 cycles of 15 s at 90°C and 60 s at 60°C. Standard curves generated using known amounts of plasmid containing the MAV-1 EIA gene were used to convert threshold cycle values for experimental samples to copy numbers of EIA DNA. Results were standardized to the nanogram (ng) amount of input DNA. Each sample was assayed in triplicate.

Real-time PCR Analysis of Gene Expression

Cytokine gene expression was quantified using reverse transcriptase (RT)-qPCR as previously described (56, 63). First, 2.5 µg of RNA were reverse transcribed using MMLV reverse transcriptase (Invitrogen) in 20 µl reactions according to the manufacturer's instructions. Water was added to the cDNA product to bring the total volume to 50 µl. cDNA was amplified using duplexed

gene expression assays for mouse CCL5 and GAPDH (Applied Biosystems). Five µl of cDNA were added to reactions containing TaqMan Universal PCR Mix and 1.25 µl each of 20X gene expression assays for the target cytokine and GAPDH. Primers used to detect β5i, PA28α, TNF-α, and GAPDH are listed in Table 2. For these measurements, 5 µl of cDNA were added to reactions containing Power SYBR Green PCR Mix (Applied Biosystems) and forward and reverse primers (each at 200 nM final concentration) in a 25 µl reaction volume. In all cases, RT-qPCR analysis consisted of 40 cycles of 15 s at 90°C and 60 s at 60°C. Quantification of target gene mRNA was normalized to GAPDH and expressed in arbitrary units as $2^{-\Delta Ct}$, where Ct is the threshold cycle and ΔCt = Ct(target) – Ct(GAPDH).

Histology

Hearts or brains were fixed in 10% formalin and embedded in paraffin. Five µm sections were stained with hematoxylin and eosin to evaluate cellular infiltrates. Sectioning and staining were performed by the University of Michigan Unit for Laboratory Animal Medicine Pathology Cores for Animal Research. Slides were viewed through an Olympus BX41 microscope and digital images were processed using Olympus DP Manager software. Images were assembled using Adobe Illustrator (Adobe Systems).

Echocardiography

In vivo echocardiography was performed as previously described (64), consistent with guidelines of the American Society of Echocardiography. Mice were anesthetized by inhaled isoflurane, chest hair was removed with Nair^{TM} (Church & Dwight), and imaging was performed using Vevo770 Ultrasound system (Visual Sonics Inc) and an RMV706 (20-60Mhz) transducer. Imaging and analysis were performed by a single blinded sonographer. LV end systolic and end diastolic dimensions (LVs and LVd), as well as systolic and diastolic wall thickness were measured from M-mode tracings to calculate ejection fraction assuming a spherical LV geometry [$(LVd^3\text{-}LVs^3)/LV\ d^3x100$)],

Statistics

Analysis for statistical significance was conducted using Prism 6 for Macintosh (GraphPad Software, Incorporated). Differences between more than two groups were analyzed using one-way analysis of variance (ANOVA) followed by Bonferroni's multiple comparison tests. Differences between two groups were analyzed using Mann-Whitney test. For viral load data, differences between groups at a given time point in log-transformed viral loads were analyzed using Student's t test. *P* values less than 0.05 were considered statistically significant.

Table 8-2. Primers and probes used for real-time PCR analysis

Target	Oligonucleotide	Sequence (5′ to 3′)
MAV-1 E1A	Forward primer	GCACTCCATGGCAGGATTCT
genomic	Reverse primer	GGTCGAAGCAGACGGTTCTTC
	Probe	TACTGCCACTTCTGC
GAPDH	Forward primer	TGCACCACCAACTGCTTAG
	Reverse primer	GGATGCAGGGATGATGTTC
β5i	Forward primer	CATTCCTGAGGTCCTTTGGTGG
	Reverse primer	ATGCGTTCCCCATTCCGAAG
PA28α	Forward primer	GTCAAAGAGAAAGAGAAGGAGGAGC
	Reverse primer	GGTGTGAAGGTTGGTCATCAGC
TNF-α	Forward primer	CCACCACGCTCTTCTGTCTAC
	Reverse primer	AGGGTCTGGGCCATAGAACT

References

1. **Rock KL, Gramm C, Rothstein L, Clark K, Stein R, Dick L, Hwang D, Goldberg AL.** 1994. Inhibitors of the proteasome block the degradation of most cell proteins and the generation of peptides presented on MHC class I molecules. Cell **78:**761-771.
2. **Groettrup M, Soza A, Kuckelkorn U, Kloetzel PM.** 1996. Peptide antigen production by the proteasome: complexity provides efficiency. Immunol Today **17:**429-435.
3. **Craiu A, Gaczynska M, Akopian T, Gramm CF, Fenteany G, Goldberg AL, Rock KL.** 1997. Lactacystin and clasto-lactacystin beta-lactone modify multiple proteasome beta-subunits and inhibit intracellular protein degradation and major histocompatibility complex class I antigen presentation. J Biol Chem **272:**13437-13445.
4. **Unno M, Mizushima T, Morimoto Y, Tomisugi Y, Tanaka K, Yasuoka N, Tsukihara T.** 2002. The structure of the mammalian 20S proteasome at 2.75 A resolution. Structure **10:**609-618.
5. **Groll M, Ditzel L, Löwe J, Stock D, Bochtler M, Bartunik HD, Huber R.** 1997. Structure of 20S proteasome from yeast at 2.4 A resolution. Nature **386:**463-471.
6. **DeMartino GN, Slaughter CA.** 1999. The proteasome, a novel protease regulated by multiple mechanisms. J Biol Chem **274:**22123-22126.
7. **Glynne R, Powis SH, Beck S, Kelly A, Kerr LA, Trowsdale J.** 1991. A proteasome-related gene between the two ABC transporter loci in the class II region of the human MHC. Nature **353:**357-360.
8. **Kelly A, Powis SH, Glynne R, Radley E, Beck S, Trowsdale J.** 1991. Second proteasome-related gene in the human MHC class II region. Nature **353:**667-668.
9. **Ortiz-Navarrete V, Seelig A, Gernold M, Frentzel S, Kloetzel PM, Hämmerling GJ.** 1991. Subunit of the '20S' proteasome (multicatalytic proteinase) encoded by the major histocompatibility complex. Nature **353:**662-664.
10. **Aki M, Shimbara N, Takashina M, Akiyama K, Kagawa S, Tamura T, Tanahashi N, Yoshimura T, Tanaka K, Ichihara A.** 1994. Interferon-gamma induces different subunit organizations and functional diversity of proteasomes. J Biochem **115:**257-269.
11. **Tanaka K.** 1994. Role of proteasomes modified by interferon-gamma in antigen processing. J Leukoc Biol **56:**571-575.
12. **Groettrup M, Kraft R, Kostka S, Standera S, Stohwasser R, Kloetzel PM.** 1996. A third interferon-gamma-induced subunit exchange in the 20S proteasome. Eur J Immunol **26:**863-869.
13. **Nandi D, Jiang H, Monaco JJ.** 1996. Identification of MECL-1 (LMP-10) as the third IFN-gamma-inducible proteasome subunit. J Immunol **156:**2361-2364.
14. **Hisamatsu H, Shimbara N, Saito Y, Kristensen P, Hendil KB, Fujiwara T, Takahashi E, Tanahashi N, Tamura T, Ichihara A, Tanaka K.** 1996.

Newly identified pair of proteasomal subunits regulated reciprocally by interferon gamma. J Exp Med **183:**1807-1816.

15. **Früh K, Gossen M, Wang K, Bujard H, Peterson PA, Yang Y.** 1994. Displacement of housekeeping proteasome subunits by MHC-encoded LMPs: a newly discovered mechanism for modulating the multicatalytic proteinase complex. EMBO J **13:**3236-3244.
16. **Driscoll J, Brown MG, Finley D, Monaco JJ.** 1993. MHC-linked LMP gene products specifically alter peptidase activities of the proteasome. Nature **365:**262-264.
17. **Dubiel W, Pratt G, Ferrell K, Rechsteiner M.** 1992. Purification of an 11 S regulator of the multicatalytic protease. J Biol Chem **267:**22369-22377.
18. **Ma CP, Slaughter CA, DeMartino GN.** 1992. Identification, purification, and characterization of a protein activator (PA28) of the 20 S proteasome (macropain). J Biol Chem **267:**10515-10523.
19. **Hutchinson S, Sims S, O'hara G, Silk J, Gileadi U, Cerundolo V, Klenerman P.** 2011. A dominant role for the immunoproteasome in CD8+ T cell responses to murine cytomegalovirus. PLoS ONE **6:**e14646.
20. **Robek MD, Garcia ML, Boyd BS, Chisari FV.** 2007. Role of immunoproteasome catalytic subunits in the immune response to hepatitis B virus. J Virol **81:**483-491.
21. **Van Kaer L, Ashton-Rickardt PG, Eichelberger M, Gaczynska M, Nagashima K, Rock KL, Goldberg AL, Doherty PC, Tonegawa S.** 1994. Altered peptidase and viral-specific T cell response in LMP2 mutant mice. Immunity **1:**533-541.
22. **Chen W, Norbury CC, Cho Y, Yewdell JW, Bennink JR.** 2001. Immunoproteasomes shape immunodominance hierarchies of antiviral CD8(+) T cells at the levels of T cell repertoire and presentation of viral antigens. J Exp Med **193:**1319-1326.
23. **Pang KC, Sanders MT, Monaco JJ, Doherty PC, Turner SJ, Chen W.** 2006. Immunoproteasome subunit deficiencies impact differentially on two immunodominant influenza virus-specific CD8+ T cell responses. J Immunol **177:**7680-7688.
24. **Kincaid EZ, Che JW, York I, Escobar H, Reyes-Vargas E, Delgado JC, Welsh RM, Karow ML, Murphy AJ, Valenzuela DM, Yancopoulos GD, Rock KL.** 2012. Mice completely lacking immunoproteasomes show major changes in antigen presentation. Nat Immunol **13:**129-135.
25. **Traenckner EB, Wilk S, Baeuerle PA.** 1994. A proteasome inhibitor prevents activation of NF-kappa B and stabilizes a newly phosphorylated form of I kappa B-alpha that is still bound to NF-kappa B. EMBO J **13:**5433-5441.
26. **Palombella VJ, Rando OJ, Goldberg AL, Maniatis T.** 1994. The ubiquitin-proteasome pathway is required for processing the NF-kappa B1 precursor protein and the activation of NF-kappa B. Cell **78:**773-785.
27. **Kalim KW, Basler M, Kirk CJ, Groettrup M.** 2012. Immunoproteasome subunit LMP7 deficiency and inhibition suppresses Th1 and Th17 but enhances regulatory T cell differentiation. J Immunol **189:**4182-4193.

28. **Basler M, Beck U, Kirk CJ, Groettrup M.** 2011. The antiviral immune response in mice devoid of immunoproteasome activity. J Immunol **187:**5548-5557.
29. **Hensley SE, Zanker D, Dolan BP, David A, Hickman HD, Embry AC, Skon CN, Grebe KM, Griffin TA, Chen W, Bennink JR, Yewdell JW.** 2010. Unexpected role for the immunoproteasome subunit LMP2 in antiviral humoral and innate immune responses. J Immunol **184:**4115-4122.
30. **Ethen CM, Hussong SA, Reilly C, Feng X, Olsen TW, Ferrington DA.** 2007. Transformation of the proteasome with age-related macular degeneration. FEBS Lett **581:**885-890.
31. **Ferrington DA, Hussong SA, Roehrich H, Kapphahn RJ, Kavanaugh SM, Heuss ND, Gregerson DS.** 2008. Immunoproteasome responds to injury in the retina and brain. J Neurochem **106:**158-169.
32. **Hussong SA, Kapphahn RJ, Phillips SL, Maldonado M, Ferrington DA.** 2010. Immunoproteasome deficiency alters retinal proteasome's response to stress. J Neurochem **113:**1481-1490.
33. **Pickering AM, Koop AL, Teoh CY, Ermak G, Grune T, Davies KJA.** 2010. The immunoproteasome, the 20S proteasome and the PA28αβ proteasome regulator are oxidative-stress-adaptive proteolytic complexes. Biochem J **432:**585-594.
34. **Ferrington DA, Husom AD, Thompson LV.** 2005. Altered proteasome structure, function, and oxidation in aged muscle. FASEB J **19:**644-646.
35. **Kotamraju S, Matalon S, Matsunaga T, Shang T, Hickman-Davis JM, Kalyanaraman B.** 2006. Upregulation of immunoproteasomes by nitric oxide: potential antioxidative mechanism in endothelial cells. Free Radic Biol Med **40:**1034-1044.
36. **Martin AB, Webber S, Fricker FJ, Jaffe R, Demmler G, Kearney D, Zhang YH, Bodurtha J, Gelb B, Ni J.** 1994. Acute myocarditis. Rapid diagnosis by PCR in children. Circulation **90:**330-339.
37. **Feldman AM, McNamara D.** 2000. Myocarditis. N Engl J Med **343:**1388-1398.
38. **Bowles NE, Ni J, Kearney DL, Pauschinger M, Schultheiss H-P, McCarthy R, Hare J, Bricker JT, Bowles KR, Towbin JA.** 2003. Detection of viruses in myocardial tissues by polymerase chain reaction. evidence of adenovirus as a common cause of myocarditis in children and adults. J Am Coll Cardiol **42:**466-472.
39. **Kuhl U, Pauschinger M, Seeberg B, Lassner D, Noutsias M, Poller W, Schultheiss HP.** 2005. Viral persistence in the myocardium is associated with progressive cardiac dysfunction. Circulation **112:**1965-1970.
40. **Tatrai E, Hartyanszky I, Jr., Laszik A, Acsady G, Sotonyi P, Hubay M.** 2011. The role of viral infections in the development of dilated cardiomyopathy. Pathol Oncol Res **17:**229-235.
41. **Pauschinger M, Bowles NE, Fuentes-Garcia FJ, Pham V, Kühl U, Schwimmbeck PL, Schultheiss HP, Towbin JA.** 1999. Detection of

adenoviral genome in the myocardium of adult patients with idiopathic left ventricular dysfunction. Circulation **99:**1348-1354.

42. **Kirk CJ, Powell SR, Miller EJ.** 2014. Assessment of cytokine-modulated proteasome activity. Methods in molecular biology (Clifton, NJ) **1172:**147-162.
43. **Adams J, Palombella VJ, Sausville EA, Adams J, Palombella VJ, Sausville EA, Johnson J, Destree A, Lazarus DD, Maas J, Pien CS, Prakash S, Elliott PJ.** 1999. Proteasome Inhibitors : A Novel Class of Potent and Effective Antitumor Agents Proteasome Inhibitors : A Novel Class of Potent and Effective Antitumor Agents. Cancer Research**:**2615-2622.
44. **Muchamuel T, Basler M, Aujay MA, Suzuki E, Kalim KW, Lauer C, Sylvain C, Ring ER, Shields J, Jiang J, Shwonek P, Parlati F, Demo SD, Bennett MK, Kirk CJ, Groettrup M.** 2009. A selective inhibitor of the immunoproteasome subunit LMP7 blocks cytokine production and attenuates progression of experimental arthritis. Nat Med **15:**781-787.
45. **Szalay G, Meiners S, Voigt A, Lauber J, Spieth C, Speer N, Sauter M, Kuckelkorn U, Zell A, Klingel K, Stangl K, Kandolf R.** 2006. Ongoing coxsackievirus myocarditis is associated with increased formation and activity of myocardial immunoproteasomes. The American Journal of Pathology **168:**1542-1552.
46. **Jäkel S, Kuckelkorn U, Szalay G, Plötz M, Textoris-Taube K, Opitz E, Klingel K, Stevanovic S, Kandolf R, Kotsch K, Stangl K, Kloetzel PM, Voigt A.** 2010. Differential Interferon Responses Enhance Viral Epitope Generation by Myocardial Immunoproteasomes in Murine Enterovirus Myocarditis. Am J Pathol **175:**510-518.
47. **Ebstein F, Kloetzel P-M, Krüger E, Seifert U.** 2012. Emerging roles of immunoproteasomes beyond MHC class I antigen processing. Cell Mol Life Sci **69:**2543-2558.
48. **Noda C, Tanahashi N, Shimbara N, Hendil KB, Tanaka K.** 2000. Tissue distribution of constitutive proteasomes, immunoproteasomes, and PA28 in rats. Biochem Biophys Res Commun **277:**348-354.
49. **Haorah J, Heilman D, Diekmann C, Osna N, Donohue TM, Ghorpade A, Persidsky Y.** 2004. Alcohol and HIV decrease proteasome and immunoproteasome function in macrophages: implications for impaired immune function during disease. Cell Immunol **229:**139-148.
50. **Frisan T, Levitsky V, Masucci MG.** 2000. Variations in proteasome subunit composition and enzymatic activity in B-lymphoma lines and normal B cells. Int J Cancer **88:**881-888.
51. **Basler M, Lauer C, Beck U, Groettrup M.** 2009. The proteasome inhibitor bortezomib enhances the susceptibility to viral infection. J Immunol **183:**6145-6150.
52. **Lee S-W, Kim J-H, Park Y-B, Lee S-K.** 2009. Bortezomib attenuates murine collagen-induced arthritis. Annals of the Rheumatic Diseases **68:**1761-1767.

53. **Schmidt N, Gonzalez E, Visekruna A, Kühl AA, Loddenkemper C, Mollenkopf H, Kaufmann SHE, Steinhoff U, Joeris T.** 2010. Targeting the proteasome: partial inhibition of the proteasome by bortezomib or deletion of the immunosubunit LMP7 attenuates experimental colitis. Gut **59:**896-906.
54. **Opitz E, Koch A, Klingel K, Schmidt F, Prokop S, Rahnefeld A, Sauter M, Heppner FL, Völker U, Kandolf R, Kuckelkorn U, Stangl K, Krüger E, Kloetzel PM, Voigt A.** 2011. Impairment of Immunoproteasome Function by β5i/LMP7 Subunit Deficiency Results in Severe Enterovirus Myocarditis. PLoS Pathog **7:**e1002233.
55. **Fehling HJ, Swat W, Laplace C, Kühn R, Rajewsky K, Müller U, von Boehmer H.** 1994. MHC class I expression in mice lacking the proteasome subunit LMP-7. Science **265:**1234-1237.
56. **Procario MC, Levine RE, McCarthy MK, Kim E, Zhu L, Chang C-H, Hershenson MB, Weinberg JB.** 2012. Susceptibility to acute mouse adenovirus type 1 respiratory infection and establishment of protective immunity in neonatal mice. J Virol **86:**4194-4203.
57. **Kremer M, Henn A, Kolb C, Basler M, Moebius J, Guillaume B, Leist M, Van Den Eynde BJ, Groettrup M.** 2010. Reduced Immunoproteasome Formation and Accumulation of Immunoproteasomal Precursors in the Brains of Lymphocytic Choriomeningitis Virus-Infected Mice. J Immunol **185:**5549-5560.
58. **Cauthen A, Welton A, Spindler KR.** 2007. Construction of mouse adenovirus type 1 mutants. Methods Mol Med **130:**41-59.
59. **Li J, Powell SR, Wang X.** 2011. Enhancement of proteasome function by PA28α overexpression protects against oxidative stress. FASEB J **25:**883-893.
60. **Chen Q, Liu J-B, Horak KM, Zheng H, Kumarapeli ARK, Li J, Li F, Gerdes AM, Wawrousek EF, Wang X.** 2005. Intrasarcoplasmic amyloidosis impairs proteolytic function of proteasomes in cardiomyocytes by compromising substrate uptake. Circ Res **97:**1018-1026.
61. **Kirk CJ, Powell SR, Miller EJ.** 2014. Assessment of cytokine-modulated proteasome activity. Methods Mol Bio **1172:**147-162.
62. **McCarthy MK, Zhu L, Procario MC, Weinberg JB.** 2014. IL-17 contributes to neutrophil recruitment but not to control of viral replication during acute mouse adenovirus type 1 respiratory infection. Virology **456-457:**259-267.
63. **McCarthy MK, Levine RE, Procario MC, McDonnell PJ, Zhu L, Mancuso P, Crofford LJ, Aronoff DM, Weinberg JB.** 2013. Prostaglandin E2 Induction during Mouse Adenovirus Type 1 Respiratory Infection Regulates Inflammatory Mediator Generation but Does Not Affect Viral Pathogenesis. PLoS ONE **8:**e77628.
64. **Zolov SN, Bridges D, Zhang Y, Lee W-W, Riehle E, Verma R, Lenk GM, Converso-Baran K, Weide T, Albin RL, Saltiel AR, Meisler MH, Russell MW, Weisman LS.** 2012. In vivo, Pikfyve generates PI(3,5)P2,

which serves as both a signaling lipid and the major precursor for PI5P. Proc Natl Acad Sci USA **109:**17472-17477.

Chapter 9:
Discussion

Overview

Adenoviruses are DNA viruses that are important causes of acute respiratory disease and myocarditis. During a viral infection, the host immune system faces the task of effectively clearing a virus while limiting local tissue damage and inflammation. The immune response to viruses can be protective, aiding in clearance of virus from the affected organs and resolution of disease caused by viral replication. Disease associated with respiratory viruses can also be caused by immune-mediated pathology. Virus-induced inflammation can be detrimental to the host, causing symptoms during acute infection and leading to damage that contributes to chronic disease. It is unclear whether the clinical manifestations of adenovirus disease are mediated by direct virus-induced tissue damage, the host immune response to the virus, or both.

The main focus of this dissertation was to identify host factors that regulate inflammatory responses and contribute to pathogenesis of acute adenovirus respiratory infection. Due to the species-specificity of adenoviruses, which precludes animal studies with a human adenovirus, I used mouse adenovirus type 1 (MAV-1) to study the pathogenesis of an adenovirus in its natural host. The role of the lipid mediator PGE_2 in immunocompetent and immunocompromised (BMT) hosts was examined in Chapters 4 and 5, respectively. In Chapter 6, I investigated the contribution of IL-17 to recruitment

of inflammatory cells and control of viral replication in the lung. In Chapters 7 and 8, I examined the role of IFN-γ and the immunoproteasome during MAV-1-induced myocarditis. By determining contributions of lipid mediators (such as PGE_2), cytokines (such as IL-17 and IFN-γ), and specific cell populations (such as T cells) to MAV-1 pathogenesis and viral clearance, we have gained insight into mechanisms of acute disease and persistence.

Chapter Summary

PGE_2 is a lipid mediator that can promote proinflammatory cytokine production and pulmonary inflammation. In Chapter 4, I used mice deficient in mPGES-1, the enzyme responsible for conversion of the intermediate PGH_2 into PGE_2, to determine the effect of PGE_2 on MAV-1 pathogenesis. I showed that while PGE_2 promotes the expression of a variety of cytokines in response to acute MAV-1 infection, PGE_2 synthesis does not appear to be essential for generating pulmonary immunity in immunocompetent mice. Adenovirus infections are an important complication for individuals who are immunocompromised due to hematopoietic stem cell transplantation. In Chapter 5, I used MAV-1 respiratory infection in an allogeneic BMT mouse model. BMT mice displayed exaggerated PGE_2 production and significantly delayed clearance of virus from the lungs. BMT-induced T cell dysfunction likely contributes to impaired virus clearance, and T cell dysfunction is independent of excess PGE_2 production.

During influenza A virus infection, PGE_2 inhibits type I IFN production and apoptosis in macrophages to promote viral replication in these cells, but not

airway epithelial cells (1). We have not observed substantial type I IFN induction in the lungs of MAV-1-infected mice, and type I IFN receptor deficiency does not substantially alter MAV-1 pathogenesis following i.n. infection (data not shown). I have detected expression of early MAV-1 genes in alveolar macrophages from bronchoalveolar lavage fluid (BALF) of infected mice (data not shown), although we do not believe that alveolar macrophages are a major target of viral replication in the lungs. It is possible that the role of PGE_2 during respiratory viral infection is virus-specific, and PGE_2 may be more important during infection by viruses that target macrophages and induce significant type I IFN production. PGE_2 also impairs antigen presentation and T cell mediated immunity during influenza A virus infection (1). In unpublished data, I have demonstrated that addition of 10 μM PGE_2 to α-CD3-stimulated splenocytes from MAV-1-infected mice impairs production of IL-2, IFN-γ, and IL-17 (data not shown). However, we observe less IFN-γ induction in mPGES-$1^{-/-}$ mice during MAV-1 infection (Figure 4-3E), suggesting that endogenous PGE_2 promotes T cell cytokine production in our model. Moreover, treatment of mice with the PGE_2 analog misoprostol significantly enhances IFN-γ production in the airways of infected mice (Figure 5-8A). These results suggest that while PGE_2 can suppress T cell responses *ex vivo*, both endogenous and exogenous PGE_2 promote production of T cell cytokines, namely IFN-γ, during MAV-1 respiratory infection *in vivo*. While PGE_2 promotes IFN-γ responses *in vivo*, IFN-γ production is not a major contributor to control of peak MAV-1 replication or MAV-1 clearance from the lung ((2) and Figure 5-5A). However, $CD8^+$ T cells do play an important role in viral clearance

because CD8$\alpha^{-/-}$ mice have significantly higher viral loads than wild-type mice at 14 dpi (Figure 5-5B). Viral clearance is unaffected in both PGE_2-deficient immunocompetent and BMT mice, indicating that neither normal nor excess PGE_2 levels suppress $CD8^+$ T cell function to impact viral clearance from the lungs.

In Chapter 6, I showed that MAV-1 induces robust Th1 and Th17 responses during MAV-1 respiratory infection. Although IL-17 contributes to recruitment of neutrophils to the airways during acute MAV-1 infection, Th17 responses are not essential for control of virus infection or for virus-induced pulmonary inflammation. In unpublished data, I have demonstrated that IL-$17^{-/-}$ mice are protected from MAV-1-induced weight loss (data not shown). This suggests that Th17 responses contribute to systemic inflammatory responses independent of the lung during MAV-1 respiratory infection. It is possible that IL-17 affects recruitment of neutrophils or another cell type to other MAV-1 target organs, such as the liver, brain, or spleen.

Adenoviruses are important causes of myocarditis. In Chapter 7, I established a model of MAV-1-induced myocarditis in neonatal mice. I demonstrate that IFN-γ is a proinflammatory mediator during MAV-1 myocarditis, and persistent MAV-1 infection may contribute to ongoing cardiac dysfunction. Although heart viral loads are similar between neonatal and adult mice, inflammation and signs of cardiac damage are not present in adult mice. In Chapter 8, I show that the immunoproteasome is significantly induced during MAV-1 myocarditis. IFN-γ is important for induction of the immunoproteasome

following MAV-1 infection, and it likely has organ-specific effects. While treatment of mice with a nonspecific proteasome inhibitor leads to decreased proinflammatory cytokine induction in the heart after MAV-1 infection, an immunoproteasome-specific inhibitor does not have seem to have a similar effect.

It is unknown whether cardiac dysfunction in MAV-1-infected neonatal mice is due to active viral replication or the immune response. However, adult mice infected with MAV-1 do not develop significant inflammation or cardiac damage (as measured by serum cardiac troponin I levels) despite similar viral loads in the heart. This suggests that immune responses are the major contributor to cardiac dysfunction in neonatal mice, rather than active viral replication. We observed less proinflammatory cytokine induction in hearts of MAV-1-infected neonatal mice treated with the proteasome inhibitor bortezomib and to a lesser extent in mice treated with the immunoproteasome inhibitor ONX 0914 (Figure 8-3 and Figure 8-4). The effect that administration of either of these compounds has on the development of cardiac dysfunction during MAV-1 infection is unknown. We may observe greater effects of these inhibitors on cardiac inflammatory responses during MAV-1 infection by altering the dose and timing of administration to target specific times post infection when immunoproteasome activity in the heart is highest. Preliminary results from a pilot experiment in which we delayed ONX 0914 treatment until 6 dpi suggest that delayed immunoproteasome inhibition leads to decreased cardiac pathology and decreased proinflammatory cytokine induction compared to vehicle-treated mice.

It is possible that the immunoproteasome plays dual roles in the heart during MAV-1-induced myocarditis. For example, immunoproteasome activity could both promote proinflammatory cytokine production and protect infected cells in the heart from oxidative stress induced by increased cytokine levels. Inhibiting immunoproteasome activity throughout the course of infection (starting at 1 dpi and continuing through 9 dpi) may cancel out any dual effects, whereas altering the timing of inhibition may reveal the different roles of the immunoproteasome during MAV-1 myocarditis.

We observed increased mortality in neonatal IFN-$\gamma^{-/-}$ mice and in neonatal mice treated with ONX 0914 after MAV-1 infection. Brains of both neonatal IFN-$\gamma^{-/-}$ and ONX 0914-treated mice showed diffuse inflammatory foci and severe hemorrhage, suggesting that early mortality in these mice may be due to excess inflammation and cell damage in the brain because of less IFN-γ-induced immunoproteasome activity. IFN-γ-induced immunoproteasome activity in the brain could be playing multiple roles during MAV-1 infection. Following i.n. and i.p. infection of 4 week old outbred Swiss Webster mice, MAV-1 antigen in brain tissue is detected primarily in endothelial cells (3). The cellular targets of MAV-1 replication in the brain may differ between neonates and adult mice. Moreover, IFN-γ production in neonatal mice may prevent spread of MAV-1 from endothelial cells to neurons or other cell types in the CNS, such as astrocytes or microglia. Although IFN-γ deficiency did not affect viral loads in the heart or the lungs, it is possible that viral loads in the brain are significantly higher in neonatal IFN-$\gamma^{-/-}$ mice compared to wild-type mice. Antiviral CD8 T cell responses in the brain may

depend on IFN-γ-induced immunoproteasome activity. Impaired production of immunoproteasome-specific peptides in infected cells in the brain due to IFN-γ deficiency or immunoproteasome inhibition could lead to reduced CD8 T cell activation. Alternatively, the primary function of the immunoproteasome in the brain may be to prevent the buildup of oxidized and damaged proteins within infected cells or neighboring cells exposed to proinflammatory cytokines. In this case, IFN-γ deficiency or immunoproteasome inhibition could lead to accumulation of toxic levels of damaged proteins within cells and excess cell death. This, in turn, could enhance the recruitment of inflammatory cells to the brain and may explain the increased mortality observed in IFN-$\gamma^{-/-}$ mice and in mice treated with ONX 0914.

Future Areas of Study

- $CD8^+$ T cell-dependent mechanisms of MAV-1 clearance
- Phenotypic and functional characteristics of $CD4^+$ and $CD8^+$ T cells recruited to lungs and heart
- Role of the immunoproteasome during MAV-1 respiratory infection
- Mechanisms of MAV-1 persistence in lungs and heart

A future goal of these projects is to elucidate the $CD8^+$ T cell-dependent mechanisms that contribute to MAV-1 clearance from the lung and heart. As stated above, IFN-γ production by $CD8^+$ T cells (or other cell types) is not required for clearance of MAV-1 from the lung. $CD8^+$ T cells kill infected target

cells by two major pathways: perforin/granzyme-mediated pathways and Fas-Fas ligand (FasL)-mediated pathways (4, 5). The Fas-mediated pathway involves engagement of TNFR1 family death receptors (Fas, TNFR1, TNFR2, and others) on target cells by $CD8^+$ T cell-expressed FasL, membrane-bound or secreted TNF-α, or TNF-related apoptosis-inducing ligand (TRAIL) (5). In mice exposed to recombinant replication-defective HAdV vectors, clearance of virus gene products from the liver is dependent on $CD8^+$ T cells (6). Clearance is unaffected in TNFR1-deficient mice, perforin-deficient mice, or dipeptidyl peptidase I-deficient mice, which are unable to process and activate GzmA or GzmB (7). However, Fas-deficient (Fas^{lpr}/Fas^{lpr}) mice display significantly delayed viral clearance from the liver, and clearance is further delayed in mice lacking both TNFR1 and Fas. TNF-α and TNFR2, but not TNFR1, play important roles in clearance of HAdV vector from the liver of infected mice, although the impaired viral clearance in TNF-α-deficient mice may be due to blunted humoral responses rather than defective $CD8^+$ T cell killing (8, 9). A separate study demonstrated that perforin accounts for the majority of cytolytic activity in target cells in the spleen of mice transduced with HAdV vector, and that FasL and TNF-α are dispensable (10). These results suggest that multiple pathways may contribute to $CD8^+$ T cell-dependent clearance of AdV after infection. Moreover, the mechanisms of infected target cell killing during AdV infection may be organ-specific, as is the case for NK-mediated control of MCMV infection (11).

Preliminary data from our lab suggests that MAV-1 clearance from the lung may be independent of perforin (data not shown). Perforin is also

dispensable for MAV-1 clearance from the brain or spleen during MAV-1-induced encephalomyelitis (12). Our laboratory is now investigating the role of Fas and TNFR1 in MAV-1 clearance from the lung and heart. It is possible that mechanisms of $CD8^+$ T cell-mediated MAV-1 clearance are relatively interchangeable, and the importance of one pathway may only become clear in the absence of another. These studies have important implications for studies of MAV-1 infection in BMT mice, which have impaired $CD8^+$ T cell activation and delayed viral clearance, and in studies of persistent MAV-1 infection, in which incomplete viral clearance may contribute to ongoing disease.

$CD8^+$ T cell-independent mechanisms are likely to play important roles in MAV-1 clearance as well. For example, cytotoxic $CD4^+$ T cells that kill target cells in an MHC class II-restricted manner have been identified in a number of viral infections (13-16). Virus-specific cytotoxic $CD4^+$ T cells can confer protection against lethal influenza virus infection in mice (17). We identified a significant population of $CD4^+GzmB^+$ T cells in the lungs of infected BALB/c mice at 7 dpi (Figure 5-3E), which likely have cytotoxic activity. It is possible that class II-restricted killing of some infected cell populations is important for complete viral clearance from the lung. Interestingly, type II alveolar epithelial cells constitutively express MHC class II and can present antigens to $CD4^+$ T cells (18-20). It is unknown whether type II alveolar epithelial cells are targets of MAV-1 infection, but they could play an important role both as APCs and as secretors of chemokines in MAV-1-infected lungs. They may also regulate activation and expansion of cytotoxic $CD4^+$ T cells during MAV-1 infection. B cells may also

contribute to clearance of MAV-1 from the lungs or heart. Neutralizing antibodies appear around 2-3 weeks post infection in the sera of mice infected i.p. with MAV-1 (21), and B cells are important for survival in mice with systemic MAV-1 infection (22). Successful clearance of HAdV from sera of human transplant recipients is associated with an increase in titers of serotype-specific antibodies (23).

The aim of future work in our laboratory is to characterize the phenotypic and functional characteristics of virus-specific $CD4^+$ and $CD8^+$ T cells in the lungs and heart during MAV-1 respiratory infection. Development of tools to study MAV-1-specific T cells will aid in this regard. The immunodominant $CD4^+$ and $CD8^+$ T cell epitopes for MAV-1 are unknown. However, creation of recombinant MAV-1 expressing immunodominant LCMV epitopes or OVA will allow for the detection of virus-specific T cell populations *in vivo*. For example, in mice infected with a recombinant MAV-1 that expresses H-$2D^b$ CD8 (GP_{33-41}) or I-A^b CD4 (GP_{61-80}) T cell receptor epitopes of LCMV, cells could be stimulated with GP_{33-41} or GP_{61-80} and then evaluated by flow cytometry for the presence of D^b-$GP_{33-41}{}^+$ $tetramer^+$ $CD8^+$ T cells or I-A^b-$GP_{61-80}{}^+$ $tetramer^+$ $CD4^+$ T cells. Similar assays could be used with a recombinant MAV-1 expressing OVA and stimulation of cells with the peptide SIINFEKL. Ongoing work in our laboratory aims to identify immunodominant MAV-1 epitopes and develop the reagents (peptides and tetramers) that would allow us to identify and characterize virus-specific T cell populations *in vivo* without the need for a recombinant virus.

We believe that virus-specific T cells likely contribute to both tissue damage and viral clearance from the lungs and heart during acute MAV-1 respiratory infection. Perforin contributes to signs of acute encephalomyelitis following i.p. infection of adult mice, supporting a role for $CD8^+$ T cells in immunopathology during MAV-1 infection (12). A previous study demonstrated a role for both $CD4^+$ and $CD8^+$ T cells in the development of CVB3 myocarditis (24), and perforin is a major contributor to severe tissue damage during CVB3 myocarditis (25). Specific mechanisms regulating the effects of T cells in the lungs or heart during MAV-1 respiratory infection have not yet been defined. To determine the protective or immunopathological effects of $CD4^+$ and $CD8^+$ T cells on MAV-1 infection, we can purify $CD4^+$ and $CD8^+$ T cells from spleens of mock or MAV-1-infected mice and transfer to naïve mice at the time of infection to examine effects on viral replication and virus-induced inflammation. Transfer of T cells deficient in specific effectors, such as perforin or Fas, will allow us to further define the mechanisms of effects that we observe. The development of a recombinant MAV-1 expressing LCMV epitopes or OVA would allow us to purify and transfer virus-specific T cells into naïve mice rather than whole $CD4^+$ and $CD8^+$ T cell populations.

Because of the important roles that $CD8^+$ T cells play in viral clearance and are likely to play during acute infection, the effects of immunoproteasome inhibition on MAV-1 infection are of considerable interest for future investigation. The immunoproteasome plays a role in the generation of CD8 T cell epitopes from a variety of viruses, included mouse cytomegalovirus, hepatitis B virus,

influenza virus, and LCMV (26-31). Although immunodominant epitopes for MAV-1 are unknown, the development of recombinant MAV-1 viruses expressing immunodominant epitopes from LCMV (as discussed above) would allow us to analyze the role of the immunoproteasome in generating virus-specific T cell epitopes during MAV-1 infection. The availability of inhibitors such as bortezomib and ONX 0914 allows us to temporally regulate proteasome activity during MAV-1 infection and will aid in assessing specific contributions of the constitutive proteasome and the immunoproteasome to viral pathogenesis. We are currently breeding $\beta5i^{-/-}$ mice, which have a severe defect in immunoproteasome assembly and will likely have a more prominent phenotype compared to use of a pharmacologic inhibitor of the immunoproteasome (32).

Another future goal of our work is to investigate mechanisms of MAV-1 persistence in the lungs and heart. I demonstrated that MAV-1 genome is present in heart tissue at 9 weeks post infection, and this is associated with cardiac hypertrophy and decreased cardiac function (Figure 7-7 and data not shown). Other work in our laboratory has demonstrated persistent MAV-1 genome in lungs of mice infected as neonates, which was associated with increased airway hyperreactivity (Megan Procario and Jason Weinberg, unpublished data). It is unknown whether these phenotypes are due to ongoing viral replication or persistent immune responses in each organ. MAV-1 DNA is detectable in the spleen, lymph nodes, brain, and kidney for up to 42 weeks post infection following i.p. inoculation (3, 33), although the specific cell types in which viral DNA persists is unknown. Persistent HAdV DNA has been demonstrated in

human tonsillar lymphocytes (34, 35). Isolation of various cell types (cardiomyocytes, fibroblasts, lung epithelial cells, lymphocytes, etc.) from hearts or lungs at long-term time points after acute MAV-1 infection will allow us to determine the cell populations that harbor persistent virus. It is likely that the adaptive immune system plays a role in ensuring that persistent MAV-1 does not replicate unchecked, as exposure to γ-irradiation increases the levels of virus detected in brains, spleens, and kidneys of outbred Swiss Webster mice persistently infected with MAV-1 (33). Sublethal irradiation or depletion of specific cell populations (such as $CD4^+$ or $CD8^+$ T cells) at late time points would allow us to determine the contribution of the adaptive immune response to control of persistent virus, although if MAV-1 persists primarily in lymphocytes then depletion of lymphocyte populations would eliminate the MAV-1 reservoir.

Conclusions

In conclusion, the work described in this dissertation has advanced our understanding of adenovirus respiratory infection. My work suggests that minimizing some host immune responses during acute infection of immunocompetent hosts may be a useful strategy to prevent excess inflammation without impacting antiviral immunity. In immunocompromised hosts in which viral clearance is impaired, interventions to restore anti-adenoviral immunity could prevent prolonged disease associated with excess viral replication. Finally, approaches to clear persistent adenovirus may lessen the impact of chronic disease in the lungs or heart. Limited treatment options exist for

human adenovirus infections. Currently, there are no antiviral agents that convincingly improve adenovirus-associated disease. A detailed understanding of the contributions of host factors to acute adenoviral disease and persistence is the first step in identifying targets to exploit for immunomodulatory therapies to improve disease in patients with adenovirus infections.

References

1. **Coulombe F, Jaworska J, Verway M, Tzelepis F, Massoud A, Gillard J, Wong G, Kobinger G, Xing Z, Couture C, Joubert P, Fritz JH, Powell WS, Divangahi M.** 2014. Targeted Prostaglandin E2 Inhibition Enhances Antiviral Immunity through Induction of Type I Interferon and Apoptosis in Macrophages. Immunity **40:**554-568.
2. **Procario MC, Levine RE, McCarthy MK, Kim E, Zhu L, Chang C-H, Hershenson MB, Weinberg JB.** 2012. Susceptibility to acute mouse adenovirus type 1 respiratory infection and establishment of protective immunity in neonatal mice. J Virol **86:**4194-4203.
3. **Kajon AE, Brown CC, Spindler KR.** 1998. Distribution of mouse adenovirus type 1 in intraperitoneally and intranasally infected adult outbred mice. J Virol **72:**1219-1223.
4. **Hoves S, Trapani Ja, Voskoboinik I.** 2010. The battlefield of perforin/granzyme cell death pathways. J Leukoc Biol **87:**237-243.
5. **Russell JH, Ley TJ.** 2002. Lymphocyte-mediated cytotoxicity. Annu Rev Immunol **20:**323-370.
6. **Abougergi MS, Gidner SJ, Spady DK, Miller BC, Thiele DL.** 2005. Fas and TNFR1, but not cytolytic granule-dependent mechanisms, mediate clearance of murine liver adenoviral infection. Hepatology **41:**97-105.
7. **Pham CT, Ley TJ.** 1999. Dipeptidyl peptidase I is required for the processing and activation of granzymes A and B in vivo. Proc Natl Acad Sci USA **96:**8627-8632.
8. **Elkon KB, Liu CC, Gall JG, Trevejo J, Marino MW, Abrahamsen Ka, Song X, Zhou JL, Old LJ, Crystal RG, Falck-Pedersen E.** 1997. Tumor necrosis factor alpha plays a central role in immune-mediated clearance of adenoviral vectors. Proc Natl Acad Sci USA **94:**9814-9819.
9. **Kafrouni MI, Brown GR, Thiele DL.** 2003. The role of TNF – TNFR2 interactions in generation of CTL responses and clearance of hepatic adenovirus infection Abstract : Deficiency or inhibition of tumor necrosis factor (TNF) significantly prolongs hepatic. Journal of Leukocyte Biology.
10. **Chen J, Hsu H-C, Zajac AJ, Wu Q, Yang P, Xu X, McPherson Sa, Li J, Curiel DT, Mountz JD.** 2006. In vivo analysis of adenovirus-specific cytotoxic T lymphocyte response in mice deficient in CD28, fas ligand, and perforin. Hum Gene Ther **17:**669-682.
11. **Tay CH, Welsh RM.** 1997. Distinct organ-dependent mechanisms for the control of murine cytomegalovirus infection by natural killer cells. J Virol **71:**267-275.
12. **Moore ML, Brown CC, Spindler KR.** 2003. T cells cause acute immunopathology and are required for long-term survival in mouse adenovirus type 1-induced encephalomyelitis. J Virol **77:**10060-10070.
13. **Hildemann SK, Eberlein J, Davenport B, Nguyen TT, Victorino F, Homann D.** 2013. High efficiency of antiviral CD4(+) killer T cells. PloS one **8:**e60420.

14. **Marshall NB, Swain SL.** 2011. Cytotoxic CD4 T cells in antiviral immunity. J Biomed and Biotechnol **2011:**954602.
15. **Sant AJ, McMichael A.** 2012. Revealing the role of CD4(+) T cells in viral immunity. J Exp Med **209:**1391-1395.
16. **Fang M, Siciliano NA, Hersperger AR, Roscoe F, Hu A, Ma X, Shamsedeen AR, Eisenlohr LC, Sigal LJ.** 2012. Perforin-dependent CD4+ T-cell cytotoxicity contributes to control a murine poxvirus infection. Proc Natl Acad Sci USA **109:**9983-9988.
17. **Brown DM, Lee S, Garcia-Hernandez MdlL, Swain SL.** 2012. Multifunctional CD4 cells expressing gamma interferon and perforin mediate protection against lethal influenza virus infection. J Virol **86:**6792-6803.
18. **Debbabi H, Ghosh S, Kamath AB, Alt J, Demello DE, Dunsmore S, Behar SM.** 2005. Primary type II alveolar epithelial cells present microbial antigens to antigen-specific CD4+ T cells. Am J Respir Cell Mol Biol **289:**L274-279.
19. **Corbière V, Dirix V, Norrenberg S, Cappello M, Remmelink M, Mascart F.** 2011. Phenotypic characteristics of human type II alveolar epithelial cells suitable for antigen presentation to T lymphocytes. Respir Res **12:**15.
20. **Cunningham AC, Milne DS, Wilkes J, Dark JH, Tetley TD, Kirby JA.** 1994. Constitutive expression of MHC and adhesion molecules by alveolar epithelial cells (type II pneumocytes) isolated from human lung and comparison with immunocytochemical findings. J Cell Sci **107 (Pt 2):**443-449.
21. **van der Veen J, Mes A.** 1973. Experimental infection with mouse adenovirus in adult mice. Arch Gesamte Virusforsche **42:**235-241.
22. **Moore ML, McKissic EL, Brown CC, Wilkinson JE, Spindler KR.** 2004. Fatal disseminated mouse adenovirus type 1 infection in mice lacking B cells or Bruton's tyrosine kinase. J Virol **78:**5584-5590.
23. **Heemskerk B, Lankester AC, van Vreeswijk T, Beersma MFC, Claas ECJ, Veltrop-Duits LA, Kroes ACM, Vossen JMJJ, Schilham MW, van Tol MJD.** 2005. Immune reconstitution and clearance of human adenovirus viremia in pediatric stem-cell recipients. J Infect Dis **191:**520-530.
24. **Henke A, Huber S, Stelzner A, Whitton JL.** 1995. The role of CD8+ T lymphocytes in coxsackievirus B3-induced myocarditis. J Virol **69:**6720-6728.
25. **Gebhard JR, Perry CM, Harkins S, Lane T, Mena I, Asensio VC, Campbell IL, Whitton JL.** 1998. Coxsackievirus B3-induced myocarditis: perforin exacerbates disease, but plays no detectable role in virus clearance. Am J Pathol **153:**417-428.
26. **Hutchinson S, Sims S, O'hara G, Silk J, Gileadi U, Cerundolo V, Klenerman P.** 2011. A dominant role for the immunoproteasome in CD8+ T cell responses to murine cytomegalovirus. PLoS ONE **6:**e14646.

27. **Robek MD, Garcia ML, Boyd BS, Chisari FV.** 2007. Role of immunoproteasome catalytic subunits in the immune response to hepatitis B virus. J Virol **81:**483-491.
28. **Van Kaer L, Ashton-Rickardt PG, Eichelberger M, Gaczynska M, Nagashima K, Rock KL, Goldberg AL, Doherty PC, Tonegawa S.** 1994. Altered peptidase and viral-specific T cell response in LMP2 mutant mice. Immunity **1:**533-541.
29. **Chen W, Norbury CC, Cho Y, Yewdell JW, Bennink JR.** 2001. Immunoproteasomes shape immunodominance hierarchies of antiviral CD8(+) T cells at the levels of T cell repertoire and presentation of viral antigens. J Exp Med **193:**1319-1326.
30. **Pang KC, Sanders MT, Monaco JJ, Doherty PC, Turner SJ, Chen W.** 2006. Immunoproteasome subunit deficiencies impact differentially on two immunodominant influenza virus-specific CD8+ T cell responses. J Immunol **177:**7680-7688.
31. **Kincaid EZ, Che JW, York I, Escobar H, Reyes-Vargas E, Delgado JC, Welsh RM, Karow ML, Murphy AJ, Valenzuela DM, Yancopoulos GD, Rock KL.** 2012. Mice completely lacking immunoproteasomes show major changes in antigen presentation. Nat Immunol **13:**129-135.
32. **Fehling HJ, Swat W, Laplace C, Kühn R, Rajewsky K, Müller U, von Boehmer H.** 1994. MHC class I expression in mice lacking the proteasome subunit LMP-7. Science **265:**1234-1237.
33. **Smith K, Brown CC, Spindler KR.** 1998. The role of mouse adenovirus type 1 early region 1A in acute and persistent infections in mice. J Virol **72:**5699-5706.
34. **Garnett CT, Erdman D, Xu W, Gooding LR.** 2002. Prevalence and quantitation of species C adenovirus DNA in human mucosal lymphocytes. J Virol **76:**10608-10616.
35. **Garnett CT, Talekar G, Mahr JA, Huang W, Zhang Y, Ornelles DA, Gooding LR.** 2009. Latent Species C Adenoviruses in Human Tonsil Tissues. J Virol **83:**2417-2428.